VNIVERSITAT DE VALÈNCIA Facultat de Química

DESARROLLO DE NUEVAS METODOLOGÍAS ANALÍTICAS DESTINADAS A LA CARACTERIZACIÓN LIPÍDICA Y PROTEICA DE LA LECHE MATERNA

Isabel Ten Doménech

Valencia, 2018

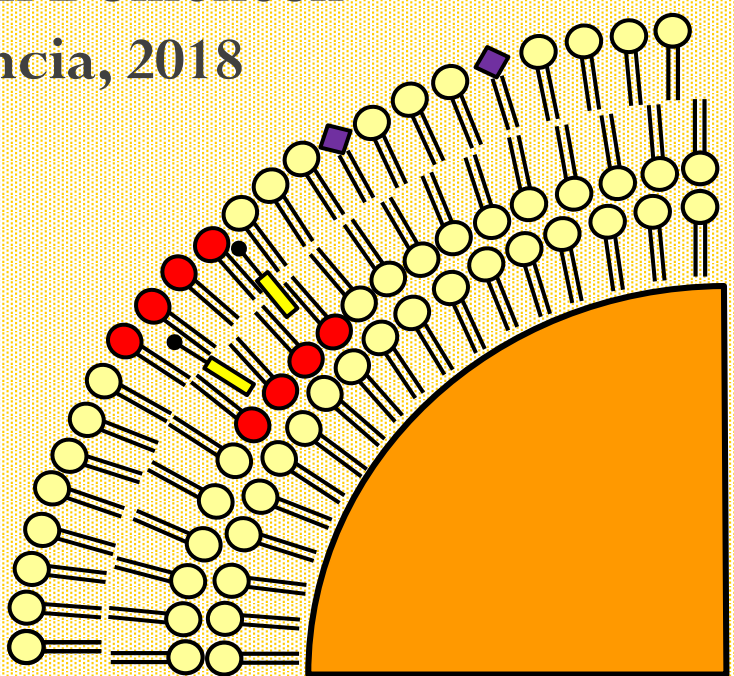

VNIVERSITAT DE VALÈNCIA

FACULTAD DE QUÍMICA

DEPARTAMENTO DE QUÍMICA ANALÍTICA

DESARROLLO DE NUEVAS METODOLOGÍAS ANALÍTICAS DESTINADAS A LA CARACTERIZACIÓN LIPÍDICA Y PROTEICA DE LA LECHE MATERNA

Memoria para alcanzar el grado de Doctor dentro del Programa de Doctorado en Química (R.D. 99/2011)

Autora:

Isabel Ten Doménech

Directores:

Dr. José Manuel Herrero Martínez

Dr. Ernesto F. Simó Alfonso

Valencia, septiembre de 2018

VNIVERSITAT DE VALÈNCIA

Facultat de Química

D. José Manuel Herrero Martínez y D. Ernesto F. Simó Alfonso, ambos catedráticos del departamento de Química Analítica de la Universidad de Valencia,

certifican

que la presente memoria, la cual lleva por título "*Desarrollo de nuevas metodologías analíticas destinadas a la caracterización lipídica y proteica de la leche materna*", constituye la Tesis Doctoral de Dña. Isabel Ten Doménech.

Asimismo, certifican haber dirigido y supervisado tanto los distintos aspectos del trabajo como su redacción.

Y para que así conste a los efectos oportunos y a petición de la interesada, firmamos la presente en Burjasot, a 26 de septiembre de 2018.

José Manuel Herrero Martínez

Ernesto F. Simó Alfonso

VNIVERSITAT DE VALÈNCIA

Prefacio

Esta Tesis se acoge a la modalidad "compendio de publicaciones", contemplada en el Reglamento de la Universidad de Valencia de 29/11/2011 (ACGUV 266/2011). De acuerdo con dicha normativa, la primera parte de la Tesis incluye un resumen global de la temática, resultados y conclusiones de los trabajos compendiados, justificando su temática y explicando la aportación original de la doctoranda. Seguidamente, se incluye una introducción general relacionada con la temática de la Tesis. A continuación, se incluyen los artículos ya publicados, los cuales corresponden en su totalidad a revistas indexadas. La doctoranda ha contribuido sustancialmente en todas las etapas de desarrollo de todos los artículos, desde la elaboración de la idea, búsqueda bibliográfica, realización experimental, análisis e interpretación de los datos, redacción y preparación del manuscrito, y seguimiento y corrección final del mismo de acuerdo con las recomendaciones de los evaluadores. Todos los artículos han sido escritos por Isabel Ten Doménech, con correcciones y revisión final por parte de los supervisores de esta Tesis.

Esta Tesis Doctoral ha sido realizada gracias a una beca predoctoral (FPU) concedida por el Ministerio de Educación, Ciencia y Deporte de España

A mi familia

AGRADECIMIENTOS

La realización de esta Tesis Doctoral no habría sido posible sin la ayuda y el apoyo de un gran número de personas.

En primer lugar, quisiera agradecer a mis directores, el Dr. José Manuel Herrero Martínez y el Dr. Ernesto F. Simó Alfonso, su ayuda y dedicación en todo este tiempo. Han sido muchos años juntos, algunos de contacto intermitente por las circunstancias. Pese a eso, los he encontrado siempre disponibles y dispuestos a ayudarme. Os complementáis en vuestras tareas, lo que hace posible los logros alcanzados.

Agradecerle también al Dr. Guillermo Ramis Ramos su disponibilidad y predisposición a ayudarme en todos los momentos en que recurrí a él solicitando ayuda.

Por otro lado, agradecer a mis compañeros del laboratorio 10. Hemos compartido momentos muy buenos y otros no tan buenos. Momentos de reírnos de auténticas tonterías. Momentos de culturizarme musicalmente (aunque sabéis qué ritmo base me gusta en realidad). Momentos de salir (aunque los menos por mi parte…). Pero también momentos de fatiga, desaliento y abandono; y momentos de tristeza personal en los que ya sabéis cómo os tengo presentes. En estos años he aprendido mucho de vosotros. Aarón, mi Aaronet, no sé si existen palabras para decir lo buen compañero y amigo que has sido para mí. Como tantas veces me has oído decir, TODO LLEGA. María Vergara, detrás de tu carácter fuerte y tu picardía, escondes una sensibilidad especial. Valentina tiene mucha suerte de tenerte como madre. Enrique, eres el chico multitarea del laboratorio, siempre dispuesto a ayudar, especialmente cuando de ordenadores y equipos se trata…Tienes claro lo que quieres, así que a por ello. No desfallezcas, pero ten siempre los pies en el suelo. Óscar, me atrevo a decir que eres el más inteligente del laboratorio, pero tampoco te pases de listo ;) Alegras el lab 10, aunque a veces te recriminemos que marees…Héctor, estás en los inicios. Creo que sabes bien

las fases que vas a vivir, pero saberlo no es igual que vivirlo. Ten ánimo y paciencia, y confía en tus posibilidades. Carol, de pronto abrupto, pero de sonrisa fácil. Constante donde las haya. Espero que veas recompensado tu esfuerzo y dedicación. No me olvido de aquellos que ya han pasado por el laboratorio (alguna incluso ha vuelto recientemente). Después de todo, tantos años han dado para mucho. María Jesús y Míriam, los dos pilares que cimentaban el laboratorio cuando llegué. Sois personas muy capaces. Perseguid aquello que merecéis. María Navarro, sensible y empática. Siempre dispuesta a anteponer las necesidades de los demás a las tuyas propias. Laura, la alegría personificada. Incansable en sus metas. Y tantos otros a los que no puedo dirigirme personalmente, pero que han dejado su huella en el lab. 10.

También agradecer a todos los compañeros de otros laboratorios, los profesores y personal del Departamento, con los que ha sido una verdadera satisfacción relacionarme y trabajar. Especial agradecimiento a María Lara, a la que personalmente llamo, mi Ángel de la Guarda.

Gracias a las lokas a y a las titis por su apoyo y confianza en este tiempo. Aunque me tenéis por lista, sabéis que lo más simple es lo que de verdad me hace reír.

Gracias también al Ministerio de Educación, Cultura y Deporte por la beca predoctoral concedida.

Y como no, agradecer también a toda mi familia su apoyo incondicional. En especial, a mis padres. Habéis ejercido de abuelos a la perfección y sin vosotros, todo esto no habría sido posible. También a mi hermana, que ha hecho de tía a la fuerza todos estos años; y a los abuelitos, siempre dispuestos a ayudarme en todo.

Por último, y no por ello menos importante, a mi marido y mis hijos. Juan, no sé si sabías en qué consistía esto del doctorado. No sé ni tan si quiera, si yo lo sabía. Has aguantado estoicamente mis quejas, mis agobios, mis incertidumbres…Siempre con palabras de ánimo y apoyo. Pero por encima de

todo, con una infinita PACIENCIA. Gracias. Miguel, Isabel y Ángela, con vosotros he aprendido a establecer prioridades, a ejercitar la paciencia y a ser humilde, que tanta falta me ha hecho siempre.

A todos vosotros, y a aquellos que, aunque no haya nombrado, han sido partícipes de este proyecto, GRACIAS.

ABREVIATURAS

FA	Ácido graso	*Fatty acid*
AA, Ara	Ácido araquidónico	*Arachidonic acid*
ALA, LnA, Ln	Ácido α-linolénico	*α-linolenic acid*
Ca	Ácido cáprico	*Capric acid*
DHA	Ácido docosahexaenoico	*Docosahexaenoic acid*
DPA	Ácido docosapentaenoico	*Docosapentaenoic acid*
EPA	Ácido eicosapentaenoico	*Eicosapentaenoic acid*
ETE	Ácido eicosatrienoico	*Eicosatrienoic acid*
GLA	Ácido γ-linolénico	*γ-linolenic acid*
La	Ácido láurico	*Lauric acid*
LA, L	Ácido linoleico	*Linoleic acid*
M	Ácido mirístico	*Myristic acid*
O	Ácido oleico	*Oleic acid*
P	Ácido palmítico	*Palmitic acid*
Pa	Ácido palmitoleico	*Palmitoleic acid*
S	Ácido esteárico	*Stearic acid*

PL	Fosfolípido	*Phospholipid*
PC	Fosfatidilcolina	*Phosphatidylcholine*
PE	Fosfatidiletanolamina	*Phosphatidylethanolamine*
PI	Fosfatidilinositol	*Phosphatidylinositol*
PS	Fosfatidilserina	*Phosphatidylserine*
SM	Esfingomielina	*Sphingomyelin*

	Proteína	*Protein*
CN	Caseína	*Casein*
HSA	Albúmina de suero humana	*Human serum albumin*
Ig	Inmunoglobulina	*Immunoglobulin*
Lf	Lactoferrina	*Lactoferrin*
Lyz	Lisozima	*Lysozyme*
sIgA	Inmunoglobulina A secretora	*Secretory immunoglobulin A*
α-La	α-Lactoalbúmina	*α-Lactalbumin*

2D	En dos dimensiones, bidimensional	*Two-dimensional*
aa	Aminoácido	*Amino acid*
ABC	Bicarbonato amónico	*Ammonium bicarbonate*
ACN	Acetonitrilo	*Acetonitrile*
Ag^+-TLC	Cromatografía de capa fina con iones de plata	*Silver ion thin-layer chromatography*
AIBN	Azobisisobutirontrilo	*Azobisisobutyronitrile*
APCI	Ionización química a presión atmosférica	*Atmospheric pressure chemical ionization*
APTMS	(3-aminopropil) trimetoxisilano	*(3-aminopropyl) trimethoxysilane*
AuNP	Nanopartícula de oro	*Gold nanoparticle*
BET	Brauner-Emmet-Teller	*Brauner-Emmet-Teller*
BGE	Electrolito de fondo	*Background electrolyte*
BHT	Butil hidroxitolueno	*Butylated hydroxytoluene*
BJH	Barret-Joyner-Halenda	*Barret-Joyner-Halenda*
C	Agente entrecruzante	*Cross-linker*

Cal	Calcinación	*Calcination*
CCP	Fosfato cálcico coloidal	*Colloidal calcium phosphate*
CE	Electroforesis capilar	*Capillary electrophoresis*
CEC	Electrocromatografía capilar	*Capillary electrocromatography*
CMC	Concentración micelar crítica	*Critical micelle concentration*
CNT	Nanotubos de carbono	*Carbon nanotubes*
CTAB	Bromuro de cetiltrimetilamonio	*Cetyl trimethyl ammonium bromide*
DB	Doble enlace	*Double bond*
df	Función discriminante	*Discriminant function*
DLS	Dispersión dinámica de luz	*Dynamic light scattering*
DTT	Ditiotreitol	*Dithiothreitol*
EDAX	Análisis por fluorescencia de rayos X por energía dispersiva	*Energy dispersive X-ray analysis*
EDMA	Dimetacrilato de etilenglicol	*Ethylene dimethacrylate*
EDTA-Na_2	Sal disódica del ácido etilendiaminotetraacético	*Ethylenediaminetetraacetic acid disodium salt*
ELSD	Detector evaporativo de dispersión de luz	*Evaporative light scattering detector*
ESI	Ionización por electroespray	*Electrospray ionization*
ESM	Material electrónico suplementario	*Electronic supplementary material*
EtOH	Etanol	*Ethanol*
Ext	Extracción química	*Chemical extraction*
FAME	Éster metílico de ácido graso	*Fatty acid methyl ester*

FMM	Nanomaterial magnético funcionalizado	*Functionalized magnetic nanomaterial*
GC	Cromatografía de gases	*Gas chromatography*
GMA	Metacrilato de glicidilo	*Glycidyl methacrylate*
HEC	Hidroxietilcelulosa	*Hydroxyethylcellulose*
HILIC	Cromatografía líquida de interacción hidrofílica	*Hydrophilic interaction liquid chromatography*
HPLC	Cromatografía líquida de alta resolución	*High performance liquid chromatography*
IAM	Iodoacetamida	*Iodoacetamide*
ICP	Plasma acoplado inductivamente	*Inductively-coupled plasma*
IDA	Ácido iminodiacético	*Iminodiacetic acid*
IEF	Isoelectroenfoque	*Isoelectric focusing*
LC	Cromatografía líquida	*Liquid chromatography*
LC-FA	Ácido graso de cadena larga	*Long chain fatty acid*
LDA	Análisis discriminante lineal	*Linear discriminant analysis*
LOD	Límite de detección	*Limit of detection*
LOQ	Límite de cuantificación	*Limit of quantitation*
M	Monómero funcional	*Functional monomer*
MAA	Ácido metacrílico	*Methacrylic acid*
MALDI	Desorción/ionización láser asistida por matriz	*Matrix-assisted laser desorbtion ionization*
MAS-NMR	Resonancia magnética nuclear con giro al ángulo mágico	*Magic angle spinning nuclear magnetic resonance*
MeOH	Metanol	*Methanol*
MFGM	Membrana de los glóbulos de grasa de la leche	*Milk fat globule membrane*

MIP	Polímero de impronta molecular	*Molecularly imprinted polymer*
MNP	Nanopartícula magnética	*Magnetic nanoparticle*
MOF	Estructuras metal-orgánicas	*Metal organic framework*
MS	Espectrometría de masas	*Mass spectrometry*
MSM	Material de sílice mesoporosa	*Mesoporous silica material*
MSP	Partícula de sílice mesoporosa	*Mesoporous silica particle*
MSPE	Extracción en fase sólida magnética	*Magnetic solid-phase extraction*
MUFA	Ácido graso monoinsaturado	*Monounsatured fatty acid*
M_w, Mr	Peso molecular	*Molecular weight*
NC	Nº de átomos de carbono	*Number of carbon atoms*
ND	Nº de dobles enlaces	*Number of double bounds*
NIP	Polímero no impreso	*Non-molecularly imprinted polymer*
NP	Nanopartícula	*Nanoparticle*
NPN	Nitrógeno no proteico	*Non-protein nitrogen*
PAGE	Electroforesis en gel de poliacrilamida	*Polyacrylamide gel electrophoresis*
PEG	Polietilenglicol	*Polyethylene glycol*
pI	Punto isoeléctrico	*Isoelectric point*
PN	Nº de partición	*Partition number*
PS-DVB	Poliestireno-divinilbenceno	*Polystyrene-divinylbenzene*
PUFA	Ácido graso poliinsaturado	*Polyunsaturated fatty acid*
RMN/ NMR	Resonancia magnética nuclear	*Nuclear magnetic resonance*

RP	Fase reversa	*Reverse-phase*
RRF	Factor de respuesta relativo	*Relative response factor*
RSD	Desviación estándar relativa	*Relative standard deviation*
SD	Desviación estándar	*Standard deviation*
SDS	Dodecilsulfato sódico	*Sodium dococyl sulfate*
SEM	Microscopía/microscopio electrónica/o de barrido	*Scanning electronic microscopy/microscope*
SFA	Ácido graso saturado	*Saturated fatty acid*
SFC	Cromatografía con fluidos supercríticos	*Supercritical fluid chromatography*
SPE	Extracción en fase sólida	*Solid-phase extraction*
T	Molécula plantilla	*Template molecule*
TAG	Triacilglicerol, triglicérido	*Triacylglycerol, triglyceride*
TEA	Trietanolamina	*Triethanolamine*
TEM	Microscopía/microscopio electrónica/o de transmisión	*Transmission electronic microscopy/microscope*
TEOS	Tetraetoxisilano/ortosilicato de tetraetilo	*Tetraethyl-orthosilicate*
TFA	ácido trifluoroacético	*Trifluoroacetic acid*
THF	Tetrahidrofurano	*Tetrahydrofuran*
TLC	Cromatografía de capa fina	*Thin layer chromatography*
Tris	Tris(hidroximetil) aminometano	*Tris(hydroxymethyl) aminomethane*
UHPLC	Cromatografía líquida de ultra alta resolución	*Ultra-high performance liquid chromatography*
α-CHCA	Ácido *α*-ciano-4-hidroxicinámico	*α-cyano-4-hydroxycinnamic acid*

ÍNDICE

ÍNDICE DE TABLAS

BLOQUE I. Introducción

BLOQUE II. Análisis de la fracción lipídica de la leche materna

BLOQUE III. Análisis de la fracción proteica de la leche materna

ÍNDICE DE FIGURAS

BLOQUE I. Introducción

BLOQUE II. Análisis de la fracción lipídica de la leche materna

BLOQUE III. Análisis de la fracción proteica de la leche materna

RESUMEN

En esta sección, de acuerdo con la normativa sobre depósito, evaluación y defensa de la Tesis Doctoral de la Universidad de Valencia aprobada por Consejo de Gobierno el 29 de noviembre de 2011 y con última modificación el 31 de octubre de 2017, se presenta un resumen global de la temática, de los principales resultados y de las conclusiones del trabajo.

Objetivos

La presente Tesis Doctoral contempla dos grandes líneas de actuación: (i) el desarrollo de métodos rápidos y sencillos de caracterización de la fracción lipídica de la leche materna, con el fin de estudiar su perfil y evolución a lo largo de la lactancia; y (ii) el desarrollo de metodologías por electroforesis en gel, electroforesis capilar (*capillary electrophoresis*, CE) y cromatografía líquida de alta resolución (*high performance liquid chromatography*, HPLC), con detección UV-visible y por espectrometría de masas (*mass spectrometry*, MS), con objeto de evaluar las proteínas lácteas de las muestras o los péptidos resultantes de la digestión de éstas.

Para la consecución de los objetivos (i) y (ii) se ha considerado la experiencia previa del grupo en técnicas cromatográficas y de electroseparación capilar y, más en concreto, en el diseño y desarrollo de soportes poliméricos para técnicas de separación miniaturizadas.

Cabe destacar que esta Tesis supone el primer contacto del grupo de investigación con muestras de leche materna. Debido a la complejidad de la matriz y considerando la potencial aportación que por parte del grupo podía hacerse, los esfuerzos de esta Tesis han ido principalmente dirigidos a la simplificación o facilitación de la etapa de tratamiento de muestra, atendiendo a la problemática existente a este fin. Así pues, se ha abordado la separación, aislamiento y preconcentración de los diferentes compuestos de interés atendiendo a su diferente naturaleza y, en el caso concreto de los fosfolípidos, incluso desde diferentes perspectivas.

Estructura

La presente memoria se divide en tres grandes bloques. El primer bloque es introductorio, haciéndose una descripción general de la composición de la leche materna y entrando más en detalle en aquellas fracciones que han sido objeto de análisis de la Tesis (**Capítulo 1**). A continuación, en el **Capítulo 2**, se recogen las principales metodologías analíticas que se han empleado para abordar el tratamiento de muestra y análisis de los dos grandes grupos de compuestos estudiados en esta Tesis: lípidos y proteínas. El capítulo se inicia con la extracción de la fracción lipídica y su posterior caracterización, para abordar posteriormente la fracción proteica y las metodologías asociadas a ésta. Por último, en el **Capítulo 3**, se muestra una visión general de las distintas estrategias utilizadas en la preparación de sorbentes en técnicas de preparación de muestra, en concreto extracción en fase sólida (*solid-phase extraction*, SPE), centrándose en aquellos materiales que han sido objeto de estudio en esta Tesis: la sílice mesoporosa, los polímeros orgánicos modificados con nanopartículas (*nanoparticle*, NP) metálicas u óxidos metálicos y los polímeros de impronta molecular *(molecularly imprinted polymer*, MIP).

El segundo bloque engloba los **Capítulos 4-7** y está dedicado al análisis de la fracción lipídica de la leche materna. El primer capítulo de este bloque se centra en el análisis del componente mayoritario de la grasa, esto es, los triglicéridos (*triacylglycerol*, TAG). Para ello, y tras proponer un método de extracción de la grasa a escala reducida, se lleva a cabo un análisis del perfil de TAG de la leche materna y se estudia la posibilidad de distinguir el origen animal de la leche en función de éste aplicando una herramienta quimiométrica de análisis, en concreto, análisis discriminante lineal (*linear discriminant analysis*, LDA). Por otra parte, los capítulos sucesivos del bloque se centran en el aislamiento y análisis de uno de los componentes minoritarios de la leche, en concreto, los fosfolípidos. Para ello, se han puesto a punto nuevos sorbentes para su uso en SPE, basados en materiales porosos de

diferente naturaleza: sílice mesoporosa, monolitos poliméricos de metacrilato de glicidilo (GMA) y posteriormente modificados con NP de magnetita; y MIP.

Por su parte, el tercer bloque abarca los **Capítulos 8** y **9** y está enfocado hacia el análisis de la fracción proteica de la leche materna y, más concretamente, a la problemática asociada a la separación de los dos grandes grupos de proteínas presentes en la leche: las caseínas (*casein*, CN) y las proteínas del suero. Dicha problemática se aborda desde dos perspectivas. Por una parte, se propone el empleo de monolitos poliméricos basados en GMA y posteriormente modificados con NP oro (AuNP) para su uso como sorbente en SPE. Por otra parte, se plantea la posibilidad de fraccionar ambos grupos de proteínas por una simple co-precipitación de las CN por la adición de iones calcio y fosfato a la leche con objeto de mejorar el rendimiento de extracción de ambas fracciones respecto al procedimiento clásico de precipitación isoeléctrica.

Resultados y conclusiones

A continuación, se describen los principales resultados obtenidos y conclusiones derivadas para cada uno de los trabajos incluidos en la Tesis Doctoral. Los trabajos han sido divididos en dos grandes grupos (A y B), correspondientes a los bloques II y III de la memoria, donde se indica de forma desglosada por capítulos (cada capítulo corresponde a una publicación) la metodología adoptada en cada uno de ellos para alcanzar los objetivos planteados, así como los resultados y conclusiones más relevantes obtenidos de los mismos.

A. Análisis de la fracción lipídica de la leche materna

A.1. Análisis de triglicéridos

En este trabajo (**Capítulo 4** de la memoria) se llevó a cabo la separación de TAG presentes en la leche materna y en la leche de otros mamíferos por HPLC en fase reversa empleando una columna particulada de "corazón fundido" (*fused core*) con detector UV-vis y detector evaporativo de dispersión de luz (*evaporative light scattering detector*, ELSD). Para la separación cromatográfica se emplearon primeramente mezclas binarias de acetonitrilo (ACN) con diferentes alcoholes (2-propanol, *n*-butanol and *n*-pentanol). De entre estos, el *n*-pentanol proporcionó los mejores resultados en cuanto a resolución y tiempo de análisis. Una vez establecido el gradiente de ACN/*n*-pentanol, se estudió el efecto de la temperatura y el caudal, seleccionándose unos valores de 10 ºC y 1 mL/min, respectivamente. Bajo las condiciones establecidas, se obtuvo un perfil de TAG donde se resolvieron de manera satisfactoria más de 50 TAG. La identificación de los picos se llevó a cabo por MS con ionización química a presión atmosférica, en la que se observó un pico molecular, la intensidad del cual dependía del grado de insaturación de la molécula de TAG, y los iones resultantes de la pérdida de las cadenas de ácidos grasos, es decir, los diglicéridos. También, se puso a punto un método extracción a escala reducida, el cual requiere unos volúmenes de reactivos y muestra inferiores al método tradicional. El método propuesto se comparó con el método tradicional en lo que al contenido total de grasa y TAG se refiere. Para la cuantificación de los TAG se llevó a cabo una calibración externa con estándares de TAG homogéneos (los tres ácidos grasos unidos a la molécula de glicerol son iguales), estableciéndose unos factores de respuesta relativos comprendidos entre 0.85-1.05. Esto permitió llevar a cabo una estimación del contenido de cada uno de los TAG en base al área de pico del cromatograma. Los resultados obtenidos por ambos métodos no presentaron diferencias significativas. Además, cabe destacar que el método de tratamiento de muestra propuesto no sólo implica una reducción en

la cantidad de reactivos necesaria, sino que, debido a la sencillez asociada a la manipulación del material requerido, permite el procesamiento de un mayor número de muestras en comparación con el método tradicional.

Por último, se llevó a cabo un estudio estadístico mediante un LDA en base a la composición de TAG de la leche de diferentes mamíferos (humana, bovina, ovina y caprina). Para ello, se seleccionaron 22 TAG comunes a todas las leches consideradas y a partir de las variables normalizadas, usadas como predictores del modelo, se obtuvo la matriz de objetos y se establecieron los conjuntos de entrenamiento y evaluación del modelo. El modelo resultante proporcionó una excelente resolución entre todas las categorías y el conjunto de evaluación fue correctamente clasificado. Esto demostró que es posible diferenciar el origen animal de la leche en base al perfil de TAG obtenido por HPLC-ELSD, lo cual puede resultar de utilidad no solo en estudios centrados en la leche materna, sino también en aquellos basados en productos derivados de la leche de otros mamíferos.

Los resultados de este trabajo se encuentran publicados en:

I. Ten-Doménech, E. Beltrán-Iturat, J.M. Herrero-Martínez, J.V. Sancho-Llopis, E.F. Simó-Alfonso, Triacylglycerol analysis in human milk and other mammalian species: small-scale sample preparation, characterization, and statistical classification using HPLC-ELSD profiles, J. Agric. Food Chem. 63 (2015) 5761–5770. doi:10.1021/acs.jafc.5b01158.

A.2. Análisis de fosfolípidos

En estos trabajos (**Capítulos 5**, **6**, y **7** de la memoria) se evaluaron diferentes materiales porosos como sorbentes de extracción en fase sólida (*solid-phase extraction*, SPE) para el aislamiento de fosfolípidos (*phospholipid*, PL) empleando fosfatidilcolina (*phosphatidylcholine*, PC) como soluto test. De entre los materiales seleccionados se encuentran los de sílice, dos de ellos mesoporosos (UVM-7 y MCM-41) y otro comercial

(**Capítulo 5**), un monolito polimérico de GMA modificado con NP de magnetita (**Capítulo 6**), y otro basado en la tecnología de impronta molecular (**Capítulo 7**).

Tras la síntesis de los materiales, se llevó a cabo su caracterización morfológica empleando microscopía electrónica de barrido (s*canning electronic microscopy*, SEM) y transmisión (*transmission electronic microscopy*, TEM) así como medidas del área superficial y el tamaño de poro. Asimismo, se abordó el mecanismo de interacción entre el analito de interés y los diferentes sorbentes. En lo que respecta a la SPE, se investigaron diferentes parámetros experimentales que afectan el proceso, como p.ej. el disolvente de carga y elución, el volumen de ruptura, la capacidad de carga y la reutilización. Para la evaluación de las recuperaciones en las diferentes variables estudiadas, se empleó un ensayo colorimétrico basado en la formación del complejo PL-ferrotiocianato de amonio. El protocolo de SPE desarrollado se aplicó satisfactoriamente a extractos de grasa de leche materna, observándose una notoria preconcentración de los analitos de interés y eliminación de lípidos no polares (TAG). Los PL extraídos fueron analizados mediante cromatografía líquida de interacción hidrofílica (*hydrophilic interaction liquid chromatography*, HILIC) acoplada a ELSD. Para ello se empleó una fase móvil a partir de mezclas de ACN-formiato amónico y agua-formiato amónico a una temperatura de 25 ºC y un caudal de 1 mL/min. También, se realizaron curvas de calibrado (externa y de adición estándar) de los PL, descartándose el posible efecto matriz (a partir de los resultados obtenidos).

En el caso de los materiales de sílice mesoporosa (*mesoporous silica material*, MSM) (**Capítulo 5**), los cuales se caracterizan por su elevada área superficial (>1000 m^2/g), su gran volumen de poro (>1 cm^3/g) y su fácil manipulación, se sintetizaron el material MCM-41 y los materiales UVM-7 puro y dopado con titanio. La síntesis de estos últimos se llevó a cabo siguiendo la ruta del complejo de atrano (o silatrano en este caso) como precursor inorgánico, y el surfactante bromuro de cetiltrimetilamonio como

plantilla y especie porógena. La eliminación del surfactante de los materiales sintetizados se llevó a cabo por dos vías: calcinación y extracción química con una mezcla ácido acético/etanol (EtOH). Como resultado, se obtuvo el material UVM-7, el cual puede describirse como un sistema de poros bimodal que contiene mesoporos intra-particulares y macroporos inter-particulares. Una vez obtenidos los materiales, se empaquetaron 10 mg de cada uno de estos en los correspondientes cartuchos de SPE.

Dentro del protocolo SPE, se estableció en primer lugar el disolvente o mezcla de disolventes más adecuado para la elución, obteniéndose los mejores resultados para la mezcla $CHCl_3$:metanol (MeOH):H_2O (3:5:2, v/v/v). Como disolventes de carga, se trabajó con una mezcla de hexano:EtOH (98:2, v/v) y con la mezcla $CHCl_3$:MeOH (2:1, v/v), proporcionando la primera de éstas los mejores resultados.

En lo que respecta al mecanismo de interacción entre el soluto test (PC) y los materiales de sílice, cabe destacar que, bajo las condiciones experimentales escogidas, las moléculas de PC se encuentran agregadas en forma de micelas invertidas, por lo que se propuso un mecanismo de interacción soluto-sorbente basado en dos pasos: (i) difusión de las micelas invertidas de PC a lo largo del sistema de poros de la sílice; y (ii) ruptura de las micelas de PC inducida por la interacción favorable con los grupos silanol de la superficie de la sílice (Si-OH···PC).

De entre los materiales testados, incluyendo el de sílice comercial (SupelClean™), el material UVM-7, en el que los restos de surfactante de la síntesis habían sido retirados por extracción química (UVM-7-Ext), proporcionó los mejores resultados. Este hecho, se atribuyó al entorno más hidrofílico (mayor proporción de grupos silanoles) del material UVM-7-Ext con respecto al MCM-41 y SupelClean™, junto con el segundo sistema de poros bimodal característico del material UVM-7. Cabe destacar que, el material UVM-7 dopado con Ti no proporcionó los resultados esperados, ya

que la interacción del Ti con los grupos fosfato de los PL no exaltó las prestaciones del material. Este hecho se atribuyó, bien a la baja disponibilidad del Ti en la superficie de los poros, ya que la mayoría de éste queda embebido dentro de las paredes del material; o bien cambios en la estructura y reducción del tamaño de poro y área superficial asociados a la introducción de Ti en la sílice. En cualquier caso, el material UVM-7-Ext proporcionó una elevada capacidad de adsorción (544 µg de PC por mg de sorbente), reutilización (más de 15 usos) y capacidad de preconcentración (hasta 16 veces).

En lo referente al material polimérico de GMA modificado con NP de magnetita (**Capítulo 6**), en primer lugar, se sintetizaron las NP por el método de co-precipitación de disoluciones acuosas de Fe^{3+} y Fe^{2+} en medio básico, obteniéndose unas NP magnéticas (*magnetic nanoparticle*, MNP) de un tamaño promedio de 12 nm (medido por TEM). Por otra parte, se sintetizó el material polimérico de GMA y dimetacrilato de etilenglicol (*ethylendimethacrylate*, EDMA), se trituró con un mortero y se tamizó hasta un tamaño de partícula de entre 125 y 200 µm. Seguidamente, el material de GMA-*co*-EDMA se silanizó y sobre éste se anclaron las MNP. La caracterización morfológica del material por SEM mostró claramente el anclaje de la magnetita sobre la superficie de éste. Por otra parte, se evaluó el contenido de hierro (previa calcinación del material) por UV-Vis y por plasma acoplado inductivamente-MS previa calcinación, obteniéndose un 1.6-1.7% de Fe (m/m). Asimismo, las isotermas de adsorción-desorción de nitrógeno empleando el modelo Brauner-Emmet-Teller (BET) mostraron que la incorporación de MNP supuso un incremento del área superficial (15.17 m^2/g) respecto al polímero sin modificar (6.14 m^2/g), lo cual contribuye a exaltar la retención de los analitos de interés.

En este trabajo, debido a las propiedades magnéticas del sorbente, el proceso de extracción se abordó de dos maneras distintas: (i) en cartuchos de SPE en los que se empaquetaron 150 mg de sorbente; y (ii) en modalidad dispersiva, también conocida como extracción en fase sólida magnética

(*magnetic solid-phase extraction*, MSPE), empleando también 150 mg de sorbente. En primer lugar, se estudió el disolvente de carga, ensayándose las mezclas $CHCl_3$:MeOH (2:1, v/v) y hexano:EtOH (98:2, v/v), obteniéndose una retención sobre el sorbente del 45 y 97%, respectivamente. Estos resultados pueden explicarse teniendo en consideración el proceso de adsorción de los PL sobre la superficie de las MNP, en el cual intervienen dos fuerzas impulsoras: (i) un aumento de la entropía debido al desplazamiento de las moléculas de disolvente alrededor de las NP por las moléculas de PL; o (ii) la atracción carga-dipolo entre la superficie cargada de las NP y el dipolo P-N de las cabezas de PL. Así pues, los resultados sugirieron que, con disolventes más polares, las MNP así como la PC se encontraban preferentemente solvatadas, lo cual va en detrimento de su interacción y, por ende, de la adsorción de PC sobre las MNP. Una vez establecido el disolvente de carga, la PC retenida se desorbió con la mezcla $CHCl_3$:MeOH (2:1, v/v).

En las condiciones de carga y elución establecidas, la capacidad de adsorción del sorbente en SPE fue superior (5.7 µg de PC por mg de sorbente) a la mostrada en dispersiva (MSPE) (3.3 µg de PC por mg de sorbente). Además, la reutilización de los cartuchos de SPE fue claramente superior (10 usos) a la mostrada en MSPE (un único uso), debido, entre otros aspectos, a la pérdida de material magnético tras el proceso de regeneración de éste.

En lo que respecta a los MIP (**Capítulo 7**), se llevó a cabo en primer lugar un estudio de pre-polimerización por espectroscopía infrarroja, en el que se estudiaron las interacciones moleculares entre la molécula plantilla (*template*, T) (PC) y el monómero funcional (*functional monomer*, M) (ácido metacrílico) en diferentes disolventes (ACN, MeOH y tetrahidrofurano). En base a esto, se seleccionó ACN como disolvente para la síntesis de los MIP. A continuación, se sintetizaron varios MIP, estudiándose la influencia de la relación molar T:M: agente entrecruzante (*cross-linker*, C) y porcentaje de iniciador radicalario. Tras su trituración y tamizado (tamaño de partícula < 100 nm), 25 mg de cada MIP, y su correspondiente polímero sin

T, se empaquetaron en sendos cartuchos de SPE. Se consideraron como disolventes de carga las mezclas $CHCl_3$:MeOH (2:1, v/v) y hexano:EtOH (98:2, v/v), siendo esta última la seleccionada finalmente; y como disolvente de elución la mezcla $CHCl_3$:MeOH (2:1, v/v). De entre los MIP sintetizados, el MIP con una relación T:M:C de 1:6:30 y un 4.2% de iniciador mostró la mejor habilidad de reconocimiento por la molécula plantilla. Seguidamente, se investigó la selectividad del MIP frente a otros PL, observándose que éste mostraba una elevada afinidad no solo por la PC, sino por otros PL como la esfingomielina y la fosfatidiletanolamina. Este fenómeno, conocido como "reactividad cruzada", es de gran utilidad para el fin que se perseguía en el trabajo: la extracción del conjunto de PL. Asimismo, el MIP mostró una buena capacidad de carga (41 μg PC por mg de sorbente) y una reutilización de al menos 20 veces para disoluciones patrón de PC y de al menos 6 veces para extractos de grasa de leche materna.

Cabe destacar que, todos los sorbentes desarrollados y empleados en los **Capítulos 5-7** suponen un ayuda adicional a la hora de preservar la integridad de la columna cromatográfica ya que, pese a que existen estudios que llevan el análisis de PL sin previa preconcentración, la etapa previa de aislamiento de PL de los extractos de grasa supone una disminución notable en el contenido de lípidos no polares (TAG) y, por consiguiente, en el frente de elución. Por otra parte, cada uno de estos trabajos representa la primera aplicación del correspondiente material a la preconcentración de PL en matrices complejas.

Los resultados de estos trabajos se encuentran publicados en:

H. Martínez Pérez-Cejuela, I. Ten-Doménech, J. El Haskouri, P. Amorós, E.F. Simó-Alfonso, J.M. Herrero-Martínez, Solid-phase extraction of phospholipids using mesoporous silica nanoparticles: application to human milk samples, Anal. Bioanal. Chem. 410 (2018) 4847–4854. doi:10.1007/s00216-018-1121-8.

I. Ten-Doménech, H. Martínez-Pérez-Cejuela, E.F. Simó-Alfonso, S. Torres-Cartas, S. Meseguer-Lloret, J.M. Herrero-Martínez, Polymer-based materials modified with magnetite nanoparticles for enrichment of phospholipids, Talanta 180 (2018) 162–167. doi:10.1016/j.talanta. 2017.12.042.

I. Ten-Doménech, H. Martínez-Pérez-Cejuela, M.J. Lerma-García, E.F. Simó-Alfonso, J.M. Herrero-Martínez, Molecularly imprinted polymers for selective solid-phase extraction of phospholipids from human milk samples, Microchim. Acta 184 (2017) 3389–3397. doi:10.1007/s00604-017-2345-6.

B. Análisis de la fracción proteica de la leche materna

En este trabajo (**Capítulo 8**) se describe un método para el aislamiento de las proteínas del suero de la leche materna mediante SPE empleando un material polimérico modificado con AuNP. En primer lugar, se procedió a la síntesis del polímero de GMA, se trituró posteriormente con un mortero y se tamizó hasta un tamaño de partícula de entre 100 y 200 µm. A continuación, se llevó a cabo la modificación de su superficie mediante reacción con amoníaco, seguida de la posterior inmovilización de las AuNP en su superficie. El contenido de Au, medido colorimétricamente previa calcinación del material, fue de un 1.3% m/m. Asimismo, las micrografías SEM mostraron la presencia de las AuNP en la superficie del sorbente. Dada la elevada afinidad que se esperaba de este material por los grupos tiol y amino, habitualmente presentes en biomoléculas como las proteínas, se decidió aplicarlo al aislamiento de éstas. Así pues, se empaquetaron 50 mg del material sintetizado, y se seleccionaron una serie de proteínas séricas como son la albúmina sérica humana (HSA), la α-lactoalbúmina (α-La), la lactoferrina (Lf) y la lisozima (Lyz). Se investigaron diferentes variables (pH, fuerza iónica) con el fin de conseguir el máximo rendimiento en el proceso de

extracción. El sorbente mostró una elevada retención (>80%) por las proteínas ácidas (HSA y α-La) a lo largo de un amplio rango de pH (3.0-9.0); mientras que para las proteínas más básicas (Lf y Lyz), las mayores retenciones se encontraron para valores de pH próximos al pI de éstas. A la vista de los resultados, se concluyó que existían diferentes mecanismos responsables de la interacción entre las proteínas y las AuNP. Por una parte, la presencia de interacciones electrostáticas entre los grupos citrato (estabilizadores de las AuNP) con dominios cargados positivamente de las proteínas, independientemente de la carga global de éstas. Por otra, también era de esperar un mecanismo de desplazamiento o de reordenamiento de la estructura de la proteína como consecuencia de su adsorción sobre la superficie, ya que a un pH próximo al pI las interacciones electrostáticas proteína-sorbente se verían minimizadas.

Bajo las mejores condiciones establecidas (pH de carga 5.0, pH de elución 12 con 0.25 M de NaCl) el sorbente SPE proporcionó excelentes recuperaciones, ofreciendo una alta permeabilidad y reutilización (más de 20 veces).

Cabe destacar que, este trabajo representa la primera aproximación centrada en la interacción de AuNP inmovilizadas sobre soportes poliméricos y las proteínas presentes en la leche, para el empleo de este tipo de materiales como sorbente de extracción en SPE. Asimismo, la viabilidad de la metodología propuesta, seguida por electroforesis en gel de poliacrilamida en presencia de dodecilsulfato sódico (*sodium docecyl sulfate-polyacrylamide gel electrophoresis*, SDS-PAGE), quedó satisfactoriamente demostrada con el aislamiento de las proteínas de interés tanto de extractos de suero de leche materna, como directamente de muestras de leche diluidas, es decir, sin haber llevado a cabo previamente la precipitación isoeléctrica de las CN.

En el estudio del **Capítulo 9** se describe un método sencillo de tratamiento de muestra para el fraccionamiento efectivo de las proteínas de la

leche materna en sus dos grupos principales: suero y CN. El protocolo de extracción consistió en la adición de iones calcio y fosfato a la leche sin ajuste previo de pH, seguido etapas de lavado y centrifugación. La combinación de ambos iones dio lugar a la precipitación de fosfato cálcico y como resultado, a una co-precipitación efectiva de las CN. Este hecho se atribuyó principalmente a que, en la leche, el fosfato inorgánico (o fosfato cálcico coloidal) y el fosfato orgánico (esterificado en la caseína a través del grupo hidroxilo del aminoácido serina) se encuentran asociados químicamente. Por otra parte, se estudió el efecto de la adición a la leche de cada uno de estos iones por separado, observándose que ambos iones eran partícipes y necesarios en el proceso de fraccionamiento.

La efectividad del fraccionamiento por co-precipitación, así como por precipitación en el punto isoeléctrico (método tradicional) se siguió por SDS-PAGE, por nano-LC-MS/MS, previa digestión de las proteínas con tripsina, y por CE. Los resultados obtenidos mostraron que, la precipitación con iones calcio y fosfato, producía una disminución significativa en la contaminación de la fracción de CN con proteínas del suero y viceversa, comparado con el método convencional de precipitación de CN. En lo referente al análisis de la leche materna por CE, se empleó un tampón isoeléctrico constituido por urea, hidroxietilcelulosa y ácido iminodiacético (pH aparente 3.1), obteniéndose un perfil electroforético en el que las principales proteínas del suero y CN se encontraban adecuadamente resueltas en un tiempo de análisis breve. Además, se aplicó satisfactoriamente la recolección de fracciones en CE acoplada a LC-MS/MS (acoplamiento fuera de línea) para la identificación de proteínas minoritarias en esta matriz compleja. Esta combinación permitió identificar proteínas tales como inmunoglobulinas, las cuales no han sido identificadas previamente mediante esta técnica separativa. Por otra parte, se llevó a cabo una clasificación de todas las proteínas identificadas en la recolección (en total 62) de acuerdo con su función molecular, el proceso biológico en el que se

encuentran involucradas y su localización en los diferentes componentes celulares.

Cabe destacar que, en lo que respecta a reactivos, instrumentación y esfuerzo, la metodología de fraccionamiento propuesta supone una aproximación de bajo coste y gran alcance para cualquiera que sea el fin que se persiga (p. ej. diferencias en el perfil electroforético de la leche materna según la etapa de lactancia o selección de biomarcadores para el diagnóstico de enfermedades). Así pues, la metodología planteada en este trabajo constituye una herramienta prometedora para acrecentar el conocimiento del proteoma de la leche materna. Los datos obtenidos en este trabajo se encuentran disponibles en el consorcio *ProteomeXchange* con el identificador PXD010315.

Los resultados de estos trabajos se encuentran publicados en:

I. Ten-Doménech, E.F. Simó-Alfonso, J.M. Herrero-Martínez, Isolation of human milk whey proteins by solid phase extraction with a polymeric material modified with gold nanoparticles, Microchem. J. 133 (2017) 320–326. doi:10.1016/j.microc.2017.03.058.

I. Ten-Doménech, E.F. Simó-Alfonso, J.M. Herrero-Martínez, Improving fractionation of human milk proteins through calcium phosphate coprecipitation and their rapid characterization by capillary electrophoresis, J. Proteome Res. (2018) (en prensa). doi:10.1021/acs.jproteome.8b00526.

BLOQUE I. INTRODUCCIÓN

CAPÍTULO 1

La leche materna

1. 1. Los beneficios de la leche materna

El libro "La Estrategia Global para la Alimentación del Lactante y el Niño Pequeño" [1], elaborado conjuntamente por la Organización Mundial de la Salud y el Fondo de las Naciones Unidas para la Infancia (*United Nations Children's Fund*, UNICEF), recomienda la lactancia materna exclusiva durante los primeros seis meses de vida del bebé y, continuar con ésta de ahí en adelante y hasta los dos años de edad, habiéndose introducido la alimentación complementaria [1,2]. Esta recomendación se ha visto respaldada por diversos estudios que relacionan la lactancia materna con una reducción del riesgo de numerosas enfermedades para el recién nacido a término (p. ej. otitis media aguda, dermatitis atópica, infecciones gastrointestinales, enfermedades del tracto respiratorio inferior, asma, obesidad, leucemia infantil y síndrome de la muerte súbita) [3], así como con varios beneficios para la madre como son un descenso en la pérdida de sangre en el postparto, una involución uterina más rápida o una reducción de enfermedades cardiovasculares [4,5]. Así pues, la leche materna ofrece una serie de beneficios a corto y largo plazo para la salud y desarrollo tanto de recién nacidos pretérmino como a término [6], así como para la madre.

1. 2. Composición de la leche materna

A diferencia de la leche en polvo, cuya composición suele variar dentro un estrecho rango, la composición de la leche materna es dinámica y varía a lo largo de la lactancia [7] e incluso dentro de una toma, a lo largo del día, entre madres, entre poblaciones [8], etc.

La leche materna pasa por tres etapas diferenciadas: el calostro, la leche de transición y la leche madura. El calostro es un líquido amarillento y cremoso que se produce incluso durante el embarazo y dura varios días (2-4)

tras el nacimiento del bebé. Este calostro es rico en proteínas (especialmente inmunoglobulinas (Ig)), vitaminas liposolubles y minerales. Inmediatamente tras el calostro, llega la leche de transición, más calórica y cuya duración es de aproximadamente dos semanas. Contiene altos niveles de grasa, lactosa y vitaminas hidrosolubles. Finalmente, de cuatro a seis semanas postparto, la leche materna se considera totalmente madura y su composición permanece relativamente constante. Dentro de esta leche madura, es posible diferenciar entre la primera leche (leche del principio de la toma) y la leche posterior (leche del final de la toma). Pese a que esta última contiene niveles más elevados de grasa que la primera [9], ambas son necesarias para asegurar un desarrollo y nutrición adecuados del bebé. La **Tabla 1.1** presenta una visión general de la composición de la leche materna.

Tabla 1.1. Composición de la leche materna.

Compuesto	**Concentración**	**Referencia**
Macronutrientes	**g/dL**	
Lípidos	3.2-4.8	[10–13]
Proteínas	0.9-1.7	[10–12,14]
Hidratos de carbono	6.2-7.8	[10–12]
Micronutrientes	**mg/dL**	
Vitaminas liposolubles	0.15-0.5	[15]
Vitaminas hidrosolubles	20-35	[15]
Minerales	130-175	[12,16]
Otros		
Agua	88%	[10]
Células	No indicado	[17]
Energía	(64-72) kcal/dL	[11,12]

1. 2. 1. Lípidos

En la leche materna, la grasa es la mayor fuente de energía del lactante, ya que contribuye entre un 40-55% a la ingesta total de energía [18]. Los lípidos de la leche se presentan en forma de glóbulos (1-10 µm) [10] emulsionados en la fase acuosa. Estos glóbulos se componen de un núcleo de triglicéridos (*triacylglycerol*, TAG), rodeados de una fina membrana de grasa (*milk fat globule membrane*, MFGM) (**Figura 1.1**). Esta membrana, compuesta principalmente por fosfolípidos (*phospholipid*, PL) y glicoproteínas, es de unos 10-20 nm de sección, actúa como emulsionante y protege los glóbulos de la coalescencia y degradación enzimática [19].

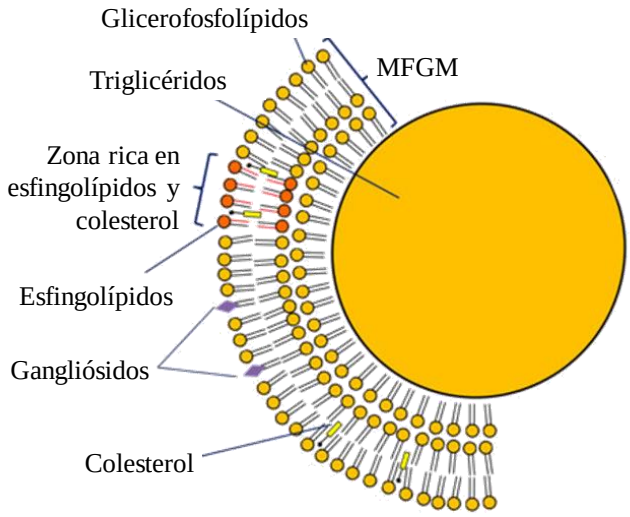

Figura 1.1. Representación esquemática de la estructura de un glóbulo de grasa de la leche.

La grasa es el macronutriente de la leche que experimenta una mayor variación. De hecho, existen muchos factores asociados a cambios en el contenido lipídico de la leche como son la etapa de lactancia, momento de la toma [9], el individuo [13] o la edad gestacional [20]. Así pues, el contenido

de grasa aumenta de aprox. 2 g/dL en el calostro a 4-4.5 g/dL a los 15 días postparto y permanece relativamente constante desde ese momento [10]. Asimismo, como ya se ha mencionado, el contenido de grasa de la leche materna aumenta a medida que se vacía el pecho de la madre, siendo de dos a tres veces superior en la leche posterior que en la leche inicial [9].

Con respecto a su composición, la grasa de la leche se compone principalmente por TAG, los cuales suponen más del 98% de la grasa total. En mucha menor medida, se encuentra la contribución de los PL y el colesterol con aprox. un 0.7% y un 0.5%, respectivamente. Recién extraída, la leche materna también contiene pequeños productos de lipolisis entre los que se incluyen ácidos grasos (*fatty acid*, FA) libres, mono- y digliceroles [18].

1. 2. 1. 1. Ácidos grasos

Los FA son componentes de los PL, TAG y ésteres de colesterol. Poseen funciones estructurales, energéticas y metabólicas. Su estructura consiste en un ácido carboxílico con una cadena alifática larga, la cual puede contener o no insaturaciones. Los FA pueden clasificarse de acuerdo con los diferentes criterios a continuación indicados:

i) Número de átomos de carbonos (*number of carbon atoms*, NC):
- FA de cadena corta: 2 a 6 carbonos.
- FA de cadena media: 8 a 14 carbonos.
- FA de cadena larga (*Long chain FA*, LC-FA): más de 16 carbonos.

ii) Presencia de dobles enlaces (*double bond*, DB) en la cadena hidrocarbonada:
- FA saturado (*saturated fatty acid*, SFA): no hay DB.
- FA insaturado: uno o más DB.

iii) Número de DB:
- FA monoinsaturado (*Monounsatured fatty acid*, MUFA): un DB.

- FA poliinsaturado (*Polyunsaturated fatty acid*, PUFA): más de un DB.

iv) Posición relativa del DB respecto al átomo de carbono terminal (omega):

- *ω*-3 FA/ *n*-3 FA.
- *ω*-6 FA/ *n*-6 FA.

v) Configuración geométrica:

- *cis*-FA.
- *trans-FA.*

vi) Fuente:

- Esencial: no sintetizado por el organismo, por lo que debe obtenerse de la dieta.
- No esencial: sintetizado por el organismo.

Por otra parte, para designar los diferentes FA, normalmente se emplea la siguiente formula: NC:ND junto con la posición relativa del carbono omega, donde ND es el número de DB (*number of double bounds*, ND). Por ejemplo, 18:2*n*-6 se corresponde con el ácido linoleico con 18 átomos de carbono, dos dobles enlaces, con el último doble enlace situado en la posición *ω*-6 (*n*-6). Las características de los lípidos en la leche se ven significativamente determinadas por su composición de FA. Concretamente, la leche materna contiene más de 200 FA. Sin embargo, muchos de ellos están presentes en concentraciones muy bajas, mientras que otros tienen una presencia más dominante [21]. En la **Tabla 1.2** se presenta la composición media de FA en la leche madura. Como se puede observar, la fracción predominante es la correspondiente a los SFA, seguido de una más o menos elevada proporción de MUFA, como p. ej. el ácido oleico (O; 18:1*n*-9).

Tabla 1.2. Principales FA presentes en la leche materna (% del total de FA). Adaptado de Patin *et al*. [22].

		Media ± SD[1] (n = 31)
SFA		
C10:0	Ácido cáprico (Ca)	1.7 ± 1.0
C12:0	Ácido láurico (La)	7 ± 3
C14:0	Ácido mirístico (M)	8 ± 3
C16:0	Ácido palmítico (P)	20 ± 2
C18:0	Ácido esteárico (S)	5.9 ± 1.2
Total		43 ± 6
MUFA		
C16:1	Ácido palmitoleico (Pa)	3.1 ± 0.9
C18:1*n*-9	Ácido oleico (O)	31 ± 4
Total		34 ± 4
***n*-6 PUFA**		
C18:2*n*-6	Ácido linoleico (LA or L)	21 ± 4
C18:3*n*-6	Ácido γ-linolénico (GLA)	0.26 ± 0.08
C20:4*n*-6	Ácido araquidónico (AA)	0.56 ± 0.14
Total		22 ± 4
***n*-3 PUFA**		
C18:3*n*-3	Ácido α-linolénico (ALA, LnA or Ln)	1.7 ± 0.6
C20:5*n*-3	Ácido eicosapentaenoico (EPA)	0.08 ± 0.07
C22:5*n*-3	Ácido docosapentaenoico (DPA)	0.24 ± 0.05
C22:6*n*-3	Ácido docosahexaenoico (DHA)	0.46 ± 0.11
Total		2.34 ± 0.18

[1]SD: desviación estándar (*standard deviation*).

Dentro del contenido de FA, los ácidos linoleico (LA; 18:2*n*-6) y α-linolénico (Ln, 18:3*n*-3), son dos PUFA esenciales, los cuales son precursores metabólicos de las series *n*-6 y *n*-3 de LC-PUFA, respectivamente, y deben

ser introducidos como tales en la dieta [23]. Una vez consumidos, estos FA se convierten en ácidos grasos de cadena más larga y más insaturada de la misma serie, como son p. ej. el ácido araquidónico (AA; C20:4*n*-6) y el ácido docosahexaenoico (DHA; C22:6*n*-3). Así pues, cabe destacar que, a diferencia de la leche de otros mamíferos, la leche materna contiene pequeñas cantidades de estos LC-PUFA como son el DHA, el AA, el ácido docosapentaenoico (DPA; C22:5*n*-3) y el ácido eicosapentaenoico (EPA; C20:5*n*-3), lo cual influye favorablemente en el desarrollo del bebé [24]. Concretamente, se ha encontrado que tanto el EPA como el DHA tienen una gran importancia para el desarrollo de la agudeza visual y sistema nervioso. Además, el DHA desempeña un papel importante en el crecimiento fetal y etapas neonatales [25].

En lo que respecta a la variabilidad en la composición de FA de la leche materna, diversas investigaciones muestran cómo la dieta de la madre durante la lactancia es uno de los factores que puede tener una influencia sobre la composición de FA de la leche [22]. Sin embargo, estos estudios no resultan concluyentes, ya que algunos de ellos se han llevado a cabo con dietas *ad libitum* y no del todo controladas, por lo que su representatividad es limitada [26].

1. 2. 1. 2. Triglicéridos

Los TAG constituyen más del 98% del total de lípidos en la leche. Su composición suele expresarse en términos de los FA presentes, aunque la disposición de los mismos es también importante [26]. De hecho, los TAG son el sustrato de las enzimas lipolíticas, por lo que su estructura es crucial para la absorción de los lípidos. La localización de los FA dentro de la molécula de TAG se designa por la numeración estereoespecífica (*sn*) (véase **Figura 1.2**).

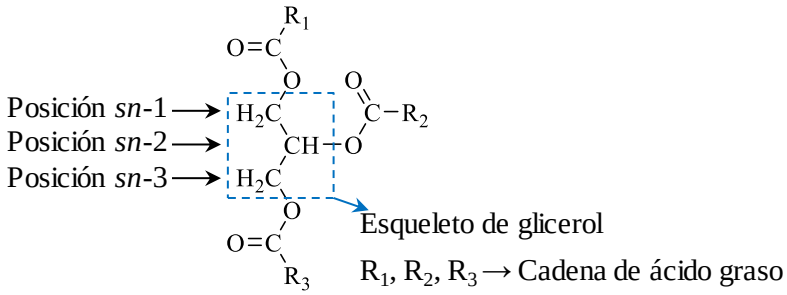

Figura 1.2. Estructura de una molécula de TAG.

La posición que ocupan los FA a lo largo del esqueleto de glicerol se preserva en gran medida. Por ejemplo, los FA de mayor abundancia en la leche materna, como son el oleico, el palmítico y el linoleico, se suelen encontrar en las posiciones *sn*-1, *sn*-2 y *sn*-3, respectivamente [27]. Esta estructura única de los TAG de la leche materna, en la cual aprox. un 70% de las posiciones *sn*-2 se encuentran esterificadas con ácido palmítico (16:0), se cree que es responsable de la eficiente absorción de los FA en el intestino [26]. Los principales TAG de la leche materna se encuentran recogidos en la **Tabla 1.3**.

Tabla 1.3. Principales TAG presentes en la leche materna [28–30].

TAG[1]	**NC:ND**	**% m/m**
MOLa	44:1	5-9
PaLS	46:1	3.4-6.6
POLa	46:1	8-14
MPO	48:1	5.6-7.0
LaOO	48:2	2-9
PPO/MOS	50:1	3-12
MOO/PPL	50:2	6-10
SOP	52:1	2.8-6.7
POO	52:2	10-33
POL	52:3	12-22

TAG[1]	NC:ND	% m/m
PLL	52:4	6-10
OOO	54:3	1-8
LOO	54:4	3.2-6.8

[1]La designación del TAG no indica la posición de los FA dentro del mismo. Para las abreviaturas, véase la **Tabla 1.2**.

Cabe mencionar que, pese a la gran variabilidad de composición de TAG en la leche materna, Morera *et al.* [30] mostraron que algunos de estos analitos pueden utilizarse como marcadores de la leche materna, ya que su concentración permanece relativamente constante bajo un amplio rango de condiciones de muestreo.

1. 2. 1. 3. Fosfolípidos

Los PL en la leche contribuyen entre un 0.2 y un 1.0% del total de lípidos [26]. Estos compuestos son fundamentales en la leche para la emulsificación de la grasa en agua, ya que, juntamente con diversas proteínas, son los principales constituyentes de la MFGM, la cual rodea las gotas de grasa segregadas por las células de las glándulas mamarias [31]. Así pues, los PL son considerados nutrientes con beneficios intrínsecos para la salud y juegan al menos tres papeles fundamentales: (i) proveer soporte estructural para la integridad de las membranas y ayudar así a llevar a cabo sus funciones; (ii) participar en la defensa de numerosas enfermedades metabólicas y neurológicas; y (iii) regular procesos biológicos básicos como la señalización de compuestos [32].

Las propiedades anfifílicas de los PL surgen de la presencia en su estructura de una cola hidrófoba y de una cabeza hidrófila. Dependiendo de su estructura y tipos de enlace, los PL suelen clasificarse en dos grandes grupos: glicerofosfolípidos y esfingolípidos. El primer grupo consiste en una cabeza polar de fosforilo esterificado en la posición *sn*-3 y dos FA

esterificados en las posiciones *sn*-1 y *sn*-2 del esqueleto de glicerol. Los glicerofosfolípidos incluyen principalmente a la fosfatidilcolina (*phosphatidylcholine*, PC), fosfatidiletanolamina (*phosphatidylethanolamine*, PE), fosfatidilinositol (*phosphatidylinositol*, PI) y fosfatidilserina (*phosphatidylserine*, PS) [33]. Por otra parte, los esfingolípidos derivan del aminoalcohol insaturado de 18 carbonos esfingosina, formando una ceramida cuando su grupo amino se une, por lo general, con un SFA. De entre ellos, la esfingomielina (*sphingomyelin*, SM) es la especie dominante y está formada por una cabeza de fosforilcolina unida a la ceramida [31] (**Figura 1.3**).

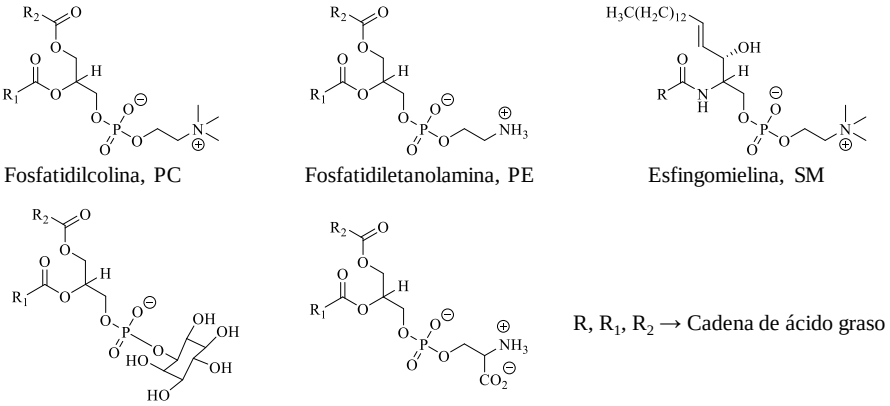

Figura 1.3. Estructura de los PL mayoritarios de la leche materna.

La **Tabla 1.4** muestra las principales clases de PL encontrados en la leche materna.

Tabla 1.4. PL mayoritarios de la leche materna.

PL (%)					
PC	**PE**	**PI**	**PS**	**SM**	**Referencia**
25 ± 5	29 ± 8	4.6 ± 1.3	5.9 ± 1.7	36 ± 7	[34]
25 ± 4	12 ± 3	7.8 ± 0.8	14 ± 2	40.2 ± 1.1	[35]
31 ± 5	12.8 ± 1.2	5.9 ± 0.5	10.4 ± 1.3	41 ± 3	[36]
30.3	26.0	6.6	9.3	27.7	[37]
23 ± 4	36 ± 4	3.5 ± 1.5	7 ± 4	31 ± 7	[25]

1. 2. 1. 4. Esteroles

La leche materna tiene un alto contenido en colesterol (10–20 mg/dL o 250–500 mg/100 g grasa) [38]. Éste es el esterol mayoritario en la leche materna y supone un 90.1% del contenido total de esteroles, seguido de desmosterol (8.6%), mientras que la cantidad de fitoesteroles en la leche es despreciable. Se ha observado que la dieta de la madre parece no tener un efecto significativo sobre el contenido de colesterol en la leche [18], si bien los beneficios funcionales de los esteroles sobre la nutrición del bebé no han sido del todo clarificados [39].

1. 2. 2. Proteínas

La fracción proteica de la leche desempeña también un papel fundamental en el alcance de los numerosos beneficios del amamantamiento. Su contenido en la leche materna disminuye rápidamente durante el primer mes de lactancia y dicha disminución se ve mucho más atenuada en meses posteriores [12,40]. En términos generales, las proteínas de la leche pueden dividirse en tres grupos: caseínas (*casein,* CN), proteínas del suero o séricas y las proteínas asociadas a la MFGM. Como ya se ha descrito, la MFGM consiste en una organización compleja de bicapa lipídica rica en proteínas

integradas y periféricas, la cual rodea un núcleo de TAG [7]. En la leche materna, las proteínas del suero son las más abundantes, mientras que las CN suponen una menor fracción. La relación o proporción suero/CN que se encuentra habitualmente en la leche materna es de 60:40, aunque ésta varía de aprox. 80:20 al inicio de la lactancia hasta 50:50 al final de la misma [41]. Por otra parte, las proteínas de MFGM, también conocidas como mucinas, representan del 1 al 4% del total de proteínas [42]. Gracias al desarrollo de la proteómica [7,42–44], más de 300 proteínas han sido identificadas en la leche materna, muchas de las cuales son activas y desempeñan diferentes funciones en la protección del lactante.

Con respecto a la función de las proteínas en la leche, cabe mencionar que muchas de ellas serán totalmente fragmentadas en el intestino y usadas como fuente de aminoácidos (aa) para el bebé. Sin embargo, algunas proteínas sufren una proteólisis parcial, quedando fragmentos biológicamente activos (p. ej. los fosfopéptidos de CN) y otras experimentan una proteólisis reducida o nula (p. ej. la lactoferrina (Lf) o la Ig A secretora (*secretory immunoglobulin A*, sIgA)). De hecho, estas últimas pueden resistir la digestión, encontrándose totalmente intactas en las heces [45].

Además de las CN, las proteínas séricas y las proteínas de la MFGM, en la leche materna se halla la fracción de nitrógeno no proteico (*non-protein nitrogen*, NPN), donde se encuentran compuestos como la urea, la creatinina o el amoniaco [46]. Por otra parte, a diferencia de en la leche de vaca, se ha descrito muy poco sobre la presencia de lo que se conoce como la fracción proteosa-peptona en la leche materna [47]. Esta fracción consiste en una mezcla compleja de péptidos, muchos de los cuales son producidos por la acción de plasmina endógena, pero otros son endógenos de la leche.

1. 2. 2. 1. Proteínas del suero

Entre las proteínas mayoritarias del suero se encuentran la α-lactoalbúmina (α-La), la Lf, la sIgA, la albúmina sérica (*human serum*

albumin, HSA) y la lisozima (*lysozyme*, Lyz) [48]. Por otra parte, existe una multitud de proteínas minoritarias presentes en la leche desempeñando funciones tales como comunicación celular, transducción de señal o respuesta inmunitaria, entre otras [7].

La α-La es la proteína más abundante de la leche materna. Constituye de un 25% a un 35% del total de proteínas. Se trata de una proteína digerible con una composición equilibrada de aa y que habitualmente presenta una alta proporción de aa esenciales. Dentro de la glándula mamaria, la α-La actúa como reguladora de la enzima galactosil transferasa, la cual es responsable de la síntesis de lactosa a partir de galactosa y glucosa [49].

La Lf, la segunda proteína más abundante en la leche (20-25%), es una proteína de unión específica al hierro que está formada por una única cadena polipeptídica. Se trata de una proteína con múltiples funciones (bacteriostática, bactericida y actividad antiviral) y es resistente a enzimas proteolíticos [50].

La HSA es también una proteína de suero abundante en la leche materna con propiedades similares a las que tiene en sangre. Sirve como fuente de aa para el lactante y se cree que esta proteína no es sintetizada por la glándula mamaria, sino que se transfiere de la circulación materna [50].

La sIgA representa alrededor del 90% del total de Ig en la leche materna [45]. Ésta consiste en un dímero de IgA unido a un componente secretor y una cadena de unión (*joining chain*, cadena J) [51]. Debido a su resistencia al ataque proteolítico, la inmunidad materna frente a diversos patógenos puede ser transferida a través de la leche. Otras Ig como la IgA, la IgM y la IgG están también presentes en la leche materna, aunque en menor concentración. A diferencia de la sIgA, éstas son fácilmente digeridas por lo que no subsistirán en el intestino delgado [45].

En la **Tabla 1.5** se recopilan algunas características sobre las proteínas de suero presentes en la leche materna.

1. 2. 2. 2. Caseínas

En la leche materna, están presentes tres tipos de subunidades de CN: β-CN, κ-CN y α_{S1}-CN. La primera, es la CN predominante en la leche materna y su contenido decrece a lo largo de la lactancia [52]. La β-CN se presenta en seis formas, las cuales varían en función del número de grupos fosforilo unidos covalentemente, desde cero (0-P) hasta cinco (5-P) [53]. Además de su función nutricional para el lactante, se cree que los fosfopéptidos de la β-CN (formados durante la digestión) facilitan la absorción del calcio y, por consiguiente, la mayor biodisponibilidad de este nutriente en la leche materna [54]. Por otra parte, la κ-CN es una proteína altamente glicosilada (aprox. 40%), la cual contiene residuos cargados de ácido siálico. Esta proteína muestra la capacidad *in vitro* de inhibir la unión de *Helicobacter pylori* a la mucosa gástrica humana [55]. En lo que respecta a la α_{S1}-CN, durante muchos años se creía que ésta estaba ausente o presente en cantidades ínfimas en la leche materna. Sin embargo, se ha comprobado que esta CN se encuentra en diferentes variantes fosforiladas (0 – P, 1 – P y 2 -P) [56].

En la leche, las CN, juntamente con fosfato cálcico, forman agregados conocidos como micelas. Estas micelas de CN, cuyo diámetro va de 50 a 500 nm, son las principales responsables del color blanco de la leche [57]. La estructura y estabilidad de las micelas de CN han sido extensamente objeto de estudio, especialmente en la leche bovina [57,58]. En el caso de la leche materna, algunos estudios han propuesto que la κ-CN se situaría en la superficie de las micelas, siendo responsable de su estabilidad frente a la precipitación de iones calcio. Así pues, la mayor naturaleza hidrofílica de la κ-CN en la leche materna, debido a su mayor grado de glicosilación, sería uno de los factores responsables del menor tamaño de las micelas de CN de la leche materna respecto a la leche bovina [53].

En la **Tabla 1.5** se recoge más información sobre las CN presentes en la leche materna.

Tabla 1.5. Peso molecular (*molecular weight*, M_w) y punto isoeléctrico (*isoelectric point*, pI) de las principales proteínas presentes en la leche materna.

Fracción	Proteína	M_w (Da)	pI
Suero	α-La	16225	4.71[a]; 4.83[b]
	HSA	69367	5.67[a]; 5.92[b]
	Lyz	16537	8.56[a]; 9.38[b]
	Lf	78357	7.23[a]; 8.51[b]
	IgA	~162000	-
	IgE	~190000	-
	IgM	~950000	-
	IgG	~153000	-
Caseínas	ß-CN	25382	5.34[a]; 5.52[b]
	α-s_1-CN	21671	5.22[a]; 5.32[b]
	κ-CN	20305	8.66[a]; 8.97[b]

[a]pI calculado a través de http://isoelectric.org/ [59].
[b]pI calculado por *Expert Protein Analysis System* disponible en https://web.expasy.org/compute_pi/ [60].

1. 2. 2. 3. Proteínas de MFGM

Seguido de la grasa, la MFGM es el componente más abundante de la leche materna [61], donde las proteínas representan un 1% de la masa del glóbulo [62]. En la leche materna, se han encontrado siete proteínas principales de la MFGM [42], las cuales están, en su mayoría, implicadas en funciones tales como comunicación celular, transducción de señal, inmunidad, metabolismo y producción de energía, entre otras.

1. 2. 3. Hidratos de carbono

Los hidratos de carbono o carbohidratos se clasifican normalmente en monosacáridos, disacáridos y oligosacáridos/polisacáridos (los tres últimos son monosacáridos unidos por enlaces glicosídicos). La lactosa es el principal carbohidrato en la leche materna (6.4-7.6 g/dL) [11] y es una gran fuente de energía para el bebé. Su contenido es menor en la leche pretérmino y el calostro, pero se mantiene más o menos constante a lo largo de la lactancia [63]. A dicho azúcar se le ha atribuido también un papel en la absorción y/o retención de calcio, aunque la manera exacta en qué lo hace no ha sido claramente establecida [64]. Además de la lactosa, la leche materna contiene aprox. un 1% de oligosacáridos neutros y alrededor de un 0.1% de oligosacáridos ácidos, los cuales son importantes para el efecto prebiótico (esencialmente bifidogénico) así como propiedades antiinfecciosas y alérgico-preventivas de la leche materna [65].

1. 2. 4. Micronutrientes: vitaminas y minerales

La leche materna también proporciona al bebé micronutrientes, incluyendo vitaminas lipo- e hidrosolubles, minerales, y minerales traza. Algunos de estos micronutrientes como la tiamina, la riboflavina, la vitamina B-6, la vitamina B-12, la colina, el retinol, la vitamina-A, la vitamina-D, el selenio y el yodo, son dependientes de la dieta de la madre; mientras que otros como el folato, el calcio, el hierro, el cobre y el zinc se ven relativamente inalterados por la ingesta o estado de la madre [66]. Independientemente de la dieta de la madre, el contenido de vitamina K es extremadamente bajo en la leche materna, y es por ello que, la Academia Americana de Pediatría recomienda una inyección de esta vitamina en los recién nacidos para evitar hemorragias [67]. Por su parte, la vitamina D también se encuentra en baja proporción en la leche materna, especialmente en lugares donde la exposición

solar de la madre es escasa. Por este motivo, es habitual aportar de manera suplementaria esta vitamina al lactante [68].

En cualquier caso, cabe destacar que, la concentración de minerales en la leche materna es menor que en cualquier sustitutivo de ésta y está mejor adaptada a los requerimientos nutricionales y capacidad metabólica de los lactantes [10].

1. 2. 5. Células

La leche materna contiene una mezcla heterogénea de células que incluye leucocitos, células epiteliales, células madre y bacterias. Indudablemente, las células no son un componente insignificante de la leche materna, pero sus funciones continúan todavía sin establecerse de un modo claro [17].

1. 3. Referencias

[1] World Health Organization, UNICEF, Global strategy for infant and young child, World Health Organization, Geneva, Switzerland, 2003.

[2] World Health Organization, Global strategy for infant and young child feeding. The optimal duration of exclusive breastfeeding, Fifthy-Fourth World Heal. Assem. (2001) 1–5.

[3] S. Ip, M. Chung, G. Raman, P. Chew, N. Magula, D. DeVine, T. Trikalinos, J. Lau, Breastfeeding and maternal and infant health outcomes in developed countries, Agency for Healthcare Research and Quality, Rockville (MD), 2007.

[4] A.I. Eidelman, R.J. Schanler, American Academy of Pediatrics Section on Breastfeeding. Breastfeeding and the use of human milk, Pediatrics 129 (2012) e827–e841. doi:10.1542/peds.2011-3552.

[5] E.B. Schwarz, R.M. Ray, A.M. Stuebe, M.A. Allison, R.B. Ness, M.S. Freiberg, J.A. Cauley, Duration of lactation and risk factors for maternal cardiovascular disease, Obstet. Gynecol. 113 (2010) 974–982. doi:10.1097/01.AOG.0000346884.67796.ca.Duration.

[6] F. Anatolitou, Human milk benefits and breastfeeding, J. Pediatr. Neonatal Individ. Med. 1 (2012) 11–18. doi:10.7363/010113.

[7] Y. Liao, R. Alvarado, B. Phinney, B. Lönnerdal, Proteomic characterization of human milk whey proteins during a twelve-month lactation period, J. Proteome Res. 10 (2011) 1746–1754. doi:10.1021/pr101028k.

[8] L.R. Mitoulas, J.C. Kent, D.B. Cox, R.A. Owens, J.L. Sherriff, P.E. Hartmann, Variation in fat, lactose and protein in human milk over 24h and throughout the first year of lactation, Br. J. Nutr. 88 (2002) 29–37. doi:10.1079/BJNBJN2002579.

[9] T. Saarela, J. Kokkonen, M. Koivisto, Macronutrient and energy contents of human milk fractions during the first six months of lactation, Acta Paediatr. 94 (2005) 1176–1181. doi:10.1080/08035250510036499.

[10] C. Shellhorn, V. Valdés, La leche humana, composicion, beneficios y comparación con la leche de vaca, Man. Lact. Para Prof. La Salud. (1995).

[11] O. Ballard, A.L. Morrow, Human milk composition: Nutrients and bioactive factors, Pediatr. Clin. North Am. 60 (2013) 49–74. doi:10.1016/j.pcl.2012.10.002.

[12] J. Bauer, J. Gerss, Longitudinal analysis of macronutrients and minerals in human milk produced by mothers of preterm infants, Clin. Nutr. 30 (2011) 215–220. doi:10.1016/j.clnu.2010.08.003.

[13] C. Agostoni, F. Marangoni, A.M. Lammardo, M. Giovannini, E. Riva, C. Galli, Breastfeeding duration, milk fat composition and developmental indices at 1 year of life among breastfed infants, Prostaglandins. Leukot. Essent. Fatty Acids. 64 (2001) 105–109. doi:10.1054/plef.2001.0248.

[14] J. Csapo, S. Salamon, Composition of the mother's milk I. Protein contents, amino acid composition, biological value. A review, Acta Univ Sapientiae Aliment. 2 (2009) 174–195.

[15] T. Sakurai, M. Furukawa, M. Asoh, T. Kanno, T. Kojima, A. Yonekubo, Fat-soluble and water-soluble vitamin contents of breast milk from Japanese women, J. Nutr. Sci. Vitaminol. 51 (2005) 239–247. doi:10.3177/jnsv.51.239.

[16] G.B. Fransson, B. Lönnerdal, Distribution of trace elements and minerals in human and cow's milk, Pediatr. Res. 17 (1983) 912–915. doi:10.1203/00006450-198311000-00015.

[17] M. Witkowska-Zimny, E. Kaminska-El-Hassan, Cells of human breast milk, Cell. Mol. Biol. Lett. 22 (2017) 1–11. doi:10.1186/s11658-017-0042-4.

[18] B. Koletzko, M. Rodriguez-Palmero, H. Demmelmair, N. Fidler, R. Jensen, T. Sauerwald, Physiological aspects of human milk lipids, Early Hum. Dev. 65 Suppl (2001) S3–S18. doi:10.1016/S0378-3782(01)00204-3.

[19] K. Dewettinck, R. Rombaut, N. Thienpont, T.T. Le, K. Messens, J. Van Camp, Nutritional and technological aspects of milk fat globule membrane material, Int. Dairy J. 18 (2008) 436–457. doi:10.1016/j.idairyj.2007.10.014.

[20] J. Bitman, L. Wood, M. Hamosh, P. Hamosh, N.R. Mehta, Comparison of the lipid composition of breast milk from mothers of term and preterm infants, Am. J. Clin. Nutr. 38 (1983) 300–312. doi:10.1093/ajcn/38.2.300.

[21] N.J. Andreas, B. Kampmann, K. Mehring Le-Doare, Human breast milk: A review on its composition and bioactivity, Early Hum. Dev. 91 (2015) 629–635. doi:10.1016/j.earlhumdev.2015.08.013.

[22] R. V Patin, M.R. Vítolo, M.A. Valverde, P.O. Carvalho, G.M. Pastore, F.A. Lopez, The influence of sardine consumption on the omega-3 fatty acid content of mature human milk, J. Pediatr. 82 (2006) 63–69.

[23] M. Giovannini, E. Riva, C. Agostoni, The role of dietary polyunsaturated fatty acids during the first 2 years of life, Early Hum. Dev. 53 (1998) S99–S107. doi:https://doi.org/10.1016/S0378-3782(98)00068-1.

[24] E.E. Birch, S. Garfield, Y. Castañeda, D. Hughbanks-Wheaton, R. Uauy, D. Hoffman, Visual acuity and cognitive outcomes at 4 years of age in a double-blind, randomized trial of long-chain polyunsaturated

fatty acid-supplemented infant formula, Early Hum. Dev. 83 (2007) 279–284. doi:10.1016/j.earlhumdev.2006.11.003.

[25] L. Wang, Y. Shimizu, S. Kaneko, S. Hanaka, T. Abe, H. Shimasaki, H. Hisaki, H. Nakajima, Comparison of the fatty acid composition of total lipids and phospholipids in breast milk from Japanese women, Pediatr. Int. 42 (2000) 14–20. doi:10.1046/j.1442-200X.2000.01169.x.

[26] R.G. Jensen, The lipids in human milk, Prog. Lipid Res. 35 (1996) 53–92. doi:10.1016/0163-7827(95)00010-0.

[27] J.C. Martin, P. Bougnoux, J.M. Antoine, M. Lanson, C. Couet, Triacylglycerol structure of human colostrum and mature milk, Lipids 28 (1993) 637–643. doi:10.1007/BF02536059.

[28] X.-Q. Zou, J.-H. Huang, Q.-Z. Jin, Z. Guo, Y.-F. Liu, L.-Z. Cheong, X.-B. Xu, X.-G. Wang, Model for human milk fat substitute evaluation based on triacylglycerol composition profile, J. Agric. Food Chem. 61 (2013) 167–175. doi:10.1021/jf304094p.

[29] I. Haddad, M. Mozzon, R. Strabbioli, N.G. Frega, A comparative study of the composition of triacylglycerol molecular species in equine and human milks, Dairy Sci. Technol. 92 (2012) 37–56. doi:10.1007/s13594-011-0042-5.

[30] S. Morera, A.I. Castellote, O. Jauregui, I. Casals, M.C. López-Sabater, Triacylglycerol markers of mature human milk, Eur. J. Clin. Nutr. 57 (2003) 1621–1626. doi:10.1038/sj.ejcn.1601733.

[31] G. Contarini, M. Povolo, Phospholipids in milk fat: composition, biological and technological significance, and analytical strategies, Int. J. Mol. Sci. 14 (2013) 2808–2831. doi:10.3390/ijms14022808.

[32] Z. Guo, A.F. Vikbjerg, X. Xu, Enzymatic modification of phospholipids for functional applications and human nutrition, Biotechnol. Adv. 23 (2005) 203–259.

doi:10.1016/j.biotechadv.2005.02.001.

[33] C.H. Huang, Mixed-chain phospholipids: structures and chain-melting behavior, Lipids 36 (2001) 1077–1097. doi:10.1007/s11745-001-0818-1.

[34] F. Giuffrida, C. Cruz-Hernandez, B. Flück, I. Tavazzi, S.K. Thakkar, F. Destaillats, M. Braun, Quantification of phospholipids classes in human milk, Lipids 48 (2013) 1051–1058. doi:10.1007/s11745-013-3825-z.

[35] X. Zou, J. Huang, Q. Jin, Z. Guo, Y. Liu, L. Cheong, X. Xu, X. Wang, Lipid composition analysis of milk fats from different mammalian species: potential for use as human milk fat substitutes, J. Agric. Food Chem. 61 (2013) 7070–7080. doi:10.1021/jf401452y.

[36] A. Sala-Vila, A.I. Castellote, M. Rodriguez-Palmero, C. Campoy, M.C. López-Sabater, Lipid composition in human breast milk from Granada (Spain): changes during lactation, Nutrition 21 (2005) 467–473. doi:10.1016/j.nut.2004.08.020.

[37] A. Sala Vila, A.I. Castellote-Bargalló, M. Rodríguez-Palmero-Seuma, M.C. López-Sabater, High-performance liquid chromatography with evaporative light-scattering detection for the determination of phospholipid classes in human milk, infant formulas and phospholipid sources of long-chain polyunsaturated fatty acids, J. Chromatogr. A 1008 (2003) 73–80. doi:10.1016/S0021-9673(03)00989-0.

[38] R.G. Jensen, Lipids in human milk, Lipids 34 (1999) 1243–1271. doi:10.1007/s11745-999-0477-2.

[39] L. Claumarchirant, E. Matencio, L.M. Sanchez-Siles, A. Alegría, M.J. Lagarda, Sterol composition in infant formulas and estimated intake, J. Agric. Food Chem. 63 (2015) 7245–7251. doi:10.1021/acs.jafc.5b02647.

[40] C. Kunz, B. Lönnerdal, Re-evaluation of the whey protein/casein ratio of human milk, Acta Pædiatrica 81 (1992) 107–112. doi:10.1111/j.1651-2227.1992.tb12184.x.

[41] B. Lönnerdal, Nutritional and physiologic significance of human milk proteins, Am. J. Clin. Nutr. 77 (2003) 1537S–1543S. doi:10.131/nr.2003.sept.295.

[42] Y. Liao, R. Alvarado, B. Phinney, B. Lönnerdal, Proteomic characterization of human milk fat globule membrane proteins during a 12 month lactation period, J. Proteome Res. 10 (2011) 3530–3541. doi:10.1021/pr200149t.

[43] X. Gao, R.J. McMahon, J.G. Woo, B.S. Davidson, A.L. Morrow, Q. Zhang, Temporal changes in milk proteomes reveal developing milk functions, J. Proteome Res. 11 (2012) 3897–3907. doi:10.1021/pr3004002.

[44] K.L. Beck, D. Weber, B.S. Phinney, J.T. Smilowitz, K. Hinde, B. Lönnerdal, I. Korf, D.G. Lemay, Comparative proteomics of human and macaque milk reveals species-specific nutrition during postnatal development, J. Proteome Res. 14 (2015) 2143–2157. doi:10.1021/pr501243m.

[45] B. Lönnerdal, Bioactive proteins in breast milk, J. Paediatr. Child Health. 49 (2013) 1–7. doi:10.1111/jpc.12104.

[46] P.F. Fox, T. Uniacke-Lowe, P.L.H. McSweeney, J.A. O'Mahony, Chapter 4. Milk Proteins, en: Encycl. Dairy Sci., 2ª ed., Springer, Switzerland, 2015: pp. 145–239. doi:10.1007/978-3-319-14892-2.

[47] A. Bezkorovainy, J.H. Nichols, D.A. Sly, Proteose-peptone fractions of human and bovine milk, Int. J. Biochem. 7 (1976) 639–645. doi:10.1016/0020-711x(76)90105-1.

[48] L.R. Woodhouse, B. Lönnerdal, Quantitation of the major whey

proteins in human milk, and development of a technique to isolate minor whey proteins, Nutr. Res. 8 (1988) 853–864. doi:10.1016/S0271-5317(88)80125-8.

[49] B. Lönnerdal, E.L. Lien, Nutritional and physiologic significance of α-lactalbumin in infants, Nutr. Rev. 61 (2003) 295–305. doi:10.131/nr.2003.sept.295.

[50] B. Lönnerdal, P. Erdmann, S.K. Thakkar, J. Sauser, F. Destaillats, Longitudinal evolution of true protein, amino acids and bioactive proteins in breast milk: a developmental perspective, J. Nutr. Biochem. 41 (2017) 1–11. doi:10.1016/j.jnutbio.2016.06.001.

[51] A.S. Goldman, The immune system of human milk: antimicrobial, antiinflammatory and immunomodulating properties, Pediatr. Infect. Dis. J. 12 (1993) 664–672. doi:10.1097/00006454-199308000-00008.

[52] C. Kunz, B. Lönnerdal, Casein and casein subunits in preterm milk colostrum and mature human milk, J. Pediatr. Gastroenterol. Nutr. 10 (1990) 454–461. doi:10.1097/00005176-199005000-00007.

[53] B.C. Dev, S.M. Sood, S. DeWind, C.W. Stattery, k-casein and ß-casein in human milk micelles: Structural studies, Arch. Biochem. Biophys. 314 (1994) 329–336. doi:10.1006/abbi.1994.1450.

[54] B. Lönnerdal, Bioactive proteins in human milk: mechanisms of action, J. Pediatr. 156 (2010) S26–S30. doi:10.1016/j.jpeds.2009.11.017.

[55] M. Strömqvist, P. Falk, S. Bergström, L. Hansson, B. Lönnerdal, S. Normark, O. Hernell, Human milk k-casein and inhibition of Helicobacter pylori adhesion to human gastric mucosa, J. Pediatr. Gastroenterol. Nutr. 21 (1995) 288–296.

[56] E.S. Sørensen, L. Møller, M. Vinther, T.E. Petersen, L.K. Rasmussen, The phosphorylation pattern of human αs1-casein is markedly different

from the ruminant species, Eur. J. Biochem. 270 (2003) 3651–3655. doi:10.1046/j.1432-1033.2003.03755.x.

[57] P.F. Fox, A. Brodkorb, The casein micelle: Historical aspects, current concepts and significance, Int. Dairy J. 18 (2008) 677–684. doi:10.1016/j.idairyj.2008.03.002.

[58] D.G. Dalgleish, M. Corredig, The Structure of the casein micelle of milk and its changes during processing, Annu. Rev. Food Sci. Technol. 3 (2012) 449–467. doi:10.1146/annurev-food-022811-101214.

[59] L.P. Kozlowski, IPC - Isoelectric Point Calculator, Biol. Direct. 11 (2016) 55. doi:10.1186/s13062-016-0159-9.

[60] ExPASy, Compute pI/Mw, (2005). Disponible en : https://web.expasy.org/compute_pi/. (Fecha de acceso: 02/06/2018).

[61] J. Charlwood, S. Hanrahan, R. Tyldesley, J. Langridge, M. Dwek, P. Camilleri, Use of proteomic methodology for the characterization of human milk fat globular membrane proteins, Anal. Biochem. 301 (2002) 314–324. doi:10.1006/abio.2001.5498.

[62] M. Cavaletto, M.G. Giuffrida, A. Conti, The proteomic approach to analysis of human milk fat globule membrane, Clin. Chim. Acta. 347 (2004) 41–48. doi:10.1016/j.cccn.2004.04.026.

[63] L.A. Nommsen, C.A. Lovelady, M.J. Heinig, B. Lönnerdal, K.G. Dewey, Determinants of energy, protein, lipid, and lactose concentrations in human milk during the first 12 mo of lactation: The DARLING Study, Am. J. Clin. Nutr. 53 (1991) 457–465. doi:10.1093/ajcn/53.2.457.

[64] H.S. Kwak, W.J. Lee, M.R. Lee, Revisiting lactose as an enhancer of calcium absorption, Int. Dairy J. 22 (2012) 147–151. doi:10.1016/j.idairyj.2011.09.002.

[65] G. Boehm, B. Stahl, J. Jelinek, J. Knol, V. Miniello, G.E. Moro,

Prebiotic carbohydrates in human milk and formulas, Acta Paediatr. 94 (2005) 18–21. doi:10.1080/08035320510043493.

[66] L.H. Allen, B vitamins in breast milk: Relative importance of maternal status and intake, and effects on infant status and function, Adv. Nutr. 3 (2012) 362–369. doi:10.3945/an.111.001172.362.

[67] P.A. Lane, W.E. Hathaway, Vitamin K in infancy, J. Pediatr. 106 (1985) 351–359. doi:https://doi.org/10.1016/S0022-3476(85)80656-9.

[68] L. Furman, Maternal vitamin D supplementation for breastfeeding infants: Will it work?, Pediatrics 136 (2015) 763–764. doi:10.1542/peds.2015-2312.

CAPÍTULO 2

Metodologías analíticas para la caracterización de las fracciones lipídica y proteica de la leche

2. 1. Determinación de lípidos

2. 1. 1. Extracción de la grasa

En 1957, Folch *et al*. [1] desarrollaron un método para el aislamiento y purificación de los lípidos totales de tejidos animales. Este método consistía en la extracción de los lípidos por homogeneización de la muestra con una mezcla de cloroformo:metanol ($CHCl_3$:MeOH) 2:1 (v/v), seguido de sucesivos lavados con agua y disoluciones salinas. Al mismo tiempo, Bligh y Dyer [2] llevaron a cabo el aislamiento de los lípidos de los músculos de peces empleando estos mismos disolventes. Dos décadas después, Hara y Radin [3] propusieron llevar a cabo la extracción de lípidos de tejidos utilizando una mezcla menos tóxica, concretamente hexano:isopropanol, mientras que Chen *et al*. [4] reemplazaron el cloroformo por diclorometano, por ser este último menos tóxico. Concretamente para muestras de leche, en el método oficial 989.05 de *AOAC International* [5], fundamentado en el estudio de Barbano *et al*. [6], la grasa de una muestra de leche es extraída empleando una mezcla de éteres. Por otra parte, se han introducido modificaciones en el método de Folch para mejorar la extracción de los lípidos polares presentes en la leche [7].

De todos los métodos anteriormente mencionados, el método de Folch y sus modificaciones han sido sin duda preponderantes en la extracción de grasa de muestras de leche [8,9]. La combinación de un disolvente apolar junto con otro polar, preferiblemente un alcohol, resulta ventajoso para la extracción de la totalidad de los lípidos (algunos de naturaleza más polar). De hecho, el disolvente polar resulta indispensable para la liberación completa de los lípidos que se encuentran formando parte de la MFGM [10].

Sin embargo, cabe destacar que todos estos métodos de extracción requieren un elevado tiempo de trabajo por lo que su automatización resulta poco factible.

2. 1. 2. Determinación de ácidos grasos

Por norma general, los FA de la leche se separan y cuantifican por cromatografía de gases (*gas chromatography*, GC) acoplada a un detector de ionización de llama, previa derivatización en sus correspondientes ésteres metílicos (*FA methyl ester*, FAME) [11,12]. Solamente algunos autores han llevado a cabo el análisis de FAME por GC seguida de espectrometría de masas (*mass spectrometry*, MS) [13,14]. El procedimiento de derivatización de FA más habitual implica una catálisis ácida o básica. La esterificación por catálisis ácida se lleva a cabo con ácido clorhídrico, ácido sulfúrico o trifluoruro de boro en MeOH; mientras que en la transesterificación de acilgliceroles por catálisis básica, se emplean hidróxido sódico o potásico en MeOH y metóxido de sodio en MeOH [15]. No obstante, el proceso de esterificación presenta algunos problemas o inconvenientes como p. ej. la alteración en la composición de FA durante la transesterificación o la pérdida por volatilidad de FAME de cadena corta [16]. Con respecto a la cuantificación de FAME, ésta se suele hacer mediante empleo de un patrón interno (p. ej. C13:0 [12], C15:0 [17], C19:0 [12], C21:0 [11], C23:0 [18]).

Pese a que estos métodos de esterificación son conocidos desde hace años y están ampliamente extendidos, se han desarrollado estrategias alternativas como la extracción y transmetilación de los FA asistidos por microondas [19].

2. 1. 3. Determinación de triglicéridos

Dado que los TAG suponen aprox. un 98% del total de lípidos de la leche, su caracterización se suele llevar a cabo utilizando el extracto de grasa completo. Entre las técnicas empleadas para la separación de TAG se encuentra la cromatografía de capa fina con iones de plata (*silver ion thin layer chromatography*, Ag^+-TLC) [20] y la cromatografía líquida de alta resolución

en fase reversa *(reverse-phase high performance liquid chromatography*, RP-HPLC) [9,18,21–23]. En Ag^+-TLC, los TAG se separan de acuerdo a su grado de insaturación, mientras que la elución de los TAG en RP-HPLC tiene lugar de acuerdo al aumento en el número de partición (*partition number*, PN) [24,25]. El PN de un TAG puede calcularse de la siguiente manera: PN = NC – 2ND, donde NC es el número de átomos de carbono y ND es el número de DB de los FA unidos a la molécula de glicerol. Por otra parte, la separación de isómeros de TAG se suele llevar a cabo por Ag^+-HPLC [26]. Autores como Dugo *et al*. han combinado ambos principios de separación dando lugar a LC en dos dimensiones (2D-LC) para caracterizar por completo los TAG de la leche [27,28], mientras que otros autores han propuesto para este fin el uso de la cromatografía con fluidos supercríticos (*supercritical fluid chromatography*, SFC) o la cromatografía de convergencia *ultra-performance*† [29].

En lo que respecta a la detección de TAG tras su separación, el detector evaporativo de dispersión de luz (*evaporative light scattering detector*, ELSD) [26] o la MS con diferentes fuentes de ionización (electroespray (*electrospray ionization*, ESI) [29–31] o química a presión atmosférica (*atmospheric pressure chemical ionization*, APCI) [21,26–28]) son los habitualmente empleados para este fin.

2. 1. 4. Determinación de fosfolípidos

El análisis de los PL de muestras de leche implica, por lo general, tres etapas fundamentales: i) extracción de lípidos de la leche; ii) aislamiento de los PL de los lípidos neutros; y iii) separación de los PL en clases. Debido a sus propiedades anfifílicas, se debe tener especial cuidado durante la etapa de

†La cromatografía de convergencia *ultra-performance* (*ultra-performance convergence chromatography*, UPC^2) aúna en un solo sistema la SFC y la LC *ultra-performance* (con altas presiones).

extracción de la grasa, ya que las proteínas presentes en la leche tienen la capacidad de estabilizar las emulsiones en las que se encuentran envueltas los PL [32]. Este hecho dificulta la completa separación de fases en la extracción líquido-líquido. Sin embargo, el reto en el análisis de PL subyace en su menor abundancia respecto a los lípidos no polares o TAG (98-99%). Para solventar este problema, se han empleado técnicas tales como la TLC [33] o la cromatografía preparativa o en columna [34], aunque la más ampliamente extendida es la extracción en fase sólida (*solid-phase extraction*, SPE) [35,36], la cual ha prevalecido por encima de éstas. En todas estas técnicas, la elución de la clase deseada de lípidos tiene lugar variando la polaridad y fuerza de la fase móvil. Con respecto a los cartuchos de SPE, materiales derivados de gel de sílice [35–39] predominan sobre otros soportes como fases enlazadas de octilo (C8) [35] o aminopropilo [40], si bien se han desarrollado materiales de empaquetamiento más sofisticados, los cuales consideran p. ej. las interacciones específicas de los PL con compuestos como el dióxido de titanio [41]. Por otra parte, existen cartuchos comerciales con sorbentes derivados de la sílice como SupelClean™ LC-Si [42], que han sido empleados para la extracción de PL de extractos de grasa de la leche [36], e incluso modificados con zirconio (HybridSPE®-Phospholipid [43]), si bien estos últimos se han empleado con el fin de eliminar la interferencia de los PL de matrices biológicas previo su análisis por LC-MS [44].

Con respecto a la separación de PL, ésta se ha llevado a cabo mediante HPLC en fase normal [8,35,45], LC de interacción hidrofílica (*hydrophilic interaction* LC, HILIC) [40,46], y en menor extensión mediante 2D-TLC [11,47]. Tras la separación cromatográfica, se han empleado técnicas de detección como ELSD [46], MS [36], detector de aerosol cargado [38] e incluso resonancia magnética nuclear (RMN) de ^{31}P [45].

Cabe destacar que el aislamiento de los PL del resto de lípidos no polares no siempre se lleva a cabo y que, por tanto, existe la posibilidad de

llevar a cabo su análisis empleando el extracto completo de grasa mediante p. ej. HPLC-ELSD [8,48].

2. 2. Determinación de proteínas

2. 2. 1. Determinación del contenido de proteínas

Para la determinación del contenido de proteínas de una muestra de alimentos, el método de Kjeldahl es el método estándar de referencia. Sin embargo, este método es lento, además de potencialmente peligroso y requiere equipamiento especializado, lo que no lo hace adecuado para el procesamiento de un gran número de muestras [49]. Por esa razón, se han empleado métodos alternativos en la determinación del contenido de proteínas como son el método de Biuret, el método de Folin-Ciocalteau, métodos de unión a colorantes (entre los que cabe destacar el método de Bradford), medidas de infrarrojo o el método de Dumas [49].

2. 2. 2. Fraccionamiento de suero y caseínas

Las proteínas de la leche pueden fraccionarse en dos grupos bien definidos: las proteínas de suero y las CN. Cuando se acidifica la muestra de leche a pH 4.6 (pH isoeléctrico) tiene lugar la coagulación de las CN y, con ello, su precipitación. A escala de laboratorio, normalmente se utiliza el HCl para la acidificación [50,51] y, en menor medida, los ácidos acético y láctico [52]. Cuando tiene lugar la acidificación de la leche a pH 4.6, el fosfato cálcico coloidal (*colloidal calcium phosphate,* CCP) (referido como fosfato inorgánico) se disuelve, de manera que, si se deja el tiempo suficiente para su disolución, se obtienen unas CN libres de CCP [49]. Sin embargo, en la precipitación isoeléctrica de CN, algunas proteínas del suero pueden coprecipitar y, asimismo, algunas CN permanecen en disolución con la

fracción sérica. En este sentido, la adición de calcio a la muestra de leche previamente ajustada al pI da lugar a una disminución en la coprecipitación de proteínas del suero con la fracción de CN [53,54]. Por otra parte, como alternativa a la precipitación isoeléctrica de CN, la fracción de CN puede aislarse por ultracentrifugación a 4 ºC (100000 x*g* durante 60 min) [55,56].

Por otra parte, a escala industrial, se han considerado métodos alternativos para disminuir la contaminación cruzada en el fraccionamiento de las proteínas de suero y CN. Entre estos métodos, se encuentra la "deconstrucción" de las micelas de CN empleando un agente quelante y su posterior reconstrucción con partículas de fosfato cálcico [57] o la precipitación de las CN por adición de fosfato seguido de etapas de congelación-atemperado [58].

2. 2. 3. Separación, identificación y caracterización de proteínas

Como ya se ha descrito, las proteínas de la leche suelen separarse en sus correspondientes clases (suero y CN) previo su análisis. Sin embargo, hay autores que llevan a cabo la determinación simultáneo de ambas fracciones mediante electroforesis bidimensional en gel de poliacrilamida (*two-dimensional polyacrylamide gel electrophoresis*, 2D-PAGE) [59]; o bien mediante electroforesis capilar (*capillary electrophoresis*, CE) [50,60–62] o LC [63,64].

En 2D-PAGE, las proteínas se separan en función de su pI en la primera dimensión (isoelectroenfoque (*isoelectric focusing*, IEF)), y en función de su tamaño (M_w) en la segunda dimensión mediante PAGE en presencia de dodecilsulfato sódico (*sodium docecyl sulfate*-PAGE, SDS-PAGE). De esta manera, la acción combinada de ambas técnicas, IEF y SDS-PAGE, permite la separación de variedades genéticas de CN y proteínas de suero así como las distintas isoformas de CN (p. ej. fosforilación y glicosilación) [65]. Cabe destacar que, para una separación efectiva de las CN

en gel, es preferible el empleo de PAGE en presencia de urea (urea-PAGE) frente a SDS-PAGE [49,66]. Esto se debe a que en urea-PAGE las proteínas se separan principalmente en base a su carga, mientras que en SDS-PAGE lo hacen en base a su tamaño. En el caso de las CN, éstas tienen una masa molecular muy similar (véase **Tabla 1.5**), por lo que la SDS-PAGE no es del todo efectiva para este fin.

La separación de proteínas por CE, donde éstas se separan en función de su relación masa/carga, tiene una serie de ventajas intrínsecas de la técnica como son velocidad, simplicidad y bajo coste [60]. De hecho, a lo largo de los años, se han revisado y recogido sistemáticamente los distintos métodos de CE para el análisis de proteínas [67–72].

En lo que respecta a LC, pueden emplearse diferentes mecanismos de separación (p. ej. exclusión molecular, RP o intercambio iónico). Concretamente, en la separación de proteínas por RP-HPLC, es necesario llevar a cabo una clarificación de la muestra previa su inyección en el cromatógrafo con el fin de suavizar o disminuir las interacciones entre proteínas y así desmantelar la organización micelar de las CN [64]. Además, tras la separación cromatográfica se suele llevar a cabo una recolección sistemática del eluato, analizándose las fracciones recogidas por SDS-PAGE [63,64].

En lo que se refiere a la identificación de proteínas, ésta se puede llevar a cabo por comparación del tiempo de retención o fortificación con patrones o estándares, por acoplamiento directo a un MS, o una vez separadas y teñidas en SDS-PAGE, por el análisis por MS de los diferentes péptidos generados tras su digestión con tripsina u otra proteasa y comparación de los péptidos observados con una base de datos [59,73]. En esta línea, se suele emplear una fuente ESI en MS o la desorción/ionización láser asistida por matriz (*matrix-assisted laser desorbtion ionization*, MALDI), cada una de las cuales con sus particulares ventajas. Así pues, MALDI es capaz de lidiar con

mezclas complejas y tolera las sales. Por su parte, ESI puede acoplarse fácilmente con técnicas de separación como LC y CE [65].

Todas las técnicas anteriormente mencionadas se encuentran incluidas en la llamada "proteómica de la leche (*milk proteomics*)", la cual se entiende como una separación sistemática, identificación y caracterización de las proteínas de la leche [73]. En la **Figura 2.1** se presenta el esquema típico del proceso proteómico para el análisis de leche.

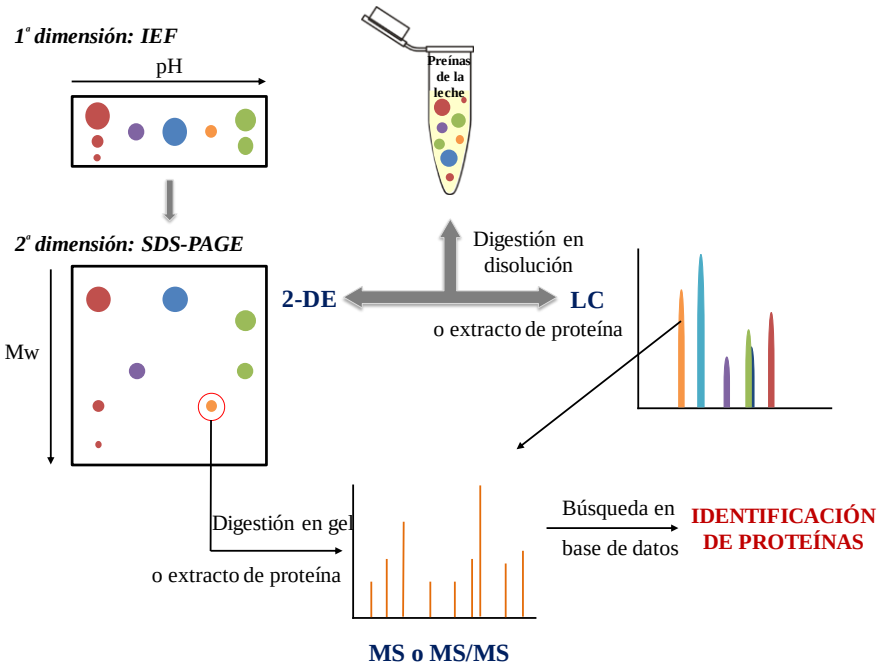

Figura 2.1. Procedimiento general de un análisis proteómico de leche. Adaptado de Le *et al*. [65].

2. 3. Referencias

[1] J. Folch, M. Lees, G.H. Sloane Stantley, A simple method for the isolation and purification of total lipides from animal tissues, J. Biol. Chem. 266 (1957) 497–509.

[2] E.G. Bligh, W.J. Dyer, A rapid method of total lipid extraction and purification, Can. J. Biochem. Physiol. 37 (1959) 911–917. doi:dx.doi.org/10,1139/cjm2014-0700.

[3] A. Hara, N.S. Radin, Lipid extraction of tissues with a low-toxicity solvent, Anal. Biochem. 90 (1978) 420–426. doi:10.1016/0003-2697(78)90046-5.

[4] I.S. Chen, C.-S.J. Shen, A.J. Sheppard, Comparison of methylene chloride and chloroform for the extraction of fats from food products, J. Am. Oil Chem. Soc. 58 (1981) 599–601. doi:10.1007/BF02672373.

[5] AOAC INTERNATIONAL, AOAC Official Method 989.05 Fat in milk, 21 (1992) 5–6.

[6] D.M. Barbano, J.L. Clark, C.E. Dunham, Comparison of Babcock and ether extraction methods for determination of fat content of milk: collaborative study, J. Assoc. Off. Anal. Chem. 71 (1988) 898–914.

[7] R. Rombaut, J. V Camp, K. Dewettinck, Analysis of phospho- and sphingolipids in dairy products by a new HPLC method, J. Dairy Sci. 88 (2005) 482–488. doi:10.3168/jds.S0022-0302(05)72710-7.

[8] L.M. Rodríguez-Alcalá, J. Fontecha, Major lipid classes separation of buttermilk, and cows, goats and ewes milk by high performance liquid chromatography with an evaporative light scattering detector focused on the phospholipid fraction, J. Chromatogr. A 1217 (2010) 3063–3066. doi:10.1016/j.chroma.2010.02.073.

[9] X. Zou, J. Huang, Q. Jin, Z. Guo, Y. Liu, L. Cheong, X. Xu, X. Wang,

Lipid composition analysis of milk fats from different mammalian species: potential for use as human milk fat substitutes, J. Agric. Food Chem. 61 (2013) 7070–7080. doi:10.1021/jf401452y.

[10] R. Rombaut, K. Dewettinck, Properties, analysis and purification of milk polar lipids, Int. Dairy J. 16 (2006) 1362–1373. doi:10.1016/j.idairyj.2006.06.011.

[11] L. Wang, Y. Shimizu, S. Kaneko, S. Hanaka, T. Abe, H. Shimasaki, H. Hisaki, H. Nakajima, Comparison of the fatty acid composition of total lipids and phospholipids in breast milk from Japanese women, Pediatr. Int. 42 (2000) 14–20. doi:10.1046/j.1442-200X.2000.01169.x.

[12] M.C. López-López, A.; Castellote-Bargalló, A. I.; López-Sabater, Comparison of two direct methods for the determination of fatty acids in human milk, Chromatographia 54 (2001) 743–747. doi:10.1007/bf02492493.

[13] C.K. Chuang, C.Y. Yeung, W.T. Jim, S.P. Lin, T.J. Wang, S.F. Huang, H.L. Liu, Comparison of free fatty acid content of human milk from Taiwanese mothers and infant formula, Taiwan. J. Obstet. Gynecol. 52 (2013) 527–533. doi:10.1016/j.tjog.2013.10.013.

[14] Z. Jiang, Y. Liu, Y. Zhu, J. Yang, L. Sun, X. Chai, Y. Wang, Characteristic chromatographic fingerprint study of short-chain fatty acids in human milk, infant formula, pure milk and fermented milk by gas chromatography–mass spectrometry, Int. J. Food Sci. Nutr. 67 (2016) 632–640. doi:10.1080/09637486.2016.1195798.

[15] M.C. Milinsk, M. Matsushita, J. V. Visentainer, C.C. De Oliveira, N.E. De Souza, Comparative analysis of eight esterification methods in the quantitative determination of vegetable oil fatty acid methyl esters (FAME), J. Braz. Chem. Soc. 19 (2008) 1475–1483. doi:10.1590/S0103-50532008000800006.

[16] J.I. Simionato, J.C. Garcia, G.T. Dos Santos, C.C. Oliveira, J.V. Visentainer, N.E. De Souza, Validation of the determination of fatty acids in milk by gas chromatography, J. Braz. Chem. Soc. 21 (2010) 520–524. doi:10.1590/S0103-50532010000300018.

[17] E. Zabo, G. Boehm, C. Beermann, M. Weyermann, H. Brenner, D. Rothenbacher, T. Desci, trans Octadecenoic acid and trans octadecadienoic acid are inversely related to long-chain polyunsaturates in human milk: Results of a large birth cohort study, Am. J. Clin. Nutr. 85 (2007) 1320–1326. doi:https://doi.org/10.1093/ajcn/85.5.1320.

[18] S. Morera, A.I. Castellote, O. Jauregui, I. Casals, M.C. López-Sabater, Triacylglycerol markers of mature human milk, Eur. J. Clin. Nutr. 57 (2003) 1621–1626. doi:10.1038/sj.ejcn.1601733.

[19] A. González-Arrojo, A. Soldado, F. Vicente, B. de la Roza-Delgado, Microwave-assisted methodology feasibility for one-step extraction and transmethylation of fatty acids in milk for GC-mass spectrometry, Food Anal. Methods 8 (2015) 2250–2260. doi:10.1007/s12161-015-0108-8.

[20] J. Fontecha, H. Goudjil, J.J. Ríos, M.J. Fraga, M. Juárez, Identity of the major triacylglycerols in ovine milk fat, Int. Dairy J. 15 (2005) 1217–1224. doi:10.1016/j.idairyj.2004.11.013.

[21] D. Gastaldi, C. Medana, V. Giancotti, R. Aigotti, F. Dal Bello, C. Baiocchi, HPLC-APCI analysis of triacylglycerols in milk fat from different sources, Eur. J. Lipid Sci. Technol. 113 (2011) 197–207. doi:10.1002/ejlt.201000068.

[22] M. Romeu-Nadal, S. Morera-Pons, A.I. Castellote, M.C. López-Sabater, Comparison of two methods for the extraction of fat from human milk, Anal. Chim. Acta 513 (2004) 457–461.

doi:10.1016/j.aca.2004.02.038.

[23] S. Morera Pons, A.I. Castellote Bargalló, M.C. López Sabater, Analysis of human milk triacylglycerols by high-performance liquid chromatography with light-scattering detection, J. Chromatogr. A 823 (1998) 475–482. doi:10.1016/S0021-9673(98)00584-6.

[24] V. Ruíz-Gutiérrez, L.-J. Barron, Methods for the analysis of triacylglycerols, J. Chromatogr. B 671 (1995) 133–168. doi:10.1016/0378-4347(95)00093-X.

[25] P. Sandra, A. Medvedovici, Y. Zhao, F. David, Characterization of triglycerides in vegetable oils by silver-ion packed-column supercritical fluid chromatography coupled to mass spectroscopy with atmospheric pressure chemical ionization and coordination ion spray, J. Chromatogr. A 974 (2002) 231–241. doi:10.1016/S0021-9673(02)01311-0.

[26] X.-Q. Zou, J.-H. Huang, Q.-Z. Jin, Z. Guo, Y.-F. Liu, L.-Z. Cheong, X.-B. Xu, X.-G. Wang, Model for human milk fat substitute evaluation based on triacylglycerol composition profile, J. Agric. Food Chem. 61 (2013) 167–175. doi:10.1021/jf304094p.

[27] P. Dugo, T. Kumm, M. Lo Presti, B. Chiofalo, E. Salimei, A. Fazio, A. Cotroneo, L. Mondello, Determination of triacylglycerols in donkey milk by using high performance liquid chromatography coupled with atmospheric pressure chemical ionization mass spectrometry, J. Sep. Sci. 28 (2005) 1023–1030. doi:10.1002/jssc.200500025.

[28] P. Dugo, T. Kumm, B. Chiofalo, A. Cotroneo, L. Mondello, Separation of triacylglycerols in a complex lipidic matrix by using comprehensive two-dimensional liquid chromatography coupled with atmospheric pressure chemical ionization mass spectrometric detection, J. Sep. Sci. 29 (2006) 1146–1154. doi:10.1002/jssc.200500476.

[29] A. Tu, Q. Ma, H. Bai, Z. Du, A comparative study of triacylglycerol composition in Chinese human milk within different lactation stages and imported infant formula by SFC coupled with Q-TOF-MS, Food Chem. 221 (2017) 555–567. doi:10.1016/j.foodchem.2016.11.139.

[30] Q. Zhou, B. Gao, X. Zhang, Y. Xu, H. Shi, L. Yu, Chemical profiling of triacylglycerols and diacylglycerols in cow milk fat by ultra-performance convergence chromatography combined with a quadrupole time-of-flight mass spectrometry, Food Chem. 143 (2014) 199–204. doi:10.1016/j.foodchem.2013.07.114.

[31] I. Haddad, M. Mozzon, R. Strabbioli, N.G. Frega, A comparative study of the composition of triacylglycerol molecular species in equine and human milks, Dairy Sci. Technol. 92 (2012) 37–56. doi:10.1007/s13594-011-0042-5.

[32] G. Contarini, M. Povolo, Phospholipids in milk fat: composition, biological and technological significance, and analytical strategies, Int. J. Mol. Sci. 14 (2013) 2808–2831. doi:10.3390/ijms14022808.

[33] T.T. Le, J. Miocinovic, T.M. Nguyen, R. Rombaut, J. Van Camp, K. Dewettinck, Improved solvent extraction procedure and high-performance liquid chromatography-evaporative light-scattering detector method for analysis of polar lipids from dairy materials, J. Agric. Food Chem. 59 (2011) 10407–10413. doi:10.1021/jf200202d.

[34] A. Sala-Vila, A.I. Castellote, M. Rodriguez-Palmero, C. Campoy, M.C. López-Sabater, Lipid composition in human breast milk from Granada (Spain): changes during lactation, Nutrition 21 (2005) 467–473. doi:10.1016/j.nut.2004.08.020.

[35] R.J. Maxwell, D. Mondimore, J. Tobias, Rapid method for the quantitative extraction and simultaneous class separation of milk lipids, J. Dairy Sci. 69 (1986) 321–325. doi:10.3168/jds.S0022-

0302(86)80408-8.

[36] A. Avalli, G. Contarini, Determination of phospholipids in dairy products by SPE/HPLC/ELSD, J. Chromatogr. A 1071 (2005) 185–190. doi:10.1016/j.chroma.2005.01.072.

[37] P. Donato, F. Cacciola, F. Cichello, M. Russo, P. Dugo, L. Mondello, Determination of phospholipids in milk samples by means of hydrophilic interaction liquid chromatography coupled to evaporative light scattering and mass spectrometry detection, J. Chromatogr. A 1218 (2011) 6476–6482. doi:10.1016/j.chroma.2011.07.036.

[38] C. Garcia, N.W. Lutz, S. Confort-Gouny, P.J. Cozzone, M. Armand, M. Bernard, Phospholipid fingerprints of milk from different mammalians determined by ^{31}P NMR: Towards specific interest in human health, Food Chem. 135 (2012) 1777–1783. doi:10.1016/j.foodchem.2012.05.111.

[39] G. Kiełbowicz, P. Micek, C. Wawrzeńczyk, A new liquid chromatography method with charge aerosol detector (CAD) for the determination of phospholipid classes. Application to milk phospholipids, Talanta 105 (2013) 28–33. doi:10.1016/j.talanta.2012.11.051.

[40] S. Gallier, D. Gragson, C. Cabral, R. Jiménez-Flores, D.W. Everett, Composition and fatty acid distribution of bovine milk phospholipids from processed milk products, J. Agric. Food Chem. 58 (2014) 10503–10511. doi:10.1021/jf101878d.

[41] M. Schwalbe-Herrmann, J. Willmann, D. Leibfritz, Separation of phospholipid classes by hydrophilic interaction chromatography detected by electrospray ionization mass spectrometry, J. Chromatogr. A 1217 (2010) 5179–5183. doi:10.1016/j.chroma.2010.05.014.

[42] C.D. Calvano, O.N. Jensen, C.G. Zambonin, Selective extraction of

phospholipids from dairy products by micro-solid phase extraction based on titanium dioxide microcolumns followed by MALDI-TOF-MS analysis, Anal. Bioanal. Chem. 394 (2009) 1453–1461. doi:10.1007/s00216-009-2812-y.

[43] Sigma-Aldrich, Supelclean™ LC-Si SPE tube, (año no indicado). Disponible en: http://www.sigmaaldrich.com/catalog/product/supelco/57051?lang=es&region=ES (Fecha de acceso: 06/04/2017).

[44] Sigma-Aldrich, HybridSPE®-Phospholipid, (año no indicado). Disponible en: http://www.sigmaaldrich.com/catalog/product/supelco/55261u?lang=es&region=ES (Fecha de acceso: 04/05/2017).

[45] G. Corona, C. Elia, B. Casetta, S. Frustaci, G. Toffoli, High-throughput plasma docetaxel quantification by liquid chromatography-tandem mass spectrometry, Clin. Chim. Acta 412 (2011) 358–364. doi:10.1016/j.cca.2010.11.010.

[46] F. Giuffrida, C. Cruz-Hernandez, B. Flück, I. Tavazzi, S.K. Thakkar, F. Destaillats, M. Braun, Quantification of phospholipids classes in human milk, Lipids 48 (2013) 1051–1058. doi:10.1007/s11745-013-3825-z.

[47] M. Russo, F. Cichello, C. Ragonese, P. Donato, F. Cacciola, P. Dugo, L. Mondello, Profiling and quantifying polar lipids in milk by hydrophilic interaction liquid chromatography coupled with evaporative light-scattering and mass spectrometry detection, Anal. Bioanal. Chem. 405 (2013) 4617–4626. doi:10.1007/s00216-012-6699-7.

[48] F. Sánchez-Juanes, J.M. Alonso, L. Zancada, P. Hueso, Distribution and fatty acid content of phospholipids from bovine milk and bovine milk fat globule membranes, Int. Dairy J. 19 (2009) 273–278. doi:10.1016/j.idairyj.2008.11.006.

[49] R. Rombaut, K. Dewettinck, J. Van Camp, Phospho- and sphingolipid content of selected dairy products as determined by HPLC coupled to an evaporative light scattering detector (HPLC–ELSD), J. Food Compos. Anal. 20 (2007) 308–312. doi:10.1016/j.jfca.2006.01.010.

[50] P.F. Fox, T. Uniacke-Lowe, P.L.H. McSweeney, J.A. O'Mahony, Chapter 4. Milk Proteins, en: Encycl. Dairy Sci., 2ª ed., Springer, Switzerland, 2015: págs. 145–239. doi:10.1007/978-3-319-14892-2.

[51] M.A. Manso, M. Miguel, R. López-Fandiño, Application of capillary zone electrophoresis to the characterisation of the human milk protein profile and its evolution throughout lactation, J. Chromatogr. A 1146 (2007) 110–117. doi:10.1016/j.chroma.2007.01.100.

[52] A.S. Egito, L. Miclo, C. López, A. Adam, J.-M. Girardet, J.-L. Gaillard, Separation and characterization of mares' milk αs1-, β-, κ-caseins, γ-casein-like, and proteose peptone component 5-like peptides, J. Dairy Sci. 85 (2002) 697–706. doi:10.3168/jds.S0022-0302(02)74126-X.

[53] I. Recio, C. Olieman, Determination of denatured serum proteins in the casein fraction of heat-treated milk by capillary zone electrophoresis, Electrophoresis 17 (1996) 1228–1233. doi:10.1002/elps.1150170710.

[54] C. Kunz, B. Lönnerdal, Human milk proteins: separation of whey proteins and their analysis by polyacrylamide gel electrophoresis, fast protein liquid chromatography (FPLC) gel filtration, and anion-exchange chromatography, Am. J. Clin. Nutr. 49 (1989) 464–470. doi:10.1016/B978-0-12-374039-7.00014-3.

[55] Y. Liao, R. Alvarado, B. Phinney, B. Lönnerdal, Proteomic characterization of human milk whey proteins during a twelve-month lactation period, J. Proteome Res. 10 (2011) 1746–1754. doi:10.1021/pr101028k.

[56] Q. Zhang, J. Cundiff, S. Maria, R. McMahon, J. Woo, B. Davidson, A. Morrow, Quantitative analysis of the human milk whey proteome reveals developing milk and mammary-gland functions across the first year of lactation, Proteomes 1 (2013) 128–158. doi:10.3390/proteomes1020128.

[57] X. Wang, X. Zhao, D. Huang, X. Pan, Y. Qi, Y. Yang, H. Zhao, G. Cheng, Proteomic analysis and cross species comparison of casein fractions from the milk of dairy animals, Sci. Rep. 7 (2017) 1–9. doi:10.1038/srep43020.

[58] T. Morçöl, Q. He, S.J.D. Bell, Model process for removal of caseins from milk of transgenic animals, Biotechnol. Prog. 17 (2001) 577–582. doi:10.1021/bp010023x.

[59] C.H. Yen, Y.S. Lin, C.F. Tu, A novel method for separation of caseins from milk by phosphates precipitation, Prep. Biochem. Biotechnol. 45 (2015) 18–32. doi:10.1080/10826068.2013.877030.

[60] E. D'Auria, C. Agostoni, M. Giovannini, E. Riva, R. Zetterström, R. Fortin, G.F. Greppi, L. Bonizzi, P. Roncada, Proteomic evaluation of milk from different mammalian species as a substitute for breast milk, Acta Paediatr. 94 (2005) 1708–1713. doi:10.1080/08035250500434793.

[61] A. Omar, N. Harbourne, M.J. Oruna-Concha, Quantification of major camel milk proteins by capillary electrophoresis, Int. Dairy J. 58 (2016) 31–35. doi:10.1016/j.idairyj.2016.01.015.

[62] J.M.L. Heck, C. Olieman, A. Schennink, H.J.F. van Valenberg, M.H.P.W. Visker, R.C.R. Meuldijk, A.C.M. van Hooijdonk, Estimation of variation in concentration, phosphorylation and genetic polymorphism of milk proteins using capillary zone electrophoresis, Int. Dairy J. 18 (2008) 548–555. doi:10.1016/j.idairyj.2007.11.004.

[63] B. Miralles, V. Rothbauer, M.A. Manso, L. Amigo, I. Krause, M. Ramos, Improved method for the simultaneous determination of whey proteins, caseins and para-κ-casein in milk and dairy products by capillary electrophoresis, J. Chromatogr. A 915 (2001) 225–230. doi:10.1016/S0021-9673(01)00617-3.

[64] G. Miranda, M.F. Mahé, C. Leroux, P. Martin, Proteomic tools characterize the protein fraction of Equidae milk, Proteomics 4 (2004) 2496–2509. doi:10.1002/pmic.200300765.

[65] N. Boumahrou, S. Andrei, G. Miranda, C. Henry, J.J. Panthier, P. Martin, S. Bellier, The major protein fraction of mouse milk revisited using proven proteomic tools, J. Physiol. Pharmacol. 60 (2009) 113–118.

[66] T.T. Le, H.C. Deeth, L.B. Larsen, Proteomics of major bovine milk proteins: Novel insights, Int. Dairy J. 67 (2017) 2–15. doi:10.1016/j.idairyj.2016.11.016.

[67] A.C.A. Veloso, N. Teixeira, I.M.P.L.V.O. Ferreira, Separation and quantification of the major casein fractions by reverse-phase high-performance liquid chromatography and urea-polyacrylamide gel electrophoresis: Detection of milk adulterations, J. Chromatogr. A 967 (2002) 209–218. doi:10.1016/S0021-9673(02)00787-2.

[68] V. García-Cañas, A. Cifuentes, Recent advances in the application of capillary electromigration methods for food analysis, Electrophoresis 29 (2008) 294–309. doi:10.1002/elps.200700438.

[69] A. Cifuentes, Recent advances in the application of capillary electromigration methods for food analysis, Electrophoresis 27 (2006) 283–303. doi:10.1002/elps.200500474.

[70] V. García-Cañas, C. Simó, M. Castro-Puyana, A. Cifuentes, Recent advances in the application of capillary electromigration methods for

food analysis and Foodomics, Electrophoresis 35 (2014) 147–169. doi:10.1002/elps.201300315.

[71] G. Álvarez, L. Montero, L. Llorens, M. Castro-Puyana, A. Cifuentes, Recent advances in the application of capillary electromigration methods for food analysis and Foodomics, Electrophoresis 39 (2017) 136–159. doi:10.1002/elps.201700321.

[72] T. Acunha, C. Ibáñez, V. García-Cañas, C. Simó, A. Cifuentes, Recent advances in the application of capillary electromigration methods for food analysis and Foodomics, Electrophoresis 37 (2016) 111–141. doi:10.1002/elps.201500291.

[73] I. Recio, L. Amigo, R. López-Fandiño, Assessment of the quality of dairy products by capillary electrophoresis of milk proteins, J. Chromatogr. B 697 (1997) 231–242. doi:10.1016/S0378-4347(97)00085-6.

[74] R. O'Donnell, J.W. Holland, H.C. Deeth, P. Alewood, Milk proteomics, Int. Dairy J. 14 (2004) 1013–1023. doi:10.1016/j.idairyj.2004.04.004.

CAPÍTULO 3

Sorbentes empleados en técnicas de extracción en fase sólida

3. 1. La extracción en fase sólida

En líneas generales, la SPE puede describirse como una técnica preparativa la cual es empleada con el fin de aislar un/os analito/s de interés en una matriz más o menos compleja (agua, orina, sangre, leche, etc.). El término viene acuñado por el hecho de que el material de soporte utilizado es un sólido, a través del cual pasa un líquido o un gas. Los analitos de interés quedan adsorbidos sobre el soporte y son posteriormente eluidos de acuerdo con sus diferentes afinidades entre el material del soporte y la fase móvil utilizada. Existen cuatro etapas definidas en el procedimiento general de SPE:

i) Acondicionamiento

En esta etapa tiene lugar la activación del sorbente al pasar por el cartucho un disolvente o mezcla de disolventes apropiados. Para sorbentes hidrofóbicos se usa generalmente MeOH o acetonitrilo (ACN), mientras que para sorbentes hidrofílicos, se emplea hexano o cloruro de metileno.

ii) Carga

En esta etapa se hace pasar la muestra a través del cartucho de manera que los analitos de interés quedan retenidos por el sorbente, mientras que el resto de componentes de la matriz pasan por la columna sin ser retenidos.

iii) Lavado

Esta etapa permite eliminar posibles restos de contaminantes que hayan quedado en el lecho y que pueden interferir en el análisis posterior de los analitos de interés.

iv) Elución

En esta etapa se eluyen los analitos de interés con un disolvente o mezcla de disolventes adecuados.

En lo que respecta a los sorbentes, estos pueden presentarse en diferentes formatos: cartuchos, jeringas, discos, capilares, puntas de pipeta o platos multipocillo. Estos últimos permiten procesar un gran número de muestras empleando un sistema semi-automático, lo que es de gran utilidad para el procesamiento de muestras biológicas. No obstante, los cartuchos continúan siendo el formato más empleado en SPE debido a la gran variedad de sorbentes disponibles comercialmente para la extracción eficaz de un gran número de analitos de interés.

En cuanto a los modos de trabajo en SPE, ésta técnica extractiva puede llevarse a cabo fuera de línea (*off-line*) (el más habitual) o en línea (*on-line*). En el modo *on-line*, hay un acoplamiento directo y automático con el sistema cromatográfico, aunque existen ciertas limitaciones asociadas, como son la incompatibilidad de los disolventes empleados con el sistema cromatográfico o el reducido caudal tolerado por el sistema de extracción, que hace las veces de precolumna [1].

En un sentido estricto, la SPE se basa en unos principios que son comunes a los procesos cromatográficos y por ello, los sorbentes empleados en SPE son, en muchos casos, similares a los empleados en las columnas de HPLC, aunque puedan diferir en formato y propiedades [2]. Así pues, los mecanismos de retención de los analitos vienen en gran medida determinados por la naturaleza del sorbente empleado, por lo que el conocimiento de sus propiedades es crucial para lograr el éxito en la extracción. La **Figura 3.1** muestra una clasificación de los principales sorbentes empleados en SPE en función de su naturaleza estructural.

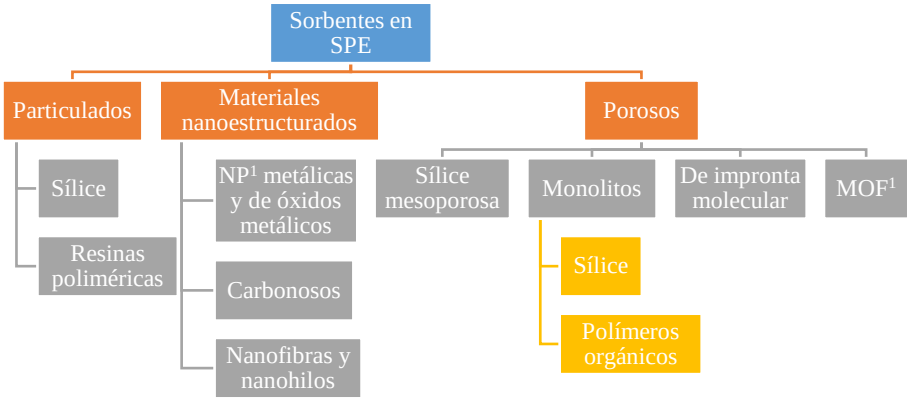

Figura 3.1. Clasificación de los principales sorbentes empleados en SPE según su naturaleza estructural. [1]Nanopartículas (*nanoparticle*, NP). [2]Estructuras metal-orgánicas (*metal organic framework*, MOF).

3. 2. Materiales particulados

Se estima que un 90% de los lechos que se fabrican para cartuchos de SPE llevan gel de sílice como material de base [3]. La sílice que normalmente se emplea en la elaboración de cartuchos para SPE es un sólido poroso amorfo con un área superficial de 50 a 500 m^2/g y un diámetro de poro de 50-500 Å [2]. En lo que respecta al tamaño de partícula, éste se encuentra, por lo general, entre los 30 y 60 µm [3,4]. La superficie de la sílice se caracteriza por la presencia de grupos silanoles libres, los cuales son responsables de muchas de sus propiedades. No obstante, la superficie de la sílice suele modificarse o enlazarse a otras especies con el fin de proporcionarle la selectividad deseada. De esta manera, se obtienen sorbentes con mecanismos de interacción tales como RP (octilo (C8), octadecilo (C18), fenilo), NP (diol, aminopropilo) o intercambio iónico (ácidos sulfónicos, aminas cuaternarias).

Pese a sus conocidas ventajas (fácil elaboración, bajo coste, elevada relación área superficial/volumen, amplia variedad de funcionalidades, etc.), sus principales desventajas yacen en su limitado rango de estabilidad de pH (pH 2 – 9) y la presencia de grupos silanoles libres en su estructura, los cuales pueden cursar un efecto negativo en la retención de ciertos analitos. Además, estos materiales de sílice presentan ciertas impurezas (especialmente metales) inherentes al proceso de elaboración, cuya presencia a niveles traza puede dar lugar a sitios no específicos de adsorción [3].

Como alternativa a los materiales basados en gel de sílice, se encuentra la alúmina, el carbono, Fluorosil® y polímeros sintéticos, entre los cuales se incluyen las resinas de poliestireno-divinilbenceno (*polystyrene-divinylbenzene*, PS-DVB), entre otros [3]. El comportamiento de estas resinas es principalmente hidrofóbico (fuerzas de Van der Waals e interacciones π-π), aunque la introducción de grupos polares (p. ej. alcohol o acetilo) han mejorado su capacidad de retención de compuestos orgánicos polares [5]. No obstante, la retención de compuestos altamente polares en matrices complejas sigue siendo una limitación de estos sorbentes.

En cualquier caso, tanto la preparación de materiales de gel de sílice particulados como de resinas poliméricas requiere de la existencia de fritas en los cartuchos de extracción. Estas fritas deberían idealmente ser lo suficientemente porosas para permitir el paso uniforme de los disolventes. Además, dado que el tamaño de las partículas no es estrictamente uniforme (sigue una distribución), las partículas más finas pueden bloquear las fritas, impidiendo así el paso del disolvente.

3. 3. Materiales nanoestructurados

El término nanomaterial hace referencia a aquel en el que al menos una de sus dimensiones se encuentra en el rango de la nanoescala, esto es,

entre 1 y 100 nm [6]. De entre las principales ventajas de estos materiales, destacan su elevada relación superficie/volumen, así como su capacidad de modificar sus propiedades fundamentales (propiedades ópticas, magnetización, temperatura de fusión, etc.). El continuo desarrollo de nanomateriales y sus aplicaciones tecnológicas en numerosas áreas hace de estos materiales un aliado indispensable en métodos de preparación de muestra. En líneas generales, el conjunto de nanomateriales puede clasificarse en: (i) cero-dimensionales (p.ej. las NP), (ii) bidimensionales (nano-*films*, nano-capas y nano-recubrimientos), y (iii) tridimensionales. Por otra parte, atendiendo a su composición, los nanomateriales pueden clasificarse en metálicos, óxidos metálicos, carbonosos, de sílice, nano-fibras y nano-hilos, y poliméricos [7].

Debido a las propiedades características de los materiales nanoestructurados (p.ej. gran área superficial) su uso como sorbentes en SPE ha sido ampliamente estudiado. Sin embargo, su uso directo se ve limitado en muchos casos por propiedades intrínsecas de los materiales. En el caso de los nanotubos de carbono (*carbon nanotube*, CNT), cuando se empaquetan en columnas o cartuchos, su tendencia a agregarse puede causar una excesiva contrapresión y reducción tanto del área superficial efectiva como de su eficiencia de adsorción. Por otra parte, si se trabaja en dispersiva, su baja densidad, su tamaño de partícula reducido y su dispersibilidad hace que su separación del medio acuoso sea difícil e incompleta, requiriendo etapas de filtración y centrifugación [8]. Esta limitación también existe para otro tipo de NP (metálicas, de sílice, etc.). Es por esto que, en muchos casos, el uso de estos materiales viene asociado o en combinación con diferentes soportes. En este sentido, en la sección 3.4.2.2. de esta Tesis, se entrará en detalle de algunas de las incorporaciones de estos nanomateriales a soportes poliméricos.

Las aplicaciones de los diferentes materiales nanoestructurados, bien directa o bien empleando soportes de anclaje, para el aislamiento o

preconcentración de una gran variedad de analitos en diferentes matrices han sido ampliamente recopiladas [7–12].

3. 4. Materiales porosos

3. 4. 1. Sílice mesoporosa

Desde su primera síntesis en 1992 realizada por "*the Mobil Oil Company"* [13], los materiales de sílice mesoporosa (*mesoporous silica material*, MSM) han recibido una especial atención debido a sus singulares características tales como su elevada área superficial (>1000 m^2/g), gran volumen de poro (>1 cm^3/g), fácil manipulación (tamaño, poro y forma), buena estabilidad química y térmica, biocompatibilidad, funcionalización interna o externa de su superficie, etc. Estas propiedades estructurales únicas, junto con su biocompatibilidad, han hecho que los MSM sean de aplicación en áreas como la catálisis [14] y la biomedicina [15], entre otras. Además, el potencial uso de estos materiales se ha ido extendiendo también al campo de la Química Analítica [16,17].

De entre los MSM, el "*Mobil Composition of Matter"* nº 41 (MCM-41) es el material más estudiado. Su síntesis, basada en la técnica sol-gel, se lleva a cabo por condensación de precursores de sílice (p. ej. tetraetil ortosilicato (*tetraethyl-orthosilicate*, TEOS)) en presencia de surfactantes catiónicos (p. ej. bromuro de cetiltrimetilamonio (c*etyl trimethyl ammonium bromide*, CTAB)), en condiciones básicas (pH = 11) y a una temperatura de entre 30 y 60 ºC. Además del material MCM-41, se han descrito otros MSM con diferente forma y sistema de poros (p.ej. SBA-15 [18] y UVM-7 [19]). Este último, desarrollado en 2002 por Amorós *et al*. [19], constituye uno de los primeros ejemplos de sistema de poros multimodal jerárquico en MSM. Así pues, el material UVM-7 puede describirse como un sistema de poros bimodal que contiene mesoporos intra-particulares y macroporos inter-

particulares, los cuales son susceptibles de ser modificados en función del tipo de surfactante, así como por variaciones en el proceso de síntesis y "envejecimiento".

Desde el punto de vista preparativo, la principal diferencia entre el material UVM-7 y MCM-41 yace en las condiciones básicas empleadas en la etapa de síntesis (pH 9 y 11, respectivamente). A menor pH, los procesos de hidrólisis y condensación se ven favorecidos, pero no así los fenómenos de redisolución. Este hecho da lugar a la formación del sistema de poros bimodal, tras la eliminación del surfactante (**Figura 3.2**). Además, el precursor inorgánico usado en la síntesis de UVM-7 es un complejo de atrano formado a partir de la transesterificación de un alcóxido en un disolvente no acuoso.

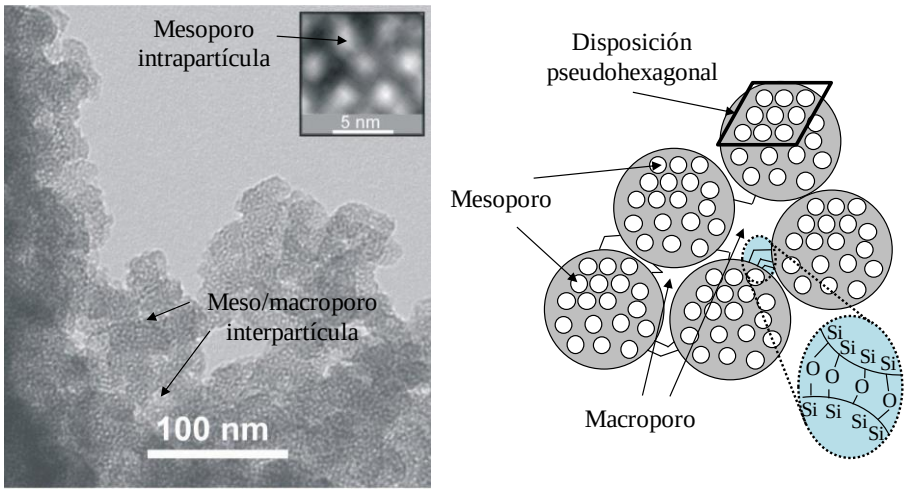

Figura 3.2. Imagen TEM y esquema del MSM UVM-7.

Cabe destacar que, las partículas de sílice mesoporosa (*mesoporous silica particle*, MSP) presentan tres posibles dominios de funcionalización: la superficie (mediante oclusión), la parte interna de los mesoporos (mediante injerto o *grafting*) y la propia matriz de sílice (mediante co-condensación) [20]. En el caso particular de la funcionalización por co-condensación, ésta permite distribuir homogéneamente el compuesto o elemento dopante (Al, Ti, V, etc.) en la superficie interna de los poros, además

de un mejor control de la morfología del material. Así pues, este tipo de partículas se pueden funcionalizar fácilmente con un diseño adecuado para aplicaciones específicas [21].

En lo que respecta a la aplicación de los MSM como sorbentes en técnicas de extracción, los materiales MCM-41 y SBA-15 se han usado extensamente como sorbentes en micro-SPE y SPE para la eliminación de contaminantes orgánicos e inorgánicos de aire y agua [22,23], así como para la preconcentración de contaminantes orgánicos como los hidrocarburos aromáticos policíclicos [24] y disruptores endocrinos [25]. Por su parte, el material UVM-7 se ha empleado de manera satisfactoria en aplicaciones de catálisis [26], sensores químicos [27] y cromatografía [28]. Sin embargo, el uso de este material con fines preparativos no ha sido descrito.

En el **Capítulo 5** de esta Tesis, se describe la aplicación del material UVM-7 puro y dopado con Ti para la extracción de PL de extractos de grasa de la leche materna.

3. 4. 2. Materiales monolíticos

El término monolito procede del griego *monólithos* y puede traducirse como “de una sola piedra”. En el contexto cromatográfico, dicho término se traduciría en un “soporte o lecho continuo”. Su aplicación con fines separativos en el campo de la cromatografía ha sido sobradamente probada, ya que constituyen una alternativa a las columnas empaquetadas, con algunas ventajas interesantes. Estos monolitos se caracterizan por tener una alta permeabilidad debido a la distribución uniforme de macroporos y mesoporos permitiendo la separación de numerosos analitos. Así pues, los macroporos (> 50 nm) proporcionan la permeabilidad necesaria para el paso del disolvente, mientras que los mesoporos (2-50 nm) proporcionan la elevada área superficial para la separación (**Figura 3.3B**).

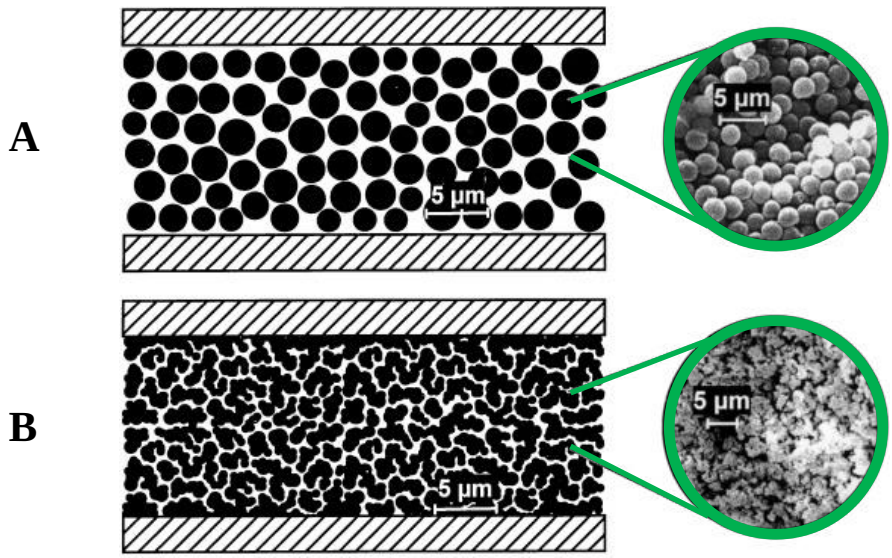

Figura 3.3. Características estructurales de un lecho empaquetado (A) y un lecho monolítico (B) [29].

En comparación con los materiales empaquetados, los materiales monolíticos ofrecen una serie de ventajas como son su alta porosidad y permeabilidad, lo cual los hace atractivos como soportes alternativos para SPE. Además, como ya se ha indicado, los materiales monolíticos no requieren de fritas y su superficie puede ser modificada fácilmente de acuerdo con el fin que se persiga.

Atendiendo a su naturaleza, los materiales monolíticos pueden clasificarse en dos grandes grupos: inorgánicos (basados en sílice) y orgánicos (basados en acrilamida, metacrilato o estireno, entre otros).

3. 4. 2. 1. Monolitos de sílice

La preparación de monolitos de sílice, con una estructura homogénea bien definida, suele llevarse a cabo mediante el proceso sol-gel [30]. Los componentes básicos en la mezcla de reacción son un precursor, un disolvente porogénico y un catalizador. Así pues, el proceso sol-gel implica la formación de una red de enlaces siloxano (Si-O-Si) a través de sucesivas hidrólisis y

policondensaciones de un alcóxido de silicio o mezcla de alcóxidos en condiciones ácidas o básicas, en presencia de un disolvente porogénico (p. ej. polietilenglicol (*polyethylene glycol*, PEG)).

La **Figura 3.4A** muestra la imagen realizada con un microscopio electrónico de barrido (*scanning electron microscope*, SEM*)* de un monolito de sílice, donde se observan claramente la estructura de los macroporos y microporos.

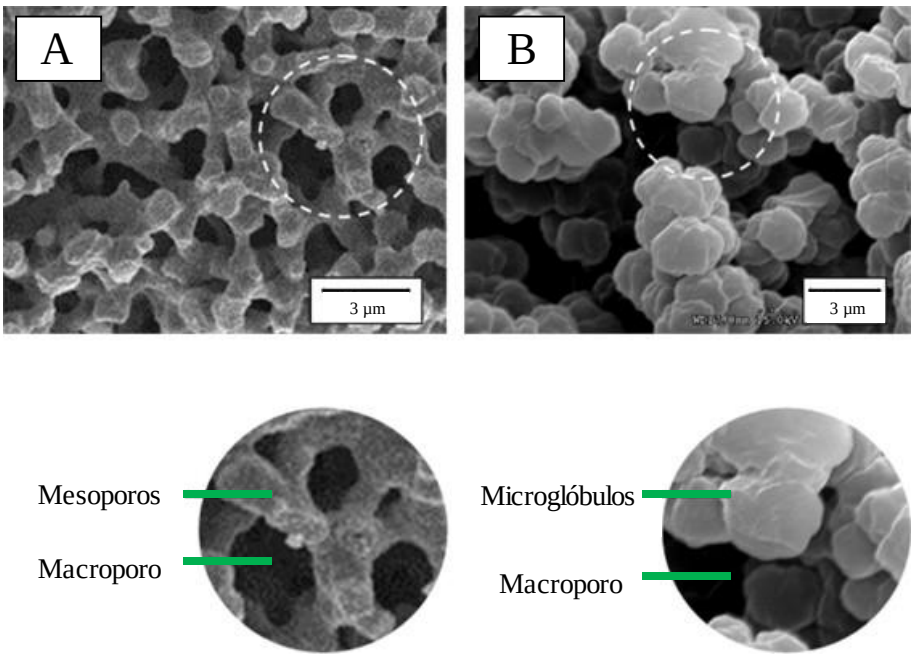

Figura 3.4. Micrografías SEM de la estructura jerárquica de un monolito de sílice con su red de macroporos y su esqueleto delgado de mesoporos (A); y estructura típica de un material monolítico polimérico con su estructura globular a partir de polímero entrecruzado (B). Adaptado de Nischang *et al.* [31].

Los monolitos de sílice ofrecen una resistencia a disolventes orgánicos y estabilidad mecánica mejores que sus homólogos poliméricos (sección 3.4.2.2.). Sin embargo, su síntesis no es sencilla y requiere un control exhaustivo de todo el proceso y, al igual que los materiales de sílice

particulados, presentan un rango estrecho de estabilidad de pH (pH 2-7). Además, el tratamiento térmico asociado a su preparación hace que el principal uso de los monolitos de sílice se haya reducido al formato capilar, siendo difícil su extensión a cartuchos de SPE u otros formatos.

Pese a estos inconvenientes, se ha descrito el uso de monolitos de sílice para el aislamiento o preconcentración de compuestos orgánicos pequeños en muestras medioambientales y biológicas [32,33]. Asimismo, existen diferentes dispositivos comerciales para extracción (columnas de centrifugación (*spin column*) y puntas de pipeta) que emplean monolitos de sílice (p.ej. MonoSpin™ y MonoTip™ de GL Sciences (Tokio, Japón)).

3. 4. 2. 2. Monolitos de polímeros orgánicos

La preparación de monolitos poliméricos se lleva a cabo normalmente vía polimerización radicalaria. La mezcla de polimerización es una combinación de monómeros entre los que se encuentra un agente entrecruzante o *cross-linker*, una mezcla porogénica de disolventes y un iniciador radicalario. La polimerización se lleva a cabo en la mayoría de los casos por calentamiento en un baño u horno, por la acción de iniciadores químicos o mediante radiación UV. Gracias al control que puede ejercerse sobre el proceso de polimerización, es posible optimizar las propiedades morfológicas de los monolitos resultantes y, por tanto, la velocidad de flujo y eficacia del sorbente. Además, la gran variedad de monómeros disponibles, así como la posibilidad de su posterior funcionalización, permite ajustarse a las interacciones especificas necesarias para conseguir una retención selectiva de los analitos de interés.

La morfología resultante de los monolitos poliméricos consiste en un sistema complejo, donde una serie de microglóbulos interconectados parcialmente agregados en racimo forman el cuerpo del polímero. Los huecos entre estos racimos de microglóbulos corresponden a los macroporos (**Figura 3.4B**).

Como ya se ha indicado, de entre los polímeros orgánicos, pueden distinguirse principalmente los basados en acrilamida, en poliestireno y en ésteres de metacrilato o acrilato. Esta Tesis, se centra en estos últimos y modificaciones de los mismos.

Cabe destacar que, pese a las buenas prestaciones de estos materiales, sus áreas superficiales relativamente bajas comparadas con sus homólogos de sílice, debido a la ausencia de una estructura micro- o mesoporosa adecuada, da lugar a una menor capacidad de carga y retenciones más débiles en aplicaciones cromatográficas. Esta menor área superficial los limita asimismo para aplicaciones basadas en la interacción con los sitios activos de la superficie como son la catálisis y la adsorción. Asimismo, pese a que el número de aplicaciones de los monolitos poliméricos es mayor que el de los monolitos de sílice, su distribución comercial es más bien limitada. A modo de ejemplo, cabe destacar los discos CIM®-*disk* de BIA Separations (Liubliana, Eslovenia), los cuales han sido aplicados para la preparación/aislamiento y purificación de moléculas de gran tamaño (proteínas, ADN y virus).

Con el fin de contrarrestar esta limitación, se han propuesto diferentes estrategias como el empleo de nuevas condiciones de polimerización, los polímeros hiperentrecruzados [34], los monolitos híbridos de sílice-orgánicos [35] o la incorporación de nanomateriales [36]. Estas aproximaciones pueden no sólo mejorar el área superficial de los sorbentes, sino que incluso facilitan el poder realizar manipulaciones de la selectividad.

Los polímeros hiperentrecruzados consisten en resinas poliméricas con una capacidad de retención acentuada debido a su gran contenido de microporos y elevada área superficial específica (> 1000 m^2/g). Por lo general, y con el fin de dotar de cierta selectividad a estas resinas, se suelen modificar

con grupos de intercambio iónico [37], pasando a ser potenciales sorbentes para p.ej. la extracción de diversos componentes de matrices acuosas [38,39].

En lo que respecta a los monolitos híbridos de sílice-orgánicos, estos aúnan las ventajas de ambos sistemas [35]: la mayor área superficial y resistencia mecánica de los monolitos de sílice, junto con la preparativa más sencilla de los monolitos orgánicos. Este tipo de monolitos híbridos ha sido empleado como sorbente de extracción de solutos orgánicos pequeños [40] e incluso para especies inorgánicas como metales traza [41].

En lo referente a la incorporación de nanomateriales, esta Tesis se centra en la incorporación de NP metálicas y óxidos metálicos, si bien existen otras posibilidades como p. ej. la incorporación de CNT [42,43].

A) Polímeros modificados con nanopartículas

Como se ha descrito anteriormente, las propiedades de muchos materiales convencionales se ven modificadas cuando se trabaja con los mismos a escala nanométrica. Esto ocurre porque, por norma general, las NP tienen una mayor relación área superficial/peso que las partículas de mayor tamaño, lo que provoca que éstas sean más reactivas [44]. Es por esto que, la incorporación de NP a monolitos orgánicos ha resultado ser un forma efectiva y prometedora de incrementar la relación superficie/volumen de estos, así como de hacerlos servir de plataforma para posteriores modificaciones químicas de su superficie [45].

En lo que respecta a la introducción de NP en los lechos monolíticos, ésta puede hacerse bien incorporando las NP en el mismo proceso de polimerización, o bien realizando un anclaje de las NP sobre la propia superficie del monolito ya formado [46]. En la primera aproximación, las NP son añadidas a la mezcla de polimerización antes de que ésta tenga lugar. Desde el punto de vista práctico, es una manera sencilla y rápida de introducirlas, pero por contraparte, esta metodología presenta varias

desventajas. En primer lugar, muchas de las NP quedan enterradas dentro de la matriz del monolito y no quedan disponibles sobre la superficie porosa para las interacciones deseadas [47]. Por otra parte, existen ciertas limitaciones respecto a la cantidad de NP que puede ser añadida a la mezcla de polimerización debido a que la polaridad de éstas puede resultar incompatible con la propia mezcla. Además, debido a estas diferencias de polaridad, la síntesis completa del monolito debe estudiarse de manera particular para cada monómero con el fin de obtener la estructura y porosidad deseadas [48]. Pese a las citadas limitaciones, esta alternativa, además de con fines cromatográficos, ha sido empleada también con fines preparativos. Así pues, Rainer *et al*. [49] han llevado a cabo una síntesis de monolitos de poli(DVB) con NP de dióxido de titanio y/o dióxido de zirconio en el interior de puntas de pipetas para el enriquecimiento de fosfopéptidos. Por su parte, Hussain *et al*. [50], de nuevo empleando puntas de pipeta como soporte, han abordado la extracción de tioninas (proteínas ricas en cisteína) empleando un monolito de PS-DVB con nano-polvo de silicato de zirconio embebido.

En cualquier caso, el anclaje de NP sobre la superficie porosa del monolito bien por unión covalente o bien por interacciones electrostáticas resulta ser la alternativa preponderante. Cabe destacar que, para este fin, se hace indispensable que el monolito de partida posea una cierta reactividad, la cual permita o facilite el anclaje de las NP. En la gran mayoría de los casos, esto se consigue empleando como monómero de partida el metacrilato de glicidilo (*glycidyl methacrylate*, GMA), el cual posee un grupo epóxido reactivo, susceptible de ser modificado químicamente una vez finalizado el proceso de polimerización. Así pues, por la apertura del anillo epóxido con p. ej. una amina secundaria pueden obtenerse monolitos amino-hidroxi funcionalizados [48] (**Figura 3.5**).

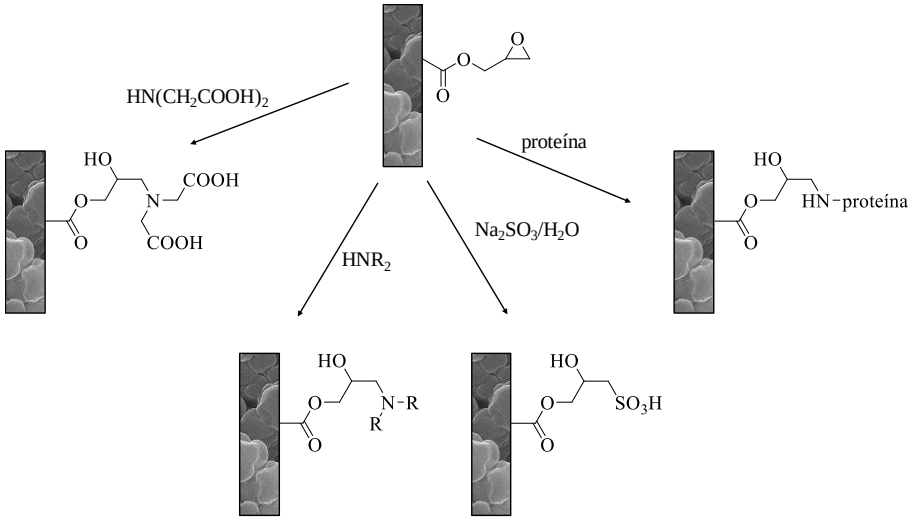

Figura 3.5. Funcionalización post-síntesis de un monolito de GMA. Adaptado de Buchmeiser *et al*. [48].

Una vez llevada a cabo la modificación del monolito base, el anclaje de las NP viene respaldado por la propia afinidad que puedan tener las NP frente a los grupos funcionales introducidos. Este es el caso de las NP de oro (AuNP), las cuales quedan inmovilizadas en la superficie del monolito de GMA en el que se ha introducido un grupo amino o un grupo tiol [36,51]. Si bien en el campo de la electrocromatografía se han descrito diversas aplicaciones centradas en el uso de monolitos modificados con NP, en lo que respecta al tratamiento de muestra existen pocas contribuciones. Así pues, Alwael *et al*. [49] han llevado a cabo el aislamiento de glicoproteínas de matrices complejas empleando monolitos de dimetacrilato de etilenglicol (*ethylendimethacrylate*, EDMA) sobre el cual han sido inmovilizadas AuNP. Por su parte, Vergara-Barberán *et al*. [52,53] han llevado a cabo la extracción de lectinas, así como la preconcentración de viscotoxinas del muérdago empleando cartuchos de SPE con un monolito base de GMA post-funcionalizado y modificado con AuNP o NP de plata (AgNP).

En el **Capítulo 8** de esta Tesis, se describe la aplicación de materiales poliméricos modificados con AuNP para la extracción selectiva de las proteínas del suero de la leche materna.

B) Polímeros magnéticos

Pese a la gran variedad de sorbentes existentes en SPE, no siempre es posible obtener unas recuperaciones satisfactorias, y el aislamiento y preconcentración de los componentes individuales puede resultar laborioso y requerir un tiempo excesivo. En este contexto, las NP magnéticas (*magnetic nanoparticle*, MNP) surgen como una alternativa a los sorbentes convencionales de SPE. Como tales, las MNP presentan una elevada área superficial, una alta capacidad de adsorción e incluso una elevada selectividad frente a ciertos analitos [54]. Así pues, el empleo de MNP ha dado lugar a lo que se conoce como SPE magnética (*magnetic SPE*, MSPE), cuyas aplicaciones, especialmente en el análisis alimentario y medioambiental, han sido recientemente recopiladas [54,55]. En la MSPE, el sorbente es introducido en la muestra donde se encuentran los analitos de interés. El contacto directo con estos analitos da lugar a la retención selectiva de los mismos sobre la superficie del sorbente. En este punto, el sorbente es separado del resto de la disolución con ayuda de un campo magnético externo (un imán), el cual se coloca sobre la pared externa del recipiente, no siendo necesario llevar a cabo una centrifugación o filtración de la muestra (**Figura 3.6**).

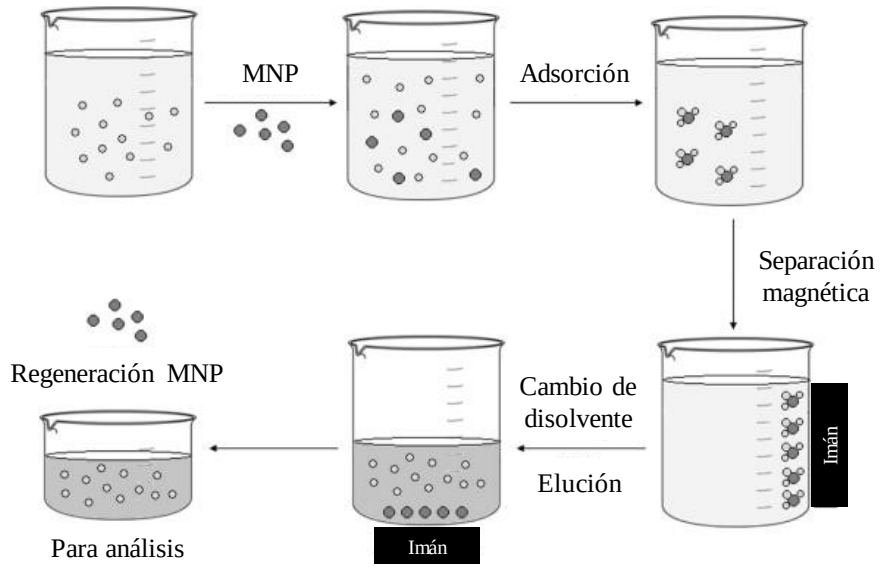

Figura 3.6. Proceso de la MSPE. Adaptado de Wierucka *et al*. [54].

La síntesis de sorbentes para MSPE se fundamenta en obtener un sorbente con propiedades magnéticas, lo que en muchos casos se consigue con la introducción de magnetita (Fe_3O_4). El método más común para la producción de NP de magnetita consiste en la coprecipitación de sales de hierro en medio básico [56]. Estas MNP desnudas son altamente reactivas químicamente y fácilmente oxidables, lo cual da lugar a pérdidas de magnetismo y estabilidad coloidal [57]. Por este motivo, una vez sintetizadas, éstas se recubren de diversos materiales como sílice, alúmina, óxidos metálicos o polímeros orgánicos para ser empleadas como sorbentes en MSPE. Debido a la gran versatilidad que ofrece la sílice, así como su alta estabilidad térmica y mecánica [54], éste es el recubrimiento más empleado, el cual se consigue vía el proceso sol-gel [58]. Además, la superficie de la sílice es susceptible de ser modificada por la unión de ligandos orgánicos e inorgánicos, dependiendo del tipo de interacción deseada (**Figura 3.7**).

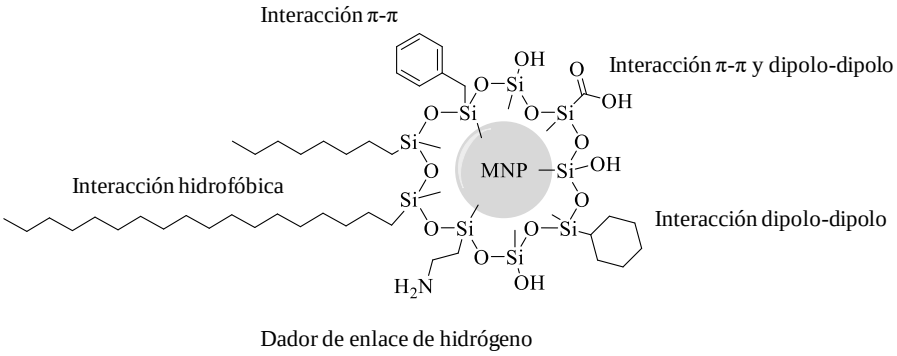

Figura 3.7. MNP de magnetita recubierta de sílice y modificada con diferentes grupos funcionales y sus procesos de interacción. Adaptado de Ibarra *et al*. [55].

De manera alternativa, el recubrimiento de las MNP puede llevarse a cabo *in situ* o post-síntesis con polímeros orgánicos como dextrano, PEG o alcohol de polivinilo [56]. Sin embargo, algunos de estos materiales magnéticos funcionalizados muestran una limitada dispersibilidad y reproducibilidad, lo que indudablemente afecta a su capacidad de adsorción. En este sentido, la inmovilización de MNP desnudas sobre sílice o soportes poliméricos puede ser una alternativa a considerar, ya que este proceso permitiría explotar por completo su potencial de interacción, como por ejemplo, con compuestos de fósforo [59,60]. Siguiendo esta línea, se han llevado a cabo algunas aproximaciones en el desarrollo de monolitos de GMA modificados con MNP. Así pues, Krenkova *et al*. han inmovilizado por interacciones electrostáticas sobre la superficie de un monolito de GMA modificado con una amina cuaternaria NP de óxido de hierro estabilizadas con citrato para la preconcentración de fosfopéptidos en digestos de CN, tanto en electrocromatografía capilar (*capillary electrocromatography*, CEC) [61], como en puntas de pipeta [62]. Por otra parte, Meseguer-Lloret *et al*. [63] han llevado a cabo la preconcentración de pesticidas organofosforados en muestras acuosas empleando cartuchos de SPE rellenos de un monolito base de GMA modificado con NP de magnetita. Sin embargo, el uso de estos

sorbentes para el aislamiento de compuestos fosforados en matrices más complejas no ha sido explorado.

En el **Capítulo 6** de esta Tesis, se describe la aplicación de materiales poliméricos modificados con MNP para la extracción selectiva de PL de la leche materna.

3. 4. 3. Polímeros de impronta molecular

La selectividad frente a un analito o grupo de analitos es en la mayoría de los casos una característica muy deseable en los sorbentes de SPE. Para este fin, y gracias al desarrollo de la tecnología de impronta molecular, se encuentran los polímeros basados en ésta (polímeros de impronta molecular (*molecularly imprinted polymer*, MIP)) [64], los cuales se basan en el reconocimiento molecular de los analitos para su retención. Dichos polímeros incluso se han desarrollado con propiedades magnéticas con el fin de acelerar y simplificar el proceso de extracción de los analitos cuando son empleados MSPE.

Los MIP consisten en polímeros estables altamente entrecruzados, cuyo reconocimiento se basa en la generación durante la polimerización de cavidades que son complementarias en tamaño, forma y funcionalidad química al analito [65]. Para la elaboración de un MIP, el analito (molécula plantilla (*template*, T)) o en su defecto un compuesto de estructura similar al analito (*dummy* o *mimmic template*) se pone en contacto con un monómero funcional (*functional monomer*, M) con grupos funcionales tales que permitan la formación de un complejo estable en presencia de un disolvente porogénico adecuado. A continuación, se añade el agente entrecruzante (*cross-linker*, C) y tiene lugar la polimerización. Una vez formado el polímero, éste se lava para eliminar la molécula plantilla, dejando así las cavidades disponibles para la posterior unión del analito de interés (**Figura 3.8**).

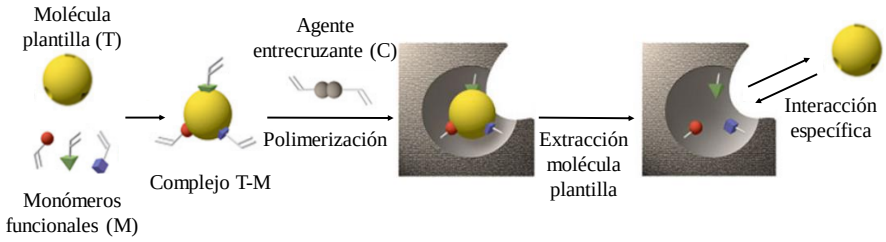

Figura 3.8. Esquema de preparación de un MIP.

A priori, cualquier compuesto químico puede ser empleado para preparar su correspondiente MIP; sin embargo, la eficiencia del proceso de impronta (o reconocimiento selectivo) solo se observa para un número limitado de compuestos. Esto se debe a que la formación de un complejo de pre-polimerización suficientemente fuerte T-M es fundamental para las propiedades de reconocimiento del polímero [66,67]. En este sentido, la formación del complejo T-M suele implicar, por lo general, interacciones de tipo no covalente (hidrofóbicas, iónicas, dipolo-dipolo, π-π o enlace de hidrógeno), pudiendo éstas ocurrir en uno o más puntos de las moléculas.

En lo que respecta a la proporción de los componentes en la mezcla de polimerización, como norma general, el agente entrecruzante se introduce en la ruta de síntesis del MIP en exceso respecto a la molécula plantilla y al monómero funcional, siendo habitual la relación T:M:C 1:4:20 para asegurar un grado de entrecruzamiento mayor del 80% y lograr una buena impresión molecular [68].

Entre los principales monómeros funcionales empleados para la síntesis de MIP no covalentes se encuentran el ácido metacrílico (*methacrylic acid*, MAA), la 4-vinilpiridina, el 2-hidroxietil metacrilato, o la acrilamida; mientras que el EDMA, el trimetacrilato de trimetilolpropano o el DVB son los agentes entrecruzantes habituales (**Figura 3.9**).

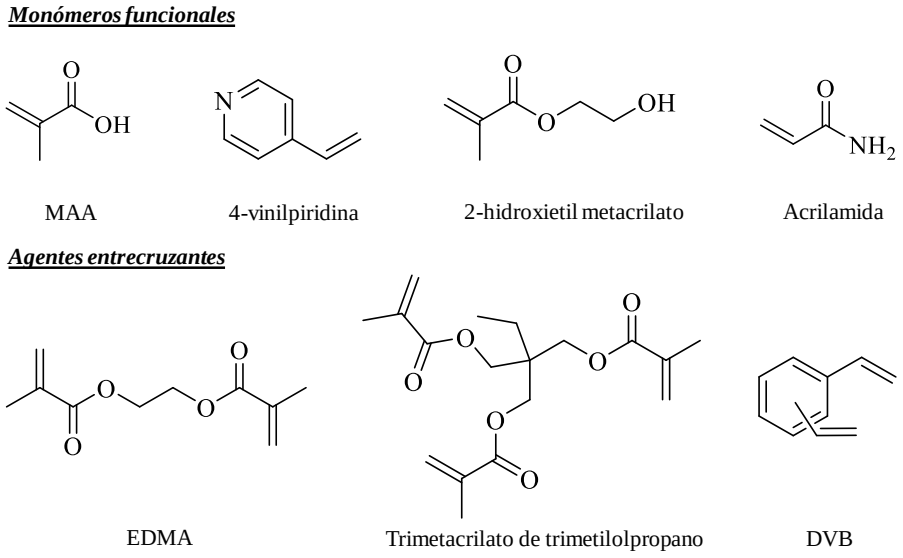

Figura 3.9. Estructuras de los principales monómeros funcionales y agentes entrecruzantes utilizados en la síntesis de MIP.

Por otra parte, la elección del disolvente porogénico es crucial para la síntesis efectiva del MIP, ya que es determinante en la interacción T-M [69]. De hecho, el disolvente puede no solo favorecer o reducir la formación del complejo T-M, sino también las interacciones intramoleculares (T-T, M-M) y/o dentro de la misma molécula. Así pues, si las uniones T-M se establecen por puentes de hidrógeno, es preferible el uso de disolventes apróticos como el ACN o el $CHCl_3$ frente agua o MeOH, ya que estos últimos competirían con los puntos de interacción de la molécula plantilla y como resultado, el reconocimiento molecular se vería mermado [70].

Cabe destacar que, determinados MIP se comportan también de manera selectiva frente a compuestos estructuralmente análogos a la molécula plantilla [31, 32]. Este fenómeno, conocido como “reactividad cruzada”, puede resultar de interés para el aislamiento selectivo de una familia de compuestos de estructura similar.

En el caso particular de los PL, existen muy pocos estudios relativos a técnicas de impronta molecular. Pegoraro *et al*. [71] han llevado a cabo la síntesis de membranas de poli(etilen-*co*-vinil alcohol) empleando PC como molécula plantilla, mientras que Jang *et al*. han desarrollado capilares recubiertos con una final película sobre su superficie interna para CEC empleando un monolito base de MAA-EDMA y *S*-ketoprofeno como *dummy template* para la separación de mezclas de PL [72]. En cualquier caso, la aplicación de la tecnología de impronta molecular con fines preparativos para PL se halla muy poco extendida.

En el **Capítulo 7** de esta Tesis, se describe la síntesis de un MIP, empleando PC como molécula plantilla, para el aislamiento selectivo de los PL de extractos de grasa de leche materna.

3. 4. 4. Estructuras metal-orgánicas

Pese a que las estructuras metal-orgánicas (*metal-organic framework*, MOF) no han tenido cabida en esta Tesis, cabe hacer alusión a ellas debido a que son un tipo de materiales porosos en auge en el campo de la Química Analítica. Los MOF consisten en una red auto-ensamblada de cationes metálicos y ligandos orgánicos (electrodadores) a través de enlaces de coordinación. La gran variedad de iones metálicos y ligandos orgánicos disponibles y las múltiples maneras de combinarlos permiten obtener diferentes diámetros de poro, así como modificar el tamaño de las cavidades dentro de la estructura tridimensional. De hecho, su capacidad de ser modificados junto con su gran área superficial (de 1000 a 10000 m^2/g [73]) y la potencial funcionalización de su estructura interna, así como su estabilidad térmica y química, han puesto en primera línea el empleo de MOF en diversas aplicaciones analíticas [11,74,75].

Pese a sus buenas características, el uso directo de MOF como micro-/nano-cristales está de algún modo limitado, ya que su empaquetamiento para

cartuchos de SPE no es sencillo y su separación en SPE dispersiva implica etapas de centrifugación o filtración. Por este motivo el uso de MOF para SPE tiene lugar, por lo general, en combinación con diferentes soportes, si bien es cierto que algunos MOF recientemente sintetizados están paliando dichos inconvenientes (p.ej. MOF magnéticos [74]).

3. 5. Referencias

[1] Z. Lin, F. Yang, X. He, X. Zhao, Y. Zhang, Preparation and evaluation of a macroporous molecularly imprinted hybrid silica monolithic column for recognition of proteins by high performance liquid chromatography, J. Chromatogr. A 1216 (2009) 8612–8622. doi:10.1016/j.chroma.2009.10.025.

[2] N.J.K. Simpson, Solid-Phase Extraction. Principles, Techniques and Applications, Marcel Dekker, Inc., New York, 2000.

[3] Lane C. Sander, Silica-based solid phase extraction, en: M.J. Telepchak, T.F. August, G. Chaney (Eds.), Forensic Clin. Appl. Solid Phase Extr., Humana Press Inc., Totowa, New Jersey, 2004: págs. 41–53.

[4] T. Nema, The application of silica monolith for solid phase extraction, National University of Singapore, 2011.

[5] C.W. Huck, G.K. Bonn, Recent developments in polymer-based sorbents for solid-phase extraction, J. Chromatogr. A 885 (2000) 51–72. doi:10.1016/S0021-9673(00)00333-2.

[6] C. Buzea, I.I. Pacheco, K. Robbie, Nanomaterials and nanoparticles: Sources and toxicity, Biointerphases 2 (2007) MR17-MR71. doi:10.1116/1.2815690.

[7] M. Ahmadi, H. Elmongy, T. Madrakian, M. Abdel-Rehim, Nanomaterials as sorbents for sample preparation in bioanalysis : A review, Anal. Chim. Acta 958 (2017) 1–21. doi:10.1016/j.aca.2016.11.062.

[8] L. Xu, X. Qi, X. Li, Y. Bai, H. Liu, Recent advances in applications of nanomaterials for sample preparation, Talanta 146 (2016) 714–726. doi:10.1016/j.talanta.2015.06.036.

[9] B. Hu, M. He, B. Chen, Nanometer-sized materials for solid-phase extraction of trace elements, Anal. Bioanal. Chem. 407 (2015) 2685–2710. doi:10.1007/s00216-014-8429-9.

[10] J. Płotka-Wasylka, N. Szczepańska, M. de la Guardia, J. Namieśnik, Modern trends in solid phase extraction: new sorbent media, TrAC - Trends Anal. Chem. 77 (2015) 23–43. doi:10.1016/j.trac.2015.10.010.

[11] J. González-Sálamo, B. Socas-Rodríguez, J. Hernández-Borges, M.Á. Rodríguez-Delgado, Nanomaterials as sorbents for food sample analysis, TrAC - Trends Anal. Chem. 85 (2016) 203–220. doi:10.1016/j.trac.2016.09.009.

[12] J. Tian, J. Xu, F. Zhu, T. Lu, C. Su, G. Ouyang, Application of nanomaterials in sample preparation, J. Chromatogr. A 1300 (2013) 2–16. doi:10.1016/j.chroma.2013.04.010.

[13] C.T. Kresge, M.E. Leonowicz, W.J. Roth, J.C. Vartuli, J.S. Beck, Ordered mesoporous molecular sieves synthesized by a liquid-crystal template mechanism, Nature 359 (1992) 710–712. doi:10.1038/359710a0.

[14] R. Luque, A.M. Balu, J.M. Campelo, M.D. Gracia, E. Losada, A. Pineda, A.A. Romero, J.C. Serrano-Ruiz, Catalytic applications of mesoporous silica-based materials, Catalysis. 24 (2012) 253–280. doi:10.1039/9781849734776.

[15] Z. Li, J.C. Barnes, A. Bosoy, J.F. Stoddart, J.I. Zink, Mesoporous silica nanoparticles in biomedical applications, Chem. Soc. Rev. 41 (2012) 2590–2605. doi:10.1039/c1cs15246g.

[16] N. Casado, D. Pérez-Quintanilla, S. Morante-Zarcero, I. Sierra, Current development and applications of ordered mesoporous silicas and other sol–gel silica-based materials in food sample preparation for xenobiotics analysis, TrAC - Trends Anal. Chem. 88 (2017) 167–184.

doi:10.1016/j.trac.2017.01.001.

[17] A. Walcarius, M.M. Collinson, Analytical chemistry with silica sol-gels: traditional routes to new materials for chemical analysis, Annu. Rev. Anal. Chem. 2 (2009) 121–143. doi:10.1146/annurev-anchem-060908-155139.

[18] D. Zhao, J. Feng, Q. Huo, N. Melosh, G.H. Fredrickson, B.F. Chmelka, G.D. Stucky, Triblock copolymer syntheses of mesoporous silica with periodic 50 to 300 angstrom pores, Science (80-.). 279 (1998) 548–552. doi:10.1126/science.279.5350.548.

[19] J. El Haskouri, D. Ortiz de Zárate, C. Guillem, J. Latorre, M. Caldés, A. Beltrán, D. Beltrán, A.B. Descalzo, G. Rodríguez-López, R. Martínez-Máñez, M.D. Marcos, P. Amorós, Silica-based powders and monoliths with bimodal pore systems, Chem. Commun. 0 (2002) 330–331. doi:10.1039/b110883b.

[20] M.C. Llinàs, D. Sánchez-García, Nanopartículas de sílice: preparación y aplicaciones en biomedicina, AFINIDAD LXXI. 565 (2014) 20–31.

[21] A.M. Morgues Bartolomé, High accesibility and chemical homogeneity in mesoporous materials: silicas, gold-containing composites and phosphates, Universitat de València, 2015.

[22] L.T. Gibson, Mesosilica materials and organic pollutant adsorption: part B removal from aqueous solution, Chem. Soc. Rev. 43 (2014) 5173–5182. doi:10.1039/C3CS60095E.

[23] L.T. Gibson, Mesosilica materials and organic pollutant adsorption: part A removal from air, Chem. Soc. Rev. 43 (2014) 5163–5172. doi:10.1039/C3CS60096C.

[24] X.-M. Wang, X.-Z. Du, H.-H. Rao, X.-Q. Lu, Determination of polycyclic aromatic hydrocarbons in water by a novel mesoporous-coated stainless steel wire microextraction combined with HPLC, J.

Sep. Sci. 33 (2010) 3239–3244. doi:10.1002/jssc.201000287.

[25] W. Cheng, H. Ma, L. Zhang, Y. Wang, Hierarchically imprinted mesoporous silica polymer: An efficient solid-phase extractant for bisphenol A, Talanta 120 (2014) 255–261. doi:10.1016/j.talanta.2013.12.001.

[26] L.J. Huerta, P. Amorós, D. Beltrán-Porter, V.C. Corberán, Selective oxidative activation of isobutane on a novel vanadium-substituted bimodal mesoporous oxide V-UVM-7, Catal. Today 117 (2006) 180–186. doi:10.1016/j.cattod.2006.05.016.

[27] A.B. Descalzo, M.D. Marcos, R. Martínez-Máñez, J. Soto, D. Beltrán, P. Amorós, Anthrylmethylamine functionalised mesoporous silica-based materials as hybrid fluorescent chemosensors for ATP, J. Mater. Chem. 15 (2005) 2721–2731. doi:10.1039/b501609f.

[28] A. Weller, E.J. Carrasco-Correa, C. Belenguer-Sapiña, A. de los Reyes Mauri-Aucejo, P. Amorós, J.M. Herrero-Martínez, Organo-silica hybrid capillary monolithic column with mesoporous silica particles for separation of small aromatic molecules, Microchim. Acta 184 (2017) 3799–3808. doi:10.1007/s00604-017-2404-z.

[29] H. Oberacher, C.G. Huber, Capillary monoliths for the analysis of nucleic acids by high-performance liquid chromatography-electrospray ionization mass spectrometry, TrAC - Trends Anal. Chem. 21 (2002) 166–174. doi:10.1016/S0165-9936(02)00304-7.

[30] K. Nakanishi, H. Minakuchi, N. Soga, N. Tanaka, Double pore silica gel monolith applied to liquid chromatography, J. Sol-Gel Sci. Technol. 8 (1997) 547–552. doi:10.1007/BF02436897.

[31] I. Nischang, Porous polymer monoliths: Morphology, porous properties, polymer nanoscale gel structure and their impact on chromatographic performance, J. Chromatogr. A 1287 (2013) 39–58.

doi:10.1016/j.chroma.2012.11.016.

[32] T. Nema, E.C.Y. Chan, P.C. Ho, Application of silica-based monolith as solid phase extraction cartridge for extracting polar compounds from urine, Talanta 82 (2010) 488–494. doi:10.1016/j.talanta.2010.04.063.

[33] X. Ma, M. Zhao, F. Zhao, H. Guo, J. Crittenden, Y. Zhu, Y. Chen, Application of silica-based monolith as solid-phase extraction sorbent for extracting toxaphene congeners in soil, J. Sol-Gel Sci. Technol. 80 (2016) 87–95. doi:10.1007/s10971-016-4054-8.

[34] J. Huang, S.R. Turner, Hypercrosslinked polymers: A review, Polym. Rev. 58 (2018) 1–41. doi:10.1080/15583724.2017.1344703.

[35] Z. Zajickova, Advances in the development and applications of organic-silica hybrid monoliths, J. Sep. Sci. 00 (2016) 1–24. doi:10.1002/jssc.201600774.

[36] Y. Lv, F.M. Alejandro, J.M.J. Fréchet, F. Švec, Preparation of porous polymer monoliths featuring enhanced surface coverage with gold nanoparticles, J. Chromatogr. A 1261 (2012) 121–128. doi:10.1016/j.chroma.2012.04.007.

[37] N. Fontanals, R.M. Marcé, F. Borrull, P.A.G. Cormack, Hypercrosslinked materials: preparation, characterisation and applications, Polym. Chem. 6 (2015) 7231–7244. doi:10.1039/c5py00771b.

[38] D. Bratkowska, A. Davies, P.A.G. Cormack, F. Borrull, D.C. Sherrington, R.M. Marcé, Hypercrosslinked strong anion-exchange resin for extraction of acidic pharmaceuticals from environmental water, J. Sep. Sci. 00 (2012) 1–8. doi:10.1002/jssc.201200451.

[39] D. Bratkowska, N. Fontanals, F. Borrull, P.A.G. Cormack, D.C. Sherrington, R.M. Marcé, Hydrophilic hypercrosslinked polymeric

sorbents for the solid-phase extraction of polar contaminants from water, J. Chromatogr. A 1217 (2010) 3238–3243. doi:10.1016/j.chroma.2009.08.091.

[40] T. Wang, Y. Chen, J. Ma, M. Chen, C. Nie, M. Hu, Y. Li, Z. Jia, J. Fang, H. Gao, Ampholine-functionalized hybrid organic-inorganic silica material as sorbent for solid-phase extraction of acidic and basic compounds, J. Chromatogr. A 1308 (2013) 63–72. doi:10.1016/j.chroma.2013.08.025.

[41] L. Zhang, B. Chen, H. Peng, M. He, B. Hu, Aminopropyltriethoxysilane-silica hybrid monolithic capillary microextraction combined with inductively coupled plasma mass spectrometry for the determination of trace elements in biological samples, J. Sep. Sci. 34 (2011) 2247–2254. doi:10.1002/jssc.201100173.

[42] L.M. Ravelo-Pérez, A. V Herrera-Herrera, J. Hernández-Borges, M.Á. Rodríguez-Delgado, Carbon nanotubes: Solid-phase extraction, J. Chromatogr. A 1217 (2010) 2618–2641. doi:10.1016/j.chroma.2009.10.083.

[43] B. Socas-Rodríguez, A. V Herrera-Herrera, M. Asensio-Ramos, J. Hernández-Borges, Recent applications of carbon nanotube sorbents in Analytical Chemistry, J. Chromatogr. A 1357 (2014) 110–146. doi:10.1016/j.chroma.2014.05.035.

[44] Hawk's Perch Technical Writing-LLC, Nanoparticle applications and uses, (2016). Disponible en: http://www.understandingnano.com/ nanoparticles.html (Fecha de acceso: 05/07/2018).

[45] E.J. Carrasco-Correa, G. Ramis-Ramos, J.M. Herrero-Martínez, Hybrid methacrylate monolithic columns containing magnetic nanoparticles for capillary electrochromatography, J. Chromatogr. A

1385 (2015) 77–84. doi:10.1016/j.chroma.2015.01.044.

[46] C. Acquah, E.M. Obeng, D. Agyei, C.M. Ongkudon, C.K.S. Moy, M.K. Danquah, Nano-doped monolithic materials for molecular separation, Separations. 4 (2017) 2–22. doi:10.3390/separations4010002.

[47] M. Navarro-Pascual-Ahuir, M.J. Lerma-García, G. Ramis-Ramos, E.F. Simó-Alfonso, J.M. Herrero-Martínez, Preparation and evaluation of lauryl methacrylate monoliths with embedded silver nanoparticles for capillary electrochromatography, Electrophoresis 34 (2013) 925–934. doi:10.1002/elps.201200408.

[48] M.R. Buchmeiser, Polymeric monolithic materials: Syntheses, properties, functionalization and applications, Polymer. 48 (2007) 2187–2198. doi:10.1016/j.polymer.2007.02.045.

[49] M. Rainer, H. Sonderegger, R. Bakry, C.W. Huck, S. Morandell, L.A. Huber, D.T. Gjerde, G.K. Bonn, Analysis of protein phosphorylation by monolithic extraction columns based on poly(divinylbenzene) containing embedded titanium dioxide and zirconium dioxide nano-powders, Proteomics. 8 (2008) 4593–4602. doi:10.1002/pmic.200800448.

[50] S. Hussain, Y. Güzel, S.A. Schönbichler, M. Rainer, C.W. Huck, G.K. Bonn, Solid-phase extraction method for the isolation of plant thionins from European mistletoe, wheat and barley using zirconium silicate embedded in poly(styrene-co-divinylbenzene) hollow-monoliths, Anal. Bioanal. Chem. 405 (2013) 7509–7521. doi:10.1007/s00216-013-7202-9.

[51] Q. Cao, Y. Xu, F. Liu, F. Švec, J.M.J. Fréchet, Polymer monoliths with exchangeable chemistries: use of gold nanoparticles as intermediate ligands for capillary columns with varying surface functionalities,

Anal. Chem. 82 (2010) 7416–7421. doi:10.1021/ac1015613.

[52] M. Vergara-Barberán, M.J. Lerma-García, E.F. Simó-Alfonso, J.M. Herrero-Martínez, Solid-phase extraction based on ground methacrylate monolith modified with gold nanoparticles for isolation of proteins, Anal. Chim. Acta 917 (2016) 37–43. doi:10.1016/j.aca.2016.02.043.

[53] M. Vergara-Barberán, M.J. Lerma-García, E.F. Simó-Alfonso, J.M. Herrero-Martínez, Polymeric sorbents modified with gold and silver nanoparticles for solid-phase extraction of proteins followed by MALDI-TOF analysis, Microchim. Acta 184 (2017) 1683–1690. doi:10.1007/s00604-017-2168-5.

[54] M. Wierucka, M. Biziuk, Application of magnetic nanoparticles for magnetic solid-phase extraction in preparing biological, environmental and food samples, TrAC - Trends Anal. Chem. 59 (2014) 50–58. doi:10.1016/j.trac.2014.04.007.

[55] I.S. Ibarra, J.A. Rodriguez, C.A. Galán-Vidal, A. Cepeda, J.M. Miranda, Magnetic solid phase extraction applied to food analysis, J. Chem. 2015 (2015) 1–13. doi:10.1155/2015/919414.

[56] S. Laurent, D. Forge, M. Port, A. Roch, C. Robic, L. Vander Elst, R.N. Muller, Magnetic iron oxide nanoparticles: Synthesis, stabilization, vectorization, physicochemical characterizations and biological applications, Chem. Rev. 108 (2008) 2064–2110. doi:10.1021/cr068445e.

[57] E. Kadar, Í.L. Batalha, A. Fisher, A.C.A. Roque, The interaction of polymer-coated magnetic nanoparticles with seawater, Sci. Total Environ. 487 (2014) 771–777. doi:10.1016/j.scitotenv.2013.11.082.

[58] A.H. Lu, E.L. Salabas, F. Schüth, Magnetic nanoparticles: Synthesis, protection, functionalization, and application, Angew. Chemie Int. Ed.

46 (2007) 1222–1244. doi:10.1002/anie.200602866.

[59] L. Weng, W.H. Van Riemsdijk, T. Hiemstra, Factors controlling phosphate interaction with iron oxides, J. Environ. Qual. 41 (2012) 628–635. doi:10.2134/jeq2011.0250.

[60] S. Zhang, H. Niu, Y. Zhang, J. Liu, Y. Shi, X. Zhang, Y. Cai, Biocompatible phosphatidylcholine bilayer coated on magnetic nanoparticles and their application in the extraction of several polycyclic aromatic hydrocarbons from environmental water and milk samples, J. Chromatogr. A 1238 (2012) 38–45. doi:10.1016/j.chroma.2012.03.056.

[61] J. Krenkova, F. Foret, Iron oxide nanoparticle coating of organic polymer-based monolithic columns for phosphopeptide enrichment, J. Sep. Sci. 34 (2011) 2106–2112. doi:10.1002/jssc.201100256.

[62] J. Krenkova, F. Foret, Nanoparticle-modified monolithic pipette tips for phosphopeptide enrichment, Anal. Bioanal. Chem. 405 (2013) 2175–2183. doi:10.1007/s00216-012-6358-z.

[63] S. Meseguer-Lloret, S. Torres-Cartas, M. Catalá-Icardo, E.F. Simó-Alfonso, J.M. Herrero-Martínez, Extraction and preconcentration of organophosphorus pesticides in water by using a polymethacrylate-based sorbent modified with magnetic nanoparticles, Anal. Bioanal. Chem. 409 (2017) 3561–3571. doi:10.1007/s00216-017-0294-x.

[64] G. Vasapollo, R. Del Sole, L. Mergola, M.R. Lazzoi, A. Scardino, S. Scorrano, G. Mele, Molecularly imprinted polymers: Present and future prospective, Int. J. Mol. Sci. 12 (2011) 5908–5945. doi:10.3390/ijms12095908.

[65] K. Haupt, A.V. Linares, M. Bompart, B.T.S. Bui, Molecular Imprinting. Topics in Current Chemistry, vol 325, en: K. Haupt (Ed.), Mol. Imprinted Polym., Springer, Berlin, Heidelberg, 2011.

[66] H.S. Andersson, I.A. Nicholls, Spectroscopic evaluation of molecular imprinting polymerization systems, Bioorg. Chem. 25 (1997) 203–211. doi:10.1006/bioo.1997.1067.

[67] M.C. Cela-Pérez, A. Lasagabáster-Latorre, M.J. Abad-López, J.M. López-Vilariño, M. V. Gónzalez-Rodríguez, A study of competitive molecular interaction effects on imprinting of molecularly imprinted polymers, Vib. Spectrosc. 65 (2013) 74–83. doi:10.1016/j.vibspec.2012.12.002.

[68] P.A.G. Cormack, A.Z. Elorza, Molecularly imprinted polymers: Synthesis and characterisation, J. Chromatogr. B 804 (2004) 173–182. doi:10.1016/j.jchromb.2004.02.013.

[69] X. Song, J. Wang, J. Zhu, Effect of porogenic solvent on selective performance of molecularly imprinted polymer for quercetin, Mater. Res. 12 (2009) 299–304. doi:10.1590/S1516-14392009000300009.

[70] M. Ávila, M. Zougagh, A. Escarpa, Á. Ríos, Molecularly imprinted polymers for selective piezoelectric sensing of small molecules, TrAC - Trends Anal. Chem. 27 (2008) 54–65. doi:10.1016/j.trac.2007.10.009.

[71] C. Pegoraro, D. Silvestri, G. Ciardelli, C. Cristallini, N. Barbani, Molecularly imprinted poly(ethylene-co-vinyl alcohol) membranes for the specific recognition of phospholipids, Biosens. Bioelectron. 24 (2008) 748–755. doi:10.1016/j.bios.2008.06.050.

[72] R. Jang, K.H. Kim, S.A. Zaidi, W.J. Cheong, M.H. Moon, Analysis of phospholipids using an open-tubular capillary column with a monolithic layer of molecularly imprinted polymer in capillary electrochromatography-electrospray ionization-tandem mass spectrometry, Electrophoresis 32 (2011) 2167–2173. doi:10.1002/elps.201100205.

[73] S.M. Cohen, Postsynthetic methods for the functionalization of metal-organic frameworks, Chem. Rev. 112 (2012) 970–1000. doi:10.1021/cr200179u.

[74] F. Maya, C. Palomino Cabello, R.M. Frizzarin, J.M. Estela, G. Turnes Palomino, V. Cerdà, Magnetic solid-phase extraction using metal-organic frameworks (MOFs) and their derived carbons, TrAC - Trends Anal. Chem. 90 (2017) 142–152. doi:10.1016/j.trac.2017.03.004.

[75] P. Rocío-Bautista, I. Pacheco-Fernández, J. Pasán, V. Pino, Are metal-organic frameworks able to provide a new generation of solid-phase microextraction coatings? – A review, Anal. Chim. Acta 939 (2016) 26–41. doi:10.1016/j.aca.2016.07.047.

BLOQUE II. ANÁLISIS DE LA FRACCIÓN LIPÍDICA DE LA LECHE MATERNA

CAPÍTULO 4

Triacylglycerol analysis in human milk and other mammalian species: small-scale sample preparation, characterization and statistical classification using HPLC-ELSD profiles

JOURNAL OF AGRICULTURAL AND FOOD CHEMISTRY

Article

pubs.acs.org/JAFC

Triacylglycerol Analysis in Human Milk and Other Mammalian Species: Small-Scale Sample Preparation, Characterization, and Statistical Classification Using HPLC-ELSD Profiles

Isabel Ten-Doménech,[†] Eduardo Beltrán-Iturat,[§] José Manuel Herrero-Martínez,*[,†] Juan Vicente Sancho-Llopis,[§] and Ernesto Francisco Simó-Alfonso[†]

[†]Department of Analytical Chemistry, Faculty of Chemistry, University of Valencia, C. Dr. Moliner 50, E-46100 Burjassot, Valencia, Spain

[§]Research Institute for Pesticides and Water, University Jaume I, E-12071 Castellón, Spain

In this work, a method for the separation of TAGs present in human milk and other mammalian species by reversed-phase high performance liquid chromatography using a core-shell particle packed column with UV and evaporative light-scattering detectors is described. Under optimal conditions, a mobile phase containing acetonitrile/*n*-pentanol at 10 ºC gave an excellent resolution between more than 50 TAG peaks. A small-scale method for fat extraction in these milks (particularly of interest for human milk samples) using minimal amounts of sample and reagents was also developed. The proposed extraction protocol and the traditional method were compared, giving similar results, with respect to the total fat and relative TAG contents. Finally, a statistical study based on linear discriminant analysis on the TAG composition of different types of milks (human, cow, sheep and goat) was carried out to differentiate the samples according to its mammalian origin.

Keywords: Human milk; Mammalian milk triacylglycerols; Fat extraction; HPLC-ELSD; Linear Discriminant Analysis.

4. 1. Introduction

According to the World Health Organization, breastfeeding is the recommended way of providing to young infants the nutrients for a healthy growth and development. This recommendation is based on knowledge that breast milk from healthy and well-fed mothers, provides sufficient energy and proper profile of nutrients to support normal growth and development of term infants, without any additional foods through the first 4 to 6 months of life [1]. Human milk constitutes a very complex fluid, which contains carbohydrates and salts in solution, caseins in colloidal dispersion, cells and cellular debris, and lipids mostly in emulsified globules [2]. Since lipids are the main energy source in human milk, contributing in 40-55% to the total energy intake, its compositional and physiological aspects have been of interest and research in the last decades and recently reviewed [3]. According to Koletzko *et al*. [4], the average amount of fat contained in human milk is *ca*. 3.8-3.9 g/100 mL, but this value varies widely. Thus, human milk is a dynamic system whose lipid composition is influenced by factors such as mother's diet [5], stage of lactation [6,7], phase of the feeding [2] and breast [2,8]. However, any difference has been observed with regard to frequency of breastfeedings [9,10] and time of day [11,12].

In spite of the good features in human milk, research to find valuable alternatives, especially when breastfeeding is not possible or may not be advisable, constitutes a high priority. To be nutritionally adequate, any substitute should have the same nutritional characteristics as breast milk. In addition, it should be hypoallergenic and palatable [13]. In this sense, commercial infant formulas, usually based on mammalian milks such as cow, buffalo, donkey, sheep, camel, and goat milk, may represent an alternative to fulfill the nutritional needs of newborns [14].

However, these milks are different from human milk in terms of chemical composition (e.g., protein and fat contents), which may cause

nutritional and immunological problems [15]. Regarding fat content, limited studies have been done so far to systematically compare the lipid composition in different mammalian milks [14].

TAGs represent 98% of total lipid fraction, and despite the changes in human milk composition, some TAGs, such as lauric acid-oleic acid-linoleic acid (LaOL), myristic acid-oleic acid-linoleic acid (MOL), can be considered as markers of the mature human milk [16]. Moreover, FAs represent 90% of these TAGs, that is, 88% of total lipid [2], and a balance ratio between ω-3 and ω-6 FAs in human milk is important to ensure the healthy growth of infants [14]. Although the analysis of FAs in human milk is much easier than TAGs evaluation, milk FAs are secreted, consumed and hydrolyzed as TAGs in globules [2]. For this reason, it is of great importance to achieve a reliable TAGs determination.

The most widely used techniques for fat extraction are based on the method developed by Folch *et al*. [17], or its modification, developed by Chen *et al*. [18]; and the AOAC Official Method 989.05 [19] based on the study of Barbano *et al*. [20]. Nevertheless, these extraction methods are time-consuming and therefore, its automation is barely possible. Modern trends in analytical chemistry move towards the simplification and miniaturization of sample preparation. This can be simply achieved by scaling down the size of previous systems or by developing new set ups and techniques [21]. Different extraction methods to accelerate and miniaturize the process (sample size and organic solvent volumes), searching for cost-effective solutions have been evaluated [22]. In spite of these benefits, few protocols [23] have been developed in human milk matrices to cover this demand.

Regarding TAGs determination in milk, several techniques such as, TLC [7,24], silver ion adsorption-TLC [25], RP-HPLC [16,23,26–28], or with Ag-HPLC [14,29], 2D-LC [30], GC [25] and tandem MS with ammonia negative ion chemical ionization [31], have been employed. From all these

techniques, RP-HPLC has been widely used, since it provides a better resolution of individual TAG molecules. Thus, these compounds are separated according to both chain length and degree of unsaturation of the FAs [32]. However, RP-HPLC for TAGs separation has been usually performed using a binary gradient ACN-isopropanol [14,27], or a linear ternary gradient ACN-dichloromethane-acetone [16,23,28]. These latter gradients led to low resolution of TAGs peaks, and the first-mentioned gave long analysis time (90 min).

In order to improve chromatographic performance in terms of throughput and/or resolution, particularly when numerous complex food extracts have to be analyzed, recent advances in LC instrumentation could be beneficial [33]. In this context several analytical strategies related to column technology have been developed in HPLC, including the use of monolithic supports, packed columns with sub-2 μm particles operating at ultra-high pressure (Ultra high performance liquid chromatography, UHPLC) or with core-shell or fused-core particles. These latter core-shell particle columns are capable of maintaining high efficiencies at increasing flow rates with the subsequent reduction of analysis time. Also, these columns operate comfortably within the pressure limits of conventional LC instruments, rivaling the performance obtained with sub-2 columns on UHPLC instruments. However, the use of these columns in conventional LC systems for TAGs separation in human milk samples has not been reported to date.

Multivariate data analysis can be used to obtain more information on major, minor, and trace components in foods [34,35]. Within these statistical tools, linear discriminant analysis (LDA) is probably one of the best known methods and it has been successfully used for the identification/differentiation of several foods, such as dairy products, oils, wines and others [36,37].

In this work, the development of analytical conditions for the extraction and RP-HPLC separation of milk fat TAGs is described. For this

purpose, a small-scale fat extraction protocol (with reduced consumption of reagents and processing time, in consistency with the recent trends in green chemistry) and in combination with the use of a fused-core HPLC column is presented and compared. In addition, on the basis of TAG profiles of milk samples from different mammalian species (human, bovine, caprine and ovine), a LDA model is applied to differentiate these matrices according to its species origin.

4. 2. Materials and methods

4. 2. 1. Chemicals

TAG standards including trilaurin (LaLaLa), trimyristin (MMM), tripalmitin (PPP), tripalmitolein (PaPaPa) and triolein (OOO) from Sigma (St. Louis, MO, USA) were employed. The following analytical grade reagents were also used: HPLC-grade ACN and MeOH were purchased from VWR Chemicals (Barcelona, Spain); reagent-grade dichloromethane, *n*-pentanol and *n*-hexane, HPLC-grade 2-propanol and *n*-butanol and anhydrous sodium sulfate, were supplied by Scharlau (Barcelona, Spain). Butylhydroxytoluene (BHT) was purchased from Fluka (Buchs SG, Switzerland).

4. 2. 2. Samples

Human milk samples (n = 15) were kindly donated by healthy well-nourished mothers in different stages of lactation (3 colostrum (1-5 days); 5 transitional milk (6-15 days); 7 mature milk (after 16 days)). All mothers, who were Caucasian, middle-class, and lived within the urban area of Valencia, consumed an unrestricted omnivorous diet. The samples were collected between the baby's feed by manual expression using a Medela Harmony™ Breastpump (Zug, Switzerland).

Bulk raw milk samples of Holstein-Friesian cows (n = 20) were collected by milking machines while milk samples of Cartera goats (n = 20) and Murciano-Granadina sheeps (n = 20) were collected by manual expression from animals in midlactation stage. All these samples were kindly donated by different farms located at *La Comunitat Valenciana*, Spain. All animals were free from mastitis or any other inflammatory diseases. They were grazed in the morning and in the afternoon were reared in stables and fed with hay, fodder grass and vegetables. After collection, milk samples were rapidly heated to 80 ºC and held at this temperature for 1.5 min in order to inactivate the lipases and to avoid TAGs hydrolysis [38].

4. 2. 3. Sample preparation

A lipid extraction method (Method I) was developed in this study. It consisted of a modification of the traditional gravimetric method [16]. Briefly, a well-mixed milk aliquot (150 µL) was placed in a centrifuge tube and 2.5 mL of a dichloromethane-MeOH solution (2:1, v/v), containing 5 µg/mL BHT to prevent lipid oxidation [24], was added. The mixture was sonicated for 10 min, vortexed for 1 min, placed in the fridge (4 ºC) for 15 min and centrifuged at 10000 rpm for 8 min. Then, 800 µL of distilled water was added, sonicated for 10 min, mixed for 1 min in the vortex and centrifuged at 10000 rpm for 8 min. The organic layer was washed with 800 µL of a saturated solution of sodium chloride, sonicated for 10 min, vortexed for 1 min and centrifuged 8 min at 10000 rpm. The organic fraction was dried with anhydrous sodium sulfate and the fat solution was then filtered with a syringe through a 0.45 µm filter, collected in a pre-weigh HPLC vial and dried under a nitrogen stream. The fat was dissolved in a 2:2:1 ACN/2-propanol/*n*-hexane (v/v/v) ternary mixture and injected in the LC system. This method was compared with that described by Morera *et al*. [16] (Method II).

4. 2. 4. High-performance liquid chromatography and mass spectrometry

An 1100 series liquid chromatograph (Agilent Technologies, Waldbronn, Germany) provided with a quaternary pump, a degasser, a thermostated column compartment, an automatic sampler, a UV-Vis diode array detector online coupled to an Agilent 385-ELSD was employed. Separation was carried out with a Kinetex™ C18 100 Å column (150 mm × 4.6 mm, 2.6 µm; Phenomenex, Torrance, CA, USA). The optimized separation conditions were: isocratic elution with a 80:20 ACN/*n*-pentanol mixture for 45 min, followed by a gradient of ACN/*n*-pentanol up to ratio 60:40 in 20 min; column temperature, 10 ºC; flow rate, 1.0 mL/min and injection volume, 10 µL. UV detection was performed at 205 ± 10 nm (360 ± 60 nm as reference). The ELSD parameters were: evaporation and nebulization temperature, 55 ºC; gas flow rate, 1.2 Standard Liters per Minute (SLM); gain factor, 1.

For TAG identification, a UPLC™ binary pump system (Acquity, Waters, Milford, USA) was interfaced to a triple quadrupole mass spectrometer (TQD, Waters, Manchester, UK) through an Atmospheric Pressure Chemical Ionization (APCI) source. The MS working conditions were as follows: probe temperature, 600 ºC; corona discharge current, 20 µA; source temperature: 120 ºC; desolvation gas flow, 800 L/h; cone gas flow, 60 L/h. Drying as well as nebulizing gas was nitrogen (Praxair, Valencia, Spain). The mass spectrometer scanned within the m/z 150-1000 range in the positive ionization mode at one scan per second.

4. 2. 5. Data treatment and statistical analysis

The area of selected TAG peaks was measured from ELSD detector, and a data matrix was constructed (see Results and Discussion Section). After

normalization of the variables, statistical data treatment was performed using SPSS (v. 15.0, Statistical Package for the Social Sciences, Chicago, IL, USA). Using a stepwise algorithm, the predictors to be included in the LDA model were selected. According to this algorithm, a predictor is considerable eligible for its inclusion in the model if the significance of its F-test exceeds the specified probability level given by the entrance threshold, F_{in}. However, the entrance of a new predictor modifies the significance of those predictors that are already present in the model. For this reason, after the inclusion of a new predictor, a rejection threshold, F_{out}, is used to decide if one of the other predictors should be removed from the model. This sequential process continues until no more predictors are eligible for entrance or removal from the model. The default probability values of F_{in} and F_{out}, 0.05 and 0.10, respectively, were adopted.

4. 3. Results and discussion

4. 3. 1. Optimization of the separation of TAGs

The initial separation conditions were adapted from a previous work for TAGs separation in vegetables oils [39]. The optimization study was performed using human milk samples. Using a flow rate of 1.5 mL/min and a column temperature of 10 ºC, a similar optimization study of mobile phase, including several binary mixtures of ACN with different alcohols (2-propanol, *n*-butanol and *n*-pentanol) at 70:30 ratio, was conducted. Using 2-propanol, poor resolution and relative long analysis time (*ca*. 50 min) were obtained. Using *n*-butanol and *n*-pentanol, analysis time and resolution improved significantly, although most peaks still overlapped. Despite this overlapping, ACN/*n*-pentanol mixture gave shorter analysis time with respect to *n*-butanol and therefore, *n*-pentanol was selected for the following studies.

Next, the influence of the content of *n*-pentanol in the 20-30% range on TAGs separation was studied. As shown in **Figure S4.1** (see Supporting Information), resolution was improved with decreasing of *n*-pentanol content. Broad peaks with separation times higher than 45 min were obtained with less than 20% *n*-pentanol. Thus, an 80:20 (v/v) ACN/*n*-pentanol mixture was selected. This mobile phase also provided a satisfactory response in ELSD. Then, the effect of column temperature on TAGs separation and detection response of UV (**Figure S4.2**, left) and ELSD (**Figure S4.2**, right) detectors was performed under isocratic conditions. As it can be seen, the TAG resolution increased when temperature decreased, with a concomitant increase both in backpressure (from 22.4 to 25.4 MPa along the 5-20 ºC range) and analysis time. Within the studied temperature interval, the TAG peaks showed satisfactory peak widths (measured at 50% peak height) ranging between 6.3-53.0 s (**Figure S4.2**, left) and 6.2-42.2 s (**Figure S4.2**, right). Regarding to detector response, UV and ELSD detection did not show significant changes in the response (measured as peak area) over the temperature range investigated. These observations in ELSD response were different from those reported in literature, where a positive [40] or negative [41] correlation with column temperature for peak area could be found. This behavior could be explained by the narrow temperature interval (5-20 ºC) considered in this study. Thus, a column temperature of 10 ºC provided the highest number of resolved peaks (30) (with peak widths ranging between 5.4 and 29.1 s) in < 65 min with a reasonable backpressure (24.1 MPa), being selected for further studies.

Next, the influence of flow rate on TAGs separation was also studied. A flow rate decrease from 1.5 mL/min to 1.0 mL/min led to an improvement in the resolution at expense of an increase of analysis time. Lower flow rates (< 1.0 mL/min) provided a significant peak broadening (peak widths ranged between 10.2 and 80.3 s and asymmetry factors comprised between 0.85-1.60) at very long separation time (> 100 min). In addition, a decrease of the ELSD

response with increasing flow rate was found, which was consistent with findings reported by several authors [40,42]. As a result, a flow rate of 1.0 mL/min was selected for further studies. Under these conditions, the late-eluting compounds were barely distinguished from baseline. In order to decrease the retention time and improve detection (peak shape), a solvent gradient step was established. Thus, the *n*-pentanol content was increased from 20% to 40% in 20 min after the first 45 min of isocratic elution with 80:20 ACN/*n*-pentanol. **Figure 4.1** shows the ELSD chromatogram obtained under these conditions, where satisfactory peak shapes for highly retained TAGs were obtained.

The performance of the developed RPLC method was compared to those of previously reported for analysis of TAGs in human milk. Most of these studies were usually conducted using conventional microparticulate columns packed with 5-µm silica particles [23,27,28], however, it should be mentioned that data of efficiency or other analytical parameters were not provided. In any case, an estimation of the number of resolved peaks of some of these works was done. These values were comprised between 17 and 22 [23,27,28], which were significantly lower than those obtained in this work (35). Also, packed columns of sub-2 µm particles operating at UPLC conditions have been applied to these samples [43,44]. To our knowledge, the work of Beccaria *et al.* [43] is the only one that has reported performance data (peak capacities values up to 170 for 114-min gradient) using three-serially coupled core-shell type C18 columns. However, the number of resolved peaks was similar to our method, which is accomplished in shorter analysis (< 65 min) using a RP column in a conventional high pressure system.

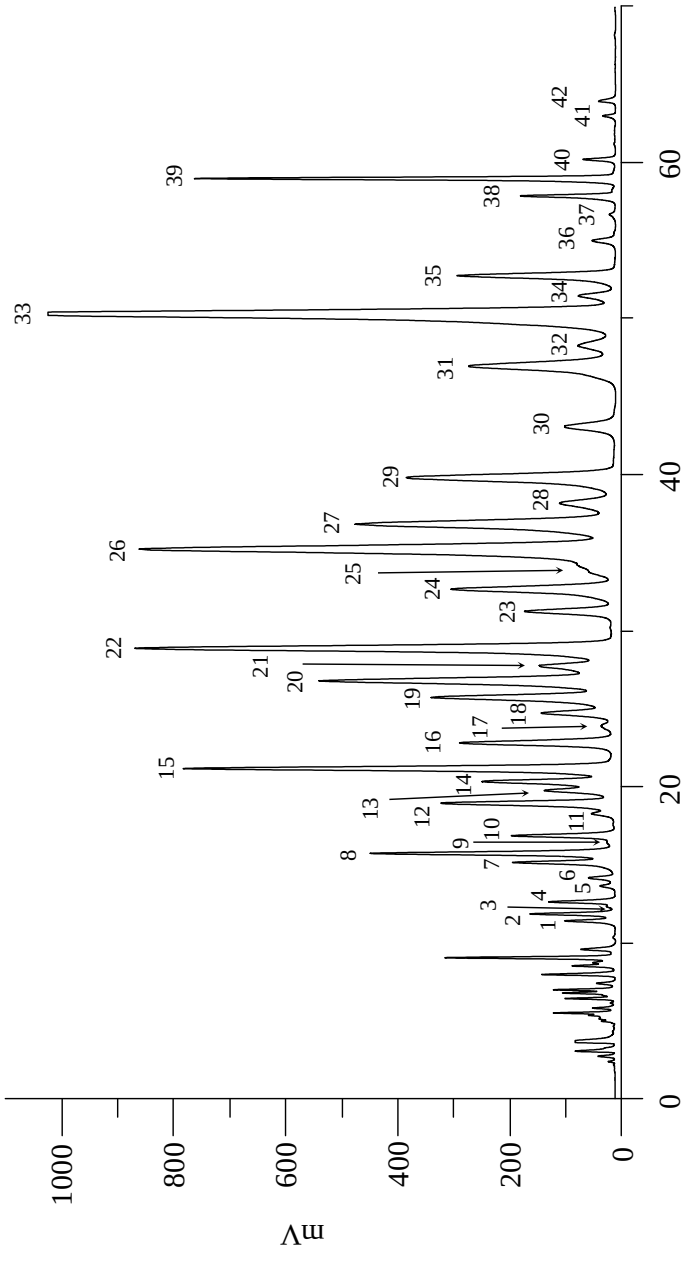

Figure 4.1. TAG profile of mature human milk. Chromatographic conditions: isocratic elution for 45 min at 80:20 ACN/*n*-pentanol followed by a linear gradient up to 60:40 ACN/*n*-pentanol in 20 min; column temperature 10 ºC; flow rate 1.0 mL/min.

4. 3. 2. Identification of TAGs

Generally, the elution of TAGs in RP-HPLC occurs according the partition number (PN) [32,45]. The PN for each individual TAG can be calculated as follows: PN = NC – 2ND, where NC is the number of carbon atoms and ND is the number of double bonds in the FAs attached to the glycerol molecule (see **Table 4.1**). However, the procedure for identifying the TAGs based on the PN is complicated due to the large number of FA constituents and rather limited to the coincidence of this parameter for several TAGs. For this reason, to achieve a reliable TAG identification, a fragmentation study resulting from the APCI-MS analysis of TAGs in the positive ionization mode was performed [46,47]. The APCI mass spectra of TAGs exhibited a protonated molecule, $[M+H]^+$, whose intensity depends on the degree of unsaturation of the TAG molecule, and $[M+H–R_{1,2,3}COOH]^+$ ions resulting from the loss of fatty acyl moieties (diacylglycerol (DAG) ions). The intensities of the protonated molecules $[M+H]^+$ formed from saturated TAGs were low or even no detected (for fully saturated TAGs), and its identification was performed according to their respective DAG ions. These results were consistent with those previously reported [45,48]. **Table 4.1** shows the *m/z* values of the protonated molecules and DAG ions found in the human milk samples studied. No distinction was made between the *sn*-1, *sn*-2 and *sn*-3 positions in the TAG species identified. It should be noted that in spite of the satisfactory resolution achieved in this work, some cases of co-elution of TAGs were observed (see **Table 4.1** and **Figure 4.1**).

Table 4.1. TAGs identified by APCI-HPLC-MS analysis of mature human milk.

Peak no.[a]	TAGs[b]	PN	$[M+H]^+$	$[M+H-R_1COOH]^+$	$[M+H-R_2COOH]^+$	$[M+H-R_3COOH]^+$
1	CaML + LaLaL	38	719.62	LaLa 439.40	LaL 519.44	-
				CaM 439.40	CaL 491.41	ML 547.47
2	CaLaO	38	693.60	CaLa 411.34	CaO 493.42	LaO 521.45
3	n. i.					
4	CaMM + LaLaM	38	667.59	CaM 439.40	-	MM 495.44
				LaLa 439.40	LaM 467.41	-
5	LaLL	40	799.68	LaL 519.44	-	LL 599.50
6	CaOL	40	773.67	CaO 493.42	CaL 491.41	OL 601.52
7	CaPL + LaML	40	747.65	CaP 467.41	CaL 491.41	PL 575.50
				LaM 467.41	LaL 519.44	ML 547.47
8	CaMO + LaLaO	40	721.63	CaM 439.40	CaO 493.42	MO 549.48
				LaLa 439.40	LaO 521.45	-
9	n. i.					
10	CaLaS + CaMP + LaLaP + LaMM	40	695.61	CaLa 411.34	CaS 495.44	LaS 523.47
				CaM 439.40	CaP 467.41	MP 523.47
				LaLa 439.40	LaP 495.44	-
				LaM 467.41	-	MM 495.44
11	MLL/PaPaETE + MPaETE + PLLn	42	827.71	ML 547.47	-	LL 599.50
			853.73	PaPa 547.47	PaETE 599.50	-
			827.71	MPa 521.45	METE 573.48	PaETE 599.50
			853.73	PL 575.50	PLn 573.48	LLn 597.50
12	LaOL	42	801.70	LaO 521.45	LaL 519.44	OL 601.52
13	CaOO	42	775.68	CaO 493.42	-	OO 603.53
14	LaPL + MML	42	775.68	LaP 495.44	LaL 519.44	PL 575.50
				MM 495.44	ML 547.47	-
15	CaPO + LaMO	42	749.67	CaP 467.41	CaO 493.42	PO 577.52
				LaM 467.41	LaO 521.45	MO 549.48
16	CaMS + CaPP + LaLaS + LaMP + MMM + OLL	42	723.65	CaM 439.40	CaS 495.44	MS 551.50
				CaP 467.41	-	PP 551.50
				LaLa 439.40	LaS 523.47	-
				LaM 467.41	LaP 495.44	MP 523.47
				MM 495.44	-	-
		44	881.76	OL 601.52		LL 599.50
17	PaOL	44	855.74	PaO 575.50	PaL 573.48	OL 601.52
18	PLL	44	855.74	PL 575.50	-	LL 599.50
19	MOL	44	829.73	MO 549.48	ML 547.47	OL 601.52
20	LaOO	44	803.71	LaO 521.45	-	OO 603.53
21	MPL	44	803.71	MP 523.47	ML 547.47	PL 575.50
22	LaPO + MMO	44	777.70	LaP 495.44	LaO 521.45	PO 577.52
				MM 495.44	MO 549.48	-
23	CaPS + LaMS + LaPP + MMP	44	751.68	CaP 467.41	CaS 495.44	PS 579.53
				LaM 467.41	LaS 523.47	MS 551.50
				LaP 495.44	-	PP 551.50
				MM 495.44	MP 523.47	-
24	OOL	46	883.76	OO 603.53	OL 601.52	-
25	PaOO	46	857.76	PaO 575.50	-	OO 603.53
26	POL	46	857.76	PO 577.52	PL 575.50	OL 601.52
27	MOO + PPaO	46	831.74	MO 549.48	-	OO 603.53
				PPa 549.48	PO 577.52	PaO 575.50

Peak no.[a]	TAGs[b]	PN	$[M+H]^+$	$[M+H-R_1COOH]^+$	$[M+H-R_2COOH]^+$	$[M+H-R_3COOH]^+$
28	PPL	46	831.74	PP 551.50	PL 575.50	-
29	LaSO + MPO	46	805.73	LaS 523.47	LaO 521.45	SO 605.55
				MP 523.47	MO 549.48	PO 577.52
30	LaPS + MMS + MPP	+46	779.71	LaP 495.44	LaS 523.47	PS 579.53
				MM 495.44	MS 551.50	-
				MP 523.47	-	PP 551.50
31	OOO	48	885.76	OO 603.53	-	-
32	SOL	48	885.76	SO 605.55	SL 603.53	OL 601.52
33	POO	48	859.77	PO 577.52	-	OO 603.53
34	PSL	48	859.77	PS 579.53	PL 575.50	SL 603.53
35	MSO + PPO	48	833.76	MS 551.50	MO 549.48	SO 605.55
				PP 551.50	PO 577.52	-
36	LaSS + MPS + PPP	+48	807.74	LaS 523.47	-	SS 607.56
				MP 523.47	MS 551.50	PS 579.53
				PP 551.50	-	-
37	n. i.					
38	SSL + SOO	50	887.81	SS 607.56	SL 603.53	-
				SO 605.55	-	OO 603.53
39	PSO	50	861.79	PS 579.53	PO 577.52	SO 605.55
40	PPS	50	835.76	PP 551.50	PS 579.53	-
41	POAra + SSO	52	889.82	PO 577.52	PAra 607.57	OAra 633.58
				SS 607.56	SO 605.55	-
42	PSS	52	863.81	PS 579.53	-	SS 607.56

[a]Peak identification number according to **Figure 4.1**; TAGs identified according to protonated molecule ($[M+H]^+$) and diacylglycerol ions ($[M+H-R_{1,2,3}COOH]^+$) observed in the APCI mass spectrum, and to the relative order of PN.

[b]Structure indicated by FA composition (e.g., OOO for triolein) using the following abbreviations: Ca, capric acid (C10.0); La, lauric acid (C12:0); M, myristic acid (C14:0); P, palmitic acid (C16.0); Pa, palmitoleic acid (C16:1); S, stearic acid (C18:0); O, oleic acid (C18:1); L, linoleic acid (C18:2); Ln, linolenic acid (C18:3); Ara, Arachidic acid (C20:0); ETE, eicosatrienoic acid (C20:3).

4. 3. 3. Small-scale extraction method and quantification

First, the evaluation of fat content using the proposed small-scale extraction method was performed. In order to evaluate the efficiency of fat extraction, the method developed here (Method I) was compared to the conventional protocol (Method II). Thus, fat was extracted and gravimetrically determined [25,26,41,42] from twelve mature human milk aliquots, six by Method I and six by Method II. The fat content obtained by Method I and II ranged between 0.021-0.029 and 0.025-0.029 g/mL,

respectively. **Table 4.2** shows the fat content (expressed as mean ± SD) obtained for both methods. No significant differences in the fat milk content between both extraction procedures were observed ($p > 0.05$, Student's *t*-test) and the results found were consistent with those described in the literature [3,23]. At sight of these results, the evaluation of TAG content was next considered.

Table 4.2. Fat content (g/mL) in human milk obtained gravimetrically by methods I and II.

Human milk aliquot	**Fat (g/mL)**	
	Method I	**Method II**
1	0.0231	0.0270
2	0.0246	0.0249
3	0.0294	0.0258
4	0.0252	0.0256
5	0.0258	0.0279
6	0.0207	0.0291
Mean ± SD	0.0248 ± 0.0029	0.0267 ± 0.0016

When performing quantification in ELSD, several authors have established that its response is linear for a wide range of concentrations [38,49]. However, some studies [50,51] have demonstrated that the response from HPLC–ELSD follows a non-linear empirical model: $A = am^b$, where A is the area of chromatographic peak, m the mass of analyte, being a and b two experimental parameters related to the ELSD configuration. Thus, each change in the instrumental working conditions would require a new estimation of these parameters. This equation can be easily linearized as follows: $\log A = b \log m + \log a$. However, the application of this equation requires the availability of each TAG identified in the target sample, which is not commercially feasible. To overcome this limitation, Heron *et al*. [51] have developed an empirical methodology to evaluate the TAG content in vegetable

oils based on the previous equation using a reduced number of standards. However, the method provided a high variability (between 1 and 40%) with respect to the real mass percentage. Another approach proposed by several authors [28,50] is based on the application of the internal normalization method as measurement of mass percentage, where a similarity in the response factors of TAGs ((relative response factors, RRF) with respect to triolein (OOO) ranged between 0.83-1.21) was assumed. In order to confirm this assumption, calibration curves of homologous TAG standards were performed and fitting equations of both linear and power models to detector response (area) *vs* mass of lipid injected were obtained. As shown in **Table 4.3**, the peak areas were well-fitted by power model equations in the mass range studied (0.5-100 µg). The limits of detection (LOD) and limits of quantification (LOQ) were also estimated for signal-to-noise ratios of 3 and 10, respectively. The results obtained for homogeneous TAG standards were: LOD (9.2-13.1) ng and LOQ (30.6-43.3) ng (see **Table 4.3**). Then, the RRF calculated for pure homogeneous TAG standards in relation to OOO were obtained, giving values close to unity, which allows a quantitative estimation of TAGs on the basis of the percentage peak area.

Table 4.3. Calibration equation coefficients (linear regression and power curve fittings), LODs and LOQs, and RRF values for TAG standards in the assayed LC-ELSD method (x = µg injected; y = peak area in mV).

	Linear regression ($y = ax + b$)			**Power curve ($y = bx^a$)**			**LOD**	**LOQ**	
TAG[a]	***a***	***b***	***r²***	***b***	***a***	***r²***	**(ng)**	**(ng)**	**RRF[b]**
LaLaLa	859.59	-856.49	0.9798	253.51	1.50	0.9995	9.2	30.6	1.0067
PaPaPa	806.75	-929.79	0.9638	198.47	1.56	0.9991	12.4	41.1	1.0475
MMM	711.87	-768.68	0.9646	186.91	1.54	0.9992	13.1	43.3	1.0357
OOO	738.15	-830.13	0.9703	208.15	1.49	0.9976	10.9	36.0	1.0000
PPP	412.05	-246.41	0.9885	217.27	1.26	0.9986	9.4	31.1	0.8471

[a]For abbreviations see **Table 4.1**.

[b]RRF values are given in relation to OOO.

The relative content of each TAG (expressed as mean ± SD) obtained is given in **Table 4.4**. As shown in **Table 4.4**, no significant differences ($p > 0.05$, Student's *t*-test) were observed between results obtained with both methods for more than 85% of the TAGs. From this study, it can be derived that Method I provided satisfactory results, both in the total fat content as in the quantitative analysis of representative TAGs. Moreover, the Method I has several advantages over the Method II. **Table 4.5** summarizes the essential features of both sample preparation methods. The Method I uses much smaller volumes of the sample and the chemical solutions (90% reduction), thus, the expense and chemical hazards are greatly reduced. Although other operational steps for both methods were quite similar, the small-scale protocol requires the use of materials such as micropipettes or small syringes, which simplifies the handling of more samples simultaneously and speeds up the isolation process of fat. In particular, the Method I allowed processing 120 samples per day (in an 8 h-working day), whereas a rate of 30 samples per day could be achieved with the Method II. A comparison between our method and the traditional Folch method for milk samples [43,52] was also done. In this protocol, the extraction step employs larger volumes of solvents (40-180 mL) of chloroform-methanol (2:1, v/v), followed by several re-extractions and washings, which results in larger experimental effort, time and amounts of residues of harmful solvents generated than the developed protocol. Consequently, the present procedure is suitable to be applied to systematic and routine characterization of lipid composition in human milk samples. Additionally, due to the small sample volume required, the proposed method offers the possibility of analyzing separate individual milk sample portions from within one feeding, allowing the characterization of possible fluctuations in the TAG composition.

Table 4.4. Relative content of each TAG in mature human milk obtained by methods I and II[a].

Peak no.[b]	TAGs[b]	Method I (*n* = 3), mean ± SD	Method II (*n* = 3), mean ± SD	*p*
1	CaML + LaLaL	0.385 ± 0.005	0.371 ± 0.019	0.057
2	CaLaO	0.612 ± 0.007	0.649 ± 0.017	0.173
3	n. i.	0.066 ± 0.003	0.091 ± 0.019	0.149
4	CaMM + LaLaM	0.508 ± 0.007	0.51 ± 0.02	0.359
5	LaLL	0.140 ± 0.003	0.146 ± 0.014	0.568
6	CaOL	0.242 ± 0.007	0.241 ± 0.006	0.866
7	CaPL + LaML	1.034 ± 0.006	0.977 ± 0.003	0.0001
8	CaMO + LaLaO	2.33 ± 0.02	2.134 ± 0.008	0.0001
9	n. i.	0.092 ± 0.007	0.10 ± 0.02	0.710
10	CaLaS + CaMP + LaLaP + LaMM	0.915 ± 0.017	0.896 ± 0.019	0.266
11	MLL/PaPaETE + MPaETE + PLLn	0.232 ± 0.009	0.243 ± 0.005	0.124
12	LaOL	2.09 ± 0.04	1.98 ± 0.06	0.055
13	CaOO	0.86 ± 0.05	0.82 ± 0.02	0.309
14	LaPL + MML	1.58 ± 0.04	1.55 ± 0.05	0.362
15	CaPO + LaMO	5.04 ± 0.07	4.86 ± 0.07	0.031
16	CaMS + CaPP + LaLaS + LaMP + MMM + OLL	1.95 ± 0.12	2.03 ± 0.04	0.302
17	PaOL	0.17 ± 0.03	0.18 ± 0.04	0.768
18	PLL	0.96± 0.07	0.96 ± 0.07	0.991
19	MOL	2.77 ± 0.06	2.760 ± 0.08	0.875
20	LaOO	4.74 ± 0.12	4.68 ± 0.07	0.507
21	MPL	1.29 ± 0.05	1.278 ± 0.015	0.795
22	LaPO + MMO	7.39 ± 0.14	7.30 ± 0.10	0.412
23	CaPS + LaMS + LaPP + MMP	1.18 ± 0.03	1.25 ± 0.02	0.051
24	OOL	2.75 ± 0.04	2.82 ± 0.12	0.445

Peak no.[b]	TAGs[b]	Method I (n = 3), mean ± SD	Method II (n = 3), mean ± SD	p
25	PaOO	0.91 ± 0.17	0.9 ± 0.2	0.748
26	POL	9.88 ± 0.21	10.1 ± 0.3	0.335
27	MOO + PPaO	5.410 ± 0.016	5.55 ± 0.05	0.010
28	PPL	1.220 ± 0.014	1.22 ± 0.05	0.947
29	LaSO + MPO	4.27 ± 0.07	4.44 ± 0.03	0.013
30	LaPS + MMS + MPP	1.036 ± 0.006	1.06 ± 0.04	0.402
31	OOO	3.65 ± 0.06	3.7 ± 0.2	0.551
32	SOL	0.97 ± 0.02	1.03 ± 0.03	0.118
33	POO	20.3 ± 0.6	20.21 ± 0.19	0.914
34	PSL	1.117 ± 0.010	1.14 ± 0.08	0.680
35	MSO + PPO	4.09 ± 0.07	4.17 ± 0.16	0.480
36	LaSS + MPS + PPP	0.55 ± 0.03	0.56 ± 0.04	0.946
37	n. i.	0.15 ± 0.02	0.117 ± 0.009	0.068
38	SSL + SOO	1.48 ± 0.04	1.43 ± 0.05	0.246
39	PSO	5.06 ± 0.13	4.9 ± 0.2	0.425
40	PPS	0.34 ± 0.03	0.35 ± 0.03	0.833
41	POAra + SSO	0.133 ± 0.006	0.139 ± 0.011	0.448
42	PSS	0.145 ± 0.002	0.157 ± 0.014	0.282

[a]Data obtained from three extractions performed the same day for each extraction method.

[b]Peak identification number, TAG information and abbreviations as indicated in **Table 4.1**.

As shown in **Table 4.4**, from 69 TAG molecular species identified, the six major TAGs found in lipid fraction in both protocols were: POO, POL, LaPO + MMO, MOO, PSO (see **Table 4.1** for abbreviations) with 20, 10, 7, 6 and 5%, respectively. The amounts of these most abundant TAGs were similar to those obtained in the literature [16,27,52]. For example, the studies of Zou *et al*. [16], in milk from Danish women, pointed out that the TAGs

were mainly composed of POO (21.52%) and POL (16.93%). These small discrepancies can be attributed to natural factors such as randomization in human milk, the physiological stage [16], and the susceptibility of human milk TAGs to dietary habits [5,44].

Table 4.5. Comparison of sample preparation protocols.

	Method I (small-scale)	**Method II** [16]
Sample volume (mL)	0.15	1.5
Extraction		
i) CH_2Cl_2:MeOH (2:1, v/v) (mL)	2.5	25
ii) Water (mL)	0.8	8
iii) Saline solution (mL)	0.8	8
Material required	10 mL centrifuge tubes, syringes, syringe filters, micropipettes	Falcon™ 50 mL conical centrifuge tubes, separating funnels, filter funnels, filter paper, pipettes, Pasteur pipettes
Samples per day	120	30

Taking into account the advantages described above for the Method I, it was extended to the other milk mammalian species (cow, sheep and goat). Thus, the total fat content varied within the ranges 0.023-0.046, 0.046-0.057 and 0.034-0.076 g/mL for cow, sheep and goat milks, respectively. These milk samples were also analyzed using the developed LC method with an excellent resolution/elution time ratio compared to those previously reported [14,16,23,27,28] (**Figure 4.2**). Similar TAG profiles (particularly for the main TAG peaks) were found than those reported in literature for these samples [14]. From these profiles, 22 common peaks, which could be easily integrated, were selected for the four mammalian species, and used for statistical treatment.

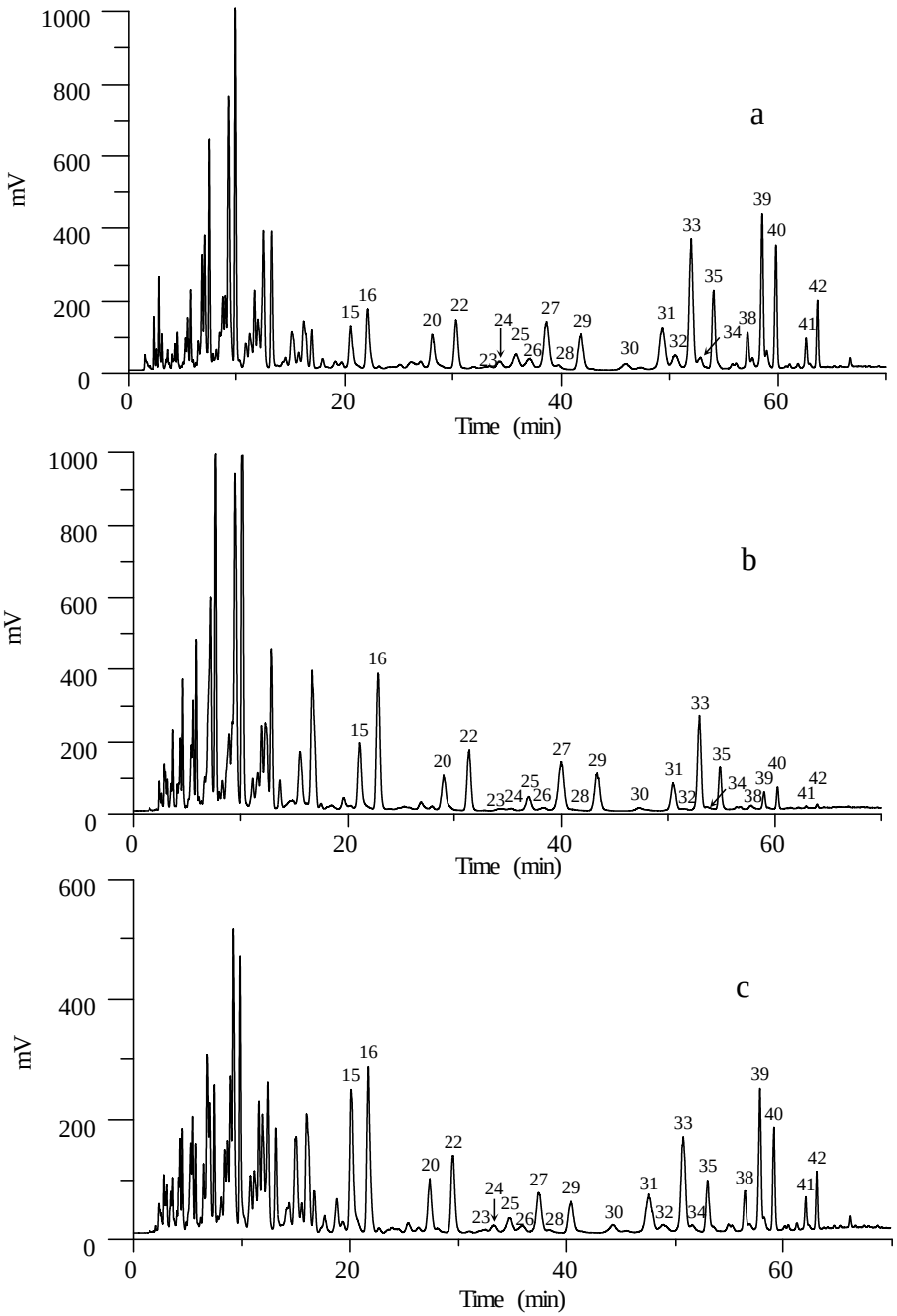

Figure 4.2. TAG profile of milk from different mammalian species: cow (a); sheep (b); goat (c). Chromatographic conditions as in **Figure 4.1**.

4. 3. 4. Classification of mammalian milks using TAG profiles with LDA model

First, to reduce the variability associated to total amount of TAGs recovered from milk samples, and to minimize the sources of variance also affecting the sum of the areas of all the peaks, normalized rather than absolute peak area were used. In order to normalize the variables, the area of each peak was divided by each one of the areas of the other 21 peaks; in this way, and taking into account that each pair of peaks should be consider only once, (22 x 21)/2 = 231 non-redundant peak area ratios were obtained to be used as predictors. Using the normalized variables, an LDA model capable of classifying the milk samples according to their respective mammalian specie was constructed. A matrix containing 75 objects which corresponded to all the milk samples analyzed was constructed. Thus, this matrix was divided in two groups of objects to constitute the training and evaluation sets. The training set was composed by 67 objects (18 milks × 3 animal mammalian species, and 13 human milk samples), while the evaluation set was constituted by the remaining samples (8 objects). A response column, containing the categories corresponding to the 4 mammalian species, was added to these matrices. When the LDA model was constructed, an excellent resolution between all the category pairs was achieved (Wilks' lambda, $\lambda_w < 0.01$). The variables selected by the SPSS stepwise algorithm, and the corresponding standardized coefficients of the model, showing the predictors with large discriminant capabilities, are given in **Table 4.6**. As shown in **Figure 4.3a**, a large resolution between the human milk from the other mammalian milks was achieved along the first discriminant function (df). As deduced from **Table 4.6**, first df was mainly constructed with the peak area ratios OOL/PaOO and POO/(POAra+SSO) (peaks labelled as 24/25 and 33/41, respectively). The projection on the second df shows a lack of capability to resolve between cow and goat milks. However, both milks were clearly

distinguished from sheep and human milks. In this case, second df was mainly constructed with the peak area ratios (CaMS+CaPP+LaLaS+LaMP+ MMM+OLL)/(MOO+PPaO) and (LaPO+MMO)/PSO. (peaks labelled as 16/27 and 22/39, respectively). According to **Figure 4.3b**, along the third df, it is not possible to distinguish between sheep and human milk, but both were markedly differentiated from cow and goat milks. As shown in **Table 4.6**, the third df was mainly constituted with the peak area ratios (CaPO+LaMO)/ (CaPS+LaMS+LaPP+MMP) and (CaMS+CaPP+LaLaS+LaMP+MMM +OLL)/OOL (peaks labelled as 15/23 and 16/24, respectively). Finally, as illustrated in **Figure 4.3c**, by using a plane oblique to the three first discriminant functions, all the possible pair of categories were very well resolved from each other.

Table 4.6. Predictors selected and corresponding standardized coefficients of the LDA model constructed to discriminate between milks obtained from different mammalian species.

Predictor[a]	**1st df**	**2nd df**	**3rd df**
Peak 15/Peak 23	-0.466	0.219	2.275
Peak 16/Peak 24	0.700	-0.302	-2.742
Peak 16/Peak 27	0.075	-2.114	2.020
Peak 16/Peak 35	-0.262	0.126	1.306
Peak 16/Peak 41	-0.395	1.559	0.128
Peak 22/Peak 39	-0.284	2.067	0.067
Peak 23/Peak 41	-0.230	-1.282	0.055
Peak 24/Peak 25	2.748	0.463	-0.143
Peak 26/Peak 40	0.949	0.263	0.243
Peak 30/Peak 33	-0.115	0.693	1.016
Peak 33/Peak 41	1.662	0.724	0.812

[a]See **Table 4.1** for peak identification.

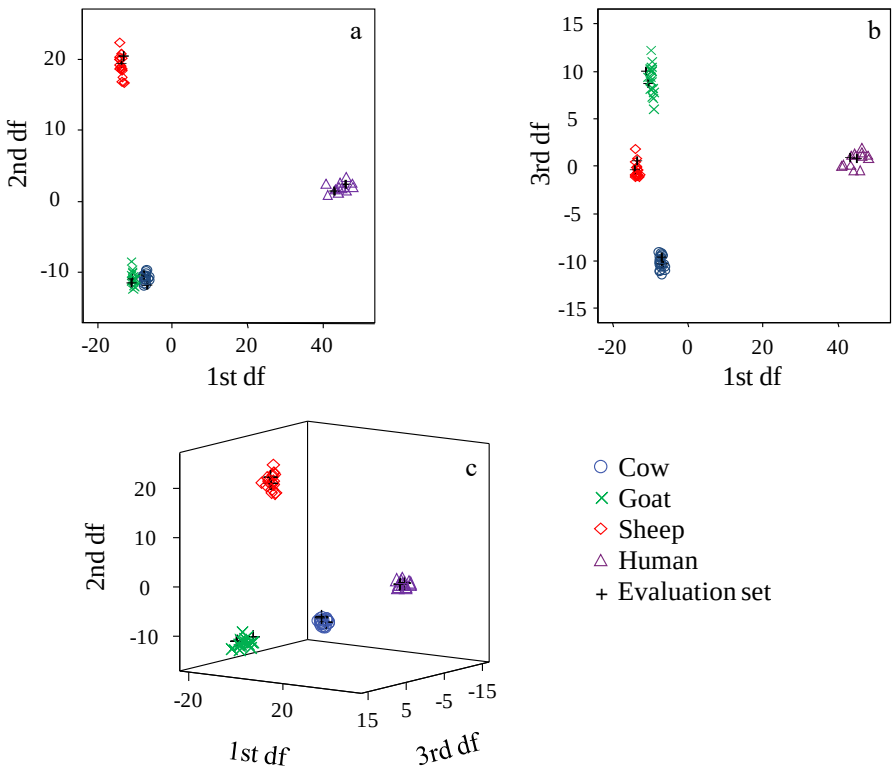

Figure 4.3. Score plots on the planes of the first and second (a), and second and third discriminant functions (df) (b), and on an oblique plane of the 3-D space defined by the three discriminant functions (c) of the LDA model constructed to discriminate between different mammalian milk species. Evaluation set samples are labeled as indicated in figure legend.

Using this model and leave-one-out validation, all the objects of the training set were correctly classified. On the other hand, the prediction capability of the model was evaluated using the evaluation set. In this case, all the objects (represented with a cross symbol in **Figure 4.3**) were correctly assigned within 95% probability level. It should be outlined that in the case of human milk samples, different period of lactation were taken, and in all cases, an excellent classification within this category was accomplished, which supports the robustness of the developed LDA model.

In summary, a highly efficient RP-HPLC-UV-ELSD method of TAGs in human milk samples has been developed. Also, a small-scale sample preparation method has been established, being particular important for human milk samples. The combination of this sample extraction protocol with HPLC-UV-ELSD technique could provide a methodology highly recommended in studies on breastfeeding and its contribution to infant growth and development. Finally, the possibility of classifying milks according to their mammalian origin by using TAG profiles obtained by HPLC-ELSD has been successfully demonstrated.

Fundings

Project CTQ2014-52765-R (MINECO of Spain and FEDER). I. T-D thanks the MINECO for an FPU grant for PhD studies.

4. 4. References

[1] M.F. Picciano, Nutrient composition of human milk, Pediatr. Clin. North Am. 48 (2001) 53–67. doi:10.1016/S0031-3955(05)70285-6.

[2] R.G. Jensen, Lipids in human milk, Lipids 34 (1999) 1243–1271. doi:10.1007/s11745-999-0477-2.

[3] S. Salamon, J. Csapó, Composition of the mother's milk II. Fat contents, fatty acid composition. A review, Acta Univ. Sapientiae, Aliment. 2 (2009) 196–234.

[4] B. Koletzko, M. Rodriguez-Palmero, H. Demmelmair, N. Fidler, R. Jensen, T. Sauerwald, Physiological aspects of human milk lipids, Early Hum. Dev. 65 Suppl (2001) S3–S18. doi:10.1016/S0378-3782(01)00204-3.

[5] G. Rocquelin, S. Tapsoba, M. Dop, F. Mbemba, P. Traissac, Y. Martin-Prével, Lipid content and essential fatty acid (EFA) composition of mature Congolese breast milk are influenced by mothers' nutritional status: impact on infants' EFA supply, Eur. J. Clin. Nutr. 52 (1998) 164–171. doi:10.1038/sj.ejcn.1600529.

[6] A. Sala-Vila, A.I. Castellote, M. Rodriguez-Palmero, C. Campoy, M.C. López-Sabater, Lipid composition in human breast milk from Granada (Spain): changes during lactation, Nutrition 21 (2005) 467–473. doi:10.1016/j.nut.2004.08.020.

[7] D. Mandel, R. Lubetzky, S. Dollberg, S. Barak, F.B. Mimouni, Fat and energy contents of expressed human breast milk in prolonged lactation, Pediatrics 116 (2005) 432–435. doi:10.1542/peds.2005-0313.

[8] F.E. Hytten, Clinical and chemicals studies in human lactation, Br. Med. J. 2 (1954) 176–179.

[9] S. Khan, A. Hepworth, D. Prime, C. Lai, N. Trengove, P. Hartmann,

Variation in fat, lactose, and protein composition in breast milk over 24 hours: associations with infant feeding patterns, J. Hum. Lact. 29 (2013) 81–89. doi:10.1177/0890334412448841.

[10] J.C. Kent, L.R. Mitoulas, M.D. Cregan, D.T. Ramsay, D.A. Doherty, P.E. Hartmann, Volume and frequency of breastfeedings and fat content of breast milk throughout the day, Pediatrics 117 (2006) e387–e395. doi:10.1542/peds.2005-1417.

[11] G. Harzer, M. Haug, I. Dieterich, P. Gentner, Changing patterns of human milk lipids in the course of the lactation and during the day, Am. J. Clin. Nutr. 37 (1983) 612–621. doi:10.1093/ajcn/37.4.612.

[12] G. Harzer, M. Haug, Dependency of human milk lipids on length of the lactation period, time of day, nursing and maternal diet, Z. Ernahrungswiss. 23 (1984) 113–125. doi: 10.1007/BF02021686.

[13] E. D'Auria, C. Agostoni, M. Giovannini, E. Riva, R. Zetterström, R. Fortin, G.F. Greppi, L. Bonizzi, P. Roncada, Proteomic evaluation of milk from different mammalian species as a substitute for breast milk, Acta Paediatr. 94 (2005) 1708–1713. doi:10.1080/08035250500434793.

[14] X.-Q. Zou, J.-H. Huang, Q.-Z. Jin, Z. Guo, Y.-F. Liu, L.-Z. Cheong, X.-B. Xu, X.-G. Wang, Model for human milk fat substitute evaluation based on triacylglycerol composition profile, J. Agric. Food Chem. 61 (2013) 167–175. doi:10.1021/jf304094p.

[15] E.I. El-Agamy, The challenge of cow milk protein allergy, Small Rumin. Res. 68 (2007) 64–72. doi:10.1016/j.smallrumres.2006.09.016.

[16] S. Morera, A.I. Castellote, O. Jauregui, I. Casals, M.C. López-Sabater, Triacylglycerol markers of mature human milk, Eur. J. Clin. Nutr. 57 (2003) 1621–1626. doi:10.1038/sj.ejcn.1601733.

[17] J. Folch, M. Lees, G.H. Sloane Stantley, A simple method for the isolation and purification of total lipides from animal tissues, J. Biol. Chem. 266 (1957) 497–509.

[18] I.S. Chen, C.-S.J. Shen, A.J. Sheppard, Comparison of methylene chloride and chloroform for the extraction of fats from food products, J. Am. Oil Chem. Soc. 58 (1981) 599–601. doi:10.1007/BF02672373.

[19] AOAC INTERNATIONAL, AOAC Official Method 989.05 Fat in milk, 21 (1992) 5–6.

[20] D.M. Barbano, J.L. Clark, C.E. Dunham, Comparison of Babcock and ether extraction methods for determination of fat content of milk: collaborative study, J. Assoc. Off. Anal. Chem. 71 (1988) 898–914.

[21] L. Ramos, J.J. Ramos, U.A.T. Brinkman, Miniaturization in sample treatment for environmental analysis, Anal. Bioanal. Chem. 381 (2005) 119–140. doi:10.1007/s00216-004-2906-5.

[22] M. Jánská, M. Tomaniová, J. Hajšlová, V. Kocourek, Appraisal of "classic" and "novel" extraction procedure efficiencies for the isolation of polycyclic aromatic hydrocarbons and their derivatives from biotic matrices, Anal. Chim. Acta 520 (2004) 93–103. doi:10.1016/j.aca.2004.05.073.

[23] M. Romeu-Nadal, S. Morera-Pons, A.I. Castellote, M.C. López-Sabater, Comparison of two methods for the extraction of fat from human milk, Anal. Chim. Acta 513 (2004) 457–461. doi:10.1016/j.aca.2004.02.038.

[24] J. Bitman, L. Wood, M. Hamosh, P. Hamosh, N.R. Mehta, Comparison of the lipid composition of breast milk from mothers of term and preterm infants, Am. J. Clin. Nutr. 38 (1983) 300–312. doi:10.1093/ajcn/38.2.300.

[25] J. Fontecha, H. Goudjil, J.J. Ríos, M.J. Fraga, M. Juárez, Identity of

the major triacylglycerols in ovine milk fat, Int. Dairy J. 15 (2005) 1217–1224. doi:10.1016/j.idairyj.2004.11.013.

[26] X. Zou, J. Huang, Q. Jin, Z. Guo, Y. Liu, L. Cheong, X. Xu, X. Wang, Lipid composition analysis of milk fats from different mammalian species: potential for use as human milk fat substitutes, J. Agric. Food Chem. 61 (2013) 7070–7080. doi:10.1021/jf401452y.

[27] D. Gastaldi, C. Medana, V. Giancotti, R. Aigotti, F. Dal Bello, C. Baiocchi, HPLC-APCI analysis of triacylglycerols in milk fat from different sources, Eur. J. Lipid Sci. Technol. 113 (2011) 197–207. doi:10.1002/ejlt.201000068.

[28] S. Morera Pons, A.I. Castellote Bargalló, M.C. López Sabater, Analysis of human milk triacylglycerols by high-performance liquid chromatography with light-scattering detection, J. Chromatogr. A 823 (1998) 475–482. doi:10.1016/S0021-9673(98)00584-6.

[29] P. Dugo, T. Kumm, M. Lo Presti, B. Chiofalo, E. Salimei, A. Fazio, A. Cotroneo, L. Mondello, Determination of triacylglycerols in donkey milk by using high performance liquid chromatography coupled with atmospheric pressure chemical ionization mass spectrometry, J. Sep. Sci. 28 (2005) 1023–1030. doi:10.1002/jssc.200500025.

[30] P. Dugo, T. Kumm, B. Chiofalo, A. Cotroneo, L. Mondello, Separation of triacylglycerols in a complex lipidic matrix by using comprehensive two-dimensional liquid chromatography coupled with atmospheric pressure chemical ionization mass spectrometric detection, J. Sep. Sci. 29 (2006) 1146–1154. doi:10.1002/jssc.200500476.

[31] H. Kallio, P. Rua, Distribution os the major fatty acids of human milk between sn-2 and sn-3 positions of triacylglycerols, J. Am. Oil Chem. Soc. 71 (1994) 985–992. doi:10.1007/BF02542266.

[32] V. Ruíz-Gutiérrez, L.-J. Barron, Methods for the analysis of

triacylglycerols, J. Chromatogr. B 671 (1995) 133–168. doi:10.1016/0378-4347(95)00093-X.

[33] O. Núñez, H. Gallart-Ayala, C.P.B. Martins, P. Lucci, New trends in fast liquid chromatography for food and environmental analysis, J. Chromatogr. A 1228 (2012) 298–323. doi:10.1016/j.chroma.2011.10.091.

[34] A.H. Pripp, Application of Multivariate Analysis: Benefits and Pitfalls, en: R.W. Hartel (Ed.), Stat. Food Sci. Nutr., Springer, New York, 2013: págs. 53–64. doi:10.1007/978-1-4614-5010-8.

[35] R. Wehrens, Linear Discriminant Analysis, en: R. Gentleman, K. Hornik, G. Parmigiani (Eds.), Chemom. with R. Multivar. Data Anal. Nat. Sci. Life Sci., Springer, Berlin, 2011: págs. 105–109.

[36] R. Karoui, J. De Baerdemaeker, A review of the analytical methods coupled with chemometric tools for the determination of the quality and identity of dairy products, Food Chem. 102 (2007) 621–640. doi:10.1016/j.foodchem.2006.05.042.

[37] M.J. Lerma-García, E.F. Simó-Alfonso, a. Méndez, J.L. Lliberia, J.M. Herrero-Martínez, Classification of extra virgin olive oils according to their genetic variety using linear discriminant analysis of sterol profiles established by ultra-performance liquid chromatography with mass spectrometry detection, Food Res. Int. 44 (2011) 103–108. doi:10.1016/j.foodres.2010.11.004.

[38] S. Morera Pons, A.I. Castellote Bargalló, M.C. López Sabater, Evaluation by high-performance liquid chromatography of the hydrolysis of human milk triacylglycerides during storage at low temperatures, J. Chromatogr. A 823 (1998) 467–474. doi:10.1016/S0021-9673(98)00273-8.

[39] M.J. Lerma-García, R. Lusardi, E. Chiavaro, L. Cerretani, A. Bendini,

G. Ramis-Ramos, E.F. Simó-Alfonso, Use of triacylglycerol profiles established by high performance liquid chromatography with ultraviolet-visible detection to predict the botanical origin of vegetable oils, J. Chromatogr. A 1218 (2011) 7521–7527. doi:10.1016/j.chroma.2011.07.078.

[40] M.M. Khandagale, J.P. Hutchinson, G.W. Dicinoski, P.R. Haddad, Effects of eluent temperature and elution bandwidth on detection response for aerosol-based detectors, J. Chromatogr. A 1308 (2013) 96–103. doi:10.1016/j.chroma.2013.07.111.

[41] A. Hazotte, D. Libong, M. Matoga, P. Chaminade, Comparison of universal detectors for high-temperature micro liquid chromatography, J. Chromatogr. A 1170 (2007) 52–61. doi:10.1016/j.chroma.2007.09.008.

[42] J.P. Hutchinson, J. Li, W. Farrell, E. Groeber, R. Szucs, G. Dicinoski, P.R. Haddad, Comparison of the response of four aerosol detectors used with ultra high pressure liquid chromatography, J. Chromatogr. A 1218 (2011) 1646–1655. doi:10.1016/j.chroma.2011.01.062.

[43] M. Beccaria, G. Sullini, F. Cacciola, P. Donato, P. Dugo, L. Mondello, High performance characterization of triacylglycerols in milk and milk-related samples by liquid chromatography and mass spectrometry, J. Chromatogr. A 1360 (2014) 172–187. doi:10.1016/j.chroma.2014.07.073.

[44] K.M. Linderborg, M. Kalpio, J. Mäkelä, H. Niinikoski, H.P. Kallio, H. Lagström, Tandem mass spectrometric analysis of human milk Triacylglycerols from normal weight and overweight mothers on different diets, Food Chem. 146 (2014) 583–590. doi:10.1016/j.foodchem.2013.09.092.

[45] P. Sandra, A. Medvedovici, Y. Zhao, F. David, Characterization of

triglycerides in vegetable oils by silver-ion packed-column supercritical fluid chromatography coupled to mass spectroscopy with atmospheric pressure chemical ionization and coordination ion spray, J. Chromatogr. A 974 (2002) 231–241. doi:10.1016/S0021-9673(02)01311-0.

[46] H.R. Mottram, Z.M. Crossman, R.P. Evershed, Regiospecific characterisation of the triacylglycerols in animal fats using high performance liquid chromatography-atmospheric pressure chemical ionisation mass spectrometry, Analyst 126 (2001) 1018–1024. doi:10.1039/b102491b.

[47] H.R. Mottram, S.E. Woodbury, R.P. Evershed, Identification of triacylglycerol positional isomers present in vegetable oils by high performance liquid chromatography/atmospheric pressure chemical ionization mass spectrometry, Rapid Commun. Mass Spectrom. 11 (1997) 1240–1252. doi:10.1002/(SICI)1097-0231(199708)11:12<1240::AID-RCM990>3.0.CO;2-5.

[48] Separation and Identification of Triacylglycerols of Peanut Oil by APCI LC/MS. Application Note AMD 31, (2001). Disponible en: www.waters.com (Fecha de acceso: 05/09/2014).

[49] A. Stolyhwo, H. Colin, M. Martin, G. Guiochon, Study of the qualitative and quantitative properties of the light-scattering detector, J. Chromatogr. A 288 (1984) 253–275. doi:10.1016/S0021-9673(01)93706-9.

[50] S. Cunha, M. Oliveira, Discrimination of vegetable oils by triacylglycerols evaluation of profile using HPLC/ELSD, Food Chem. 95 (2006) 518–524. doi:10.1016/j.foodchem.2005.03.029.

[51] S. Heron, M.-G. Maloumbi, M. Dreux, E. Verette, A. Tchapla, Method development for a quantitative analysis performed without any

standard using an evaporative light-scattering detector, J. Chromatogr. A 1161 (2007) 152–156. doi:10.1016/j.chroma.2007.05.101.

[52] I. Haddad, M. Mozzon, R. Strabbioli, N.G. Frega, A comparative study of the composition of triacylglycerol molecular species in equine and human milks, Dairy Sci. Technol. 92 (2012) 37–56. doi:10.1007/s13594-011-0042-5.

4. 5. Supporting Information

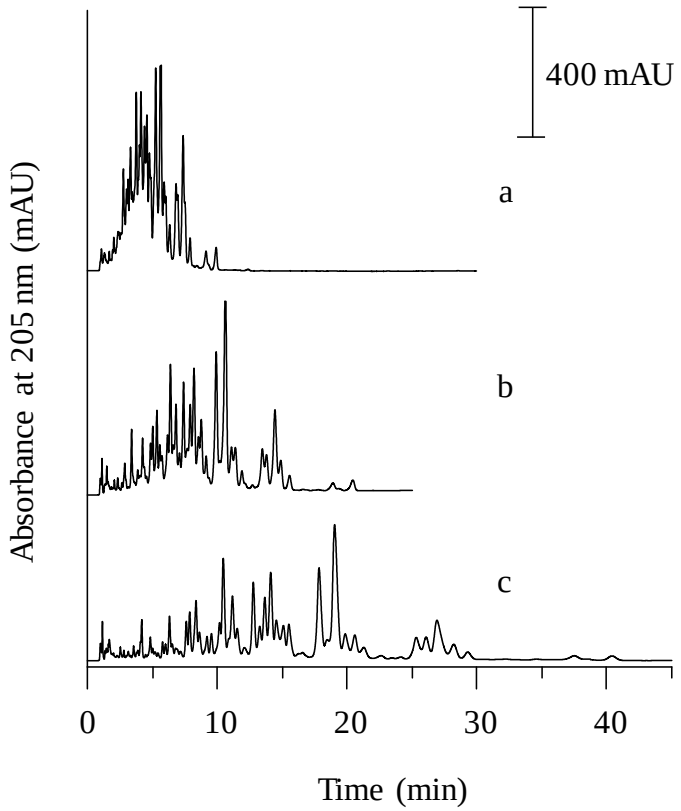

Figure S4.1. Influence of *n*-pentanol content on TAGs separation in mature human milk: 70:30 (a), 75:25 (b) and 80:20 (c) ACN/*n*-pentanol. Chromatographic conditions: isocratic elution; column temperature, 10 ºC; flow rate, 1.5 mL/min.

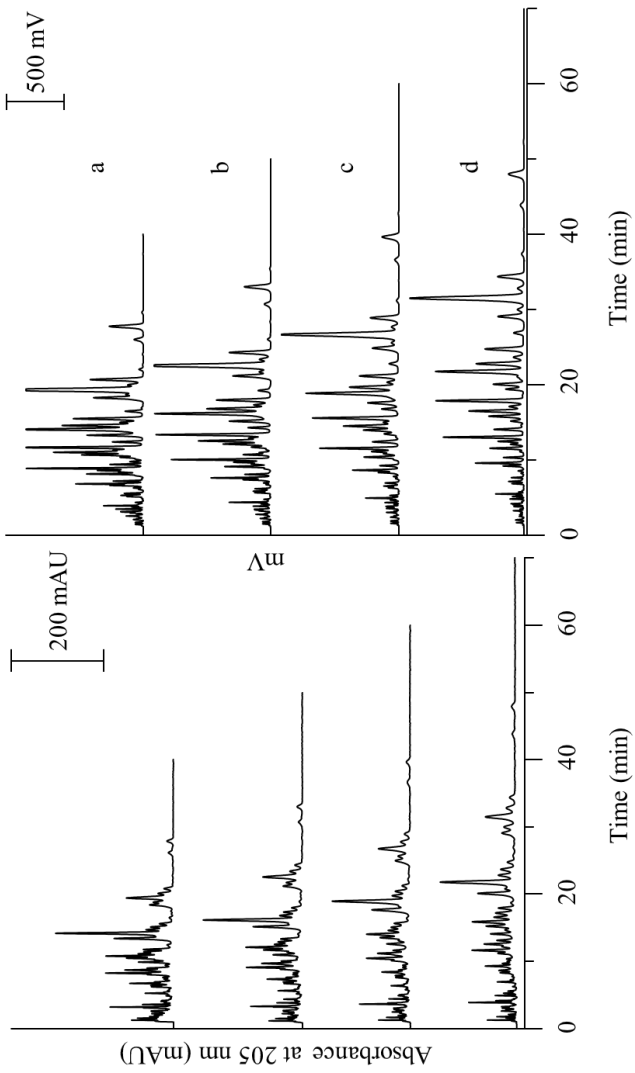

Figure S4.2. Influence of column temperature on TAGs separation in mature human milk using UV (left) and ELSD detector (right): 20 (a), 15 (b), 10 (c) and 5 ºC (d). Chromatographic conditions: isocratic elution, 80:20 ACN/*n*-pentanol; flow rate, 1.5 mL/min.

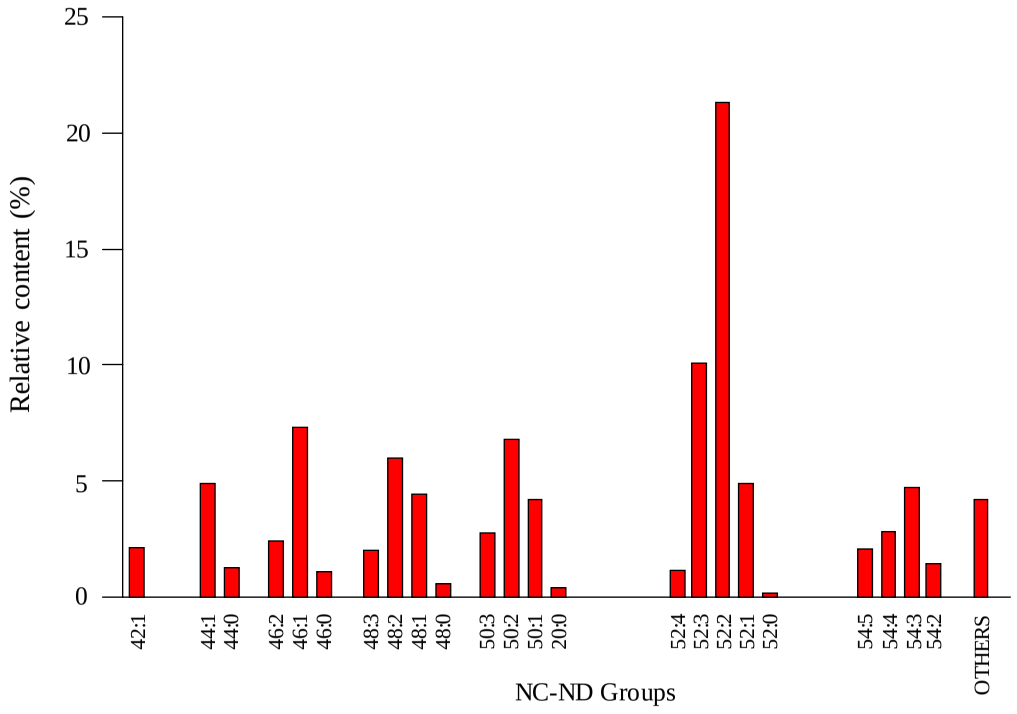

Figure S4.3. TAG molecular weight distribution (expressed as NC:ND groups) in human milk.

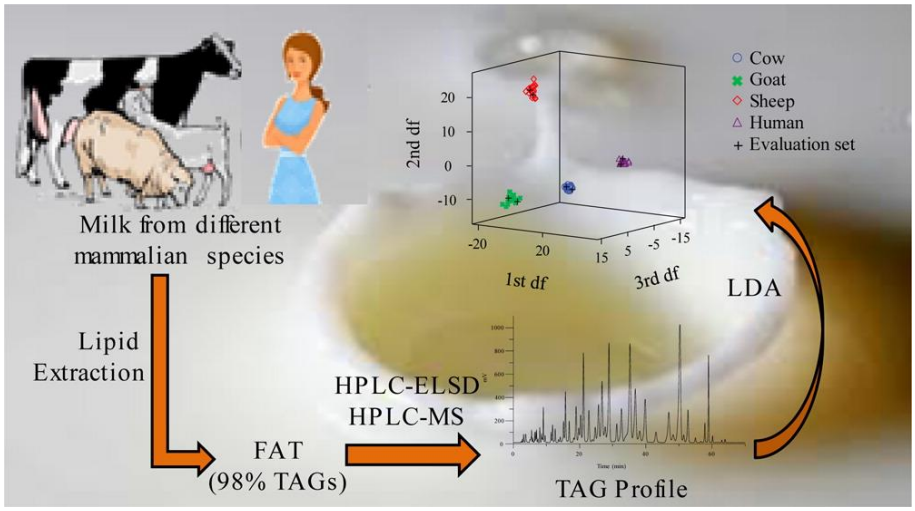
Milk from different mammalian species
Lipid Extraction
FAT (98% TAGs)
HPLC-ELSD
HPLC-MS
TAG Profile
LDA
Cow
Goat
Sheep
Human
Evaluation set
2nd df
1st df
3rd df

CAPÍTULO 5

Solid-phase extraction of phospholipids using mesoporous silica nanoparticles. Application to human milk samples

Analytical and Bioanalytical Chemistry
https://doi.org/10.1007/s00216-018-1121-8

RESEARCH PAPER

Solid-phase extraction of phospholipids using mesoporous silica nanoparticles: application to human milk samples

Héctor Martínez Pérez-Cejuela[1] · Isabel Ten-Doménech[1] · Jamal El Haskouri[2] · Pedro Amorós[2] · Ernesto F. Simó-Alfonso[1] · José Manuel Herrero-Martínez[1]

Received: 2 January 2018 / Revised: 19 April 2018 / Accepted: 1 May 2018

[1] Department of Analytical Chemistry, Faculty of Chemistry, University of Valencia, Dr Moliner 50, 46100 Burjassot, Valencia, Spain

[2] Institute of Material Science (ICMUV), University of Valencia, Catedrático José Beltrán 2, 46980 Paterna, Valencia, Spain

In this study, MSMs with bimodal pore systems (namely, UVM-7), MCM-41 silica and a commercial silica-based material were evaluated as SPE sorbents for the isolation of PLs using PC as test compound. Morphological characterization (including TEM, surface and size pore measurements) of these materials was carried out. The mechanism of interaction of the target analyte with the MSMs was also studied. With regard to the SPE process, several experimental parameters that affect the extraction performance (e.g., loading and elution solvent, breakthrough volume, loading capacity and reusability) were investigated. The recommended protocol was applied to the extraction of PLs in human milk fat samples. The extracted PLs were then determined by HILIC using ELSD. This work reports the first application of silica-based mesoporous materials to preconcentrate PLs in these complex matrices.

Keywords: Mesoporous silica material; UVM-7; Phospholipids; SPE; HILIC-ELSD.

5. 1. Introduction

MSMs, synthesized for the first time in 1992 by the Mobile Oil Corporation [1], have received extensive attention due to their distinctive features such as high surface area (>1000 m^2/g), large pore volume (>1 cm^3/g), easy tailoring of morphology (size, pore and shape), good chemical and thermal stability, suitable biocompatibility, internal and/or external surface functionalization, etc. These unique structural properties together with their biocompatibility have made these MSMs preferred materials in several fields such as catalysis [2] and biomedicine [3], amongst others. However, the potential use of these materials in analytical chemistry has been only partially exploited [4].

The standard procedure for the synthesis of MSPs is based in the sol-gel technique, where silica precursors (e.g., TEOS) condensate in the presence of cationic surfactants (e.g., CTAB) under basic conditions, between 30 and 60 ºC. Although MCM-41 is the most studied and applied mesoporous silica-based material, other MSPs with different shape and porous systems have been also described (e.g., SBA-15 [5] and UVM-7 [6]). The later material, developed by Amorós and co-workers, constituted one of the first examples of hierarchical multimodal pore systems in MSMs. Thus, UVM-7 material has a bimodal pore system that combines the presence of intra-particle mesopores and inter-particle macropores, whose modulation depends on both the surfactant used and the procedural variables.

In particular, raw and functionalized MCM-41 and SBA-15 materials have been widely used to remove organic and inorganic contaminants from air and water [7,8] as well as to preconcentrate organic pollutants such as polycyclic aromatic hydrocarbons [9] and endocrine disrupting compounds [10] as sorbents in micro/SPE modes.

On the other hand, UVM-7 has been successfully used in several applications such as catalysis [11], chemosensory [12] and chromatography [13]. However, the use of this material has not been reported for sample treatment purposes.

PLs are considered as nutrients with intrinsic health benefits and play at least three major roles, which are to provide structural assurance for the integrity of membranes and help carry out their functions, to involve many metabolism-related and neurological diseases, and to regulate basic biological processes as signaling compounds [14]. Natural occurrence and structural characteristics of PLs depend on the source (e.g., food, animal organ or microorganism). Depending on their backbone and bonding types, they are generally classified into two main groups: glycerolphospholipids and sphingolipids.

The challenge in PLs analysis arises from their low abundance with respect to other compounds present in the matrix such as neutral lipids, saccharides, or other small molecules. Thus, extracting PLs from complex biological matrix is usually an indispensable requirement. To address this problem, 2D-TLC [15,16] or column chromatography [17] have been commonly adopted techniques. Alternatively, to isolate PLs from different matrices, SPE procedures using various sorbents (e.g., commercial silica-based material [18], titanium dioxide [19], titania-coated silica core-shell composites [20]) have been also described. However, most of these studies did not report extraction performance values of these analytes neither loading capacity and reusability issues. Due to the amphiphilic nature of PLs, their selective isolation is not a straightforward process, and therefore, the development and application of novel sorbents is highly encouraged.

In this sense, Sinyaeva *et al.* [21,22] have recently described the dynamics of sorption of PC by mesoporous composites based on MCM-41. They revealed that these structured MSMs are characterized by a high

adsorption capacity with respect to the tested PL, due to the highly ordered mesoporous structures. Despite this finding, to our knowledge, the use of MSMs as SPE sorbent to isolate/preconcentrate PLs from real samples has not been explored to date.

In this work, the synthesis and characterization of MSMs (pure and doped with variable amounts of titanium) with bimodal pore systems has been described. The resulting materials were used as simple and cost-effective SPE sorbents for the extraction of PLs followed by their analysis by HILIC coupled to ELSD. Several experimental factors related to the SPE protocol were established. Then, a comparison in terms of extraction performance of the selected MSM with a commercial silica gel based material [23] (hereinafter "SupelClean™") was performed. The recommended SPE method was successfully applied to the extraction and determination of PLs in human milk fat samples, since the knowledge of this complex sample is of great importance to further understand its intrinsic benefits for both full and preterm infants.

5. 2. Experimental

5. 2. 1. Reagents and materials

HPLC-grade ACN, *n*-hexane, MeOH, acetic acid glacial and chloroform were supplied by VWR Chemicals (Barcelona, Spain); reagent-grade dichloromethane, EtOH, *n*-hexane, anhydrous sodium sulfate, sodium chloride, sodium hydroxide and ammonia were purchased from Scharlab (Barcelona, Spain); TEOS, triethanolamine (TEA) and CTAB were obtained from Sigma-Aldrich (St. Louis, MO, USA); ammonium formate and titanium (IV) butoxide were supplied by Fluka (Buchs SG, Switzerland); iron (III) chloride 6-hydrate ($FeCl_3 \cdot 6H_2O$) and ammonium thiocyanate were supplied by Panreac (Barcelona, Spain); L-α-PC (soy bean, 95%) was

purchased from Avanti Polar Lipids (Alabaster, AL, USA); SM (chicken egg yolk, ≥ 95%), L-α-PE (egg yolk, ≥ 97%) were from Sigma-Aldrich. Deionized water (Barnstead deionizer, Sybron, Boston, Mass., U.S.A.) was used in all procedures.

Empty propylene cartridges (1 mL) and frits (20 µm pore size) were supplied by Análisis Vínicos (Tomelloso, Spain). Commercial silica gel based cartridges (SupelClean™ LC-Si (1 g sorbent, 6 mL volume)) were obtained from Supelco (Sigma-Aldrich).

Mature human milk samples were kindly donated by healthy well-nourished women. The samples were collected between the baby's feed by manual expression using a Medela Harmony™ Breastpump (Zug, Switzerland). After collection, milk samples were rapidly heated to 80 ºC and held at this temperature for 1.5 min in order to inactivate the lipases and to avoid triglycerides hydrolysis [24].

5. 2. 2. Instrumentation

Transmission electron microscope (TEM) images of MSMs were obtained using Jeol (Tokyo, Japan) model JEM-1010 microscope operated at 100 kV. A dispersion of these materials was made in pure EtOH by sonication, and 0.05 mL of this suspension was placed on a 200-mesh Cu grid coated with a holey amorphous carbon film. The EtOH was evaporated prior to TEM analysis. Images were obtained using a MegaView III camera provided with the AnalySIS image data acquisition system.

Scanning electron microscope (SEM) images were obtained with a Hitachi S-4800 (Ibaraki, Japan). For this purpose, the silica materials were sputter-coated with a thin layer of Au/Pd.

Surface area, pore size and volume were measured by porosimetry using nitrogen adsorption-desorption isotherms. The isotherms were recorded

with a Micromeritics ASAP2020 automated sorption analyzer. The specific surface areas were calculated from the adsorption data in low-pressure range using Brauner-Emmet-Teller (BET) model. Pore size was determined following the Barret-Joyner-Halenda (BJH) model on the adsorption branch of the isotherms.

Dynamic light scattering (DLS) for particle size determination was done with a Malvern Zetasizer ZS (Malvern, United Kingdom).

^{29}Si magic angle spinning nuclear magnetic resonance (MAS NMR) spectra were recorded on a Varian Unity 300 spectrometer (PA, USA) operating at 79.5 MHz, with a magic angle spinning speed of at least 4.0 kHz.

The Stewart assay for the quantification of PLs [25] was performed by measuring in UV-vis with a diode-array UV-vis spectrophotometer with a single pulsed xenon lamp (model 6305, Jenway, Staffordshire, UK) provided with a 1 cm optical-path quartz cell (Hellma, Müllheim, Germany).

Centrifugation steps were conducted in a Hettich® EBA 21 laboratory centrifuge with rotor 1116 (radius of 97 mm) and adapters 1631 (Sigma, Osterode am Harz, Germany). Evaporation under vacuum was accomplished using a miVac sample concentrator (SP Scientific, Warminster, PA).

Chromatographic separation of PLs and their determination was made with an 1100 series liquid chromatograph (Agilent Technologies, Waldbronn Germany) provided with a quaternary pump, a degasser, a thermostated column compartment, an automatic sampler, and an Agilent 385-ELSD (see Electronic Supplementary Material (ESM) for chromatographic conditions).

5. 2. 3. Preparation of MSMs (MCM-41 and UVM-7)

The method used to prepare both materials, denoted as atrane route, is based on the use of: (i) complexes that include TEA-related ligand species (i.e. “atranes”; silatranes in the present case) as hydrolytic inorganic precursors;

and (ii) surfactants as templating and porogen species [6,26,27]. In both cases, the same reagent with a molar ratio of Si: TEA: CTAB: H_2O = 2: 7: 0.5: 180 under pH controlled conditions (through the addition of a NaOH solution) was used to synthesize either MCM-41 (10 < pH < 11) or UVM-7 (8 < pH < 9) materials. Thus, MCM-41 was synthesized as follows: 0.49 g of NaOH were dissolved in 23 mL of TEA. Afterwards, 10.5 mL of TEOS were added, and the solution was heated at 150 °C for 5 min. After cooling the solution at 100 °C, 4.68 g of CTAB were added while stirring. Then, 80 mL water were added with vigorous stirring at a temperature of 60 °C. The white suspension was kept for 24 h at room temperature and the mesoporous powder was filtrated, washed with water and EtOH and air-dried. The UVM-7 silica was synthesized following the same method, but without addition of NaOH. In this case, only 2 h of aging time were necessary before filtering. The final porous materials (MCM-41 and UVM-7) were obtained removing the surfactant from the as-synthesized powders. This was carried out by two ways: pyrolysis of the samples at 550 ºC for 5 h and chemical extraction of the surfactant using an acetic acid/EtOH solution (*ca.* 1 g of silica powder, 10 mL of glacial acetic acid and 100 mL of EtOH 99%; t = 12-24 h at 60 ºC). The synthesis of Ti-UVM-7 material (with a Si/Ti = 25, 5 M ratio) was carried out by using exactly the same protocol described for the UVM-7 silica, and mixing the TEOS and titanium (IV) butoxide with TEA in the first preparation step. The reagent molar ratio used was: 2-x Si: x Ti: 7 TEA: 0.5 CTAB: 180 H_2O [26].

5. 2. 4. Fat extraction and analysis of human milk

Extraction of the lipid fraction from human milk samples was carried out according to Folch *et al*. [28] with minor modifications [29]. Thus, 1.5 mL of milk were dispersed in dichloromethane:MeOH (2:1, v/v). After removing the aqueous phase, the lower dichloromethane phase, containing the lipid fraction, was washed with a salt solution and evaporated under vacuum. The

final residue was re-dissolved in 5 mL hexane-EtOH (98:2, v/v). The lipid extract solution was percolated through the cartridge following the SPE protocol described below. The eluted fraction was dried under vacuum, re-dissolved in a known volume of $CHCl_3$:MeOH (2:1, v/v) (200 µL) and injected into the HPLC system.

5. 2. 5. SPE protocol

For the preparation of the SPE cartridges, 10 mg of the MSMs were packed between two frits into 1 mL empty propylene cartridges. Prior to extraction, activation and equilibration of the sorbent was done with 1 mL of MeOH and 1 mL of hexane-EtOH (98:2, v/v), respectively. Then, 500 µL of a PC solution of 4000 µg/mL prepared in hexane-EtOH (98:2, v/v) were percolated through the SPE cartridge. Before eluting the retained PC with $CHCl_3$:MeOH:H_2O (3:5:2, v/v/v) (500 µL), a washing step with hexane (500 µL) was done. All SPE fractions (loading, washing and elution) were collected and their PC content was quantified separately by Stewart assay [25] (measurement of absorbance at 488 nm). Then, the sorbent was regenerated with 1 mL of $CHCl_3$:MeOH:H_2O (3:5:2, v/v/v) followed by 1 mL of MeOH. All experiments were carried out in triplicate.

5. 3. Results and discussion

5. 3. 1. Characterization of the MSMs

As commented above, the preparation of final porous silica-based materials requires removing the surfactant from the as-synthesized mesoporous powders. The common approach to carry out this process is by pyrolysis. It is well-known that this type of treatment leads to a relatively high condensation of the silica walls, which involves new siloxane links at the cost

of reducing the relative proportion of terminal silanol groups [30]. However, it should be desirable to achieve a high density of silanol groups on the surface of the silica for certain analytical applications. To address this end, mild chemical extraction of the surfactant can be adopted. In this study, the two treatments, calcination (Cal) and chemical extraction (Ext), were conducted with UVM-7 materials. The synthesized MSMs were characterized by SEM and TEM (see ESM, **Figure S5.1**). For comparison, the conventional MCM-41 material and SupelClean™ were also included. As observed in ESM **Figure S5.1a**, the UVM-7 silica presents rough surfaces resulting from the aggregation of clusters with a large porosity between them. These clusters were constructed by aggregation of pseudo-spherical mesoporous primary nanoparticles with sizes of 15-30 nm (see ESM, **Figure S5.1d**). Additionally, UVM-7 materials doped with different ratios of Ti were prepared (see Preparation of MSMs). No significant changes in the SEM micrographs of these materials were observed compared to the pure silica.

SEM micrograph confirms the larger dimensions of the MCM-41 particles (in the 200-2000 nm range) (see ESM, **Figure S5.1b**) compared to the UVM-7 primary ones. Besides, the TEM image of the MCM-41 material (see ESM, **Figure S5.1e**) shows the presence of large domains with a hexagonal ordered disposition of the mesopores. On the other hand, the morphology of the SupelClean™ (see ESM, **Figure S5.1c**) commercial material includes relatively large grains (with a homogeneous size of *ca.* 50 μm). The TEM image shows that the internal organization of this solid is conformed by aggregation of non-porous particles (with sizes comprised between 5-10 nm) (see ESM, **Figure S5.1f**) being its clustered nature the responsible of a disordered inter-particle textural porosity.

Then, the surface area and pore-size distribution of the prepared MSMs were determined from the nitrogen adsorption-desorption isotherms (see ESM, **Figure S5.2** and **S5.3**). In UVM-7 silica-based materials, both calcined and chemically extracted, two adsorption steps are evidenced (see

ESM, **Figure S5.2a** and **S5.2b**). The first step, observed at intermediate partial pressures ($0.2 < P/P_0 < 0.5$), is caused by the capillary condensation of nitrogen into the mesoporous channels, and it is characteristic of Type IV isotherms. The second step, at a high relative pressure ($P/P_0 > 0.8$), corresponds to the filling of the large pores among the primary nanoparticles. The UVM-7 supports doped with Ti show a decrease in the N_2 adsorbed volume as compared with the pure UVM-7-Cal or UVM-7-Ext, respectively. As shown in **Table 5.1**, the surface area and pore volume of the doped Ti-UVM-7 materials show lower values than their UVM-7 pure silica counterparts. For MCM-41, only one condensation step is observed in the nitrogen adsorption-desorption isotherm (see ESM, **Figure S5.2c**), with the characteristic sharp shape of mesoporous materials. Thus, both materials display the existence of mesopores with similar pore size (2.8-3.0 nm), but in the case of UVM-7, a second large pore system with values close to 33 nm, due to the aggregation of primary nanoparticles, is evidenced (see **Table 5.1** and ESM, **Figure S5.3**). A single nitrogen adsorption step is also found for the SupelClean™ material, although it extends over a broad range of pressure values (see ESM, **Figure S5.2**). This leads to a pore size distribution much wider than the observed for the MCM-41, with a central value of *ca.* 9 nm (see ESM, **Figure S5.3**). Additionally, the surface areas and pore volumes of MCM-41 and SupelClean™ are lower than those obtained for the UVM-7 based materials (see **Table 5.1**).

Table 5.1. Surface area, pore size and pore volume of silica materials studied.

Silica family	Removal of surfactant	Si/Ti	S_{BET} (m^2/g)	Pore size (nm)[a] (small pore)	Pore size (nm) (large pore)	V (cm^3/g) (small pore)	V (cm^3/g) (large pore)	V (cm^3/g) (total pore)
UVM-7	Calcination	-	1122	2.77	34.22	0.87	1.94	2.81
		25	1046	2.81	44.01	0.89	1.31	2.20
		5	896	2.53	36.30	0.67	0.84	1.51
	Chemical extraction	-	1275	2.99	33.46	1.13	2.26	3.39
		25	1053	3.10	46.14	0.99	1.62	2.61
		5	1054	2.68	35.64	0.83	0.86	1.69
MCM-41	Chemical extraction	-	657	2.80	-	0.39	-	0.39
SupelClean™	-	-	488		9.09	-	0.38	0.38

[a]Pore diameters calculated by using the BJH model on the adsorption branch of the isotherms.

In order to evaluate the silica condensation degree in the tested silica-based materials, a ^{29}Si MAS NMR spectroscopic study was conducted (see ESM, **Figure S5.4**). Both samples (UVM-7-Ext and SupelClean™) show spectra typical of silica exhibiting three partially overlapped signals falling in the *ca.* -90 to -120 ppm range, which are associated to Q^2 (*ca.* -90 ppm), Q^3 (*ca.* -100 ppm) and Q^4 (*ca.* -110 ppm) Si-sites. The results of the deconvolution of the spectra of ESM **Figure S5.4** are gathered in **Table S5.1**. The lower $Q^4/(Q^2+Q^3)$ ratio for UVM-7-Ext (*ca.* 1.02) in comparison with SupelClean™ (*ca.* 1.72) suggests that the former possess a silica network with lower condensation degree, and therefore with more free silanol groups (more hydrophilic). On the other hand, $Q^4/(Q^2+Q^3)$ values close to 1 are also observed for MCM-41 materials, in which the surfactant removal was carried out through chemical procedures.

5. 3. 2. Evaluation of MSMs as SPE sorbents

SPE is a well-known extraction technique based on the partition of a solute between a mobile liquid phase and a solid stationary phase. To accomplish a SPE optimization, the conditions of loading, washing and elution steps are of critical importance. In this sense, previous kinetic studies of Sinyaeva and co-workers [22] showed that PC dissolved in this solvent provided a high adsorption capacity with high rate of mass transfer on MCM-41 materials. In addition, in a previous work [31], loading and washing solutions consisting of hexane resulted in suitable solvents for a good extraction performance of PLs in SPE. Taking into account all these considerations, a PC solution in hexane:EtOH (98:2, v/v) (200 µg PC per mg of sorbent) was selected and loaded onto UVM-7. An excellent retention (*ca*. 98%) was achieved in this material.

It should be noted that, in non-aqueous systems, such as hexane, PC forms reverse (inverted) micelles (critical micelle concentration (CMC) from

20 to 50 µg/mL) [22,32]. In our case, the PC concentration used was above CMC values, which gave reverse micelles with an average diameter *ca.* 2 nm (see DLS measurements in ESM **Figure S5.5a**). This value was close to the range reported in crude soybean oil [32]. Under these experimental conditions, where the interaction of polar head groups of PC molecules (inner surface of PC inverse micelles) with the hydrophilic silica surface (rich in silanol groups) is not favored, a feasible interaction mechanism (in two-steps) should be considered. A first step would imply the diffusion of reverse micelles along the pore systems (size-exclusion mechanism). In the second stage, the free silanol groups in silica surface would induce somehow a rupture of the PC micelles and hence promote the Si-OH···PC interactions.

In any case, the proposed mechanism is not exclusive of the UVM-7 silica. Any other silica material (as we commented below) with a similar density of silanol groups at the surface should behave in a similar way. Indeed, the different porosity of the silica architecture (pore size and shape) can favor or prevent the diffusion of micelles along the pore network. On the other hand, the formation of large PL mixed micelles and vesicles cannot be discarded, although these large aggregates (with relatively large sizes) result inadequate to penetrate the pore system.

Then, several elution solvents were tested (see **Figure 5.1**). As observed, the introduction of water in mixtures $CHCl_3$-MeOH provided an enhancement in recoveries, reaching values of (101 ± 4) and (95 ± 6)% for Si/Ti-25-UVM-7-Cal and UVM-7-Cal, respectively. The presence of more polar solvents may induce changes in the structuration and orientation of the PC molecules (adsorbed onto silica surface) to form normal (direct) micelles by increasing the number of hydrogen bonds with PC polar head group. Moreover, this fact was reflected in the smaller average size of normal micelles (0.8 nm; see ESM, **Figure S5.5b**) compared to reverse micelles (2 nm) since hydrophobic tails of PC molecules can be assembled tighter than

PC head groups. Thus, $CHCl_3$:MeOH:H_2O (3:5:2, v/v/v) was selected as elution solvent for further studies.

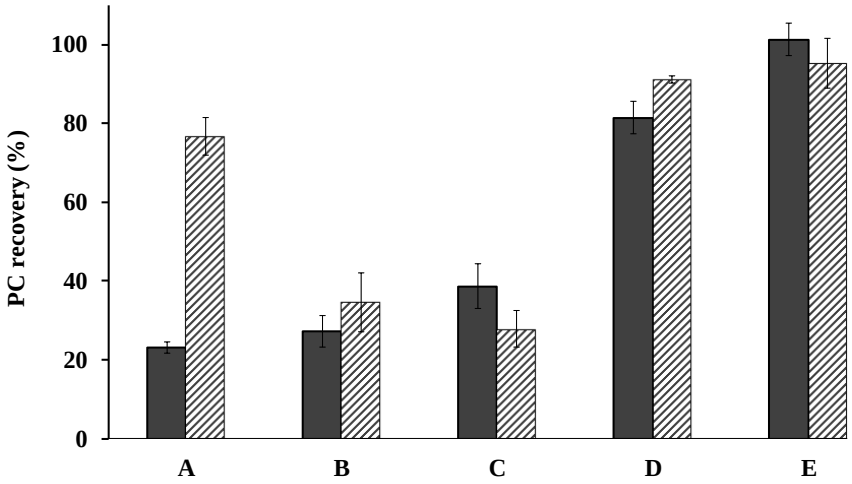

Figure 5.1. Influence of elution solvent on PC recovery on Si/Ti-25-UVM-7-Cal-SPE (bold bars) and UVM-7-Cal-SPE (stripped bars) cartridges. Elution solvent: MeOH (A); $CHCl_3$:MeOH (2:1, v/v) (B); $CHCl_3$:MeOH (3:5, v/v) (C); $CHCl_3$:MeOH:H_2O (3:5:1, v/v/v) (D); $CHCl_3$:MeOH: H_2O (3:5:2, v/v/v) (E).

Table 5.2 shows the PC content in the percolated (loading) and elution fractions for the different synthesized MSMs using two different loading solvents. $CHCl_3$:MeOH mixture (2:1, v/v) was included since it is commonly used to extract lipids [33,34]. However, the proposed organic solvent mixture (hexane:EtOH (98:2, v/v)) with greater hydrophobic character provided better results when working with these materials. From all the porous materials tested, UVM-7-Ext provided the best extraction performance, even better than MCM-41 and SupelClean™. These results can be explained as follows. The intraparticle mesopores both in UVM-7 and MCM-41 solids (see **Table 5.1**) are slightly larger than the PC micelles size. Therefore, only a certain interaction around the mesopore entrances should be expected. However, in

the case of UVM-7, the existence of a secondary large pore system is crucial for the diffusion of PC micelles and posterior adsorption of PC molecules. On the other hand, the incorporation of Ti to the UVM-7 silica system did not improve significantly the PC retention with respect pure silica. This result was unexpected, since the interaction between phosphate groups and Ti-based materials has been previously described [19,20].This fact might be attributed to different causes: (i) the low availability of Ti into the pore surface, since most of it remains embedded inside pore walls; (ii) the introduction of Ti element disturbs the order and reduces the pore size and surface area, which is a drawback to reach a desirable interaction.

Regarding SupelClean™, although its surface area was only 488 m^2/g, its average pore size (9 nm), together with its wide pore size distribution (see ESM, **Figure S5.3**), contribute to diffusion and retention of the target analyte. In any case, the larger voids among particles in UVM-7 silicas (four times bigger) when compared to SupelClean™, together with the existence of more regular cage-like inter-particle pores, confer to UVM-7 solids a greater ability to interact with host species such as PC micelles. Indeed, the adsorption capacity of the SupelClean™ was lower than UVM-7-Ext (169 and 544 µg/mg of sorbent, respectively); and even lower when, in accordance with literature [18,35], the $CHCl_3$:MeOH mixture (2:1, v/v) was employed (see **Figure 5.2**).

Apart from these considerations, NMR measurements also showed a higher density of silanol groups in the UMV-7 surface. Thus, the synergistic effect of the better accessibility and higher hydrophilic surface of the UVM-7-Ext silica seems to be the key to explain its best performance. Therefore, this material was selected for further studies.

Table 5.2. Percentage of PC in the percolated (loading) and elution fractions using the MSM-SPE cartridges.

Silica material	Loading[a] (%)	Elution[b] (%)	Loading[c] (%)	Elution[b] (%)
Si-UVM-7-Ext	1.3 ± 0.8	95 ± 5	43.7 ± 0.8	52 ± 6
Si-UVM-7-Cal	2.0 ± 1.8	44 ± 9	60 ± 13	31 ± 17
Si/Ti-5-UVM-7-Ext	4 ± 4	73.2 ± 0.4	52 ± 10	17.7 ± 1.5
Si/Ti-5-UVM-7-Cal	38 ± 2	57.3 ± 0.5	53 ± 2	25 ± 5
Si/Ti-25-UVM-7-Ext	1.0 ± 0.6	92 ± 9	65 ± 8	20 ± 10
Si/Ti-25-UVM-7-Cal	2.0 ± 0.6	96 ± 13	43 ± 2	50 ± 12
MCM-41-Ext	50 ± 6	59 ± 2	78 ± 3	10 ± 3
SupelClean™	15 ± 7	88 ± 18	79.8 ± 1.5	24.1 ± 1.7

[a] Loading solvent: Hexane:EtOH (98/2, v/v).

[b] Elution solvent: $CHCl_3$:MeOH:H_2O (3:5:2, v/v/v).

[c] Loading solvent: $CHCl_3$:MeOH (2:1, v/v).

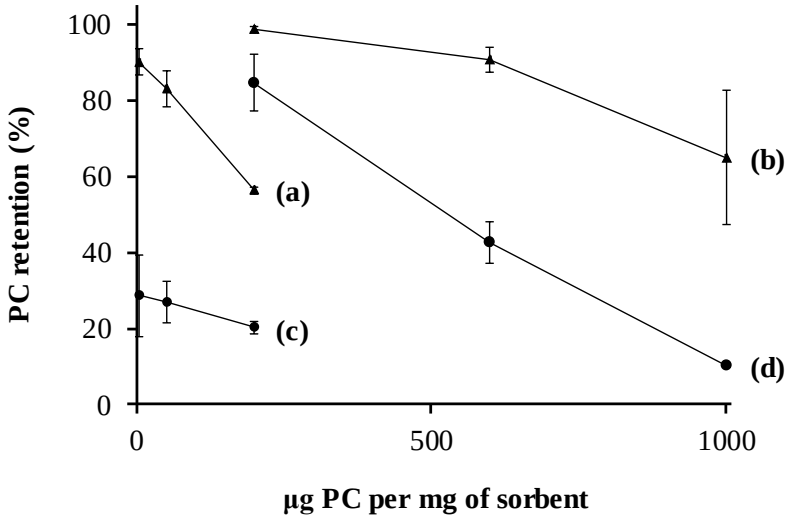

Figure 5.2. Adsorption capacity of UVM-7-Ext (▲) and SupelClean™ (●) sorbents in different loading solvents: $CHCl_3$:MeOH (2:1, v/v) (a, c) and hexane:EtOH (98:2, v/v) (b, d).

5. 3. 3. Analytical features of the selected MSM

As mentioned above, the adsorption capacity of UVM-7-Ext was determined to be 544 µg of PC per mg of sorbent. This value is significantly higher than that previously reported for this analyte in a molecularly imprinted-based SPE sorbent [31] and typical bed capacity of SPE cartridges [36].

The reusability of the UVM-7-Ext-SPE cartridges was also evaluated using the SPE protocol described in the Experimental Section. After 15 uses, excellent performance with a recovery of (94 ± 4)% for PC was achieved. Apart from this excellent reusability, another non-negligible strength is the low amount of sorbent used (10 mg) compared to other home-made (150 mg) [20] or commercial cartridges (1000 mg) [18]. This implies the possibility of manufacturing several SPE cartridges from a single synthesis of the UVM-7

material, which undoubtedly makes this SPE protocol economically very attractive.

On the other hand, breakthrough volume of the UVM-7-Ext-SPE cartridges was studied by analyzing the recoveries of PC after loading different sample volumes (0.5-8 mL) containing a constant amount of PC (200 µg per mg of sorbent). With a sample loading volume of 8 mL, recovery of PC was (97 ± 2) %, which indicated that no significant compound loss (analyte breakthrough) took placed.

Then, preconcentration capacity was investigated by loading 8 mL of PC and eluting with 0.1, 0.25 or 0.5 mL, which corresponds to a preconcentration factor (PCF) of 80, 32 and 16, respectively. After applying the SPE protocol, percentage of PC found in the elution fraction was (18 ± 12), (93 ± 15) and (97 ± 4) for 0.1, 0.25 or 0.5 mL, respectively. These results suggest that to ensure quantitative and reproducible recoveries, an elution volume of 0.5 mL should be used.

Under the selected conditions, a multi-standard solution of PC, SM and PE (500 µL, 1000 µg/mL each) was percolated through the SPE cartridge. Recovery value for this mixture of PLs was (94 ± 4)%. This result confirmed the suitability of the selected sorbent for the simultaneous extraction of these compounds.

5. 3. 4. Extraction and analysis of PLs from lipid extracts of milk

The applicability of the UVM-7-Ext SPE cartridge to fat extracts of human milk was tested following the procedure described in Experimental Section, and the eluates were analyzed by HILIC-ELSD. External calibration curves for the quantitative evaluation of PLs were constructed based on peak area versus mass of analyte. The response of ELSD detector was linear ($r > 0.998$) in the range of 150-600 µg/mL. Standard addition calibration

curves were also conducted, being the samples solutions spiked with different PL contents (30-120 μg). No significant differences between the slopes of both types of calibration curves were found, which discarded any matrix effect from human milk samples using the MSM-SPE method.

Besides, LODs and LOQs were also estimated on the basis of signal-to-noise ratio (S/N = 3 and 10, respectively). The LOD and LOQ values were less than 3.5 and 11.7 μg/mL, respectively.

The content of the PLs present in the milk fat extract was 2.1, 0.7 and 0.8 mg per g of fat for PE, PC and SM, respectively. **Figure 5.3** shows the chromatograms of the human milk fat sample before and after extraction with UVM-7-Ext SPE cartridge. A significant reduction of nonpolar lipids and an increase in ELSD signals of PLs in the elution fraction (continuous line) when compared to the crude fat extract (dashed line) were observed. This demonstrates the suitability of the MSM to be applied in clean-up and preconcentration steps for further analysis of PLs present in complex samples.

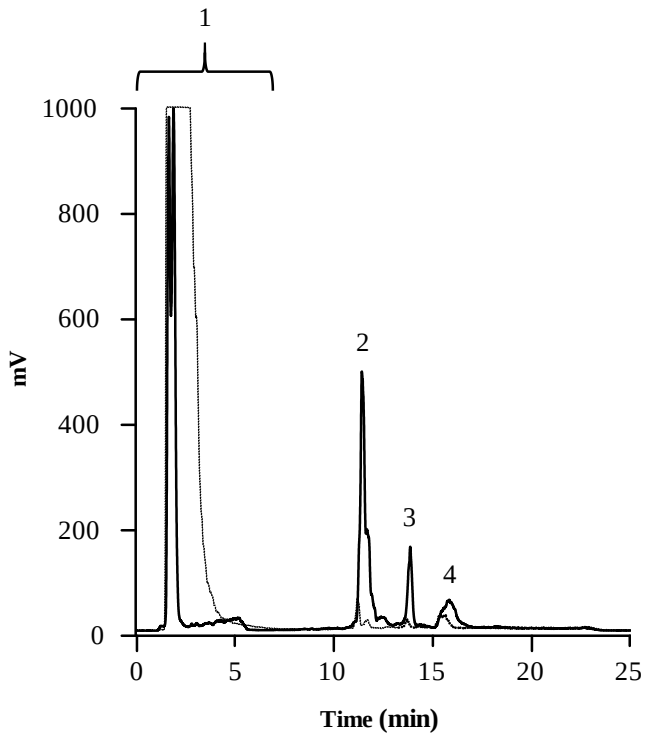

Figure 5.3 HILIC-ELSD chromatograms of human milk fat extract obtained without (dashed line) and with (continuous line) UVM-7-Ext SPE treatment. Peak identification: (1) nonpolar lipids, (2) PE, (3) PC and (4) SM. For SPE and HILIC-ELSD conditions, see Experimental Section and ESM, respectively.

5. 4. Conclusions

In this work, several MSMs (MCM-41, pure and Ti-doped UVM-7) have been prepared following the atrane route. The potential use of the synthesized MSMs as SPE sorbents for PLs extraction has been studied. At the same time, a commercial silica-based material (SupelClean^{TM}) has been considered. The feasible interaction mechanism of the target analyte (PC) with the silica materials was described in two stages: (i) diffusion of PC reverse

micelles along the pore systems; and (ii) rupture of PC micelles by silanol groups inducing a favored Si-OH···PC interaction. From all the MSMs materials tested, UVM-7 with a mild chemical extraction of surfactant provided the best results. This fact is due to the more hydrophilic environment (free silanol groups) of UVM-7-Ext with respect to MCM-41 and SupelClean™, jointly with the second large pore system of UVM-7-like materials. The adsorption capacity (544 μg of PC per mg of sorbent), reusability (up to 15 reuses) and preconcentration capacity (up to 16) of the UVM-7-Ext are features of great importance for sample treatment purposes. The potential use of the UVM-7-Ext as SPE sorbent was also demonstrated by its application to human milk fat extracts. This treatment provided an effective clean-up of sample (particularly to remove triglycerides) and enrichment of PLs prior their determinations by HPLC-ELSD. Besides, this protocol preserves the structural integrity of HILIC column. Consequently, UVM-7-like materials deserve to be considered as attractive SPE sorbents for the extraction of PLs from biological samples.

Acknowledgments

Project CTQ2014-52765-R (MINECO of Spain and FEDER), MAT2015-64139-C4-2-R (MEyC-Retos) and PROMETEO/2016/145 (Generalitat Valenciana). I. T-D thanks the MINECO for an FPU grant for PhD studies.

Conflict of interest

The authors declare that they have no conflict of interest.

5. 5. References

[1] C.T. Kresge, M.E. Leonowicz, W.J. Roth, J.C. Vartuli, J.S. Beck, Ordered mesoporous molecular sieves synthesized by a liquid-crystal template mechanism, Nature 359 (1992) 710–712. doi:10.1038/359710a0.

[2] R. Luque, A.M. Balu, J.M. Campelo, M.D. Gracia, E. Losada, A. Pineda, A.A. Romero, J.C. Serrano-Ruiz, Catalytic applications of mesoporous silica-based materials, Catalysis 24 (2012) 253–280. doi:10.1039/9781849734776.

[3] Z. Li, J.C. Barnes, A. Bosoy, J.F. Stoddart, J.I. Zink, Mesoporous silica nanoparticles in biomedical applications, Chem. Soc. Rev. 41 (2012) 2590–2605. doi:10.1039/c1cs15246g.

[4] N. Casado, D. Pérez-Quintanilla, S. Morante-Zarcero, I. Sierra, Current development and applications of ordered mesoporous silicas and other sol–gel silica-based materials in food sample preparation for xenobiotics analysis, TrAC - Trends Anal. Chem. 88 (2017) 167–184. doi:10.1016/j.trac.2017.01.001.

[5] D. Zhao, J. Feng, Q. Huo, N. Melosh, G.H. Fredrickson, B.F. Chmelka, G.D. Stucky, Triblock copolymer syntheses of mesoporous silica with periodic 50 to 300 angstrom pores, Science 279 (1998) 548–552. doi:10.1126/science.279.5350.548.

[6] J. El Haskouri, D. Ortiz de Zárate, C. Guillem, J. Latorre, M. Caldés, A. Beltrán, D. Beltrán, A.B. Descalzo, G. Rodríguez-López, R. Martínez-Máñez, M.D. Marcos, P. Amorós, Silica-based powders and monoliths with bimodal pore systems, Chem. Commun. 0 (2002) 330–331. doi:10.1039/b110883b.

[7] L.T. Gibson, Mesosilica materials and organic pollutant adsorption:

part B removal from aqueous solution, Chem. Soc. Rev. 43 (2014) 5173–5182. doi:10.1039/C3CS60095E.

[8] L.T. Gibson, Mesosilica materials and organic pollutant adsorption: part A removal from air, Chem. Soc. Rev. 43 (2014) 5163–5172. doi:10.1039/C3CS60096C.

[9] X.-M. Wang, X.-Z. Du, H.-H. Rao, X.-Q. Lu, Determination of polycyclic aromatic hydrocarbons in water by a novel mesoporous-coated stainless steel wire microextraction combined with HPLC, J. Sep. Sci. 33 (2010) 3239–3244. doi:10.1002/jssc.201000287.

[10] W. Cheng, H. Ma, L. Zhang, Y. Wang, Hierarchically imprinted mesoporous silica polymer: An efficient solid-phase extractant for bisphenol A, Talanta 120 (2014) 255–261. doi:10.1016/j.talanta.2013.12.001.

[11] L.J. Huerta, P. Amorós, D. Beltrán-Porter, V.C. Corberán, Selective oxidative activation of isobutane on a novel vanadium-substituted bimodal mesoporous oxide V-UVM-7, Catal. Today 117 (2006) 180–186. doi:10.1016/j.cattod.2006.05.016.

[12] A.B. Descalzo, M.D. Marcos, R. Martínez-Máñez, J. Soto, D. Beltrán, P. Amorós, Anthrylmethylamine functionalised mesoporous silica-based materials as hybrid fluorescent chemosensors for ATP, J. Mater. Chem. 15 (2005) 2721–2731. doi:10.1039/b501609f.

[13] A. Weller, E.J. Carrasco-Correa, C. Belenguer-Sapiña, A. de los Reyes Mauri-Aucejo, P. Amorós, J.M. Herrero-Martínez, Organo-silica hybrid capillary monolithic column with mesoporous silica particles for separation of small aromatic molecules, Microchim. Acta 184 (2017) 3799–3808. doi:10.1007/s00604-017-2404-z.

[14] Z. Guo, A.F. Vikbjerg, X. Xu, Enzymatic modification of phospholipids for functional applications and human nutrition,

Biotechnol. Adv. 23 (2005) 203–259. doi:10.1016/j.biotechadv.2005.02.001.

[15] J.G. Parsons, S. Patton, Two-dimensional thin-layer chromatography of polar lipids from milk and mammary tissue, J. Lipid Res. 8 (1967) 696–698.

[16] F. Sánchez-Juanes, J.M. Alonso, L. Zancada, P. Hueso, Distribution and fatty acid content of phospholipids from bovine milk and bovine milk fat globule membranes, Int. Dairy J. 19 (2009) 273–278. doi:10.1016/j.idairyj.2008.11.006.

[17] R.J. Maxwell, D. Mondimore, J. Tobias, Rapid method for the quantitative extraction and simultaneous class separation of milk lipids, J. Dairy Sci. 69 (1986) 321–325. doi:10.3168/jds.S0022-0302(86)80408-8.

[18] P. Donato, F. Cacciola, F. Cichello, M. Russo, P. Dugo, L. Mondello, Determination of phospholipids in milk samples by means of hydrophilic interaction liquid chromatography coupled to evaporative light scattering and mass spectrometry detection, J. Chromatogr. A 1218 (2011) 6476–6482. doi:10.1016/j.chroma.2011.07.036.

[19] C.D. Calvano, O.N. Jensen, C.G. Zambonin, Selective extraction of phospholipids from dairy products by micro-solid phase extraction based on titanium dioxide microcolumns followed by MALDI-TOF-MS analysis, Anal. Bioanal. Chem. 394 (2009) 1453–1461. doi:10.1007/s00216-009-2812-y.

[20] Q. Shen, H.-Y. Cheung, TiO_2/SiO_2 core-shell composite-based sample preparation method for selective extraction of phospholipids from shrimp waste followed by hydrophilic interaction chromatography coupled with quadrupole time-of-flight/mass spectrometry analysis, J. Agric. Food Chem. 62 (2014) 8944–8951. doi:10.1021/jf503040p.

[21] L.A. Sinyaeva, N.A. Belanova, S.I. Karpov, V.F. Selemenev, F. Roessner, Dynamics of the sorption of phosphatidylcholine by mesoporous composites based on MCM-41, Russ. J. Phys. Chem. A 90 (2016) 2254–2261. doi:10.1134/S003602441611025X.

[22] L.A. Sinyaeva, S.I. Karpov, N.A. Belanova, F. Roessner, V.F. Selemenev, Characteristics of the mass transfer of phosphatidylcholine during its sorption on mesoporous composites based on MCM-41, Russ. J. Phys. Chem. A 89 (2015) 2278–2284. doi:10.1134/S0036024415120298.

[23] Sigma-Aldrich, Supelclean™ LC-Si SPE tube, (año no indicado). http://www.sigmaaldrich.com/catalog/product/supelco/57051?lang=es&region=ES (Fecha de acceso: 06/04/2017).

[24] S. Morera Pons, A.I. Castellote Bargalló, M.C. López Sabater, Evaluation by high-performance liquid chromatography of the hydrolysis of human milk triacylglycerides during storage at low temperatures, J. Chromatogr. A 823 (1998) 467–474. doi:10.1016/S0021-9673(98)00273-8.

[25] J.C.M. Stewart, Colorimetric determination of phospholipids with ammonium ferrothiocyanate, Anal. Biochem. 104 (1980) 10–14. doi:10.1016/0003-2697(80)90269-9.

[26] S. Cabrera, J. El Haskouri, C. Guillem, J. Latorre, A. Beltrán-Porter, D. Beltrán-Porter, M.D. Marcos, P. Amorós, Generalised syntheses of ordered mesoporous oxides: The atrane route, Solid State Sci. 2 (2000) 405–420. doi:10.1016/S1293-2558(00)00152-7.

[27] J. El Haskouri, J.M. Morales, D. Ortiz De Zárate, L. Fernández, J. Latorre, C. Guillem, A. Beltrán, D. Beltrán, P. Amorós, Nanoparticulated silicas with bimodal porosity: Chemical control of the pore sizes, 47 (2008) 8267–8277. doi:10.1021/ic800893a.

[28] J. Folch, M. Lees, G.H. Sloane Stantley, A simple method for the isolation and purification of total lipides from animal tissues, J. Biol. Chem. 266 (1957) 497–509.

[29] I.S. Chen, C.-S.J. Shen, A.J. Sheppard, Comparison of methylene chloride and chloroform for the extraction of fats from food products, J. Am. Oil Chem. Soc. 58 (1981) 599–601. doi:10.1007/BF02672373.

[30] R.K. Iler, The chemistry of silica: Solubility, polymerization, colloid and surface properties and biochemistry of silica, Wiley, New York, 1979.

[31] I. Ten-Doménech, H. Martínez-Pérez-Cejuela, M.J. Lerma-García, E.F. Simó-Alfonso, J.M. Herrero-Martínez, Molecularly imprinted polymers for selective solid-phase extraction of phospholipids from human milk samples, Microchim. Acta 184 (2017) 3389–3397. doi:10.1007/s00604-017-2345-6.

[32] S. Manjula, I. Kobayashi, R. Subramanian, Characterization of phospholipid reverse micelles in nonaqueous systems in relation to their rejection during membrane processing, Food Res. Int. 44 (2011) 925–930. doi:10.1016/j.foodres.2011.01.059.

[33] F. Giuffrida, C. Cruz-Hernandez, B. Flück, I. Tavazzi, S.K. Thakkar, F. Destaillats, M. Braun, Quantification of phospholipids classes in human milk, Lipids 48 (2013) 1051–1058. doi:10.1007/s11745-013-3825-z.

[34] T.P.L. Ferraz, M.C. Fiúza, M.L.A. Dos Santos, L. Pontes De Carvalho, N.M. Soares, Comparison of six methods for the extraction of lipids from serum in terms of effectiveness and protein preservation, J. Biochem. Biophys. Methods 58 (2004) 187–193. doi:10.1016/j.jbbm.2003.10.008.

[35] A. Avalli, G. Contarini, Determination of phospholipids in dairy

products by SPE/HPLC/ELSD, J. Chromatogr. A 1071 (2005) 185–190. doi:10.1016/j.chroma.2005.01.072.

[36] Sigma-Aldrich, SPE Cartridge (Tube) Configuration Guide, (2016). http://www.sigmaaldrich.com/analytical-chromatography/sample-preparation/spe/tube-configuration-guide.printerview.html (Fecha de acceso: 26/09/2016).

5. 6. Electronic Supplementary Material

5. 6. 1. Chromatographic conditions for HILIC-ELSD

Separation was performed with a Kinetex™ HILIC 100 Å column (150 mm × 4.6 mm, 2.6 µm; Phenomenex, Torrance, CA, USA). Mobile phases consisted of ACN-ammonium formate 100 mM (A, 97:3, v/v) and water-ammonium formate 100 mM (B, 97:3, v/v). The chromatographic separation was carried out using the following gradient: 0-3.5 min, 100% A; 11 min, 15% B and kept during 10 min. Column temperature, 25 ºC; flow rate, 1.0 mL/min and injection volume, 20 µL. The ELSD parameters were: evaporation and nebulization temperature, 80 and 40 ºC, respectively; gas flow rate, 1.4 Standard Litres per Minute (SLM); gain factor, 1.

5. 6. 2. Characterization of mesoporous silica materials

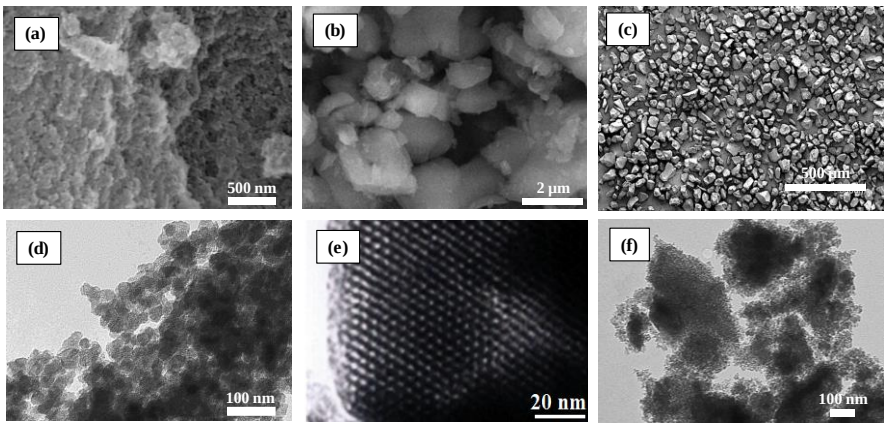

Figure S5.1. SEM (a-c) and TEM (d-f) images of mesoporous silica UVM-7-Ext (a) and (d), MCM-41 (b) and (e) and SupelClean™ (c) and (f).

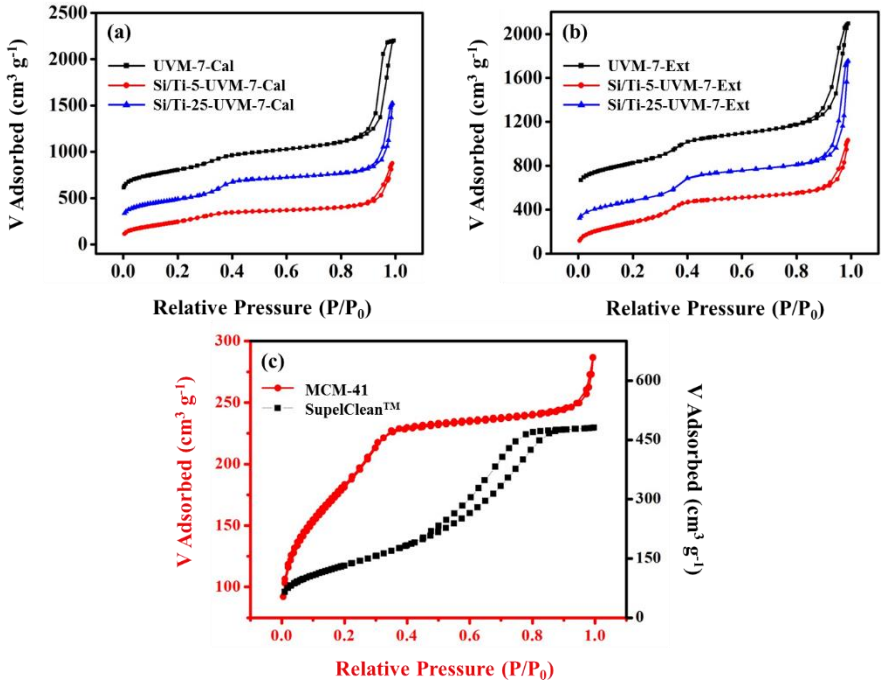

Figure S5.2. N_2 adsorption-desorption isotherms of mesoporous silica UVM-7 materials with calcination (a), with chemical extraction of the surfactant (b) and MCM-41 and SupelClean™ (c).

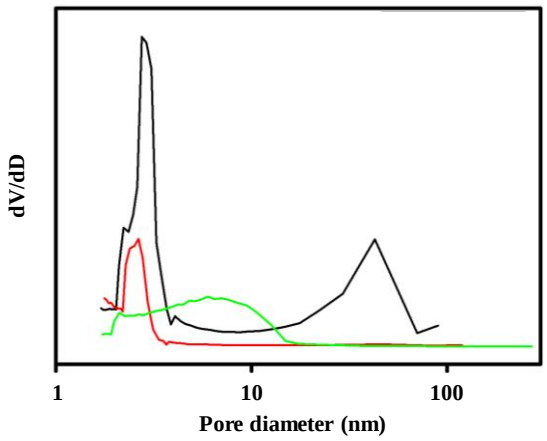

Figure S5.3. Pore size distribution of mesoporous silica UVM-7-Ext (black), MCM-41 (red) and SupelClean™ (green).

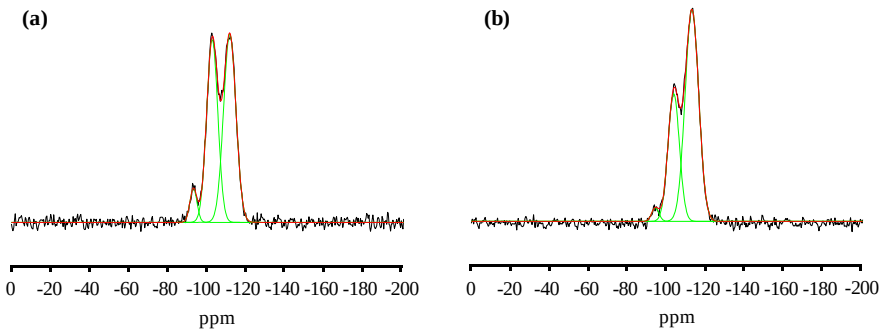

Figure S5.4. ^{29}Si MAS NMR spectra of mesoporous silica UVM-7-Ext (a) and SupelClean™ (b).

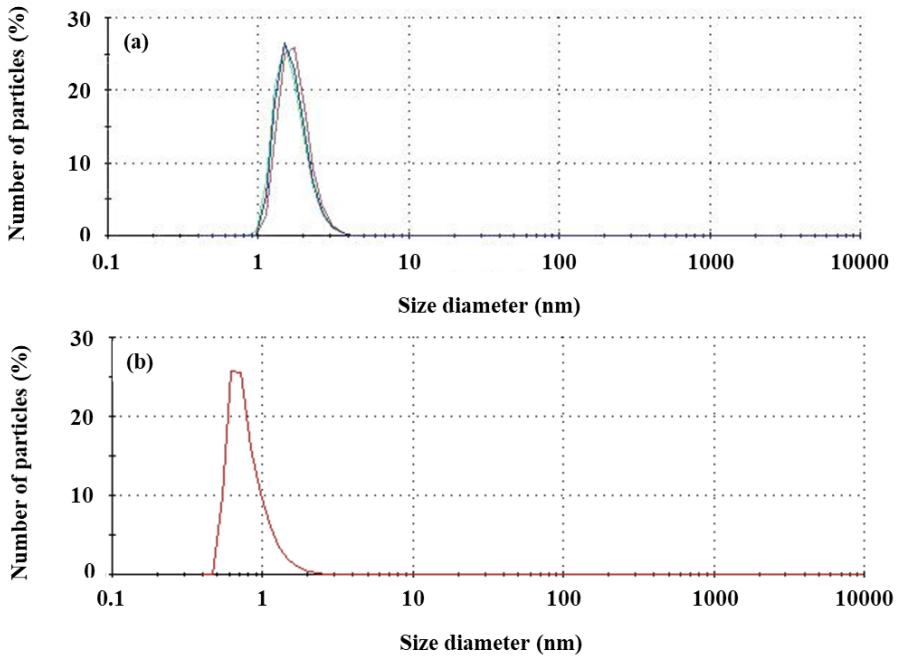

Figure S5.5. Size distribution by number of PC reverse micelles in hexane:EtOH (98:2, v/v) (a) and PC normal micelles in $CHCl_3$:MeOH:H_2O (3:5:2, v/v/v).

Table S5.1. Deconvolution of ^{29}Si-MAS NMR spectra of UVM-7-Ext and commercial silica.

	UVM-7-Ext		**SupelClean™**	
Si (Q^n)	**δ (ppm)**	**Relative intensity (%)**	**δ (ppm)**	**Relative intensity (%)**
Q^4	-111.3	50.6	-112.7	63.2
Q^3	-102.3	44.2	-103.3	34.5
Q^2	-92.7	5.2	-92.7	2.3

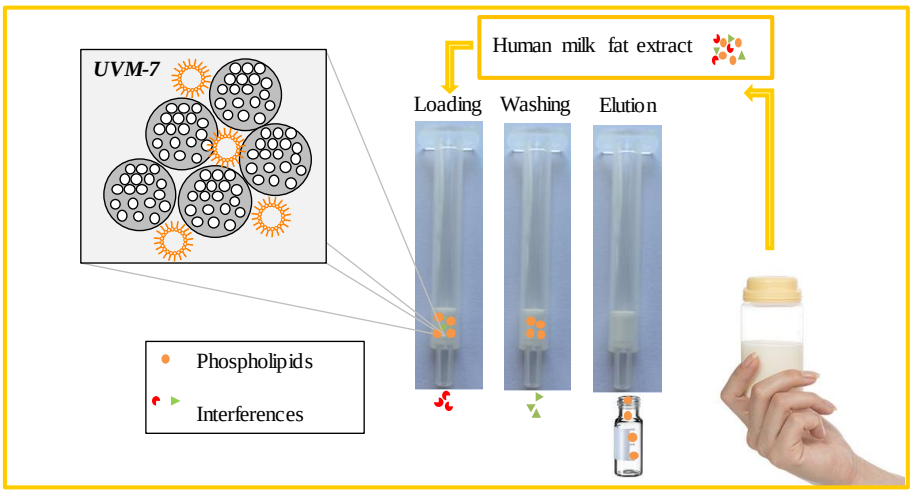
UVM-7
Human milk fat extract
Loading
Washing
Elution
Phospholipids
Interferences

CAPÍTULO 6

Polymer-based materials modified with magnetite nanoparticles for enrichment of phospholipids

Talanta 180 (2018) 162–167

Contents lists available at ScienceDirect

Talanta

journal homepage: www.elsevier.com/locate/talanta

Polymer-based materials modified with magnetite nanoparticles for enrichment of phospholipids

I. Ten-Doménech[a], H. Martínez-Pérez-Cejuela[a], E.F. Simó-Alfonso[a], S. Torres-Cartas[b], S. Meseguer-Lloret[b], J.M. Herrero-Martínez[a,*]

[a] Department of Analytical Chemistry, University of Valencia, C/Doctor Moliner 50, 46100 Burjassot, Valencia, Spain
[b] Instituto de Investigación para la Gestión Integrada de Zonas Costeras, Universitat Politècnica de València, C/Paranimf 1, 46730 Grao de Gandía, Spain

A polymeric material modified with MNPs has been synthesized and evaluated as sorbent both for SPE and dispersive MSPE of PLs in human milk samples. The synthesized sorbent was characterized by scanning electron microscopy and its iron content was also determined. Several experimental variables that affect the extraction performance (e.g., loading solvent, breakthrough volume and loading capacity) were investigated and a comparison between conventional SPE and MSPE modalities was done. The proposed method was satisfactorily applied to the analysis of PLs in human milk fat extracts in different lactation stages and the extracted PLs were determined by means of hydrophilic interaction liquid chromatography using evaporative light scattering detection.

Keywords: Magnetic polymer-based material; Solid-phase extraction; Phospholipids; Human milk; Hydrophilic interaction liquid chromatography-evaporative light scattering detection.

6. 1. Introduction

Human breast milk can be considered as the optimum food for all infants, since it satisfies the nutritional requirements for a healthy growth and development. Among the different human milk nutrients, about 50% of total energy intake comes from the lipid fraction of milk [1]. Within this fraction, PLs are basic constituents of the milk fat globule membrane, showing emulsifying properties and, moreover, their implication in many biological processes (e.g., brain development in newborn infants) has been demonstrated [2]. The total amount of PLs in human milk ranges from 0.5 to 1.0 g per 100 g of fat [3] and their distribution, given as percentage of total PLs, is: PC 28-35%, PE 28-30%, SM 25-38%, PI 5-9% and PS 3-9% [4,5].

Due to the amphiphilic nature of PLs, their quantitative analysis is not a straightforward process. To characterize and quantify PLs in both biological and food matrices, HILIC, either coupled with ELSD [6] or with MS [7], has been satisfactorily applied.

However, the challenge in PLs analysis arises from their low abundance with respect to nonpolar TAGs (98-99%). To address this problem, several techniques, such as 2D-TLC [8,9], column chromatography [10] and SPE [5–7] have been employed.

In this context, magnetic materials have recently emerged as extraction sorbents (namely, MSPE) in the analysis of food samples and other matrices [11,12]. These sorbents can be easily handled by the application of an external magnetic field (a magnet arranged outside the extraction vessel), thereby avoiding additional centrifugation or filtration steps. A usual strategy to synthesize functionalized magnetic nanomaterials (FMMs) is to coat the core of MNPs with silica via sol-gel process [13]. Alternatively, polymer-coated MNPs can be accomplished by physical/chemical adsorption or surface coating with specific ligands, depending on specific applications. However,

some of these FMMs showed limited dispersibility and reproducibility, which undoubtedly affect to their adsorption performance. In this sense, the immobilization of bare MNPs onto silica or polymeric supports could be an alternative approach to be considered. This procedure would allow to fully exploit their interaction capabilities, as for instance, with phosphorus-based compounds [14,15].

Recently, organic polymers have been synthesized by in situ preparation and evaluated as alternative stationary phases to replace conventional packing materials [16]. These materials show some advantages, such as their high stability, low cost, ease of preparation and very low resistance to flow. Particularly, polymeric monoliths based on GMA have been recently employed as platform in the synthesis of novel sorbents with different functionalities for sample preparation purposes [16–18]. However, the use of GMA as support for the attachment of MNPs has been only slightly explored [19,20]. Although these supports have been applied to the enrichment of phosphorous-compounds in aqueous samples (with a reduced number of possible interferences), their application to the isolation of PLs in more complex matrices (lipid matrices) has not been explored.

The aim of this work was the evaluation of a composite material, which combines the advantages of MNPs and GMA polymers to selectively extract PLs from real complex matrices such as human milk. The sorbent was prepared from a ground GMA-*co*-EDMA polymer, subsequently modified with a silanizing agent, to which MNPs were attached. This procedure provides a sorbent with a surface coated with bare MNPs, which are available to interact with the phosphate groups present in PLs. The prepared material was evaluated both in conventional SPE and in MSPE to extract PC from standard solutions. The features of this material as extraction sorbent (such as extraction recoveries, reusability, etc) were studied. After conventional SPE or MSPE treatment, HILIC-ELSD analysis was carried out. To our

knowledge, this is the first work dealing with PLs isolation from human milk fat extracts using a polymeric sorbent modified with MNPs.

6. 2. Materials and methods

6. 2. 1. Chemicals and reagents

HPLC-grade ACN, MeOH and chloroform were purchased from VWR Chemicals (Barcelona, Spain); reagent-grade dichloromethane, EtOH, *n*-hexane, sulfuric acid and hydrochloric acid, anhydrous sodium sulfate, sodium hydroxide, ascorbic acid and ammonia were supplied by Scharlab (Barcelona, Spain); GMA, EDMA, *o*-phenanthroline monohydrate, SM (chicken egg yolk, ≥ 95%) and L-α-PE (egg yolk, ≥ 97%) were obtained from Sigma-Aldrich (St. Louis, MO, USA); azobisisobutyronitrile (AIBN), BHT and ammonium formate were supplied by Fluka (Buchs SG, Switzerland); cyclohexanol, 1-dodecanol, (3-aminopropyl)trimethoxysilane (APTMS), 2-nitrophenol and acetone were purchased from Alfa-Aesar (Karlsruhe, Germany); ferrous chloride ($FeCl_2 \cdot 4H_2O$), ferric chloride ($FeCl_3 \cdot 6H_2O$), citric acid monohydrate and ammonium thiocyanate were supplied by Panreac (Barcelona, Spain); ammonium iron (II) sulfate hexahydrate (Mohr's salt) was obtained from Probus (Badalona, Spain); L-α-PC (soy bean, 95%) was purchased from Avanti Polar Lipids (Alabaster, AL, USA).

Deionized water (Barnstead deionizer, Sybron, Boston, Mass., U.S.A.) was used in all procedures.

Empty propylene cartridges (3 mL) and frits (20 µm pore size) were supplied by Análisis Vínicos (Tomelloso, Spain).

6. 2. 2. Instrumentation

Polymerization protocol was carried out using a vacuum oven (Memmert, Schwabach, Germany).

TEM images of the MNPs were obtained using a Jeol (Tokyo, Japan) model JEM-1010 microscope operated at 100 kV. Images were obtained using a MegaView III camera provided with the AnalySIS image data acquisition system.

SEM images were obtained with a Hitachi S-4800 (Ibaraki, Japan) integrated with backscattered electron detector (Bruker, Germany).

Surface areas were measured by porosimetry using nitrogen adsorption-desorption isotherms. The isotherms were recorded with a Micromeritics ASAP2020 automated sorption analyzer. The specific surface areas were calculated from the adsorption data in low-pressure range using BET model.

Inductively-coupled plasma MS (ICP-MS) measurements were conducted with an Agilent 7900 ICP-MS (Agilent Technologies, Waldbronn, Germany).

For UV-Vis measurements, an 8453 diode-array UV-Vis spectrophotometer (Agilent Technologies) was used.

Centrifugation steps were conducted in a Hettich® EBA 21 laboratory centrifuge with rotor 1116 and adapters 1631 (Sigma, Osterode am Harz, Germany).

Evaporation under vacuum was accomplished using a miVac sample concentrator (SP Scientific, Warminster, PA).

Chromatographic separation and determination of PLs was made with an 1100 series liquid chromatograph (Agilent Technologies) provided with a quaternary pump, a degasser, a thermostated column compartment, an

automatic sampler, a UV-Vis diode array detector online coupled to an Agilent 385-ELSD (see Supporting Information for chromatographic and detection conditions).

6. 2. 3. Preparation of MNPs

Fe_3O_4 nanoparticles were synthesized through the co-precipitation method from aqueous Fe^{3+}/Fe^{2+} salt solutions with a ratio 2:1 by the addition of ammonia [13,21] (see Supporting Information).

6. 2. 4. Synthesis and silanization of GMA-*co*-EDMA material

The synthesis of GMA-*co*-EDMA polymeric material was based on a previous work [22]. The obtained polymeric material was ground with a mortar and sieved to particle sizes between 125 and 200 μm.

For the silanization, 3 g of the powdered material were placed in a glass flask with 75 mL of a 65 mM APTMS solution in acetone and allowed to react for 3 h at 60 ºC (water bath) under stirring. Then, the silanized material was filtered, washed with EtOH, dried at 60 ºC and stored in a desiccator until use.

6. 2. 5. Functionalization of silanized GMA-based material with MNPs

The attachment of the MNPs was carried out following the method described by Meseguer-Lloret and co-workers [20]. Thus, the silanized powdered material (2.5 g) was placed into a doubled PTFE fritted 60 mL propylene syringe. Several fractions (15 × 5 mL) of a 1000 μg/mL dispersion of MNPs in EtOH-water (1:1, v/v) were passed through the syringe under continuous stirring, while remaining liquid was removed by gravity at a flow

rate of 0.5 mL/min. After that, a brown colored powder, corresponding to the MNPs-modified material, was obtained. To remove the excess of MNPs, the material was washed with 100 mL of an EtOH-water solution (1:1, v/v), followed by 15 mL of EtOH. Then, the MNPs-modified material was dried in an oven at 60 ºC and stored in a desiccator until use. The synthesis route to obtain the MNPs-modified material is shown in **Figure 6.1**.

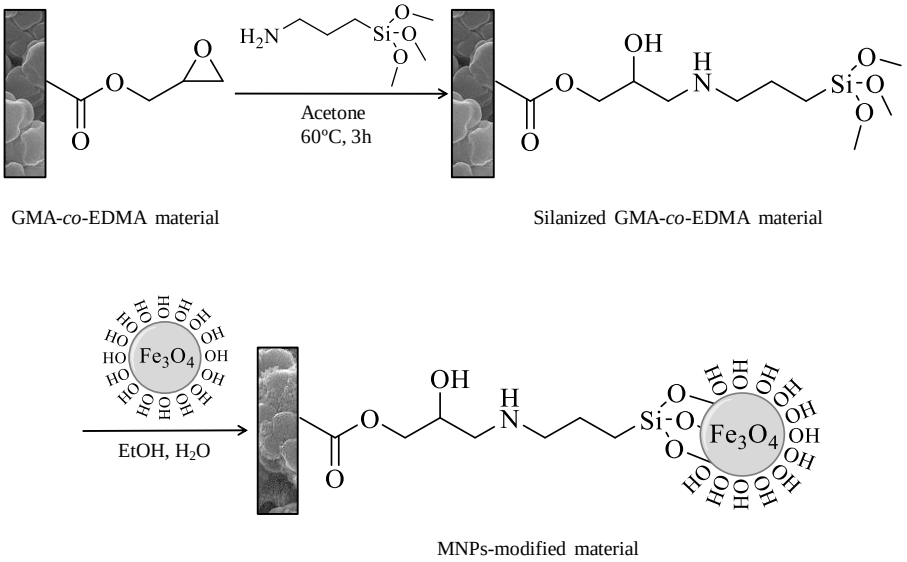

Figure 6.1. Scheme of modification with APTMS of the poly(GMA-*co*-EDMA) material and subsequent functionalization with MNPs.

Fe content of the MNPs-modified material was evaluated in triplicate using both UV-Vis [23] and ICP-MS (see Supporting Information).

6. 2. 6. SPE protocol

For the preparation of the SPE cartridges, 150 mg of the MNPs-modified material was packed between two frits into 3 mL empty propylene cartridges. To compact the material, the sorbent was washed under vacuum with 15 mL of an EtOH-water solution (1:1, v/v) (**Figure S6.2A**). Activation

and equilibration of the sorbent was done with MeOH and hexane-EtOH (98:2, v/v), respectively. Then, 500 µL of a PC solution of 500 µg/mL prepared in this later solvent were percolated through the SPE cartridge. Before eluting retained PC with $CHCl_3$:MeOH (2:1, v/v) (500 µL), a washing step with hexane (500 µL) was done. Throughout the SPE process, PC in the loading, washing and elution fractions was quantified by Stewart assay [24]. Then, the sorbent was regenerated with $CHCl_3$ followed by MeOH. The same procedure was also applied to the GMA-*co*-EDMA polymer (blank).

6. 2. 7. MSPE protocol

To carry out the MSPE, 150 mg of MNPs was placed in a glass tube and were conditioned with MeOH followed by hexane-EtOH (98:2, v/v). To collect MNPs in all extraction steps, a neodymium magnet was placed on the wall of the glass tube until no turbidity in the supernatant was observed (**Figure S6.2B**). Then, 5 mL of a PC standard solution (50 µg/mL) were added and the mixture was vortexed for 1 min. Using the magnet, the supernatant solution was discarded, and the sorbent was washed with 5 mL of hexane. Next, retained PC was desorbed with 5 mL $CHCl_3$:MeOH (2:1, v/v). PC content in each fraction was spectrophotometrically quantified at 488 nm [24].

6. 2. 8. Fat extraction and analysis of human milk

In order to extract lipids from human milk samples, the extraction method described by Folch *et al*. [25] with minor modifications was applied (see Supporting Information). The fat extract was re-dissolved in 5 mL hexane-EtOH (98:2, v/v) and percolated through the cartridge following the protocol described in Section 6.2.6. The eluted fraction was dried under vacuum, re-dissolved in a known volume of $CHCl_3$:MeOH (2:1, v/v) (250 – 500 µL) and injected in the HPLC system.

6. 3. Results and discussion

6. 3. 1. Characterization of the MNPs-modified material

As described in Section 6.2.5, the anchoring of MNPs onto the polymeric support became noticeable with a change of color from white to brown. Additionally, SEM micrographs of materials were performed (**Figure 6.2**). As it can be seen, MNPs are successfully attached to the polymeric surface.

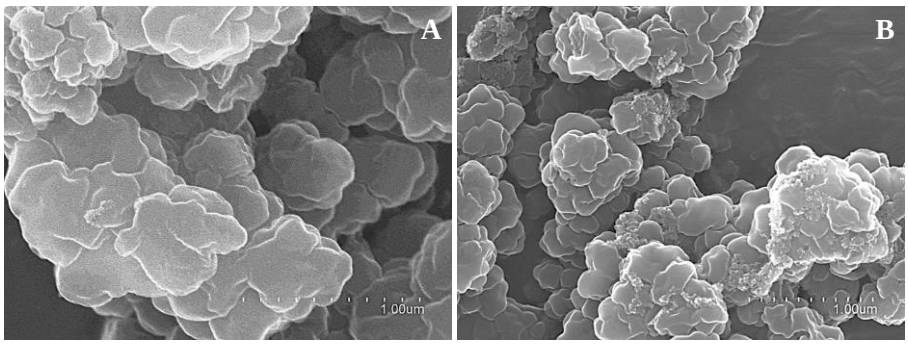

Figure 6.2. SEM micrographs of (GMA-c*o*-EDMA) material without MNPs (A) and modified with MNPs (B).

On the other hand, iron content of the MNPs-modified material was evaluated using both UV-Vis and ICP-MS. Thus, UV-Vis spectroscopy analysis showed the presence of (1.69 ± 0.08) wt% Fe, being ICP-MS analysis ((1.59 ± 0.03) wt% Fe) consistent with this value. The application of a statistical *t*-test to these data showed no significant differences at the 95% confidence level. In this work, iron percentage is in the range content reported for other organic polymers modified with iron oxide nanoparticles (1% [19] and 3.7% [26]), where the measurements were performed by energy dispersive X-ray analysis (EDAX). Additionally, the surface area of the resulting modified polymer was evaluated. The analysis of this material showed a significantly higher surface area (15.17 m^2/g) compared to that of the

unmodified polymer (6.14 m^2/g). This increase in surface area results in an additional benefit to the retention of target analytes.

6. 3. 2. Selection of SPE conditions with the MNPs-modified material

The selection of an appropriate solvent is of major concern to optimize a SPE process. Since our aim was to use the MNPs-modified material to extract PLs from lipid extracts, several solvents were selected to load the sample solution. Initially, a $CHCl_3$:MeOH mixture (2:1, v/v) was chosen, since this is the solvent commonly used to extract lipids [27–30]. However, when this solvent mixture was employed, 55% of the loaded amount of PC (250 µg of PC) was lost. For this reason, organic solvent mixtures with greater hydrophobic character, which are able to dissolve fat-based matrices containing PLs, were considered [31]. Thus, the same amount of PC (250 µg of PC) dissolved in hexane-EtOH (98:2, v/v) was percolated through the SPE cartridge. PC content found in the percolated fraction was accounted for only 3% of initial PC. Several studies [15,32] have described that the adsorption of PLs on the surface of MNPs could be explained taking into account two driving forces: i) an entropy increase due to displacement of solvent molecules around NPs by the PL molecules or ii) charge-dipole attraction between the charged NPs and the P-N dipole of the PL headgroups. The results suggested that when more polar solvents were employed, MNPs as well as PC were preferentially swollen, which had a detrimental effect on their interaction, and consequently, in PC adsorption.

Once established the loading solvent, an appropriate washing step was introduced. Since the hydrophobic character of hexane can be suitable to remove matrix nonpolar components (e.g., TAGs) without jeopardizing PLs adsorption onto the MNPs, it was initially selected as washing solvent. Next, retained PC was desorbed with $CHCl_3$:MeOH (2:1, v/v), since the polarity of the mixture was expected to compete with PC-MNPs interaction, thus

ensuring high extraction efficiency of the target analytes. Following the described procedure, no loss of PC was observed in the washing step, and PC recovery in the elution fraction reached values above 95%.

Under the selected conditions, solutions of SM and PE (500 µL, 500 µg/mL each) were percolated through the SPE cartridge. Recovery values for these PLs were 92% and 93%, respectively. The SPE protocol was also applied to a GMA-*co*-EDMA cartridge (without MNPs), and recovery values around 40% for all investigated PLs were obtained. These results confirmed that the attached MNPs onto the GMA-based polymer played an important role in the adsorption of these compounds.

6. 3. 3. Analytical features of the MNPs-SPE cartridge

First, increased amounts of PC standard were percolated through the MNPs-cartridge following the extraction protocol described in Section 6.2.6. It was intended to establish the maximum loading capacity of the MNPs-cartridge for PC adsorption. **Figure 6.3** shows that after loading 1000 µg of PC (6.7 µg of PC/ mg of sorbent), adsorption on the MNPs-cartridge diminishes substantially (*ca*. 60%). Thus, the adsorption capacity of the MNPs-cartridge was established in 5.7 µg of PC per mg of polymer.

Then, the breakthrough volume, defined as the sample volume that can be loaded on the sorbent bed without loss of the analytes, was evaluated. Thus, variable volumes of PC standard solutions (0.5 – 5.0 mL), keeping constant the total amount of PC (1.7 µg PC/ mg of sorbent), were percolated through the MNPs-cartridge and the SPE protocol was applied. In the range assayed, no significant losses of PC (< 4%) were observed (spectrophotometrically quantified [24]).

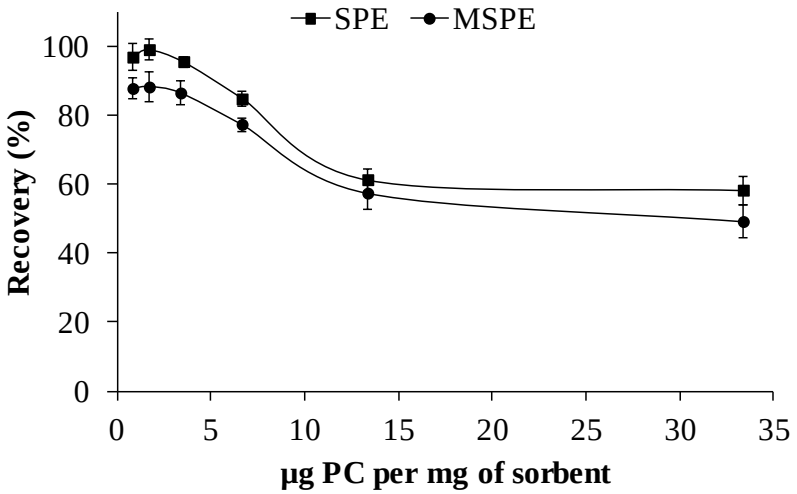

Figure 6.3. Adsorption capacity at increasing PC amounts of the MNPs material in SPE and MSPE modes.

The reusability of the SPE columns was evaluated (250 µg of PC) using the proposed procedure. A single MNPs-SPE column was repeatedly used (n = 10) using the regeneration protocol described in Section 6.2.6. An excellent performance with recoveries higher than 88% for PC was observed.

6. 3. 4. Extraction of PC in the MSPE mode

The MSPE protocol using the MNPs-modified material under application of an external magnetic field was developed (see Section 6.2.7). For this purpose, several parameters previously studied in the conventional SPE procedure were adapted to MSPE. In order to compare the performance in both modalities, the same amount of sorbent (150 mg) was employed. First, adsorption capacity was evaluated with 5 mL of PC standard solutions (125 – 5000 µg of PC). Recovery of PC followed the same trend found for SPE, although the values found were lower (see **Figure 6.3**). Since sonication has been proved to increase the efficiency of desorption of analytes from a solid sorbent [33,34], the elution step was assisted by sonication at two levels:

250 and 2000 µg of PC. In this study, however, sonication improved only slightly the recoveries (1-5%) and therefore, desorption assisted with sonication was not further considered. Thus, the loading capacity of the MNPs-modified material in MSPE was established in 3.3 µg of PC/ mg of polymer.

Then, reusability of the MNPs-modified material used in MSPE was evaluated (250 µg of PC). For this purpose, the regeneration and conditioning processes carried out for the SPE cartridges were adopted. In MSPE, extraction capacity of the MNPs material in MSPE was reduced in its first use up to 53%, so that the MNPs modified polymer should not be used more than one time in this sorption modality. The reason for this limited reusability may be attributed to the following reasons. On the one hand, a loss of mass of the MNPs-modified material after the regeneration process, since the sorbent was initially weighed and washed once using different solvents ($CHCl_3$, MeOH and hexane-EtOH (98:2, v/v)). On the other hand, the bare MNPs can undergo a loss in their magnetic properties upon direct exposing to certain surrounding environment (e.g., solvents), which produces a destabilization effect caused by electrostatic, hydrophobic or hydrogen bond interactions [35]. In fact, the magnetic field has a greater effect on the solvents with stronger hydrogen bond and becomes an obstacle to the diffusion of solute molecules [36].

As stated before, PC recoveries obtained via conventional SPE and via MSPE were comparable, although slightly better results were found in the first approach. However, regeneration process seems to be determining in MSPE, and to continue with this approach would imply the use of large amounts of sorbent. On the other hand, the SPE protocol simplifies largely the handling of more samples simultaneously, which would accelerate the clean-up process of fat extracts. For this reason, the SPE approach was selected for further studies.

6. 3. 5. Extraction and analysis of PLs from lipid extracts of milk

The applicability of the MNPs-modified material was evaluated percolating through the SPE-cartridge human milk fat extracts. Thus, the protocol described in Section 6.2.8 was followed, and the analysis of PC, PE and SM was accomplished by HILIC-ELSD. To evaluate quantitatively these three PLs, external calibration curves for each PL (20 - 400 μg/mL in $CHCl_3$:MeOH (2:1, v/v)) were constructed. Peak area *vs* mass of lipid values were fitted both to linear and power models (**Table S6.1**). Since linear regression gave reasonable coefficients of determination for all analytes, in the adopted concentration range, it was selected for quantitation studies. LODs and LOQs were determined from 3 and 10 signal-to-noise ratio, respectively. As shown in **Table S6.1**, LODs are comprised between 1.4 and 3.5 μg/mL, and LOQs between 4.8 and 11.7 μg/mL. To evaluate precision of the HILIC-ELSD method in terms of retention times and peak areas, a multi-component standard solution (100 μg/mL) was injected 3 times per day for 3 days. For all the analytes considered, relative standard deviations (RSD) lower than 2.5% were obtained.

Figure S6.3 shows the chromatograms of a human milk fat extract before and after applying the SPE protocol with the MNPs-based sorbent. A significant decrease of nonpolar lipids and a large enhancement of signals corresponding to PLs are observed in the elution fraction (continuous line) with respect to the untreated fat extract (dashed line). This fact confirms the suitability of the MNPs-modified material to be used as sorbent in SPE for clean-up and preconcentration purposes, allowing further characterization of target analytes (PLs). On the other, considering the complexity of milk matrices and the unavailability of an analyte-free milk sample, a recovery study using the standard addition method was conducted. Thus, a human milk sample (5 mL) was fortified at four concentration levels (between 10 and 50 μg/mL) and these spiked samples were analyzed after applying the

MNPs-SPE procedure. Recovery values of the spiked PLs were comprised between 83 and 90%, which suggests that their extraction was unaffected by the matrix.

Then, reusability of the MNPs-SPE cartridges for fat extracts was also evaluated. For this purpose, fat extracts were dissolved in 5 mL of hexane-EtOH (98:2, v/v) and the adsorption-elution cycle was repeated 6 times using the same MNPs-SPE cartridge. To evaluate retention, the total content of PLs was estimated before and after applying the SPE protocol by the Stewart assay [24]. **Figure S6.4** shows recovery values of PLs from human milk fat extracts as a function of increasing number of reuses. It can be seen that the sorbent demonstrates an appropriate performance for fat analysis at least for three consecutive uses (RSD 8.0%).

Finally, the content of PLs of several human milk samples in different lactation stages (colostrum, transitional, and mature milk) was determined using the described protocol. As shown in **Table S6.2**, some variability in the PL levels can be observed among the analyzed human milk samples. In all cases, the amount of PLs is in good agreement with the data reported for these compounds in human milk samples [29,37]. Additionally, a decrease in PL content as lactation progresses is observed, which is in accordance with the findings previously reported [3,38].

The developed method was also compared with other extraction methods [5,6,39–44], being SPE the commonly used technique [5,6,39–41]. Regarding recoveries, our values were similar to those reported in literature [5,6,39,41,43], which demonstrates the suitability of the procedure. Concerning LODs and LOQs, our SPE protocol gave comparable values to those reported using ELSD [6], but higher than those obtained using more sophisticated techniques, such as MS [39,43]. In addition, the amount of sorbent in the SPE cartridges for PLs analysis ranges from 25 mg for home-made cartridges [41] to 1000 mg for commercial cartridges [5,45]. In

this sense, the amount employed in this work (150 mg) allows us to prepare several SPE cartridges (*ca.* 15) from the bulk MNPs-modified material. Additionally, since some sorbents reported [45,46] might not be affordable for all laboratories, our home-made cartridges represent undoubtedly a potential alternative.

6. 4. Conclusions

In this work, a polymeric material was successfully functionalized with MNPs and then used as sorbent for the extraction of PLs from human milk samples. Subsequently, the extracted PLs were separated and quantified by HILIC-ELSD. To our knowledge, the present study is the first work in using a MNPs-modified material as sorbent for the extraction of PLs from this complex matrix. The use of bare Fe_3O_4 NPs attached to the surface of the polymeric support constitutes a favorable platform for the selective interaction of phosphorous-compounds, such as PLs. Although the magnetic functionalized material could be used both in SPE and MSPE, the SPE procedure presented some advantages (e.g., slightly higher recoveries, better reusability and a large high-throughput) over the MSPE methodology.

The performance of the MNPs-SPE cartridge was demonstrated by its application to human milk fat samples, where an effective clean-up of sample (particularly to remove neutral lipids) and preconcentration of PLs was accomplished. Following this methodology, it is possible an accurate determination of PLs by HILIC-ELSD while the structural integrity of the HPLC column is guaranteed. Thus, the proposed methodology represents a promising alternative for the extraction of PLs from biological samples.

Acknowledgments

Project CTQ2014-52765-R (MINECO of Spain and FEDER) and PROMETEO/2016/145 (Generalitat Valenciana). I. T-D thanks the MINECO for an FPU grant for PhD studies.

6. 5. References

[1] R.G. Jensen, Lipids in human milk, Lipids 34 (1999) 1243–1271. doi:10.1007/s11745-999-0477-2.

[2] L. Wang, Y. Shimizu, S. Kaneko, S. Hanaka, T. Abe, H. Shimasaki, H. Hisaki, H. Nakajima, Comparison of the fatty acid composition of total lipids and phospholipids in breast milk from Japanese women, Pediatr. Int. 42 (2000) 14–20. doi:10.1046/j.1442-200X.2000.01169.x.

[3] J. Bitman, L. Wood, M. Hamosh, P. Hamosh, N.R. Mehta, Comparison of the lipid composition of breast milk from mothers of term and preterm infants, Am. J. Clin. Nutr. 38 (1983) 300–312. doi:10.1093/ajcn/38.2.300.

[4] R.G. Jensen, The lipids in human milk, Prog. Lipid Res. 35 (1996) 53–92. doi:10.1016/0163-7827(95)00010-0.

[5] A. Avalli, G. Contarini, Determination of phospholipids in dairy products by SPE/HPLC/ELSD, J. Chromatogr. A 1071 (2005) 185–190. doi:10.1016/j.chroma.2005.01.072.

[6] P. Donato, F. Cacciola, F. Cichello, M. Russo, P. Dugo, L. Mondello, Determination of phospholipids in milk samples by means of hydrophilic interaction liquid chromatography coupled to evaporative light scattering and mass spectrometry detection, J. Chromatogr. A 1218 (2011) 6476–6482. doi:10.1016/j.chroma.2011.07.036.

[7] M. Schwalbe-Herrmann, J. Willmann, D. Leibfritz, Separation of phospholipid classes by hydrophilic interaction chromatography detected by electrospray ionization mass spectrometry, J. Chromatogr. A 1217 (2010) 5179–5183. doi:10.1016/j.chroma.2010.05.014.

[8] J.G. Parsons, S. Patton, Two-dimensional thin-layer chromatography of polar lipids from milk and mammary tissue, J. Lipid Res. 8 (1967)

696–698.

[9] F. Sánchez-Juanes, J.M. Alonso, L. Zancada, P. Hueso, Distribution and fatty acid content of phospholipids from bovine milk and bovine milk fat globule membranes, Int. Dairy J. 19 (2009) 273–278. doi:10.1016/j.idairyj.2008.11.006.

[10] R.J. Maxwell, D. Mondimore, J. Tobias, Rapid method for the quantitative extraction and simultaneous class separation of milk lipids, J. Dairy Sci. 69 (1986) 321–325. doi:10.3168/jds.S0022-0302(86)80408-8.

[11] M. Wierucka, M. Biziuk, Application of magnetic nanoparticles for magnetic solid-phase extraction in preparing biological, environmental and food samples, TrAC - Trends Anal. Chem. 59 (2014) 50–58. doi:10.1016/j.trac.2014.04.007.

[12] I.S. Ibarra, J.A. Rodriguez, C.A. Galán-Vidal, A. Cepeda, J.M. Miranda, Magnetic solid phase extraction applied to food analysis, J. Chem. 2015 (2015) 1–13. doi:10.1155/2015/919414.

[13] A.H. Lu, E.L. Salabas, F. Schüth, Magnetic nanoparticles: Synthesis, protection, functionalization, and application, Angew. Chemie Int. Ed. 46 (2007) 1222–1244. doi:10.1002/anie.200602866.

[14] L. Weng, W.H. Van Riemsdijk, T. Hiemstra, Factors controlling phosphate interaction with iron oxides, J. Environ. Qual. 41 (2012) 628–635. doi:10.2134/jeq2011.0250.

[15] S. Zhang, H. Niu, Y. Zhang, J. Liu, Y. Shi, X. Zhang, Y. Cai, Biocompatible phosphatidylcholine bilayer coated on magnetic nanoparticles and their application in the extraction of several polycyclic aromatic hydrocarbons from environmental water and milk samples, J. Chromatogr. A 1238 (2012) 38–45. doi:10.1016/j.chroma.2012.03.056.

[16] T. Nema, E.C.Y. Chan, P.C. Ho, Applications of monolithic materials for sample preparation, J. Pharm. Biomed. Anal. 87 (2014) 130–141. doi:10.1016/j.jpba.2013.05.036.

[17] M. Vergara-Barberán, M.J. Lerma-García, E.F. Simó-Alfonso, J.M. Herrero-Martínez, Solid-phase extraction based on ground methacrylate monolith modified with gold nanoparticles for isolation of proteins, Anal. Chim. Acta 917 (2016) 37–43. doi:10.1016/j.aca.2016.02.043.

[18] I.D. Vukoje, E.S. Džunuzović, D.R. Lončarević, S. Dimitrijević, S.P. Ahrenkiel, J.M. Nedeljković, Synthesis, characterization, and antimicrobial activity of silver nanoparticles on poly(GMA-co-EGDMA) polymer support, Polym. Compos. (2015) 1–9. doi:10.1002/pc.23684.

[19] J. Krenkova, F. Foret, Iron oxide nanoparticle coating of organic polymer-based monolithic columns for phosphopeptide enrichment, J. Sep. Sci. 34 (2011) 2106–2112. doi:10.1002/jssc.201100256.

[20] S. Meseguer-Lloret, S. Torres-Cartas, M. Catalá-Icardo, E.F. Simó-Alfonso, J.M. Herrero-Martínez, Extraction and preconcentration of organophosphorus pesticides in water by using a polymethacrylate-based sorbent modified with magnetic nanoparticles, Anal. Bioanal. Chem. 409 (2017) 3561–3571. doi:10.1007/s00216-017-0294-x.

[21] C. Yang, G. Wang, Z. Lu, J. Sun, J. Zhuang, W. Yang, Effect of ultrasonic treatment on dispersibility of Fe_3O_4 nanoparticles and synthesis of multi-core Fe_3O_4/SiO_2 core/shell nanoparticles, J. Mater. Chem. 15 (2005) 4252–4257. doi:10.1039/b505018a.

[22] E.J. Carrasco-Correa, G. Ramis-Ramos, J.M. Herrero-Martínez, Methacrylate monolithic columns functionalized with epinephrine for capillary electrochromatography applications, J. Chromatogr. A 1298

(2013) 61–67. doi:10.1016/j.chroma.2013.05.013.

[23] P. Serra-Mora, Y. Moliner-Martínez, R. Herráez-Hernández, J. Verdú-Andrés, P. Campíns-Falcó, Simplifying iron determination with o-phenanthroline in food ashes using 2-nitrophenol as an acid-base indicator, Food Anal. Methods 9 (2016) 1150–1154. doi:10.1007/s12161-015-0294-4.

[24] J.C.M. Stewart, Colorimetric determination of phospholipids with ammonium ferrothiocyanate, Anal. Biochem. 104 (1980) 10–14. doi:10.1016/0003-2697(80)90269-9.

[25] J. Folch, M. Lees, G.H. Sloane Stantley, A simple method for the isolation and purification of total lipides from animal tissues, J. Biol. Chem. 266 (1957) 497–509.

[26] J. Krenkova, F. Foret, Nanoparticle-modified monolithic pipette tips for phosphopeptide enrichment, Anal. Bioanal. Chem. 405 (2013) 2175–2183. doi:10.1007/s00216-012-6358-z.

[27] C. Lopez, V. Briard-Bion, O. Menard, F. Rousseau, P. Pradel, J.-M. Besle, Phospholipid, sphingolipid, and fatty acid compositions of the milk fat globule membrane are modified by diet, J. Agric. Food Chem. 56 (2008) 5226–5236. doi:10.1021/jf7036104.

[28] L.M. Rodríguez-Alcalá, J. Fontecha, Major lipid classes separation of buttermilk, and cows, goats and ewes milk by high performance liquid chromatography with an evaporative light scattering detector focused on the phospholipid fraction, J. Chromatogr. A 1217 (2010) 3063–3066. doi:10.1016/j.chroma.2010.02.073.

[29] F. Giuffrida, C. Cruz-Hernandez, B. Flück, I. Tavazzi, S.K. Thakkar, F. Destaillats, M. Braun, Quantification of phospholipids classes in human milk, Lipids 48 (2013) 1051–1058. doi:10.1007/s11745-013-3825-z.

[30] T.P.L. Ferraz, M.C. Fiúza, M.L.A. Dos Santos, L. Pontes De Carvalho, N.M. Soares, Comparison of six methods for the extraction of lipids from serum in terms of effectiveness and protein preservation, J. Biochem. Biophys. Methods 58 (2004) 187–193. doi:10.1016/j.jbbm.2003.10.008.

[31] K.M. Marakulina, R. V. Kramor, Y.K. Lukanina, M. V. Kozlov, L.N. Shishkina, Application of UV- and IR-Spectroscopy to analyze the formation of complexes between sphingomyelin and phenolic antioxidants, Moscow Univ. Chem. Bull. 67 (2012) 185–191. doi:10.3103/S0027131412040098.

[32] B. Yuan, L.L. Xing, Y.D. Zhang, Y. Lu, Z.H. Mai, M. Li, Self-assembly of highly oriented lamellar nanoparticle-phospholipid nanocomposites on solid surfaces, J. Am. Chem. Soc. 129 (2007) 11332–11333. doi:10.1021/ja074235n.

[33] R.S. Davidson, A. Safdar, J.D. Spencer, B. Robinson, Applications of ultrasound to organic chemistry, Ultrasonics 25 (1987) 35–39. doi:10.1016/0041-624X(87)90009-6.

[34] R. Sitko, B. Gliwinska, B. Zawisza, B. Feist, Ultrasound-assisted solid-phase extraction using multiwalled carbon nanotubes for determination of cadmium by flame atomic absorption spectrometry, J. Anal. At. Spectrom. 28 (2013) 405–410. doi:10.1039/C2JA30328K.

[35] D.P. Joshi, G. Pant, N. Arora, S. Nainwal, Effect of solvents on morphology, magnetic and dielectric properties of (α-Fe_2O_3@SiO_2) core-shell nanoparticles, Heliyon 3 (2017) 1–16. doi:10.1016/j.heliyon.2017.e00253.

[36] F. Moosavi, M. Gholizadeh, Magnetic effects on the solvent properties investigated by molecular dynamics simulation, J. Magn. Magn. Mater. 354 (2014) 239–247. doi:10.1016/j.jmmm.2013.11.012.

[37] G. Contarini, M. Povolo, Phospholipids in milk fat: composition, biological and technological significance, and analytical strategies, Int. J. Mol. Sci. 14 (2013) 2808–2831. doi:10.3390/ijms14022808.

[38] H. Shoji, T. Shimizu, N. Kaneko, K. Shinohara, S. Shiga, M. Saito, K. Oshida, T. Shimizu, M. Takase, Y. Yamashiro, Comparison of the phospholipid classes in human milk in Japanese mothers of term and preterm infants, Acta Paediatr. 95 (2006) 996–1000. doi:10.1080/08035250600660933.

[39] Q. Shen, H.-Y. Cheung, TiO_2/SiO_2 core-shell composite-based sample preparation method for selective extraction of phospholipids from shrimp waste followed by hydrophilic interaction chromatography coupled with quadrupole time-of-flight/mass spectrometry analysis, J. Agric. Food Chem. 62 (2014) 8944–8951. doi:10.1021/jf503040p.

[40] C. Ferreiro-Vera, F. Priego-Capote, M.D. Luque de Castro, Comparison of sample preparation approaches for phospholipids profiling in human serum by liquid chromatography-tandem mass spectrometry, J. Chromatogr. A 1240 (2012) 21–28. doi:10.1016/j.chroma.2012.03.074.

[41] I. Ten-Doménech, H. Martínez-Pérez-Cejuela, M.J. Lerma-García, E.F. Simó-Alfonso, J.M. Herrero-Martínez, Molecularly imprinted polymers for selective solid-phase extraction of phospholipids from human milk samples, Microchim. Acta 184 (2017) 3389–3397. doi:10.1007/s00604-017-2345-6.

[42] C.D. Calvano, O.N. Jensen, C.G. Zambonin, Selective extraction of phospholipids from dairy products by micro-solid phase extraction based on titanium dioxide microcolumns followed by MALDI-TOF-MS analysis, Anal. Bioanal. Chem. 394 (2009) 1453–1461. doi:10.1007/s00216-009-2812-y.

[43] S.K. Kailasa, H.F. Wu, Surface modified $BaTiO_3$ nanoparticles as the matrix for phospholipids and as extracting probes for LLME of hydrophobic proteins in Escherichia coli by MALDI-MS, Talanta 114 (2013) 283–290. doi:10.1016/j.talanta.2013.05.032.

[44] C. Pegoraro, D. Silvestri, G. Ciardelli, C. Cristallini, N. Barbani, Molecularly imprinted poly(ethylene-co-vinyl alcohol) membranes for the specific recognition of phospholipids, Biosens. Bioelectron. 24 (2008) 748–755. doi:10.1016/j.bios.2008.06.050.

[45] Sigma-Aldrich, Supelclean™ LC-Si SPE tube, (año no indicado). Disponible en: http://www.sigmaaldrich.com/catalog/product/supelco/57051?lang=es&region=ES (accessed April 6, 2017).

[46] Sigma-Aldrich, HybridSPE®-Phospholipid, (año no indicado). Disponible en: http://www.sigmaaldrich.com/catalog/product/supelco/55261u?lang=es&region=ES (accessed May 4, 2017).

6. 6. Supporting Information

6. 6. 1. Experimental

6. 6. 1. 1. Chromatographic and detection conditions

Separation was carried out with a Kinetex™ HILIC 100 Å column (150 mm × 4.6 mm, 2.6 µm; Phenomenex, Torrance, CA, USA). Mobile phases consisted of ACN-ammonium formate 100 mM (A, 97:3, v/v) and water-ammonium formate 100 mM (B, 97:3, v/v). The chromatographic separation was carried out using the following gradient: 0-3.5 min, 100% A; in 11 min, 15% B is reached and kept during 10 min. Column temperature, 25 ºC; flow rate, 1.0 mL/min and injection volume, 20 µL. The ELSD parameters were: evaporation and nebulization temperature, 80 and 40 ºC, respectively; gas flow rate, 1.4 Standard Litres per Minute (SLM); gain factor, 1.

6. 6. 1. 2. Preparation of MNPs

180 mL of 62 mM Fe^{3+} and 31 mM Fe^{2+} aqueous solutions were placed into a two-neck round-bottom flask with a glass condenser under nitrogen atmosphere. The solution was heated until reaching 50 ºC, at which point 12.5 mL of concentrated ammonia were added under vigorous stirring. After 30 min, the temperature was raised to 90 ºC and the mixture was kept for another 30 min at this temperature. The MNPs were collected on the flask wall with a neodymium magnet, washed with water and EtOH several times to remove excess of reagents and dried at 60 ºC for 30 min. The average diameter of the synthesized Fe_3O_4 nanoparticles, measured by TEM, was *ca*. 12 nm (see **Figure S6.1**).

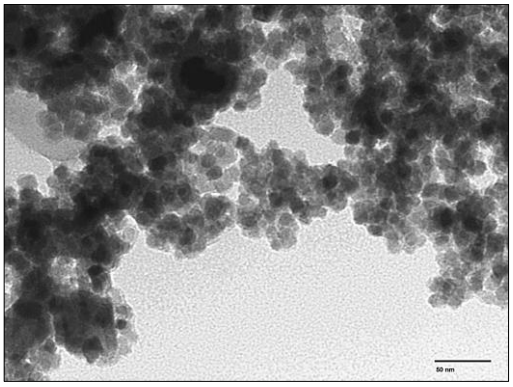

Figure S6.1. TEM image of synthesized Fe_3O_4 nanoparticles.

6. 6. 1. 3. Fe content determination by UV-Vis and ICP-MS

For UV-Vis, 25 mg of the dried methacrylate material modified with Fe_3O_4 was calcined at 550 ºC for 2.5 h. Then, the ashes (which contained the iron material) were treated with 2 mL HCl-water (1:1, v/v) for 60 min at 60 ºC under stirring. The resulting solution was subjected to the colorimetric determination of Fe based on the formation of the red *o*-phenantroline complex. A stock solution of 200 µg/mL of Fe (II) was prepared from Mohr's salt and a calibration curve (0.8-4 µg/mL) was constructed. Similarly, ashes from calcination of 25 mg of the Fe_3O_4 modified material were digested with nitric acid, and the resulting solution was subjected to ICP-MS analysis.

6. 6. 1. 4. Fat extraction

1.5 mL of milk were dispersed in dichloromethane: MeOH (2:1, v/v) and the mixture was shaken for 15 min and later centrifuged at 6000 rpm (3904 *g*) for 8 min. Then, the aqueous phase was removed and the lower dichloromethane phase, containing lipids, was washed with a salt solution and evaporated under vacuum.

6. 6. 1. 5. SPE and MSPE protocol

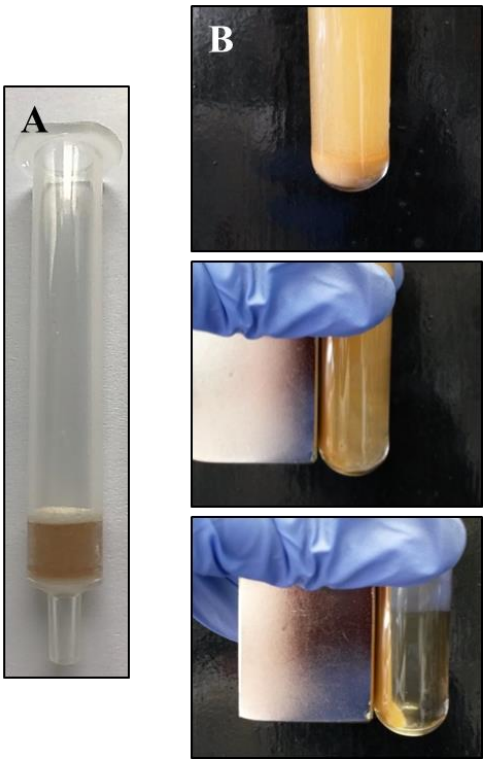

Figure S6.2. SPE cartridge with polymeric material modified with MNPs (A); scheme of separation of the MNPs-modified material with a magnet in the extraction steps (B).

Table S6.1. Calibration curves (peak area vs µg injected) and lLOD and LOQ for determination of PLs in HILIC-ELSD.

PLs	Power	Linear	LOD (µg/mL)	LOQ (µg/mL)
PE	$y = 417.1x^{1.250}$; $r^2 = 0.9996$	$y = 931.6x - 1422.7$; $r^2 = 0.9965$	1.4	4.8
PC	$y = 640.1x^{1.089}$; $r^2 = 0.9995$	$y = 794.2x - 145.6$; $r^2 = 0.9983$	2.6	8.8
SM	$y = 471.6x^{1.045}$; $r^2 = 0.9989$	$y = 543.8x - 140.0$; $r^2 = 0.9980$	3.5	11.7

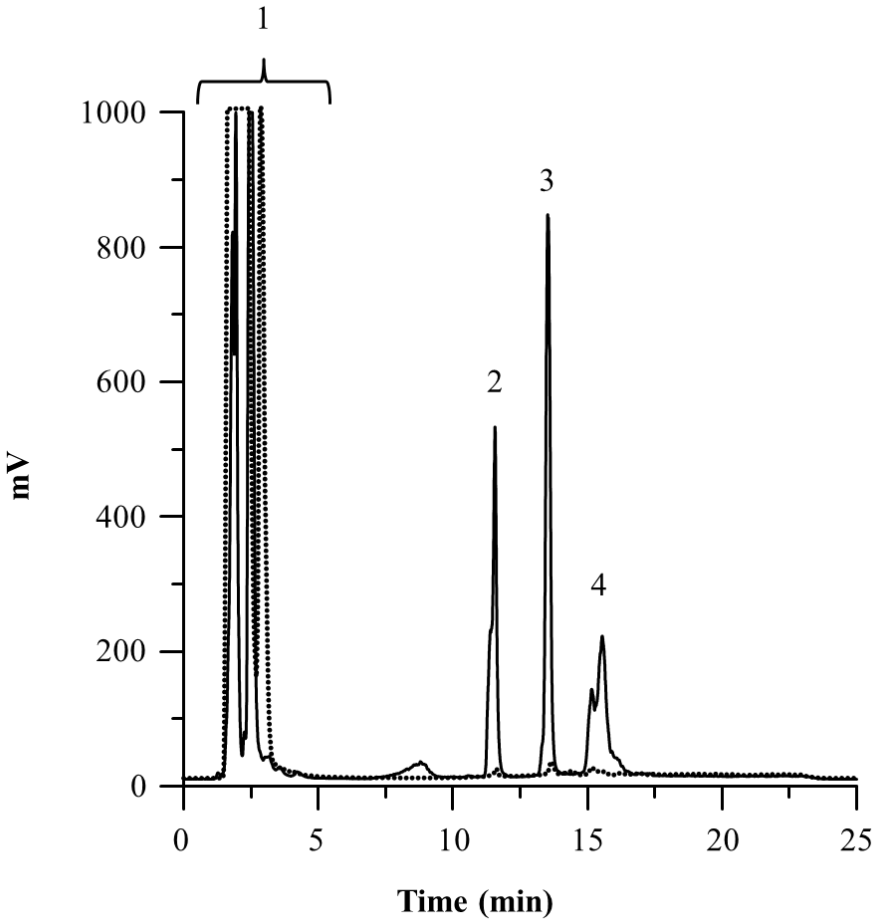

Figure S6.3 HILIC-ELSD chromatograms of human milk fat extract obtained without (dashed line) and with (continuous line) MNPs-SPE treatment. For extraction procedure of MNPs-SPE see Section 6.2.6 and for HILIC-ELSD conditions see above. Peak identification: (1) nonpolar lipids, (2) PE, (3) PC and (4) SM.

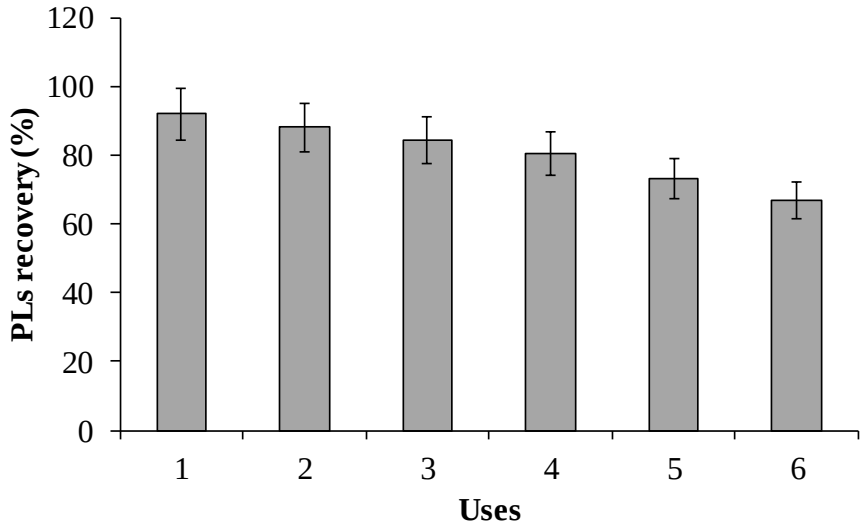

Figure S6.4. Recovery values of PLs from human milk fat extracts in SPE as a function of increasing number of reuses.

Table S6.2. Content of PE, PC and SM content (mean ± SD in mg per g of fat, n = 3) in human milk at different stages of lactation.

PL	Colostrum	Transitional milk	Mature milk
PE	3.2 ± 0.7	1.6 ± 0.2	1.2 ± 0.5
PC	4.4 ± 1.1	2.0 ± 0.2	1.3 ± 0.6
SM	3.9 ± 1.3	1.8 ± 0.2	1.3 ± 0.4

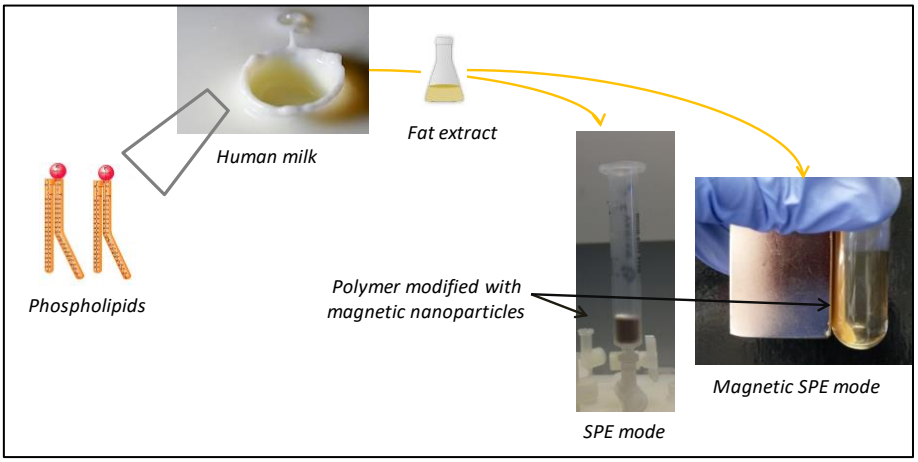
Human milk
Fat extract
Phospholipids
Polymer modified with
magnetic nanoparticles
SPE mode
Magnetic SPE mode

CAPÍTULO 7

Molecularly imprinted polymers for selective solid-phase extraction of phospholipids from human milk samples

Microchim Acta (2017) 184:3389–3397
DOI 10.1007/s00604-017-2345-6

ORIGINAL PAPER

Molecularly imprinted polymers for selective solid-phase extraction of phospholipids from human milk samples

Isabel Ten-Doménech[1] · Héctor Martínez-Pérez-Cejuela[1] · María Jesús Lerma-García[1] · Ernesto Francisco Simó-Alfonso[1] · José Manuel Herrero-Martínez[1]

[1] Department of Analytical Chemistry, Faculty of Chemistry, University of Valencia, Dr. Moliner 50, 46100 Burjassot, Spain

The authors describe a method for the extraction and determination of PLs from human milk fat by using a MIP as the sorbent material and liquid chromatography for detection. The MIP was synthesized by thermal polymerization using L-α-PC as the template, MAA as the functional monomer, EDMA as the cross-linker, and ACN as the porogenic solvent. The resulting MIP was employed as a sorbent for SPE of PLs from human milk fat samples. The extracted PLs were then determined by means of HILIC in combination with ELSD. Variables affect the extraction efficiency (such as the porogenic solvent, template/functional monomer/cross-linker (T:M:C) ratio and extraction conditions) were optimized. The selectivity of the MIP over PLs different from PC was investigated, and the adsorption capacity, breakthrough volume and reusability of the MIP was determined. The MIP displays a satisfactory loading capacity (*ca.* 41 μg PC per g of sorbent) and a high affinity and selectivity for PC and structurally related PLs such as SM and L-α-PE. The MIP can be reused at least 20 times in case of PL standards, and at least 6 times in case of human milk fat samples.

Keywords: Breast milk; Methacrylate; Polar lipids; Selective; Solid-phase extraction; Template.

7. 1. Introduction

PLs are basic constituents of the milk fat globule membranes and play an important functional, structural and metabolic role. Their amphiphilic properties derive from the presence of a hydrophobic tail, an interfacial region of intermediated polarity and a hydrophilic head. They are divided into two main groups: glycerolphospholipids and sphingolipids. The former group consists of a polar phosphoryl headgroup esterified to the *sn*-3 position and two FAs esterified at the *sn*-1 and *sn*-2 positions of the glycerol backbone. They include principally PC, PE, PI and PS [1]. On the other hand, sphingolipids are derived from the aliphatic amino alcohol sphingosin, forming a ceramide when its amino group is linked, generally, with a saturated FA. SM is the dominant species and it is composed of a phosphorylcholine head group linked to the ceramide [2]. The most abundant PLs in milk fat, expressed as percentage of total PLs, are: PC 35%, PE 30%, SM 25%, PI 5% and PS 3% [3].

The analysis of milk PLs requires different steps: fat extraction from milk; in some cases, isolation of PL fraction from other lipid classes; separation and detection of the different PL classes and or species. In fact, the challenge in PLs analysis arises from their low abundance (0.5-1%) with respect to the nonpolar TAGs, as well as the simultaneous occurrence of a number of positional and structural isomers [4]. Several authors focus on the PLs fraction without a prior fractionation step and in a single run [5–7]. However, several techniques, such as 2D-TLC [8,9], column chromatography [10] and SPE [3,4,11] have been employed to isolate the PL fraction (polar fraction) from the other lipid classes. By the same line of clean-up and/or pre-concentration, MIPs have been a focus of research as a consequence of their molecular recognition properties [12]. The imprinted polymer matrix is created by the copolymerization of a functional monomer/template molecule complex with a cross-linking agent in the presence of a porogenic solvent [13].

In principle, any chemical compound can be used to prepare a corresponding MIP. However, the efficiency of the imprinting process is reported only for a limited number of compounds. The formation of a sufficient strong pre-polymerization complex between the template molecule and the functional monomer species is critical to the subsequent recognition properties of the polymer [14,15]. In the specific case of phospholipid analysis, only a few studies related with molecular imprinting technique have been described [16,17]. However, these systems have not been applied for sample treatment purposes.

Regarding the separation of phospholipid classes, it has been accomplished, in general, by means of normal phase-HPLC [3,5,6] and in less extension by HILIC [11,18].

The aim of this work was the synthesis of a MIP for PLs using PC as template molecule. The molecular recognition ability of the resulting polymers was evaluated following an SPE protocol. The selectivity of the MIP towards other PLs different from PC was also investigated as well as its adsorption capacity, breakthrough volume and reusability. The extraction protocol was then applied to human milk fat samples in order to isolate PLs from the nonpolar fraction.

7. 2. Experimental

7. 2. 1. Reagents and materials

HPLC-grade ACN, MeOH, $CHCl_3$ and tetrahydrofuran (THF) were purchased from VWR Chemicals (Barcelona, Spain); reagent-grade dichloromethane, EtOH and n-hexane and anhydrous sodium sulfate, were supplied by Scharlau (Barcelona, Spain). BHT and ammonium formate were purchased from Fluka (Buchs SG, Switzerland). Iron (III) chloride 6-hydrate

and ammonium thiocyanate were supplied by Panreac (Barcelona, Spain). L-α-PC (soy bean, 95%) was purchased from Avanti Polar Lipids (Alabaster, AL, USA). SM (chicken egg yolk, ≥95%), PE (egg yolk, ≥97%), acetic acid, MAA, EDMA, AIBN were obtained from Sigma-Aldrich (St. Louis, MO, USA).

Human milk samples (n = 9) were kindly donated by healthy well-nourished mothers in different stages of lactation. The samples were collected between the baby's feed by manual expression using a Medela Harmony™ Breastpump (Zug, Switzerland). After collection, milk samples were rapidly heated to 80 ºC and held at this temperature for 1.5 min in order to inactivate the lipases and to avoid triglycerides hydrolysis [19].

7. 2. 2. Instrumentation

SEM micrographs were taken with a scanning electron microscope (S-4100, Hitachi, Ibaraki, Japan) equipped with a field emission gun, and an EMIP 3.0 image data acquisition system (Rontec, Normanton, UK). For these measurements, the materials were sputter-coated with a thin layer of Au/Pd.

Attenuated total reflection FT-IR spectra of powdered materials (MIPs and their corresponding non-molecularly imprinted polymers (NIPs)) and template molecule were obtained with a DuraSamplIR II accessory from Smiths Detection Inc. (Warrington, UK) equipped with a nine reflection diamond/ZnSe DuraDisk plate, installed on a Bruker FTIR spectrometer (Bremen, Germany) model Tensor 27 with a KBr beamspliter and a DLaTGS detector. Spectra were accomplished from 4000 to 600 cm^{-1} in the absorbance mode at a 2 cm^{-1} resolution with 100 scans.

The Stewart assay for the quantification of PLs [20] was carried out by measuring in UV-vis with an 8453 diode-array UV-vis spectrophotometer (Agilent Technologies, Waldbronn, Germany).

Centrifugation steps were conducted in a Hettich® EBA 21 laboratory centrifuge (Sigma, Osterode am Harz, Germany).

Evaporation under vacuum was accomplished using a miVac sample concentrator (SP Scientific, Warminster, PA).

Chromatographic determination of PLs was made with an 1100 series liquid chromatograph (Agilent Technologies, Waldbronn, Germany) provided with a quaternary pump, a degasser, a thermostated column compartment, an automatic sampler, a UV-vis diode array detector online coupled to an Agilent 385-ELSD. Chromatographic conditions are described in the Electronic Supplementary Material.

7. 2. 3. Preparation and characterization of MIPs

Prior to the preparation of MIP, an appropriate selection of porogenic solvent was done. For this purpose, PC, MAA and mixtures of PC-MAA (1:4 molar ratio) were prepared in MeOH, THF and ACN. After sonicating for 10 min, the solubility of PC in the different solvents was observed and the FT-IR spectra of all solutions were measured. Afterwards, several MIPs (using PC as template) and their corresponding NIPs were synthesized by preparing the polymerization mixtures included in **Table S7.1**. These polymerization mixtures were prepared by mixing a functional monomer (MAA), a cross-linker (EDMA), a porogenic solvent (ACN) and an initiator (AIBN). The polymerization mixture was sonicated for 10 min, degassed with nitrogen for 5 min and allowed to react into a thermostated water bath at 60 ºC during 20 h. After the polymerization, the polymer was removed from the vial and ground with a mortar. Then, a Soxhlet extraction with MeOH-acetic acid (95:5, v/v) was used to remove the template from the material until no template was detected in the washing solution. The polymers were finally rinsed with MeOH to remove the remaining acetic acid and dried at 60 ºC for 8 h. The

polymer was then sieved with a steel sieve with sizes < 100 µm. A total amount of *ca.* 1200 mg of each sorbent was obtained.

MIPs and NIPs were characterized by studying their morphology (SEM micrographs) and chemical composition (FT-IR spectra).

7. 2. 4. MIP-SPE protocol

For the preparation of the SPE cartridges, 25 mg of each polymer (MIP or NIP) were packed between two frits (20 µm pore size, Análisis Vínicos, Tomelloso, Spain) into 1 mL empty propylene cartridge (Análisis Vínicos). Activation of the sorbent was done with MeOH (1 mL) and equilibration was done with hexane-EtOH (98:2, v/v) (1 mL). Then, 250 µL of a PC solution of 2000 µg/mL prepared in this solvent were loaded on the SPE material. After this step, the material was washed with hexane (250 µL). Retained PC was eluted with $CHCl_3$:MeOH (2:1, v/v) (250 µL). Along the SPE process, PC content of the eluate after the different steps (loading, washing and elution) was quantified by Stewart assay [20] (measurement of absorbance at 488 nm). Next, the sorbent surface was regenerated with 1 mL of $CHCl_3$ followed by 1 mL of MeOH. In order to confirm the recognition ability of the material, the same procedure was applied for PC extraction using the respective NIPs.

On the other hand, selectivity of both MIP and NIP was evaluated by measuring the recognition towards two structural analogues of PC template (SM and PE). For this purpose, 250 µL of a SM or PE solution of 2000 µg/mL prepared in hexane-EtOH (98:2, v/v) was loaded onto the SPE cartridges, and the eluates were quantified spectrophotometrically [20].

7. 2. 5. Human milk samples treatment and analysis

Lipid extraction of human milk samples was performed following the gravimetric method described by Folch *et al*. [21] with minor modifications. Briefly, milk aliquots (1.5 mL) were dispersed with a dichloromethane: MeOH (2:1, v/v) mixture, shaken during 15 min and centrifuged at 6000 rpm for 8 min. After removing the aqueous phase and performing washing steps, the lower dichloromethane phase, containing lipids, was evaporated under vacuum, and the final residue was re-dissolved in 5 mL of hexane-EtOH (98:2, v/v). The fat extract solution was percolated through the cartridge following the procedure described above. Then, the eluted fraction (1 mL) was dried under nitrogen stream, re-dissolved in a known volume of $CHCl_3$:MeOH (2:1, v/v) (250 – 500 µL) and injected in the chromatograph.

7. 3. Results and discussion

7. 3. 1. Choice of materials

In the synthesis of MIPs, the choice of the chemical reagents is of primary importance in order to obtain efficient MIPs. In particular, the role of monomer is critical to create highly specific cavities for the subsequent adsorption of the template molecule. The vast majority of MIPs have been synthesized using acrylic-based polymers, especially MAA as functional monomer and EDMA as the cross-linker. The extensive use of MAA is due to its capability to act both as hydrogen bond and proton donor and as hydrogen bond acceptor. These properties result adequate to favor its interaction with the hydrophilic head group of PLs (see **Figure 7.1**). Taking into account these considerations, poly(MAA-*co*-EDMA) was employed as the host for molecular imprinting of PLs.

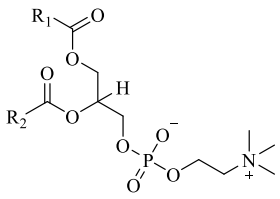

Phosphatidylcholine, PC

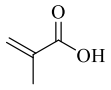

Methacrylic acid, MAA

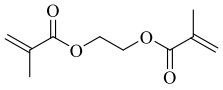

Ethylene dimethacrylate, EDMA

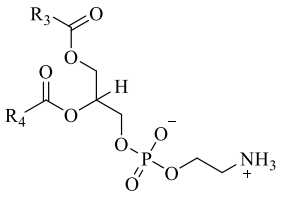

Phosphatidylethanolamine, PE

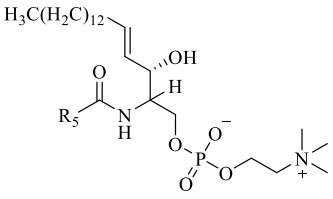

Sphingomyelin, SM

Figure 7.1. Representation of chemical structures of the template molecule (PC), functional monomer (MAA) and cross-linker (EDMA) used in the polymerization mixture and phospholipids (PE and SM) used to investigate MIP selectivity. Hydrocarbon tails of fatty acids are designated as R1 to R5.

7. 3. 2. Prepolymerization studies

Within the amphiphilic nature of PLs, PC presents higher solubility in nonpolar solvents such as hexane or $CHCl_3$ than in polar aprotic solvents (e.g., ACN). On the other hand, the carboxyl oxygen present in its structure can act as hydrogen bonding acceptor. This fact allows PC to be easily dissolved in polar protic solvents such as EtOH or MeOH.

In MIP preparation, the interaction between the template molecule and the functional monomer is strongly affected by the polarity of the solvent. This functional monomer-solvent interaction has a critical impact on the structure of imprinting sites [22]. Thus, the solvent can favor or reduce the monomer-template complexation or even their intra-or/and self-intramolecular interactions [15]. For this reason, it is essential to investigate

the interactions between the template, functional monomer and cross-linker with different solvents in the polymerization mixture.

In this sense, the mechanism of interaction of PC with MAA in MeOH, THF and ACN was explored by FT-IR. Firstly, solutions of PC in the absence of MAA were prepared. As expected, PC was easily dissolved in MeOH, confirming a strong interaction between the solvent and template molecule through hydrogen bonding formation. In THF, PC was dissolved after sonication; but using ACN, PC remained only partially dissolved. These later observations are reflected in their respective FT-IR spectra (**Figure 7.2A**), where the carbonyl stretching band ($\upsilon_{C=O}$) of PC at 1737 cm^{-1} shifts to 1740 cm^{-1} in MeOH, but it remains almost invariable in THF and ACN. Additionally, a band at 1717 cm^{-1} arises from the formation of hydrogen bonds between MeOH and carboxyl groups of PC.

Next, the FT-IR spectra of MAA solutions in MeOH, THF and ACN were studied (**Figure 7.2B**). It has been well-established that MAA is found in equilibrium between the monomeric and dimeric forms, which is affected by its interaction with the solvent [15,23]. Thus, three different bands can be observed in the FT-IR spectra of MAA at approximately 1735, 1719 and 1698 cm^{-1}. These bands are attributed to free carboxylic group (monomer), the inter-association of MAA and solvent molecules (liberated carbonyl group) and cyclic dimers of MAA, respectively [24]. The intensity of the band that evidences dimerization of MAA is higher for MeOH, followed by ACN and far behind by THF. On the other hand, THF presents an intense band for the liberated carbonyl group due to its capacity as hydrogen-bond acceptor. Several reports have described that dimerization of MAA molecules diminishes the template-monomer complex [15,23], resulting in fewer imprinted sites. Despite this, its overall effect seems to be beneficial in MIPs, since the number of non-selective background sites is reduced [23,25].

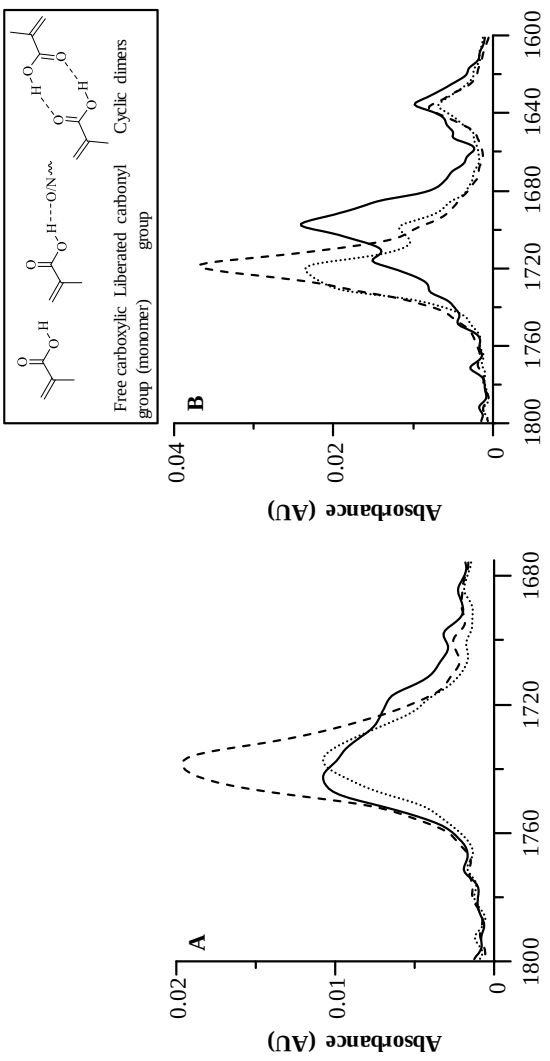

Figure 7.2. FT-IR spectra of carbonyl stretching band ($\upsilon_{C=O}$) of: PC (A) and MAA (B) in MeOH (bold line), THF (dashed line) and ACN (dotted line).

Next, PC-MAA solutions (ratio 1:4) in the above mentioned solvents were investigated. First of all, it is worth noting that PC was completely dissolved in ACN in the presence of MAA. This fact can be attributed to the hydrogen bond formation between PC and MAA, which would confirm the interaction between the monomer and the template molecule in the pre-polymerization mixture. With respect to FT-IR spectra of these solutions, the carbonyl region of the monomer and template overlaps. This hinders the confirmation of hydrogen bonding between PC and MAA. Taking into account all above results, ACN was selected as porogen for the MIP synthesis since the complexation PC-MAA was satisfactorily guaranteed, thus predominating the imprinting process over dimerization.

7. 3. 3. Influence of experimental variables on MIP performance

Since our aim was to use MIPs to extract PLs from lipid extracts, several solvents were selected for loading the sample solution. Thus, a $CHCl_3$:MeOH mixture (2:1, v/v) was chosen, since it is the solvent commonly used to extract lipids [5–7,26]. Some authors [27] have also proposed organic solvent mixtures with large hydrophobic character (e.g., hexane-EtOH) to dissolve fat-based matrices containing PLs. To study the performance of both solvents, a PC solution at 2000 μg/mL (250 μL) was applied to the MIP 1 and its corresponding NIP (see **Table S7.1**). The amount of retained PC on the polymer was calculated by subtracting the concentration of PC found in the percolated solution (measured spectrophotometrically [20]) with respect to the initial concentration loaded.

When $CHCl_3$:MeOH (2:1, v/v) was considered, (91 ± 6)% of the amount of PC initially loaded onto MIP 1 was lost, whereas with hexane-EtOH (98:2, v/v), a retention of (58 ± 4)% was found. These results suggested that the retention of PC was accomplished mainly by both electrostatic interactions and hydrogen bond formation, although non-specific

interactions also occurred. Taking into account these results, this latter mixture was selected as the loading solvent for further experiments. After loading the sample solution in the SPE cartridge, a suitable washing step was introduced. For this purpose, hexane was used since it can remove matrix non-polar components (such as TAGs). Remaining adsorbed PC was finally eluted with the conventional $CHCl_3$:MeOH (2:1, v/v) mixture. The washing and elution fractions were collected and their PC content was also evaluated spectrophotometrically [20]. Using this protocol, no loss of PC was evidenced in washing step, and the recovery of PC in the collected elution fraction reached values above 95%.

Once the SPE protocol was established, it was applied to the different sorbents prepared (see **Table S7.1**). Several parameters were investigated: (a) initiator content and (b) template/functional monomer/cross-linker (T:M:C) molar ratio. The respective experiments are described in the Electronic Supplementary Material. As a result of this study, MIP 3 (T:M:C of 1:10:30 and 4.2% of initiator) was selected for further experiments.

7. 3. 4. Characterization and evaluation of selected MIP

MIP 3 and its corresponding NIP were characterized through its morphological and chemical composition by SEM and FT-IR. As shown in **Figure S7.1**, SEM micrographs reflect a lower average size for the MIP globules than for the NIP, suggesting some influence of the template on the particle growth during the polymerization process.

FT-IR spectra of pure PC, MIP 3 and NIP 3 were measured (see **Figure 7.3**). Spectrum of PC presents various characteristic stretching bands: CH_2 at 2800-3000 cm^{-1}; C=O at 1737 cm^{-1}; P=O, C-O-C at 1300-1100 cm^{-1}; $P\text{-}O^-$ at 1091 cm^{-1}; P-O-C at 1062 cm^{-1} and $(CH_3)_3N$ at 968 cm^{-1} [28,29]. MIP and NIP 3 show identically FT-IR spectra, which indicates that these polymers have a similar backbone. Phosphate bands and $(CH_3)_3N$ band cannot be

observed in MIP, which demonstrates that template molecules were successfully removed from the MIP in cleaning step. Besides, several distinctive bands at 3600, 3000, 1725 and 1300-1000 cm^{-1} indicate the -OH in the carboxyl of MAA, and =C-H, C=O and C-O-C stretching vibrations, respectively [30]. These results suggest that MAA and EDMA were successfully interlinked.

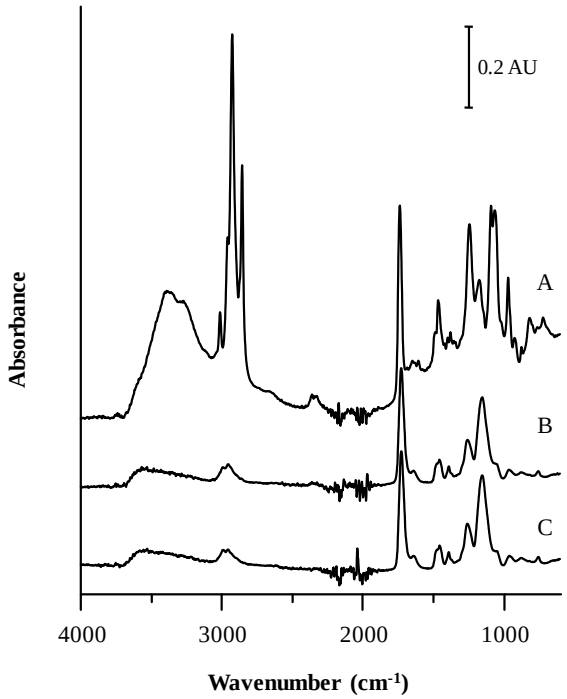

Figure 7.3. FT-IR spectra of PC (A), MIP 3 (B) and NIP 3 (C).

The adsorption capacity of the MIP and NIP cartridges was determined to be 40.8 and 22.6 µg/mg of polymer, respectively (see description in the Electronic Supplementary Material). These results reflect the intrinsic molecular recognition ability and selective adsorption for PC of MIP over NIP.

Then, the breakthrough volume of MIP was established. For this purpose, different loading sample volumes (0.25 - 10 mL) containing a constant amount of PC (500 µg) were percolated through to cartridge.

Recoveries ranged from 93 to 98% in the range assayed, indicating that no significant compound loss (analyte breakthrough) occurred.

The presence of imprinted cavities in the polymeric network of MIPs enables the selectively rebinding of the template molecule. Additionally, selectivity of the MIP towards compounds structurally related to the template molecule has been also reported [31,32]. This phenomenon is known as cross-reactivity and may be of interest to selectively isolate a family of compounds in a particular matrix. Thus, selectivity of both polymers (MIP 3 and NIP 3) to retain two structural related compounds of PC template (500 μg of SM and PE, respectively; see **Figure 7.1**) was also evaluated. Following the protocol described in Experimental Section, retention values on MIP 3 were determined to be (98 ± 2)% for both PLs, while PE and SM retention on NIP 3 were (40 ± 2) and (50 ± 4.4)%, respectively. These results confirmed that MIP exhibited high selective binding affinity for PC and some structure-related PLs, and can be applied to extract PLs. Considering that target analytes are particularly retained through electrostatic interactions and hydrogen bonding, selective templated binding sites of the MIP might be attributed mainly to the polar "head" of PL. The cross-reactivity showed by MIP 3 was of much interest for the purpose of this study.

7. 3. 5. Extraction and analysis of PLs from lipid extracts of milk

To demonstrate the applicability of the prepared MIP, fat extracts of human milk samples were loaded onto the selected MIP, and treated following the procedure described in Experimental Section. To determine the content of the three PLs in these milk samples, the analysis by HILIC-ELSD was accomplished. To obtain a quantitative evaluation of PLs, external calibration curves were constructed by injecting six standard solutions (prepared in $CHCl_3$:MeOH (2:1, v/v)) in the range 20-400 μg/mL. Calibration equations and other figures of merit (LODs, LOQs and precision) are described in the

Electronic Supplementary Material. The chromatograms of a human milk sample before and after extraction with MIP 3 are given in **Figure 7.4**. Peak identification of PLs was performed by comparing retention times with those of the standards, and when required also by spiking the sample with the standards. **Figure 7.4** shows a significant decrease of nonpolar lipids and a large enhancement of signals corresponding to PLs in the elution fraction (continuous line) with respect to the untreated fat extract (dashed line). This fact confirms the efficiency of the MIP to be used as clean-up and preconcentration step, allowing further characterization of target analytes (PLs).

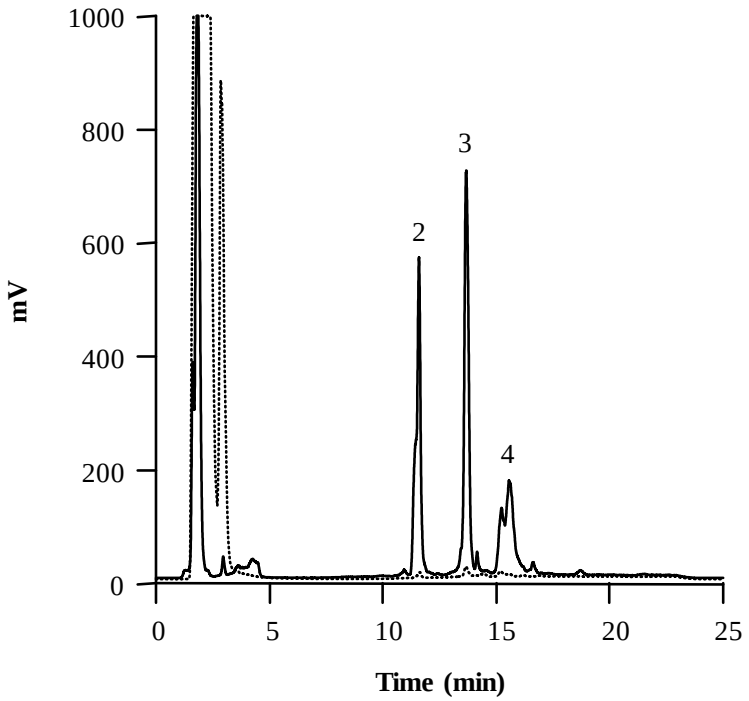

Figure 7.4. HILIC-ELSD chromatograms of human milk fat extract before (dashed line) and after (continuous line) MIP-SPE treatment. For extraction procedure of MIP-SPE and HPLC-ELSD conditions (see Experimental Section and Electronic Supplementary Material, respectively). Peak identification: (1) nonpolar lipids, (2) PE, (3) PC and (4) SM.

Then, the accuracy of the method in human milk samples was also evaluated through a recovery study. Considering the complexity of matrix of this sample and the unavailability of an analyte-free milk sample, the standard addition method was used. For this purpose, a human milk sample (5 mL) was fortified at four concentration levels (10-50 μg/mL) and these spiked samples were analyzed after using the MIP-SPE procedure. The average spiked recoveries (n = 3) of the PLs in samples ranged from 75 to 88% for all analytes investigated. The RSD values found were comprised between 5-8%. These results show that PLs extraction was not affected by the matrix from human milk samples using the MIP-SPE method.

Next, the content of each PL was evaluated by analyzing several human milk samples in different lactation stages (colostrum, transitional and mature milk, **Table 7.1**). Some variability in the PL levels can be observed among the analyzed human milk samples; in any case, their content is within the range previously reported [2, 6].

Table 7.1. PE, PC and SM content (mg per g of fat) in human milk at different stages of lactation.

	PE (mean ± SD)	**PC (mean ± SD)**	**SM (mean ± SD)**
Colostrum (n = 3)	3.7 ± 1.2	5.2 ± 1.4	4.3 ± 0.6
Transitional milk (n = 3)	1.8 ± 0.7	2.2 ± 0.9	2.0 ± 0.7
Mature milk (n = 3)	1.4 ± 0.3	1.8 ± 0.3	1.5 ± 0.2

7. 3. 6. Reusability and reproducibility of the MIP-SPE cartridges

The reusability of the columns was evaluated using the optimal MIP (n = 20) for the analysis of 250 μL of a PC solution of 2000 μg/mL. Excellent performance with recoveries higher than 90% for PC was achieved. Additionally, reusability for fat extracts was evaluated. For this purpose, fat

extracts (8-75 mg) were dissolved in 5 mL of hexane-EtOH (98:2, v/v), being the adsorption-elution cycle repeated 6 times using the same MIP. To evaluate retention, total PLs were estimated before and after applying the SPE protocol by the Stewart assay [20]. In any case, the percolated fraction was also injected in the chromatograph to confirm the absence of PLs. There was no remarkable reduction in the adsorption capacity of the MIP adsorbent (retention values ranged between 95 and 98%), which indicates a good stability of MIP.

The reproducibility of the MIPs was investigated by using three batches prepared on different days. The adsorption capacity to PC was measured in triplicate for each batch, being its average value 38.7 μg/mg (with RSD 7.1%). This indicates that the fabrication method exhibits acceptable reproducibility.

To illustrate the advantages of the MIP as a novel extraction material, a comparative study of our method with other reported sample preparation protocols is presented in **Table 7.2**. Unfortunately, in most reported studies [3,16,33,34], analytical parameters (LODs, LOQs and recoveries of PLs) were not mentioned. Regarding LODs, our values are comparable to those reported using ELSD [4], and were higher when MS was used as detector system [35,36]. Concerning extraction recoveries, our values were similar to those reported in literature [3,4,35,36]. To our knowledge, the consumable materials of some sorbents reported [37,38] are relative expensive, whereas our starting materials are cheaper and easily available. Besides this, the suitable reusability of our sorbent, combined with the possibility of manufacturing several SPE cartridges (*ca*. 50) from the bulk MIP material (see Experimental Section), undoubtedly makes this protocol economically attractive.

Table 7.2. An overview on recently reported nanomaterial-based methods for preconcentration and determination of PLs.

Sorbent used	Extraction procedure	Coupled technique	Matrix	PLs studied	LOD (µg/mL)	LOQ (µg/mL)	Recovery (%)	Refs.
Silica gel base material	SPE	NP-LC-ELSD	Dairy products	PC, PE, PI, PS, SM	-	-	96	[3,37]
Silica gel base material	SPE	HILIC-ELSD	Bovine and donkey milk	PC, PE, PI, PS, SM	1.68 - 4.04	1.70 - 4.05	89.99	[4,37]
TiO_2 beads	Micro-SPE	MALDI-TOF-MS	Dairy products	PC, PE, PI, PS, SM	-	-	-	[33]
HOA–$BaTiO_3$ NPs	LLME	MALDI-TOF	*Escherichia coli*	PS, L-α-PA	0.16 - 0.28	-	96.6 - 99.4	[36]
Titania-coated silica (TiO_2/SiO_2) core-shell composites	SPE	HILIC-MS/MS	Shrimp waste	PC, PE, PI, PS	0.12 - 0.25	0.37 - 0.78	74.2 - 102.4	[35]
Zirconia-bonded silica particles	SPE	LC-TOF-MS	Human serum	Lyso-PC, PC, lyso-	-	-	-	[34,38]
Poly(ethylene-co-vinyl alcohol) base MIM using PC as template	Permeability	UV	-	PC	-	-	-	[16]
Methacrylate base MIP using PC as template	SPE	HILIC-ELSD	Human milk	PC, PE, SM	1.4 - 3.5	4.8 - 11.7	75 - 88	Present work

Abbreviations: NP, normal-phase; HOA–$BaTiO_3$ NPs, 12-hydroxy octadecanoic acid-modified barium titanate nanoparticles; LLME, liquid–liquid microextraction; PA, phosphatidic acid sodium salt; MIM, molecularly imprinted membrane.

7. 4. Conclusions

In this work, a novel and selective MIP-SPE sorbent prepared by bulk polymerization using PC as template molecule has been synthesized. The sorbent has been applied to the extraction of PLs in human milk fat samples, followed by HILIC-ELSD analysis. To our knowledge, the present study is the first work to use imprinting process for PLs extraction in these matrices.

A pre-polymerization study was firstly conducted. On the basis of molecular interactions between template and functional monomer in solution by FT-IR spectroscopy, ACN was chosen as suitable porogen. Then, imprinted polymers were synthesized and the influence of the template/functional monomer/cross-linker molar ratios, percentage of initiator as well as the extraction conditions were investigated. The MIP with a molar ratio of 1:6:30 and 4.2% of initiator showed the best recognition ability for PC.

The use of PC as a template generated molecularly imprinted sites with size, shape, and functionality suitable for a remarkable selective extraction of PLs. The retention of these compounds was attributed to hydrogen bonds and electrostatic interactions.

The selective potential of the MIP was demonstrated by its application to human milk fat samples. This treatment resulted in an effective clean-up of sample (particularly to remove neutral lipids) and preconcentration (10 to 20 times). This fact allows an accurate determination of PLs by HILIC-ELSD, without jeopardizing the structural integrity of HPLC column. In summary, the present MIP-SPE method is cost-effective and selective, with a satisfactory sorbent reusability (up to 20 and 6 reuses, for standard solutions and fat extracts, respectively). However, our SPE protocol gave LODs higher than those obtained using more sophisticated techniques such MS detection.

In any case, our extraction methodology represents a promising alternative for the isolation of PLs from biological samples.

Acknowledgments

Project CTQ2014-52765-R (MINECO of Spain and FEDER) and PROMETEO/2016/145 (Generalitat Valenciana). I. T-D thanks the MINECO for an FPU grant for PhD studies.

7. 5. References

[1] C.H. Huang, Mixed-chain phospholipids: structures and chain-melting behavior, Lipids 36 (2001) 1077–1097. doi:10.1007/s11745-001-0818-1.

[2] G. Contarini, M. Povolo, Phospholipids in milk fat: composition, biological and technological significance, and analytical strategies, Int. J. Mol. Sci. 14 (2013) 2808–2831. doi:10.3390/ijms14022808.

[3] A. Avalli, G. Contarini, Determination of phospholipids in dairy products by SPE/HPLC/ELSD, J. Chromatogr. A 1071 (2005) 185–190. doi:10.1016/j.chroma.2005.01.072.

[4] P. Donato, F. Cacciola, F. Cichello, M. Russo, P. Dugo, L. Mondello, Determination of phospholipids in milk samples by means of hydrophilic interaction liquid chromatography coupled to evaporative light scattering and mass spectrometry detection, J. Chromatogr. A 1218 (2011) 6476–6482. doi:10.1016/j.chroma.2011.07.036.

[5] L.M. Rodríguez-Alcalá, J. Fontecha, Major lipid classes separation of buttermilk, and cows, goats and ewes milk by high performance liquid chromatography with an evaporative light scattering detector focused on the phospholipid fraction, J. Chromatogr. A 1217 (2010) 3063–3066. doi:10.1016/j.chroma.2010.02.073.

[6] F. Giuffrida, C. Cruz-Hernandez, B. Flück, I. Tavazzi, S.K. Thakkar, F. Destaillats, M. Braun, Quantification of phospholipids classes in human milk, Lipids 48 (2013) 1051–1058. doi:10.1007/s11745-013-3825-z.

[7] C. Lopez, V. Briard-Bion, O. Menard, F. Rousseau, P. Pradel, J.-M. Besle, Phospholipid, sphingolipid, and fatty acid compositions of the milk fat globule membrane are modified by diet, J. Agric. Food Chem.

56 (2008) 5226–5236. doi:10.1021/jf7036104.

[8] J.G. Parsons, S. Patton, Two-dimensional thin-layer chromatography of polar lipids from milk and mammary tissue, J. Lipid Res. 8 (1967) 696–698.

[9] F. Sánchez-Juanes, J.M. Alonso, L. Zancada, P. Hueso, Distribution and fatty acid content of phospholipids from bovine milk and bovine milk fat globule membranes, Int. Dairy J. 19 (2009) 273–278. doi:10.1016/j.idairyj.2008.11.006.

[10] R.J. Maxwell, D. Mondimore, J. Tobias, Rapid method for the quantitative extraction and simultaneous class separation of milk lipids, J. Dairy Sci. 69 (1986) 321–325. doi:10.3168/jds.S0022-0302(86)80408-8.

[11] M. Schwalbe-Herrmann, J. Willmann, D. Leibfritz, Separation of phospholipid classes by hydrophilic interaction chromatography detected by electrospray ionization mass spectrometry, J. Chromatogr. A 1217 (2010) 5179–5183. doi:10.1016/j.chroma.2010.05.014.

[12] W.J. Cheong, S.H. Yang, F. Ali, Molecular imprinted polymers for separation science: A review of reviews, J. Sep. Sci. 36 (2012) 609–628. doi:10.1002/jssc.201200784.

[13] J. O'Mahony, A. Molinelli, K. Nolan, M.R. Smyth, B. Mizaikoff, Towards the rational development of molecularly imprinted polymers: 1H NMR studies on hydrophobicity and ion-pair interactions as driving forces for selectivity, Biosens. Bioelectron. 20 (2005) 1884–1893. doi:10.1016/j.bios.2004.07.036.

[14] H.S. Andersson, I.A. Nicholls, Spectroscopic evaluation of molecular imprinting polymerization systems, Bioorg. Chem. 25 (1997) 203–211. doi:10.1006/bioo.1997.1067.

[15] M.C. Cela-Pérez, A. Lasagabáster-Latorre, M.J. Abad-López, J.M.

López-Vilariño, M. V. Gónzalez-Rodríguez, A study of competitive molecular interaction effects on imprinting of molecularly imprinted polymers, Vib. Spectrosc. 65 (2013) 74–83. doi:10.1016/j.vibspec.2012.12.002.

[16] C. Pegoraro, D. Silvestri, G. Ciardelli, C. Cristallini, N. Barbani, Molecularly imprinted poly(ethylene-co-vinyl alcohol) membranes for the specific recognition of phospholipids, Biosens. Bioelectron. 24 (2008) 748–755. doi:10.1016/j.bios.2008.06.050.

[17] R. Jang, K.H. Kim, S.A. Zaidi, W.J. Cheong, M.H. Moon, Analysis of phospholipids using an open-tubular capillary column with a monolithic layer of molecularly imprinted polymer in capillary electrochromatography-electrospray ionization-tandem mass spectrometry, Electrophoresis 32 (2011) 2167–2173. doi:10.1002/elps.201100205.

[18] M. Russo, F. Cichello, C. Ragonese, P. Donato, F. Cacciola, P. Dugo, L. Mondello, Profiling and quantifying polar lipids in milk by hydrophilic interaction liquid chromatography coupled with evaporative light-scattering and mass spectrometry detection, Anal. Bioanal. Chem. 405 (2013) 4617–4626. doi:10.1007/s00216-012-6699-7.

[19] S. Morera Pons, A.I. Castellote Bargalló, M.C. López Sabater, Evaluation by high-performance liquid chromatography of the hydrolysis of human milk triacylglycerides during storage at low temperatures, J. Chromatogr. A 823 (1998) 467–474. doi:10.1016/S0021-9673(98)00273-8.

[20] J.C.M. Stewart, Colorimetric determination of phospholipids with ammonium ferrothiocyanate, Anal. Biochem. 104 (1980) 10–14. doi:10.1016/0003-2697(80)90269-9.

[21] J. Folch, M. Lees, G.H. Sloane Stantley, A simple method for the isolation and purification of total lipides from animal tissues, J. Biol. Chem. 266 (1957) 497–509.

[22] X. Song, J. Wang, J. Zhu, Effect of porogenic solvent on selective performance of molecularly imprinted polymer for quercetin, Mater. Res. 12 (2009) 299–304. doi:10.1590/S1516-14392009000300009.

[23] Y. Zhang, D. Song, L.M. Lanni, K.D. Shimizu, Importance of functional monomer dimerization in the molecular imprinting process, Macromolecules 43 (2010) 6284–6294. doi:10.1021/ma101013c.

[24] K. ElMiloudi, M. Benygzer, S. Djadoun, N. Sbirrazzuoli, S. Geribaldi, FT-IR spectroscopy and hydrogen bonding interactions in poly(styrene-co-methacrylic acid)/poly(styrene-co-4-vinyl pyridine) blends, Macromol. Symp. 230 (2005) 39–50. doi:10.1002/masy.200551140.

[25] Y. Zhang, D. Song, J.C. Brown, K.D. Shimizu, Suppression of background sites in molecularly imprinted polymers via urea-urea monomer aggregation, Org. Biomol. Chem. 9 (2011) 120–126. doi:10.1039/c0ob00637h.

[26] T.P.L. Ferraz, M.C. Fiúza, M.L.A. Dos Santos, L. Pontes De Carvalho, N.M. Soares, Comparison of six methods for the extraction of lipids from serum in terms of effectiveness and protein preservation, J. Biochem. Biophys. Methods 58 (2004) 187–193. doi:10.1016/j.jbbm.2003.10.008.

[27] K.M. Marakulina, R. V. Kramor, Y.K. Lukanina, M. V. Kozlov, L.N. Shishkina, Application of UV- and IR-Spectroscopy to analyze the formation of complexes between sphingomyelin and phenolic antioxidants, Moscow Univ. Chem. Bull. 67 (2012) 185–191. doi:10.3103/S0027131412040098.

[28] M.B. Abramson, W.T. Norton, R. Katzman, Study of ionic structures in phospholipids by infrared spectra, J. Biol. Chem. 240 (1965) 2389–2395.

[29] J. Nzai, A. Proctor, Determination of phospholipids in vegetable oil by Fourier transform infrared spectroscopy, J. Am. Oil Chem. Soc. 75 (1998) 1281–1289. doi:10.1007/s11746-998-0173-x.

[30] Q. Su, C. Zeng, Y. Tang, D.E. Finlow, M. Cao, Evaluation of diazepam-molecularly imprinted microspheres for the separation of diazepam and its main metabolite from body fluid samples, J. Chromatogr. Sci. 50 (2012) 608–614. doi:10.1093/chromsci/bms039.

[31] M.J. Lerma-García, M. Zougagh, A. Ríos, Magnetic molecular imprint-based extraction of sulfonylurea herbicides and their determination by capillary liquid chromatography, Microchim. Acta. 180 (2013) 363–370. doi:10.1007/s00604-013-0942-6.

[32] E. Caro, R.M. Marcé, P.A.G. Cormack, D.C. Sherrington, F. Borrull, On-line solid-phase extraction with molecularly imprinted polymers to selectively extract substituted 4-chlorophenols and 4-nitrophenol from water, J. Chromatogr. A 995 (2003) 233–238. doi:10.1016/S0021-9673(03)00543-0.

[33] C.D. Calvano, O.N. Jensen, C.G. Zambonin, Selective extraction of phospholipids from dairy products by micro-solid phase extraction based on titanium dioxide microcolumns followed by MALDI-TOF-MS analysis, Anal. Bioanal. Chem. 394 (2009) 1453–1461. doi:10.1007/s00216-009-2812-y.

[34] C. Ferreiro-Vera, F. Priego-Capote, M.D. Luque de Castro, Comparison of sample preparation approaches for phospholipids profiling in human serum by liquid chromatography-tandem mass spectrometry, J. Chromatogr. A 1240 (2012) 21–28.

doi:10.1016/j.chroma.2012.03.074.

[35] Q. Shen, H.-Y. Cheung, TiO_2/SiO_2 core-shell composite-based sample preparation method for selective extraction of phospholipids from shrimp waste followed by hydrophilic interaction chromatography coupled with quadrupole time-of-flight/mass spectrometry analysis, J. Agric. Food Chem. 62 (2014) 8944–8951. doi:10.1021/jf503040p.

[36] S.K. Kailasa, H.F. Wu, Surface modified $BaTiO_3$ nanoparticles as the matrix for phospholipids and as extracting probes for LLME of hydrophobic proteins in Escherichia coli by MALDI-MS, Talanta 114 (2013) 283–290. doi:10.1016/j.talanta.2013.05.032.

[37] Sigma-Aldrich, Supelclean™ LC-Si SPE tube, (año no indicado). Disponible en: http://www.sigmaaldrich.com/catalog/product/supelco /57051?lang=es&region=ES (Fecha de acceso: 06/04/2017).

[38] Sigma-Aldrich, HybridSPE®-Phospholipid, (año no indicado). Disponible en: http://www.sigmaaldrich.com/catalog/product/supelco /55261u?lang=es&region=ES (Fecha de acceso: 04/05/2017).

[39]† I. Mijangos, F. Navarro-Villoslada, A. Guerreiro, E. Piletska, I. Chianella, K. Karim, A. Turner, S. Piletsky, Influence of initiator and different polymerisation conditions on performance of molecularly imprinted polymers, Biosens. Bioelectron. 22 (2006) 381–387. doi:10.1016/j.bios.2006.05.012.

[40]† C.E. Carraher, Jr., Free radical chain polymerization (addition polymerization), en: J.J. Lagowski (Ed.), Polym. Chem., 6ª ed., Marcel Dekker, Inc., New York, 2003. doi:10.1039/c4py01415d.

[41]† E. Caro, R.M. Marcé, F. Borrull, P.A.G. Cormack, D.C. Sherrington, Application of molecularly imprinted polymers to solid-phase

† Only included in Supplementary Material.

extraction of compounds from environmental and biological samples, TrAC - Trends Anal. Chem. 25 (2006) 143–154. doi:10.1016/j.trac.2005.05.008.

7. 6. Electronic Supplementary Material

7. 6. 1. Instrumentation

Separation of PLs classes was carried out with a Kinetex™ HILIC 100 Å column (150 mm × 4.6 mm, 2.6 µm; Phenomenex, Torrance, CA, USA, http://www.phenomenex.com/). Mobile phases consisted of ACN-ammonium formate 100 mM (A, 97:3, v/v) and water-ammonium formate 100 mM (B, 97:3, v/v). The chromatographic separation was carried out using the following gradient: 0-3.5 min, 100% A; 11 min, 15% B and kept during 10 min. Column temperature, 25 ºC; flow rate, 1.0 mL/min and injection volume, 20 µL. The ELSD parameters were: evaporation and nebulization temperature, 80 and 40 ºC, respectively; gas flow rate, 1.4 Standard Litres per Minute (SLM); gain factor, 1.

7. 6. 2. Influence of experimental variables on MIP performance

In this study, four MIPs and their corresponding NIPs were prepared via bulk polymerization method following the non-covalent approach. In particular, two different template/functional monomer/cross-linker (T:M:C) molar ratios and percentage of initiator were studied. As shown in **Table S7.1**, lower percentage of initiator enhanced the recognition ability of MIPs prepared with a 1:4:20 molar ratio, while scarcely affected to MIPs with a 1:10:30 molar ratio. The presence of a higher content of initiator usually leads to the formation of a larger number of free radicals, a larger number of growing nuclei, giving as a result rigid and less selective materials [39]. Additionally, larger initiator contents might lead an increase in the heat reaction, which could disrupt the T-M complex and therefore the selectivity of MIPs [39,40]. However, at high content of monomer the interaction with template could be easily favored, being the initiator content a less determining

factor. On the other hand, molar ratio 1:10:30 led to more selective MIPs under the conditions assayed. These results can be attributed to the fact that an excess of functional monomer relative to the template is usually required to favor T-M complex formation and to maintain its integrity during polymerization [41]. Moreover, considering that PC is a large molecule, steric hindrance in the formation of the T-M complex might be overcome with a higher proportion of MAA. As shown in **Table S7.1**, MIP 3 and MIP 4 exhibited similar recognition ability, although MIP 3 provided slightly higher retention. For these reasons, it was selected for further experiments.

Table S7.1. Polymerization mixture composition, T:M:C[1] molar ratio and percentage of retained PC by the MIPs and NIPs.

	PC	MAA	EDMA	AIBN[2]	ACN	T:M:C	%Retention	RSD (%)
MIP1	0.184	0.736	3.68	4.2	5	1:04:20	58	7.7
NIP1	-	0.736	3.68		5		42	8.3
MIP2	0.184	0.736	3.68	2.1	5	1:04:20	86	8.4
NIP2	-	0.736	3.68		5		47	8.6
MIP3	0.184	1.84	5.52	4.2	5	1:10:30	98	1.9
NIP3	-	1.84	5.52		5		52	4.5
MIP4	0.184	1.84	5.52	2.1	5	1:10:30	88	5
NIP4	-	1.84	5.52		5		55	6.2

[1]T:M:C = template/functional monomer/cross-linker.

[2]with respect to total monomers.

7. 6. 3. SEM micrographs of MIP/NIP 3

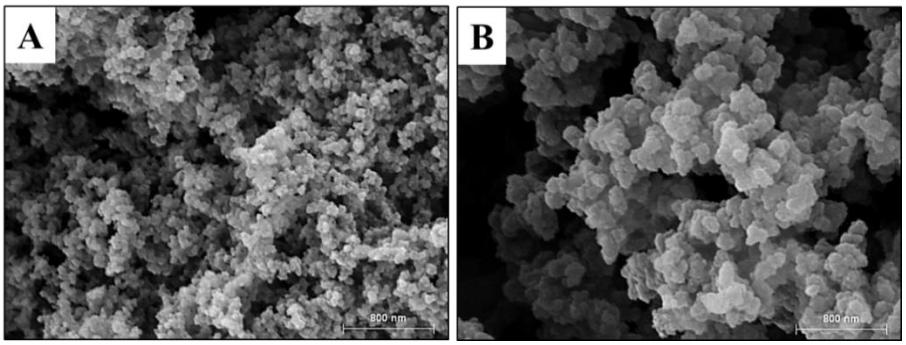

Figure S7.1. SEM micrographs of MIP 3 (A) and NIP 3 (B) measured at 30000x.

7. 6. 4. Characterization and evaluation of selected MIP

The capacity of the MIP/NIP is considered as the maximum amount of a compound that can be retained on the imprinted polymer when particular extraction conditions are applied. Thus, increasing amounts of PC standard were percolated through the MIP and NIP under the recommended extraction protocol. **Figure S7.2** indicates that after loading 1000 µg of PC, retention in NIP dramatically decreased, whereas retention in MIP remained unchanged. These results reflect that the recognition ability of MIP included both specific and non-specific interactions; whereas retention of PC in NIP was only attributed to this later adsorption mechanism. Thus, once non-specific cavities are covered, selective templated binding sites of the MIP start gaining importance.

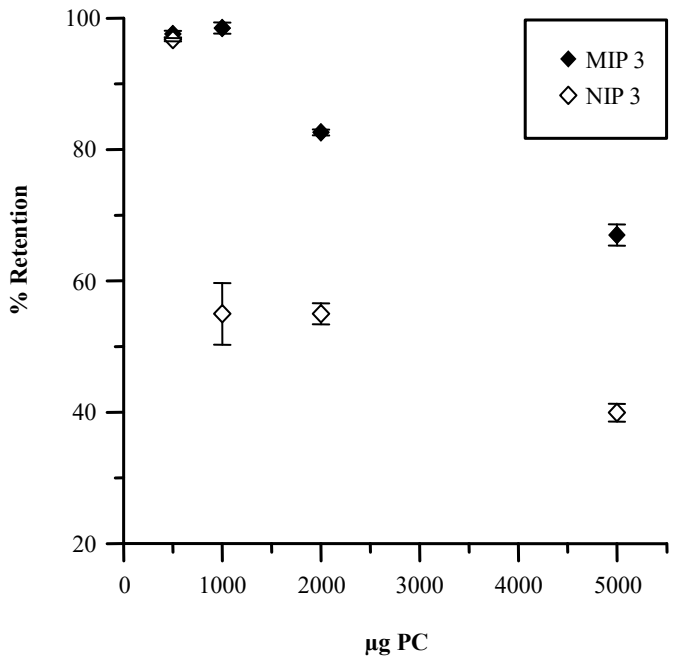

Figure S7.2. Adsorption capacity of MIP 3 and NIP 3 cartridges at increasing PC amounts.

7. 6. 5. Analytical figures of merit

Calibration equations were calculated by applying both linear and power models to the detector response (area) and mass of lipid values. **Table S7.2** shows that the peak areas fit reasonably well to the linear model in the adopted concentration range. The LODs and LOQs of the analytes were based on a signal-to-noise ratio (S/N) = 3 and 10, respectively. As it can be observed in **Table S7.2**, LOD values range from 1.4 to 3.5 µg/mL and LOQs from 4.8 to 11.7 µg/mL. The precision of the method (intra and inter-day conditions) of retention times and peak areas, given as RSD, was calculated from a standard solution (prepared at a concentration of 100 µg/mL) injected 3 times per day during 3 days. Thus, the RSD values were lower than 2.5% for all the analytes considered.

Table S7.2. Calibration curve parameters (peak area *vs* µg injected), LOD and LOQ for standard PLs in the HILIC-ELSD method.

	PE	**PC**	**SM**
Power	$y = 417.1x^{1.250}$; $r^2 = 0.9996$	$y = 640.1x^{1.089}$; $r^2 = 0.9995$	$y = 471.6x^{1.045}$; $r^2 = 0.9989$
Linear	$y = 931.6x - 1422.7$; $r^2 = 0.9965$	$y = 794.2x - 145.6$; $r^2 = 0.9983$	$y = 543.8x - 140.0$; $r^2 = 0.9980$
LOD (µg/mL)	1.4	2.6	3.5
LOQ (µg/mL)	4.8	8.8	11.7

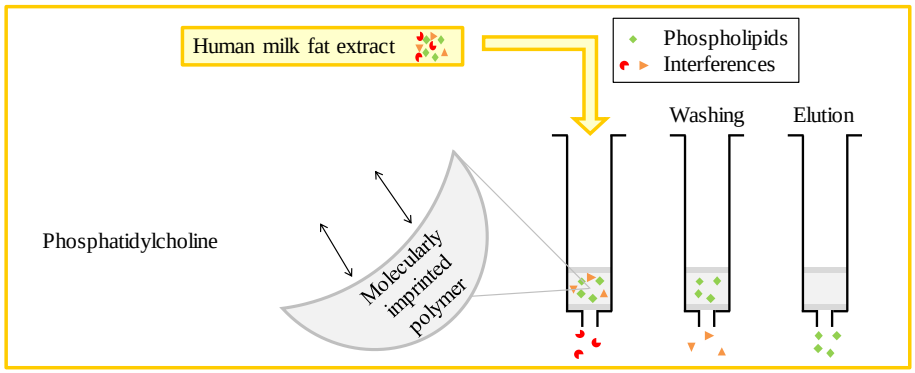
Human milk fat extract
Phospholipids
Interferences
Washing
Elution
Phosphatidylcholine
Molecularly imprinted polymer

BLOQUE III. ANÁLISIS DE LA FRACCIÓN PROTEICA DE LA LECHE MATERNA

CAPÍTULO 8

Isolation of human milk whey proteins by solid-phase extraction with a polymeric material modified with gold nanoparticles

Microchemical Journal 133 (2017) 320–326

Contents lists available at ScienceDirect

Microchemical Journal

journal homepage: www.elsevier.com/locate/microc

Isolation of human milk whey proteins by solid phase extraction with a polymeric material modified with gold nanoparticles

Isabel Ten-Doménech *, Ernesto Francisco Simó-Alfonso, José Manuel Herrero-Martínez *

Department of Analytical Chemistry, University of Valencia, C. Doctor Moliner 50, E-46100, Burjassot, Valencia, Spain

This work describes a method for the isolation of human milk whey proteins by SPE with a polymeric material modified with AuNPs. HSA, α-La, Lf and Lyz were selected as target proteins to establish the performance of SPE support. Several experimental variables (pH and ionic strength) that affect the SPE protocol were investigated to achieve the maximum extraction efficiency. Under optimal conditions, the SPE sorbent gave excellent recoveries, and offered a high permeability and reusability (more than 20 times). The feasibility of this methodology was successfully demonstrated by isolating the target proteins (from milk whey extract) and from a direct dilution of human milk samples (without isoelectric precipitation of CNs).

Keywords: Gold nanoparticles; Glycidyl methacrylate polymer; Human milk Whey proteins; Solid-phase extraction.

8. 1. Introduction

Human milk is considered the optimal way of providing young infants with the necessary nutrients for healthy growth and development. It comprises a very complex fluid, which contains carbohydrates and salts in solution, CNs in colloidal dispersion, cells and cellular debris, and lipids mostly in emulsified globules [1]. In particular, the protein fraction in milk plays an important role in achieving many of the benefits of breast-feeding. Total protein content in human milk represents *ca*. 1%, from which approximately 5% is bound to the fat globule membrane [2]. The variety of proteins contained in human milk is wide. These include CNs (*ß*-CN, *κ*-CN, α_{s1}-CN) and whey proteins such as *α*-La, Lf, Igs (sIgA, IgM, IgG), HSA, and Lyz [3]. In human milk, the whey fraction contains the majority of the protein (80% in early lactation and 60% in mature milk) [3], whereas CNs represent a smaller fraction.

Separation of human milk CNs is usually carried out through precipitation at their pI (pH 4.6). However, some whey proteins may coprecipitate with CNs at this pH [4]. This problem might be partially overcome by adding Ca^{2+} during the pH adjustment [2]. However, rapid and direct isolation of human milk whey proteins without prior precipitation of CNs has not been reported to date.

SPE is an increasingly useful sample preparation technique. It is used either to preconcentrate or to purify analytes of interest from a great variety of sample matrices. In particular, this technique is a widely employed alternative for separation and enrichment purposes in protein analysis schemes and proteomic techniques [5,6]. RP and to a lesser extent ion-exchange are the most commonly used SPE materials for protein isolation. In particular, normal phase sorbents (including HILIC supports) have been preferred for glycosylated proteins and peptides [7,8]. Nevertheless, the availability of novel sorbents for proteins species is limited at present [6,9].

In this field of sample pre-treatment, porous polymer monoliths have recently undergone a rapid growing [10,11]. Their simple in situ preparation, high permeability, stability along wide pH-range, and versatile surface chemistry offer a wide range of possibilities and represent an alternative to usual packed materials in SPE cartridges. Particularly, GMA is a commonly used "starting material" to provide polymers with different chromatographic properties (ion exchange, hydrophobic/hydrophilic, chiral, etc.) [12–15]. It is due to the active epoxy groups contained in this material, being susceptible of undergoing functionalization, which makes GMA a potential tool in the development of novel sorbents for SPE.

AuNPs have unique properties such as special stability, multiple surface functionalities, and great biocompatibility [16]. In the last years, their mechanisms of interaction with proteins have been deeply discussed [17–19]. Thus, several mechanisms such as hydrophobic and hydrogen bonding attractions; electrostatic adsorption; covalent attachment to the AuNP ligand; direct linkage of aa on the AuNP surface or rearrangement in the protein structure [17] can be involved. For instance, Brewer *et al*. [18] have suggested two possible hypotheses for the interaction between proteins and citrate-coated AuNPs (as those used in this study): an electrostatic binding and a displacement reaction. The first hypothesis is related to the attraction between the positive surface residues of the protein and the negative charge from the citrate-coated Au surfaces, whereas the second phenomenon involves a displacement of citrate by other stronger binding ligands such as amines or thiol functionalities; which are present in protein structures. This last hypothesis also considers structural changes (displacement by the protein in its native structure or denaturation of the protein on the surface) that can occur as a result of adsorption on the surface while the protein displaces the citrate stabilizer. In this way, these structural changes, which depend on protein conformational flexibility [19], expose the hydrophobic residues and present

specific functional groups able to interact by dispersive and van der Waals forces with the Au surface.

However, the combination of AuNPs with organic polymers to extract and enrich proteins from complex matrices has been slightly explored. In this sense, the use of GMA as reactive monomer has allowed the feasible functionalization of monolithic columns with different sulfur-ligands (e.g., cysteamine and cystamine) to provide platforms on which AuNPs can be attached [20–22]. However, the application of this novel composite material as sorbent in sample preparation has been scarcely reported [23]. Recently, our research group has successfully developed a polymeric material functionalized with AuNPs as SPE sorbent for isolation of model proteins (bovine serum albumin and cytochrome C) [24].

The aim of this study was the application of a SPE sorbent based on the modification of a polymeric support with AuNPs for the isolation of human milk whey proteins. Several conditions (e.g., pH, ionic strength, additives) for an effective extraction and elution of whey proteins (α-La, HSA, Lf and Lyz) were studied. Loading capacity and regenerative ability of the SPE monolithic material was also evaluated. The ability of the developed sorbent to isolate human milk whey proteins was tested following two approaches: with and without prior extraction of target proteins. This work represents the first application of SPE sorbents modified with AuNPs for the direct extraction of human milk whey proteins with a simple sample dilution.

8. 2. Experimental

8. 2. 1. Chemicals and reagents

GMA, EDMA, ACN and MeOH were purchased from Scharlab (Barcelona, Spain). AIBN was supplied by Fluka (Buchs, Switzerland). AuNP

suspension (particle size, 20 nm, $6.54 \cdot 10^{11}$ particles/mL, stabilized with sodium citrate) and Coomassie Blue were provided from Alfa Aesar (Landcashire, United Kingdom). Sodium acetate, monosodium, disodium and trisodium phosphate and orthophosphoric acid were supplied from Merck (Darmstadt, Germany). Ammonium persulfate, acrylamide, bisacrylamide, HSA, α-La, Lf, Lyz, gold (III) chloride trihydrate, HCl, 2-mercaptoethanol, HNO_3, potassium bromide, SDS, tetramethylethylenediamine, tris(hydroxymethyl)-aminomethane (Tris), acetic acid, and trisodium citrate were obtained from Sigma-Aldrich (St. Louis, MO, USA). A molecular-weight-size protein standard (6.5 to 200 kDa) was also provided by Sigma-Aldrich. Deionized water (Barnstead deionizer, Sybron, Boston, Mass., U.S.A.) was used in all procedures.

Stock solutions of each protein (1 mg/mL) were prepared by dissolving appropriate amounts of each protein in deionized water, and working standard solutions were obtained by dilution of the stock solutions. Phosphate buffers of 25 mM at several pH values were prepared by mixing appropriate amounts of Na_3PO_4, Na_2HPO_4, NaH_2PO_4 and/or H_3PO_4 according to the required pH.

8. 2. 2. Instrumentation

SEM images were obtained with a Hitachi S-4800 (Ibaraki, Japan) integrated with backscattered electron detector (Bruker, Germany). For these measurements, the polymeric materials were coated with a very thin-layer of conductive carbon.

Elemental analysis of synthesized material was performed using an EA 1110 CHNS elemental analyzer (CE Instruments, Milan, Italy). The determination of Au in synthetized materials and Bradford protein assay were carried out by measuring in UV-vis with an 8453 diode-array UV-vis spectrophotometer (Agilent Technologies, Waldbronn, Germany).

SDS-PAGE experiments were performed using a vertical minigel Hoefer SE260 Mighty Small system (Hoefer, MA, USA).

Centrifugation steps were conducted in a Sigma 2-15 laboratory centrifuge with rotors No. 12141 and No. 12148 (Sigma, Osterode am Harz, Germany).

8. 2. 3. Preparation and functionalization of GMA-based polymer

The GMA-*co*-EDMA polymeric material was based on a previous work [13]. Briefly, a polymerization mixture was prepared in a 10 mL glass vial by weighing appropriate amounts of GMA (20 wt%), EDMA (5 wt%), cyclohexanol (70 wt%) and 1-dodecanol (5 wt%). AIBN (1 wt% with respect to monomers) was added as initiator. This mixture was sonicated for 5 min and then purged with nitrogen to remove oxygen for 10 more min. The polymerization was carried out in an oven at 60 ºC for 24 h. Next, the polymeric material was washed with methanol to remove the porogenic solvents and possible unreacted monomers. Then, the monolithic bulk material was ground with a mortar and sieved with a steel sieve with sizes between 100 - 200 µm. The synthesized powder porous material was treated with aqueous 4.5 M ammonia in a round bottomed-flask at 60 ºC (water bath) for 2 h under continuous stirring. Upon completion of the reaction, the material was washed with ultra-pure water to remove the excess of ammonia until the eluent was neutral. The poly(GMA-*co*-EDMA) powdered material functionalized with amino group was obtained for further use. Elemental analysis of this bulk material indicated the presence of 1.84 wt% nitrogen (1.31 mmol /g monolith).

8. 2. 4. Functionalization of amino modified GMA-co-EDMA powder material with AuNPs

The amino modified powder material (400 mg) was placed in a Falcon tube and then 20 mL AuNPs solution were added. The mixture was allowed to react under stirring for 10 h. The attachment of the AuNPs to the amino GMA-*co*-EDMA powder was evidenced in the pinkish tone. Then, the material was washed with sodium citrate solution at pH 6.6 in order to remove the non-attached AuNPs. The route of synthesis of the AuNP-modified material is shown in **Figure S8.1**. The material was characterized by SEM and its Au content was evaluated as follows. Firstly, the dried methacrylate material with AuNPs was calcined at 550 ºC for 1 h. Then, the ashes (which contained the gold material), were treated with freshly prepared *aqua regia* for 90 min at 60 ºC under stirring. The resulting solution was subjected to the colorimetric determination of Au based on the formation of the yellow-orange bromoaurate $AuBr_4^-$ complex [25]. A stock solution of 200 µg/mL of Au(III) was prepared from its chloride salt and a calibration curve (1 - 30 µg/mL) was constructed. A content of 1.3 wt% Au was found in this sorbent.

8. 2. 5. SPE protocol

For the preparation of the SPE cartridges, fifty milligrams of AuNP-modified polymer was packed between two frits (1/16', 20 µm, Análisis Vínicos, Tomelloso, Spain) into 1 mL empty propylene cartridge (Análisis Vínicos) (see **Figure S8.2A**). Activation and equilibration of the sorbent was done with ACN (200 µL) and water (500 µL), respectively. Then, 200 µL of protein standard were loaded on the SPE material at a flow rate of 0.1 mL/min. After the loading step, the material was washed with 25 mM phosphate buffer (200 µL). Retained proteins were eluted with 25 mM phosphate buffer at pH 12.0 containing 0.25 M NaCl (200 µL). Along the SPE process, the

proteins left in the effluent (loading solution), washing and elution fractions were quantified by Bradford assay [26]. Thus, a calibration curve up to 200 µg/mL of HSA was prepared in the proper solvents. Next, the sorbent surface was regenerated with water at 80 ºC during 2 h. The same SPE protocol was applied to a blank sorbent constituted by the GMA-*co*-EDMA polymer.

8. 2. 6. Samples

Mature human milk samples were kindly donated by healthy well-nourished mothers. All mothers, who were Caucasian, middle-class, average age 31, and lived within the urban area of Valencia, consumed an unrestricted omnivorous diet. The samples were collected between the baby's feed by manual expression using a Medela Harmony Breastpump (Zug, Switzerland). After collection, milk samples were kept at -20 ºC until their use.

8. 2. 7. Extraction of human milk whey proteins by SPE

The extraction of whey proteins was based on the method described by Recio and Olieman [27]. An aliquot of 10 mL of a milk sample was placed in a centrifuge tube and 1.25 mL of acetic acid/sodium acetate buffer of pH 4.6 were added. After 20 min in an ice bath [28], the sample was centrifuged (10000 rpm) for 15 min. The supernatant fraction was kept at -20 ºC until analysis. The protein content of the whey fraction was also estimated by Bradford assay. Then, this solution was 1:5 diluted with phosphate buffer (pH 5) and an aliquot (500 µL) was passed through the SPE sorbent. The elution was performed as described above and an aliquot of 20 µL was loaded into the gel.

On the other hand, human milk samples were directly loaded into the cartridge after dilution (1:20) with deionized water. The target analytes (whey

proteins) were eluted from the SPE column using a solution containing 10 mM NaOH, 250 mM NaCl and 60 mM $CaCl_2$, and an aliquot of 20 µL was loaded into the gel.

8. 2. 8. SDS-PAGE analysis

SDS-PAGE of proteins was carried out with 40% acrylamide/bis-acrylamide solution, and standard discontinuous buffer systems as described by Laemmli [29]. The protein bands were visualized with staining using Coomassie Blue. Molecular sizes of the model proteins were analyzed by comparison with an SDS-PAGE standard marker.

8. 3. Results and discussion

8. 3. 1. Interaction of proteins with AuNPs

As previously discussed in Introduction Section, the interaction of proteins onto AuNP surfaces is a complex phenomenon ruled by different forces. In the particular case of human milk, there are major differences in physical and chemical properties between CNs and whey proteins, which can be exploited to provide several potential molecular interactions with AuNPs. For instance, CNs present strong hydrophobic regions, and a low content of cysteine residues, whereas the whey proteins provide both hydrophobic and hydrophilic regions and a large content of cysteine residues. Moreover, these latter proteins are soluble in aqueous media and relatively resistant to the precipitation in the presence of di- and polyvalent ions [30]. On the other hand, there are few studies related to the interaction between human proteins and AuNPs, and they all occur in aqueous solution [17,31]. However, any work focused on the immobilization of AuNPs onto polymeric supports and its interaction with milk proteins as extraction platforms has been described. Our

preliminary study [24] has showed that, the surfaces of AuNPs bound to GMA-based polymers can effectively retain protein species.

In order to extend the application of this material to direct isolation of proteins in complex matrices (e.g., human milk), a SPE column containing sieved (100-200 µm) polymeric particles modified with AuNPs was prepared. These small-sized particles showed low flow resistance during the sample loading and elution process. SEM characterization of this material (see **Figure S8.2B**) showed the typical three-dimensional monolith network with through channels, being the polymer surface modified with AuNPs.

8. 3. 2. Study of SPE protocol using AuNP-modified polymeric material

The protein – AuNP surface interaction may be modulated by the pH or charge screening via controlling the ionic strength of the medium. For this reason, the effect of sample pH (3.0 – 11.0) on the loading SPE step was first studied (**Figure 8.1**). Solutions (200 µL) containing either 200 µg/mL of HSA (pI 4.7), α-La (pI 5.0), Lf (pI 8.7) or Lyz (pI 11.0) were selected as test solutes to perform the sorption studies. As shown in **Figure 8.1**, large retentions (>80%) for acidic proteins in the loading step were obtained along wide pH range (3.0 - 9.0), whereas for basic proteins, the highest adsorptions were found close to their respective pI values. Then, the washing step was done at the same pH values as those studied in the loading step. As shown in **Figure 8.1**, for α-La and HSA, significant losses were obtained at pH 9.0 (up to 41%), whereas for Lf and Lyz these losses were found at pH 3.0. These results are in agreement with the discussion given in the Introduction Section. Thus, on the one hand, favorable electrostatic interactions may occur regardless of the overall charge of the protein, where citrate interacts with positively charged surface groups or domains of the proteins [19], which supports the idea that the pI is not the only parameter to evaluate the protein's charge [32]. On the other hand, for Lf and Lyz, the displacement mechanism

or the rearrangements in the protein structure upon adsorption could be additional driving forces for their adsorption onto Au surfaces, since at pH close to the pI, the electrostatic interactions between the protein molecule and the sorbent are minimized. At sight of these results, a pH range between 5 and 7 was selected as compromise to achieve the highest extraction recoveries for all the proteins investigated.

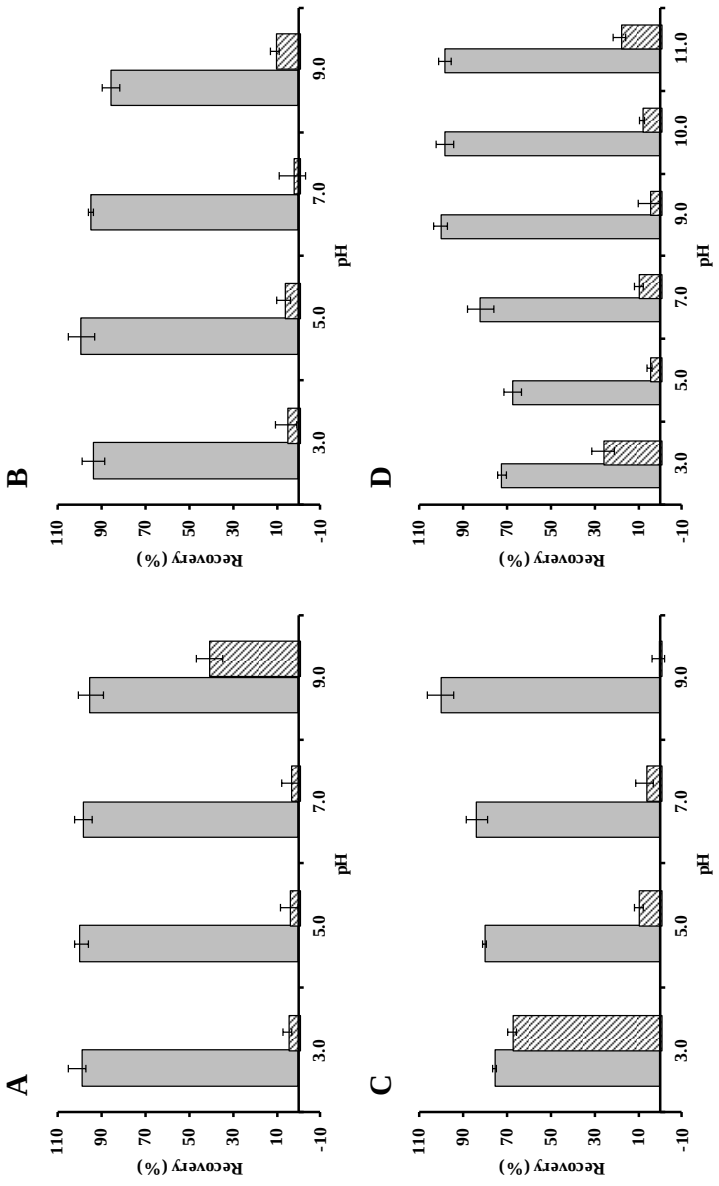

Figure 8.1. Influence of pH on the loading (grey) and washing (striped) steps for α-La (A); HSA (B); Lf (C) and Lyz (D).

Regarding the elution step, 25 mM phosphate buffer (pH 12) was initially employed for the desorption of proteins from the AuNP surface [24]. Acceptable recoveries were found for HSA, α-La and Lyz (> 70%); however, the recovery of Lf was close to 50%. This behavior can be explained by the electrostatic repulsion between protein molecules with citrate-capped AuNPs and/or between adjacent adsorbed protein molecules onto Au surface.

It is well-known that, the ionic strength has a large effect on the adsorption capacity [33]. Thus, salt molecules raise surface tension of the solution; diminish the electrostatic interaction between dispersed molecules, and alter the surface activity of protein molecules [34]. This increase of the surface tension of the solution encourages the exposure of the inner hydrophobic regions of the protein solution.

Therefore, the influence of ionic strength in the elution solution was studied by increasing NaCl concentration up to 1.0 M (**Figure 8.2A**). As it can be seen, an increase in NaCl content gave an improvement in the extraction efficiencies both for Lf and Lyz reaching values above 80%; however, a sharp decrease in recoveries was evidenced for α-La at concentrations higher than 0.25 M. This behavior could be explained as follows: at high ionic strengths, the desorption of Lf and Lyz might be favoured due to a screening of the surface charges, which led to the reduction of electrostatic interactions between these proteins and Au surface [33]. However, in the case of acidic proteins, an increase in the salt content hindered the electrostatic repulsions, which had a detrimental effect on their desorption. Considering these results, a salt concentration of 0.25 M was selected for further studies.

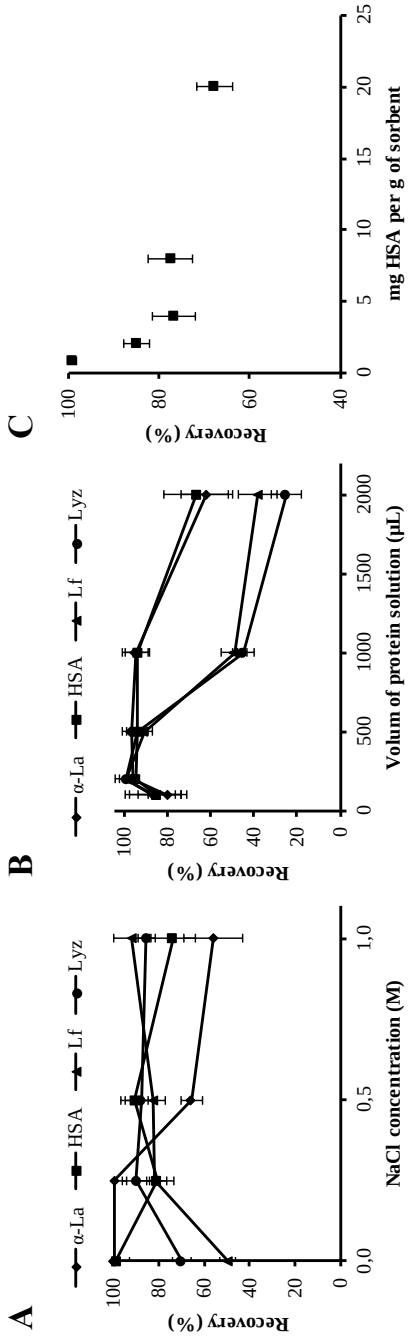

Figure 8.2. Effect of ionic strength (A) and sample volume (B) on the recoveries of α-La, HSA, Lf and Lyz; adsorption capacity (C) of GMA-based polymer modified with AuNPs at increasing amounts of HSA.

Additionally, a generic GMA-based polymer was used as sorbent under the optimal conditions found for the AuNPs-modified material. Lower retentions were obtained for all proteins (*ca*. 25% for HSA and Lf, and *ca*. 50% for α-La and Lyz) in the control polymer, which confirmed the selectivity of the synthesized material.

Another important parameter in SPE that affects the extraction efficiency is the breakthrough volume. To establish this parameter, increasing sample volumes (from 100 to 2000 µL; constant amount of protein, 1000 µg) of standard protein solutions were percolated through the SPE cartridge. High recoveries (90-98%) up to 1000 µL were achieved for HSA and α-La; however, a decrease in the recovery values of Lf and Lyz were observed at volumes > 500 µL (**Figure 8.2B**). For this reason, a volume of 500 µL was chosen for further SPE studies.

The loading capacity of AuNPs-modified material (50 mg) was also established by passing increasing amounts of HSA, giving a maximum value of (13.6 ± 0.8) mg per g of sorbent (**Figure 8.2C**). This capacity value was slightly higher than those found for porous particle sorbents, which were *ca*. 5 mg of analyte (under the proper condition) per g of material [35].

According to Xu *et al*. [20], rinsing with water at elevated temperatures (80 ºC) allowed a satisfactory regeneration of AuNP-modified columns after treatment with different ligands. In this work, the regeneration of the AuNP-modified material was carried out by washing it with water at 80 ºC for 2 h, obtaining recoveries *ca*. 90% of the original capacity. Following this protocol, the reusability of the cartridges was hence guaranteed for more than 20 times [24]. Besides, the developed polymeric sorbent showed a large stability over a wide pH range compared to the conventional silica-based supports. Another aspect to be considered is that these typical supports show large tendency to clogging and offer a poor reusability. In our case, the

resulting polymeric sorbent provided some residual permeable porous monolithic structure, which reduced the probability of sorbent clogging.

8. 3. 3. Application to human milk whey proteins

To demonstrate the feasibility of the proposed extraction method for the retention of proteins with different pI, a standard mixture of four whey proteins (HSA, α-La, Lf and Lyz) was firstly tested. For this purpose, a sample solution containing 50 µg/mL of each protein was prepared at pH 5, and the extraction process detailed above was conducted. The different fractions were subjected to SDS-PAGE under reducing conditions (presence of 2-mercaptoethanol) as illustrated in **Figure 8.3**. In addition, a standard mixture of these proteins without pretreatment was loaded in the gel (lane 2). The whey proteins were identified according to their molecular weight as follows: Lf (Mr ~ 78 kDa), HSA (Mr ~ 69 kDa), Lyz (Mr ~ 16.5 kDa) and α-La (Mr ~ 14 kDa). These latter two bands could not be completely resolved. In addition, a band at Mr ~ 55 kDa was found, which was ascribed to HSA, due to an uncompleted reaction with 2-mercaptoethanol [36]. Lanes 3 and 4 (loading and washing fractions, respectively) did not clearly show the presence of any band of target proteins. When the elution fraction was loaded in the gel, the standard proteins were easily distinguished (lane 5).

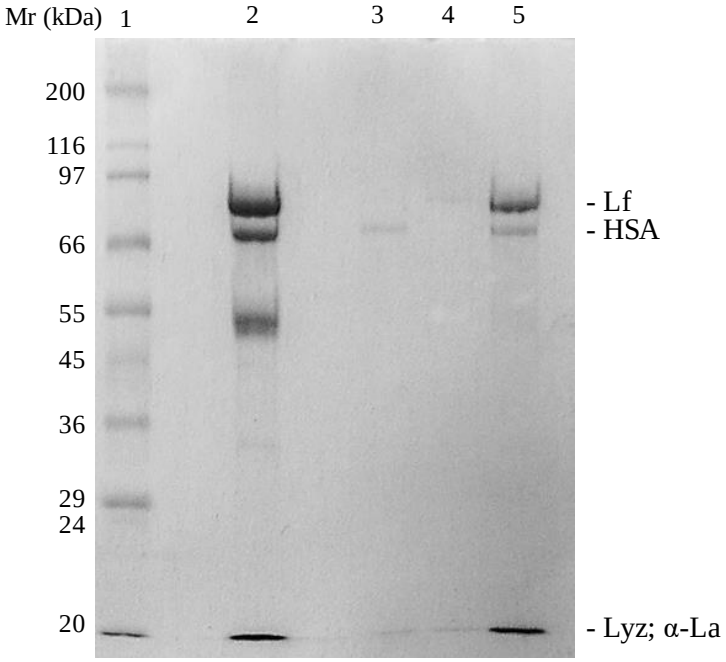

Figure 8.3. SDS-PAGE analysis of a standard mixture of α-La, HSA, Lf and Lyz. Identification: lane 1, molecular weight marker; lane 2, protein mixture at 200 μg/mL each, without pre-treatment; lane 3, loading step solution in phosphate buffer (pH 5) passing through the GMA-based polymer modified with AuNPs; lane 4, washing step solution in phosphate buffer (pH 5); lane 5: elution step solution with phosphate buffer (pH 12) and 0.25 M NaCl.

Then, the sorbent was applied to the isolation of whey proteins from a human milk sample. For this purpose, the whey protein fraction was obtained following the extraction process described in Section 8.2.7, and a dilution of the extract was percolated through the cartridge. Next, SDS-PAGE analysis of the collected fractions was carried out. **Figure 8.4** shows the SDS-PAGE analysis of human milk whey extract without (lane 2) and with SPE treatment (lane 3) under reducing conditions. Apart from the four whey proteins studied, the presence of two bands located at ~ 64 and ~ 28 kDa, which were attributed to sIgA-heavy and light chain, respectively, were observed. This identification of the sIgA forms was consistent with the findings found by Almogren *et al.*

[37]. Although the band at ca. 28 kDa might be also ascribed to the typical molecular weight range of casein subunits, the absence of this band in non-reducing SDS-PAGE discarded this assumption [38] (see **Figure S8.3**). Besides, an additional band for sIgA, at approximately 83 kDa, might be also present, but it was masked by the prominent band of Lf. As can be shown in **Figure 8.4**, all proteins were satisfactorily retained in the loading and washing fractions (lane 3 and 4, respectively). With respect to the elution fraction, the four whey proteins as well as other relevant proteins (e.g., sIgA) present in the whey fraction of milk were distinguished, which proved the effectiveness of the developed sorbent.

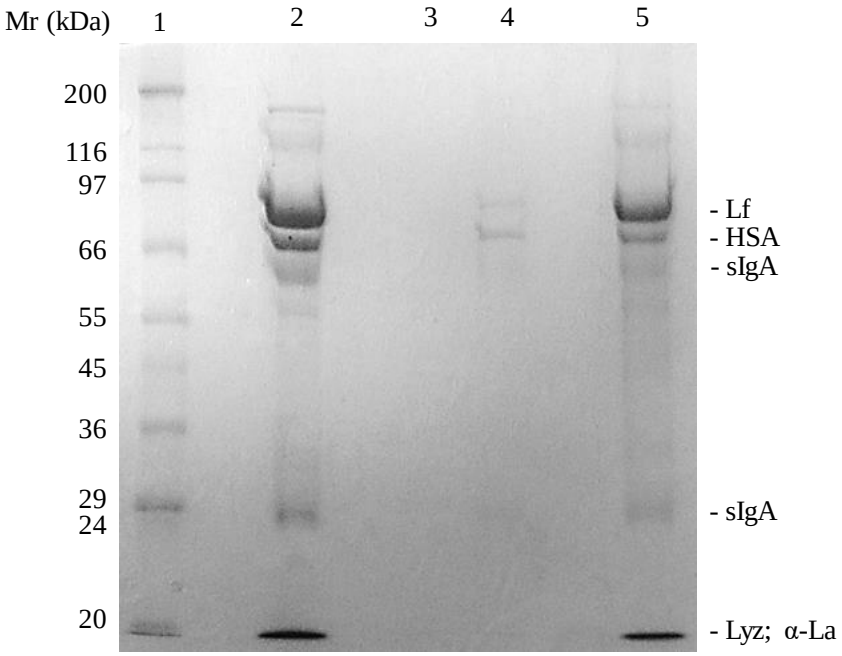

Figure 8.4. SDS-PAGE analysis of a whey extract 1:5 diluted with phosphate buffer (pH 5). Identification: lane 1, molecular weight marker; lane 2, whey extract without pre-treatment; lane 3, loading step solution; lane 4, washing step solution in phosphate buffer (pH 5); lane 5, elution step solution with phosphate buffer (pH 12) and 0.25 M NaCl.

In order to achieve an alternative protocol to the classical isolation of whey proteins by isoelectric precipitation of CNs, human milk samples were simply diluted and percolated through the SPE-cartridge. For this purpose, the SPE protocol described above was slightly modified. The loading step was accomplished at pH 7 to avoid undesirable CNs precipitation; achieving a strong retention of whole proteins; however, when the elution step was performed with phosphate buffer at pH 12 containing 0.25 M NaCl, an uncomplete elution of both types of proteins in the collected fraction was evidenced (**Figure S8.4**).

Kunz *et al.* [2] have reported that the use of calcium salts improves separation of whey and CNs in milk samples. Thus, the addition of calcium may facilitate the release of whey proteins from CNs due to hydrophobic interaction, repulsive forces, or entrapment. In this context, there is an interesting point that merits investigation: the addition of Ca^{2+} to the elution solvent. To avoid the risk of calcium phosphate precipitation in this solution, phosphate buffer was also replaced by sodium hydroxide to adjust the pH. Then, the Ca^{2+} concentration was varied between 5 to 80 mM. A 60 mM Ca^{2+} was enough for a distinct separation of whey proteins and CNs, giving a satisfactory elution of whey proteins in the collected fraction, whereas the CNs did not appear in the gel (**Figure 8.5**, lane 4).

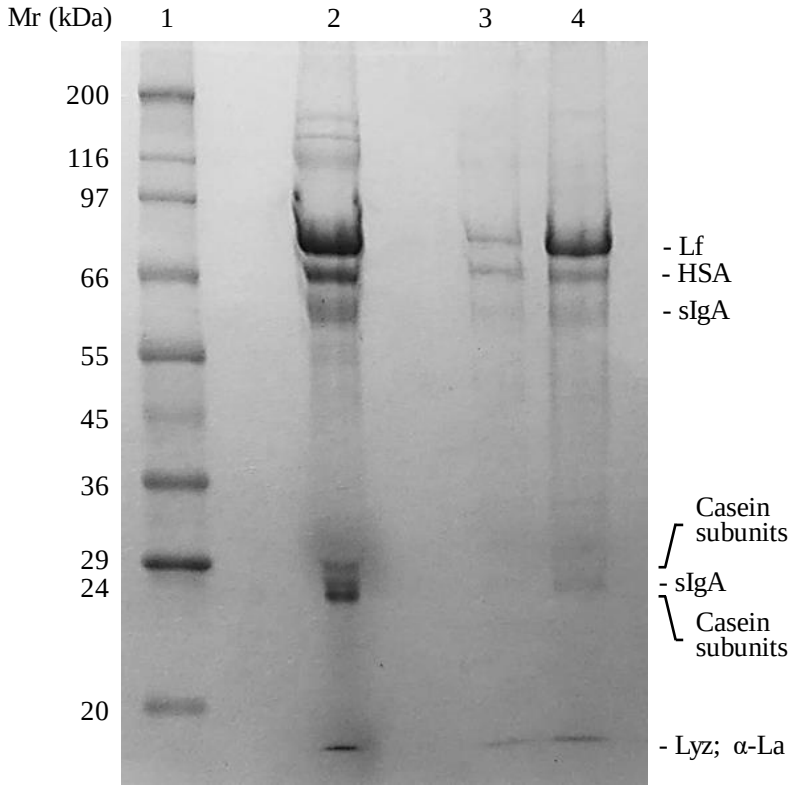

Figure 8.5. SDS-PAGE analysis of a milk sample 1:20 diluted with water. Identification: lane 1, molecular weight marker; lane 2, milk sample without pre-treatment; lane 3, loading step solution; lane 4, elution step solution with NaOH 0.01 M, 0.25 M NaCl and 60 mM $CaCl_2$.

8. 4. Conclusions

This work describes a simple, cost-effective, selective and reliable SPE protocol for the isolation of human milk whey proteins using a methacrylate polymeric sorbent modified with AuNPs. Several variables of the SPE procedure have been optimized and protein recoveries have been evaluated by using Bradford assay. The results showed that large retentions (>90%) can be achieved for all whey proteins by a proper adjust of the pH of the loading and washing solution. Then, the whey proteins were desorbed

from the AuNPs surface after a careful selection of pH and ionic strength of the eluent. The developed polymeric sorbent showed a large stability over a wide pH range, high permeability and reusability (more than 20 uses without significant losses in recoveries) compared to the conventional silica-based supports. The effectiveness of the proposed methodology was firstly demonstrated by the isolation of whey proteins from human milk samples (after isoelectric precipitation of CNs) and from a simple dilution of milk samples. This work represents a novel and feasible approach of SPE sorbents modified with AuNPs for the direct extraction of human milk whey proteins as promising alternative to the conventional precipitation protocol.

Acknowledgements

This work was supported by project CTQ2014-52765-R (MINECO of Spain and FEDER) and PROMETEO/2016/145 (Generalitat Valenciana). I. T-D thanks the MECD for an FPU grant for PhD studies. The authors also thank Dr. Salomé Laredo-Ortíz and Dr. Enrique Navarro-Raga from the Atomic spectroscopy and Microscopy sections of the SCSIE (University of Valencia), respectively, for their help in elemental analysis and SEM measurements.

8. 5. References

[1] R.G. Jensen, Lipids in human milk, Lipids 34 (1999) 1243–1271. doi:10.1007/s11745-999-0477-2.

[2] C. Kunz, B. Lönnerdal, Human milk proteins: separation of whey proteins and their analysis by polyacrylamide gel electrophoresis, fast protein liquid chromatography (FPLC) gel filtration, and anion-exchange chromatography, Am. J. Clin. Nutr. 49 (1989) 464–470. doi:10.1016/B978-0-12-374039-7.00014-3.

[3] B. Lönnerdal, Nutritional and physiologic significance of human milk proteins, Am. J. Clin. Nutr. 77 (2003) 1537S–1543S. doi:10.131/nr.2003.sept.295.

[4] T. Nagasawa, I. Kiyosawa, M. Takase, Lactoferrin and serum albumin of human casein in colostrum and milk, J. Dairy Sci. 57 (1974) 1159–1163. doi:10.3168/jds.S0022-0302(74)85030-7.

[5] W. Chen, J. Shen, X. Yin, Y. Yu, Optimization of microfabricated nanoliter-scales solid-phase extraction device for detection of gel-separated proteins in low abundance by matrix-assisted laser desorption/ionization mass spectrometry, Rapid Commun. Mass Spectrom. 21 (2007) 35–43. doi:10.1002/rcm.

[6] M.R. Bladergroen, Y.E.M. van der Burgt, Solid-phase extraction strategies to surmount body fluid sample complexity in high-throughput mass spectrometry-based proteomics, J. Anal. Methods Chem. 2015 (2015) 1–8. doi:10.1155/2015/250131.

[7] L.R. Ruhaak, C. Huhn, C.A.M. Koeleman, A.M. Deelder, M. Wuhrer, Robust and high-throughput sample preparation for (semi-)quantitative analysis of N-glyscosylation profiles for plasma samples, Methods Mol. Biol. 893 (2012) 371–385. doi:10.1007/978-1-61779-

885-6.

[8] S. Mysling, G. Palmisano, P. Højrup, M. Thaysen-Andersen, Utilizing ion-pairing hydrophilic interaction chromatography solid phase extraction for efficient glycopeptide enrichment in glycoproteomics, Anal. Chem. 82 (2010) 5598–5609. doi:10.1021/ac100530w.

[9] Z. Du, Y. Yu, X.-W. Chen, J.-H. Wang, The isolation of basic proteins by solid-phase extraction with multiwalled carbon nanotubes, Chem. - A Eur. J. 13 (2007) 9679–9685. doi:10.1002/chem.200700784.

[10] D.R. Bunch, S. Wang, Applications of monolithic solid-phase extraction in chromatography-based clinical chemistry assays, Anal. Bioanal. Chem. 405 (2013) 3021–3033. doi:10.1007/s00216-013-6761-0.

[11] A. Namera, T. Saito, Advances in monolithic materials for sample preparation in drug and pharmaceutical analysis, TrAC - Trends Anal. Chem. 45 (2013) 182–196. doi:10.1016/j.trac.2012.10.017.

[12] D. Sýkora, F. Svec, J.M.J. Fréchet, Separation of oligonucleotides on novel monolithic columns with ion-exchange functional surfaces, J. Chromatogr. A 852 (1999) 297–304. doi:10.1016/S0021-9673(99)00004-7.

[13] E.J. Carrasco-Correa, G. Ramis-Ramos, J.M. Herrero-Martínez, Methacrylate monolithic columns functionalized with epinephrine for capillary electrochromatography applications, J. Chromatogr. A 1298 (2013) 61–67. doi:10.1016/j.chroma.2013.05.013.

[14] B. Preinerstorfer, W. Lindner, M. Lämmerhofer, Polymethacrylate-type monoliths functionalized with chiral amino phosphonic acid-derived strong cation exchange moieties for enantioselective nonaqueous capillary electrochromatography and investigation of the chemical composition of the monolithic polyme, Electrophoresis 26

(2005) 2005–2018. doi:10.1002/elps.200410380.

[15] J. Dong, J. Ou, X. Dong, R. Wu, M. Ye, H. Zou, Preparation and evaluation of rigid porous polyacrylamide-based strong cation-exchange monolithic columns for capillary electrochromatography, J. Sep. Sci. 30 (2007) 2986–2992. doi:10.1002/jssc.200700402.

[16] Y.-C. Yeh, B. Creran, V.M. Rotello, Gold nanoparticles: preparation, properties, and applications in bionanotechnology, Nanoscale 4 (2012) 1871–1880. doi:10.1039/c1nr11188d.

[17] S.H. De Paoli Lacerda, J.J. Park, C. Meuse, D. Pristinski, M.L. Becker, A. Karim, J.F. Douglas, Interaction of gold nanoparticles with common human blood proteins, Am. Chem. Soc. Nano. 4 (2010) 365–379. doi:10.1021/nn9011187.

[18] S.H. Brewer, W.R. Glomm, M.C. Johnson, M.K. Knag, S. Franzen, Probing BSA binding to citrate-coated gold nanoparticles and surfaces, Langmuir 21 (2005) 9303–9307. doi:10.1021/la050588t.

[19] W.R. Glomm, Ø. Halskau, A.-M.D. Hanneseth, S. Volden, Adsorption behavior of acidic and basic proteins onto citrate-coated Au surfaces correlated to their native fold, stability, and pI, J. Phys. Chem. B. 111 (2007) 14329–14345. doi:10.1021/jp074839d.

[20] Y. Xu, Q. Cao, F. Švec, J.M.J. Fréchet, Porous polymer monolithic column with surface-bound gold nanoparticles for the capture and separation of cysteine-containing peptides, Anal. Chem. 82 (2010) 3352–3358. doi:10.1021/ac1002646.

[21] Y. Lv, F.M. Alejandro, J.M.J. Fréchet, F. Švec, Preparation of porous polymer monoliths featuring enhanced surface coverage with gold nanoparticles, J. Chromatogr. A 1261 (2012) 121–128. doi:10.1016/j.chroma.2012.04.007.

[22] Q. Cao, Y. Xu, F. Liu, F. Švec, J.M.J. Fréchet, Polymer monoliths with

exchangeable chemistries: use of gold nanoparticles as intermediate ligands for capillary columns with varying surface functionalities, Anal. Chem. 82 (2010) 7416–7421. doi:10.1021/ac1015613.

[23] X. Wang, Y. Du, H. Zhang, Y. Xu, Y. Pan, T. Wu, H. Hu, Fast enrichment and ultrasensitive in-situ detection of pesticide residues on oranges with surface-enhanced Raman spectroscopy based on Au nanoparticles decorated glycidyl methacrylate-ethylene dimethacrylate material, Food Control. 46 (2014) 108–114. doi:10.1016/j.foodcont.2014.04.035.

[24] M. Vergara-Barberán, M.J. Lerma-García, E.F. Simó-Alfonso, J.M. Herrero-Martínez, Solid-phase extraction based on ground methacrylate monolith modified with gold nanoparticles for isolation of proteins, Anal. Chim. Acta 917 (2016) 37–43. doi:10.1016/j.aca.2016.02.043.

[25] W.A.E. McBryde, J.H. Yoe, Colorimetric determination of gold as bromoaurate, Anal. Chem. 20 (1948) 1094–1099. doi:10.1021/ac60023a034.

[26] M.M. Bradford, A rapid and sensitive method for the quantitation of microgram quantities of protein utilizing the principle of protein-dye binding, Anal. Biochem. 72 (1976) 248–254. doi:10.1016/0003-2697(76)90527-3.

[27] I. Recio, C. Olieman, Determination of denatured serum proteins in the casein fraction of heat-treated milk by capillary zone electrophoresis, Electrophoresis 17 (1996) 1228–1233. doi:10.1002/elps.1150170710.

[28] P.F. Fox, T. Uniacke-Lowe, P.L.H. McSweeney, J.A. O'Mahony, 4.3.1 Acid (isoelectric) precipitation, en: Dairy Chem. Biochem., Springer, Switzerland, 2015: pág. 151. doi:10.1007/978-3-319-14892-2.

[29] U.K. Laemmli, Cleavage of structural proteins during the assembly of the head of bacteriophage T4, Nature 227 (1970) 680–685. doi:10.1038/227680a0.

[30] C.R. Chandan, Milk composition, physical and processing characteristics, en: Y.H. Hui (Ed.), Handb. Food Prod. Manuf., Wiley-Interscience, New Jersey, 2007: págs. 356–359.

[31] Y. Liu, R. Guo, The interaction between casein micelles and gold nanoparticles, J. Colloid Interface Sci. 332 (2009) 265–269. doi:10.1016/j.jcis.2008.12.043.

[32] Y.-M. Chen, C.-J. Yu, T.-L. Cheng, W.-L. Tseng, Colorimetric detection of lysozyme based on electrostatic interaction with human serum albumin-modified gold nanoparticles, Langmuir 24 (2008) 3654–3660. doi:10.1021/la7034642.

[33] J. Sun, Y. Su, S. Rao, Y. Yang, Separation of lysozyme using superparamagnetic carboxymethyl chitosan nanoparticles, J. Chromatogr. B 879 (2011) 2194–2200. doi:10.1016/j.jchromb. 2011.05.052.

[34] W.-Y. Chen, Z.-C. Liu, P.-H. Lin, C.-I. Fang, S. Yamamoto, The hydrophobic interactions of the ion-exchanger resin ligands with proteins at high salt concentrations by adsorption isotherms and isothermal titration calorimetry, Sep. Purif. Technol. 54 (2007) 212–219. doi:10.1016/j.seppur.2006.09.008.

[35] Sigma-Aldrich, SPE Cartridge (Tube) Configuration Guide, (2016). Disponible en: http://www.sigmaaldrich.com/analytical-chromatography/sample-preparation/spe/tube-configuration-guide.printerview.html (Fecha de acceso: 26/09/2016).

[36] G. Colombo, M. Clerici, D. Giustarini, N. Portinaro, S. Badalamenti, R. Rossi, A. Milzani, I. Dalle-Donne, A central role for intermolecular

dityrosine cross-linking of fibrinogen in high molecular weight advanced oxidation protein product (AOPP) formation, Biochim. Biophys. Acta 1850 (2015) 1–12. doi:10.1016/j.bbagen.2014.09.024.

[37] A. Almogren, B.W. Senior, M.A. Kerr, A comparison of the binding of secretory component to immunoglobulin A (IgA) in human colostral S-IgA1 and S-IgA2, Immunology 120 (2007) 273–280. doi:10.1111/j.1365-2567.2006.02498.x.

[38] A. Kuizenga, N.J. van Haeringen, A. Kijlstra, SDS-minigel electrophoresis of human tears, Invest. Ophthalmol. Vis. Sci. 32 (1991) 381–386.

8. 6. Supplementary data

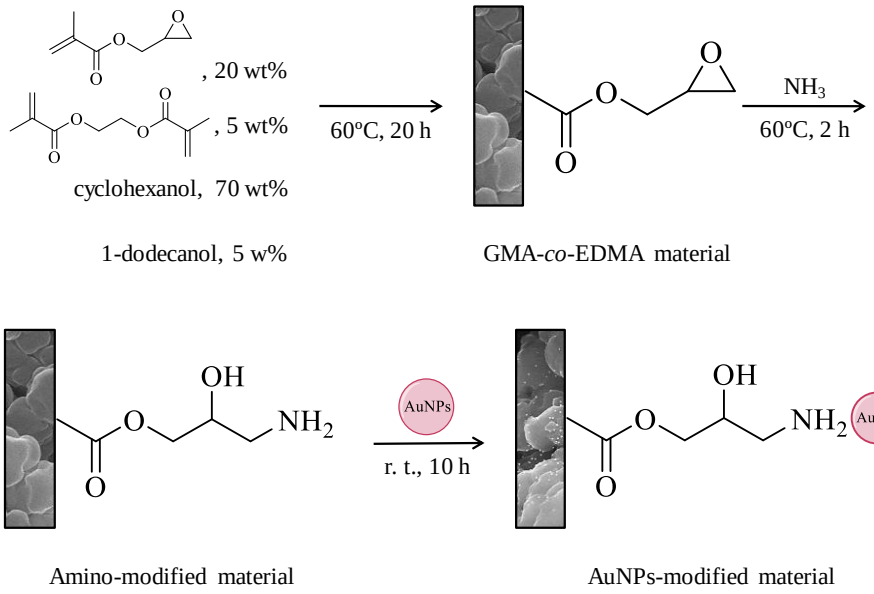

Figure S8.1. Scheme of preparation of AuNP-modified polymeric material from poly(GMA-*co*-EDMA).

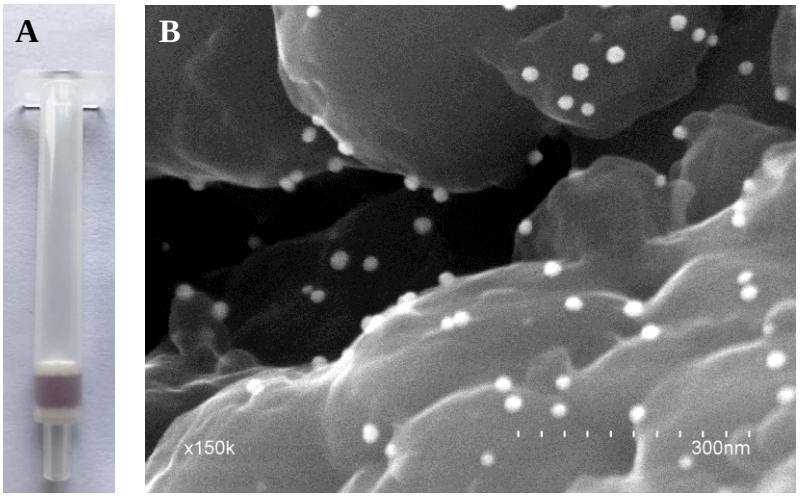

Figure S8.2. SPE cartridge with polymeric material modified with AuNPs (A) and SEM micrograph of the sorbent (B).

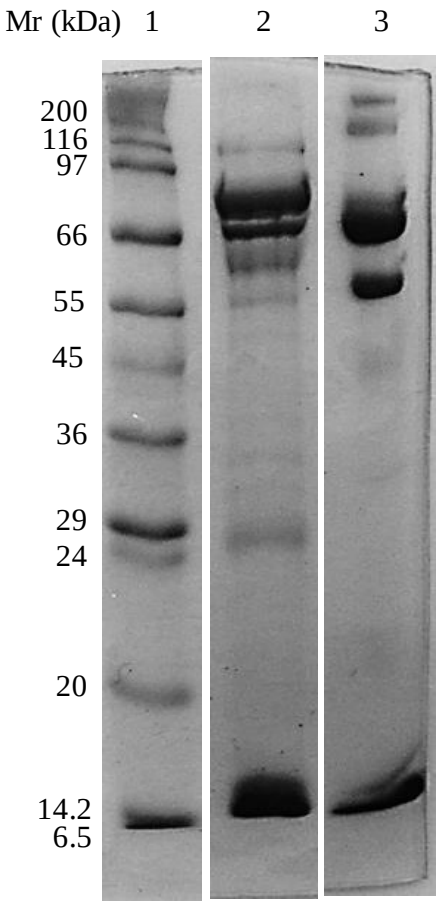

Figure S8.3. SDS-PAGE analysis of a whey extract diluted with phosphate buffer (pH 5). Identification: lane 1, molecular weight marker; lane 2, whey extract under reducing conditions; lane 3, whey extract under non-reducing conditions.

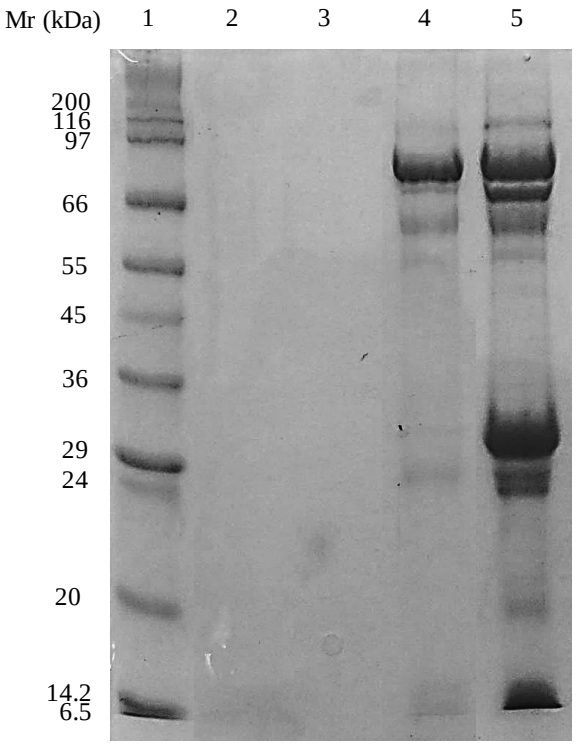

Figure S8.4. SDS-PAGE analysis of a milk sample 1:20 diluted with water. Identification: lane 1, molecular weight marker; lane 2, loading step solution; lane 3, washing step solution in phosphate buffer (pH 7); lane 5, elution step solution with phosphate buffer (pH 12) and 0.25 M NaCl; lane 6, milk sample without pre-treatment.

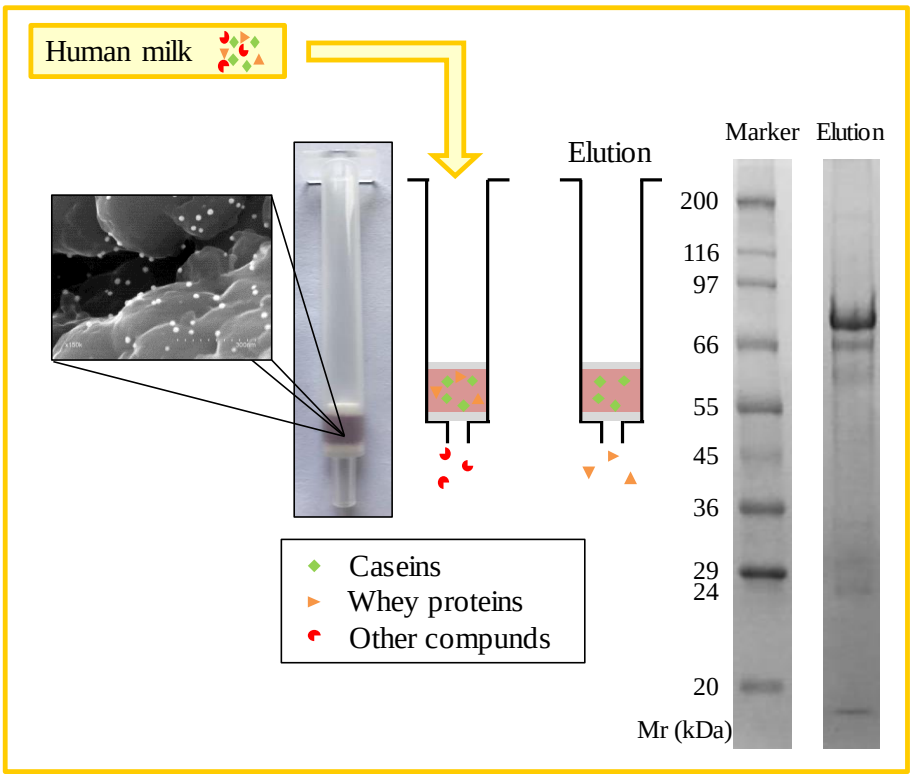
Human milk
Elution
Marker
Elution
200
116
97
66
55
45
36
29
24
20
Mr (kDa)
Caseins
Whey proteins
Other compunds

CAPÍTULO 9

Improving fractionation of human milk proteins through calcium phosphate coprecipitation and their rapid characterization by capillary electrophoresis

Journal of proteome research
Article
Cite This: J. Proteome Res. XXXX, XXX, XXX−XXX
pubs.acs.org/jpr

Improving Fractionation of Human Milk Proteins through Calcium Phosphate Coprecipitation and Their Rapid Characterization by Capillary Electrophoresis

Isabel Ten-Doménech,* Ernesto Francisco Simó-Alfonso, and José Manuel Herrero-Martínez*
Department of Analytical Chemistry, University of Valencia, C. Doctor Moliner 50, E-46100 Burjassot, Valencia, Spain

This work describes a simple sample pretreatment method for the fractionation of human milk proteins (into their two main groups: whey and CNs) prior to their analysis. The protein extraction protocol is based on the addition of calcium phosphate to non-adjusted pH human milk. The combination of calcium ions with phosphate results in an effective coprecipitation of CNs. To assess the suitability of this fractionation protocol, the protein extracts were analyzed by SDS-PAGE, LC-MS/MS, and CE analysis. The results evidence a significant decrease in contamination of casein fraction with whey proteins and vice versa compared with the conventional isoelectric precipitation of CNs. In addition, CE fraction collection coupled to LC-MS/MS (off-line coupling) has been successfully applied to the identification of minor proteins in this complex matrix. The methodology presented here constitutes a promising tool to enlarge the knowledge of human milk proteome. Data are available via ProteomeXchange with identifier PXD010315.

Keywords: Calcium phosphate fractionation; Human milk whey proteins; Human milk caseins; Capillary electrophoresis; Fraction collection.

9. 1. Introduction

Human milk has been settled as the best way of providing both full and preterm infants with the essential nutrients for a healthy growth and development [1]. Human milk constituents include water (88%), macronutrients (lipids, proteins and carbohydrates), micronutrients (fat- and water-soluble vitamins, minerals) and others (cells). The protein fraction of milk plays a key role in achieving many of the beneficial outcomes of breastfeeding. Milk proteins can be divided into three groups: CNs, whey proteins and proteins associated with the MFGM. Whey proteins are the most abundant proteins in human milk, whereas CNs represent a smaller fraction. On the other hand, MFGM proteins (also known as mucins) represent 1 - 4% of total milk protein content [2]. CNs, together with calcium phosphate, form aggregates of several thousand individual protein molecules known as CN micelles, whose structure and stability have been extensively studied (especially in bovine milk) [3,4].

Fractionation of milk proteins is usually accomplished on acidification to pH 4.6 (the isoelectric pH), where coagulation of CNs occurs, and they precipitate readily out of solution. However, some whey proteins may coprecipitate with CNs at this pH and the other way round [5]. In this sense, the addition of calcium to pH adjusted milk resulted in a marked decreased of whey proteins in the CN fraction [6,7]. On the other hand, alternative methods to overcome the cross-contamination such as the deconstruction of CN micelles using a chelating agent and later reconstruction with calcium phosphate particles [8] or precipitation of CNs by adding phosphate followed by a freezing-thawing step [9] have been considered.

However, these fractionation approaches have been usually applied to bovine milk and in a lesser extent to human milk. At this point, it should be noted that composition of human milk proteins differs substantially from bovine milk and, as a result, their fractionation may be affected. Thus, CNs

represent 40% of total proteins in human milk as opposite to ~75% in bovine milk. Additionally, most of the CN are in the β-CN fraction, which is phosphorylated (P) at six levels from 0 (0 - P) to 5 (5 – P), and in the κ-CN fraction. Unlike bovine milk, human milk contains only a very small amount of a protein corresponding to α_{s1}-CN [10].

Dealing with separation and identification of milk proteins, several techniques have been used to this end. On one hand, separation of milk proteins has been carried out by means of 2D-PAGE [11], CE [12,13] and LC [14]. With respect CE, where individual proteins are separated according to their charge to mass ratio, several well-known advantages such as speed, simplicity and low-operation costs are guaranteed [12]. In fact, CE methods for the analysis of milk proteins have been systematically reviewed [15]. On the other hand, the so-called "milk proteomics", understood as the systematic separation, identification and characterization of proteins from milk [16] is gaining more and more attention. However CE for human milk analysis has been only scarcely applied [13], and its combination with off-line MS for identification of minor proteins has not been reported to date.

The aim of this study was the implementation of an easy fractionation protocol of human milk proteins through a simple calcium phosphate precipitation and their subsequent characterization with SDS-PAGE, CE and MS. In addition, an attempt of identification of minor proteins without a depletion step via off-line coupling of CE to MS is also proposed. This work represents the first alternative of isoelectric precipitation of CNs in human milk samples prior to their analysis through more sophisticated techniques.

9. 2. Material and methods

9. 2. 1. Chemicals, reagents and samples

MeOH and sodium hydroxide were purchased from Scharlau (Barcelona, Spain); Coomassie Blue was provided from Alfa Aesar (Landcashire, United Kingdom). Sodium acetate was supplied from Merck (Darmstadt, Germany). α-La, CN from bovine milk, HSA, Lf, Lyz, ammonium persulfate, 2-mercaptoethanol, acetic acid, acrylamide, α-cyano-4-hydroxycinnamic acid (α-CHCA), ammonium bicarbonate (ABC), bisacrylamide, brilliant blue R, bromophenol blue, dithiothreitol (DTT), formic acid, glycerol, glycine, hydrochloric acid, iodoacetamide (IAM), SDS, tetramethylethylenediamine, TFA, and Tris were obtained from Sigma-Aldrich (St. Louis, MO, USA). A molecular-weight-size protein standard (6.5 to 200 kDa) was also provided by Sigma-Aldrich; Hydroxyethylcellulose (HEC; average molecular mass, 27000) was from Polysciences (Warrington, PA, USA); Calcium chloride dihydrate was purchased from Panreac (Barcelona, Spain); Urea and iminodiacetic acid (IDA) were from Fluka (Buchs SG, Switzerland); Acetone (reagent grade) and potassium dihydrogen phosphate were supplied by VWR Chemicals (Barcelona, Spain); Ethylenediaminetetraacetic acid disodium salt dihydrate (EDTA-Na_2) was supplied by Probus (Badalona, Spain).

Mature human milk samples were kindly donated by healthy well-nourished mothers from the urban area of Valencia (Spain). The samples were collected between the baby's feed by manual expression using a Medela Harmony Breastpump (Zug, Switzerland). After collection, milk samples were kept at -20 ºC until their use.

9. 2. 2. Instrumentation

SDS-PAGE experiments were performed using a vertical minigel Hoefer SE260 Mighty Small system (Hoefer, MA, USA).

Centrifugation steps were conducted in a MICRO STAR 17R laboratory centrifuge (VWR, Barcelona, Spain).

CE experiments were conducted on an Agilent 7100 Capillary Electrophoresis System equipped with a diode array spectrophotometric detector. Fused-silica uncoated capillaries (33.5 cm × 50 µm I.D. × 375 µm O.D.) from Supelco (Bellefonte, PA, USA) were used.

LC–MS/MS analyses were carried out after in-gel or in-solution digestion of the samples with an Eksigent nanoLC-2D plus system (Dublin, CA, USA) with a MS nanoESI qQTOF (5600 TripleTOF, AB Sciex) via an ESI interface (San Jose, CA, USA).

MALDI-TOF/TOF analyses were performed after in-gel digestion of the samples with a MALDI-TOF/TOF 5800 AB Sciex.

9. 2. 3. Precipitation of caseins

An aliquot of 250 µL of human milk was placed in an Eppendorf tube and 7.5 µL of 2 M $CaCl_2$ followed by 7.5 µL of 0.5 M KH_2PO_4 pH 6.0 were added. After 30 min of mechanical stirring the tube was centrifuged at 13300 rpm (17000 ×*g*) for 10 min at 20 ºC and the supernatant, which corresponded to the whey fraction of milk was transferred to an empty tube and different aliquots were subjected either to SDS-PAGE, LC-MS/MS or CE analysis. Then, the pellet (CN fraction) was washed three times with 80 mM $CaCl_2$ solution. For SDS-PAGE and LC-MS/MS analysis, a final wash with acetone was done and the pellet was re-dissolved in 250 µL of 0.02 M Tris, 2% (w/v) SDS, 0.1 M EDTA-Na_2 at pH 6.0. For CE analysis, the pellet was

washed consecutively with 250 µL of 10% (v/v) acetic acid/ 1 M sodium acetate, 250 µL of water and 250 µL of acetone and eventually re-dissolved in 250 µL of 20 mM ABC pH 8.2. Two parallel precipitations, where calcium and phosphate were added alone were also carried out ("Ca precipitation" and "Phosphate precipitation", respectively).

For comparison, isoelectric precipitation of CNs was carried out. Briefly, an aliquot of 250 µL of human milk was place in an Eppendorf tube to which 30 µL of 10% (v/v) acetic acid/1 M sodium acetate pH 4.6 were added. The mixture was kept for 20 min at 4 ºC and centrifuged at 13300 rpm for 10 min at 4 ºC. The supernatant (whey fraction) was transferred to a clean tube for its posterior analysis and the pellet (CN fraction) was washed three times with 250 µL of 0.4% (v/v) acetic acid/ 0.4 M sodium acetate. As described above, the CN fraction was washed and re-dissolved according to the subsequent analysis.

9. 2. 4. SDS-PAGE analysis

SDS-PAGE experiments were carried out by mixing 10 µL of the sample solution with 10 µL of Laemmli solution under reducing conditions. The mixture was loaded into a gel with 40% acrylamide/bis-acrylamide solution, and standard discontinuous buffer systems [17]. To visualize the protein bands, the gel was stained with Coomassie Blue dye and destained with a MeOH-acetic acid-water (40:10:50; v/v/v) solution. Molecular sizes of the model proteins were analyzed by comparison with an SDS-PAGE standard marker (6.5 to 200 kDa).

9. 2. 5. In-gel and in-solution digestion

Gel samples were digested with sequencing grade trypsin (Promega) as described elsewhere [18]. One hundred ng of trypsin was used. The

digestion mixture was dried in a vacuum centrifuge, and re-suspended in 11 µL of 2% ACN, 0.1% TFA.

For sample solutions, 10 µL of each sample were reduced by 2 mM DTT (final volume, V_f = 25 µL) for 20 minutes at 60 ºC. The thiol groups were alkylated with 5.5 mM IAM (V_f = 30 µL) for 30 minutes at room temperature in the dark. The excess of IAM was quenched with 10 mM DTT (V_f = 60 µL) at 37 ºC for 1 hour. 500 ng of trypsin were added (V_f = 65 µL) and digestion was let overnight. All the reagents were prepared in 50 mM ABC. The protein digestion was stopped with 5 µL of 10 % TFA in water. The mixtures final volume was 70 µL.

9. 2. 6. MALDI-TOF/TOF

One µL of digested sample solutions were spotted onto the MALDI target plate. After the droplets were air-dried at room temperature, 1 µL of matrix (5 mg/mL α-CHCA in 0.1% TFA-ACN/H_2O (1:1, v/v)) was added and allowed to air-dry at room temperature. The resulting mixtures were analysed by MALDI-TOF/TOF in positive reflectron mode (3000 shots every position). Five of the most intense precursors (according to the threshold criteria: minimum signal-to-noise: 10, minimum cluster area: 500, maximum precursor gap: 200 ppm, maximum fraction gap: 4) were selected for every position for the MS/MS analysis. MS/MS data was acquired using the default 1kV MS/MS method. The MS and MS/MS information was sent to MASCOT via the Protein Pilot (AB Sciex).

To identify proteins, database search was performed on Expasy database with protein specific sequences. Searches were done with tryptic specificity allowing one missed cleavage and a tolerance on the mass measurement of 100 ppm in MS mode and 0.9 Da for MS/MS ions. Carbamidomethylation of Cys was used as a fixed modification and oxidation

of Met and deamidation of Asn and Gln as variable modifications. Proteins showing score higher than homology or significance threshold were identified with confidence ≥ 95%.

9. 2. 7. LC-MS/MS

Five µL of sample was loaded onto a trap column (NanoLC Column, 3 µm C18-CL, 350 µm x 0.5 mm; Eksigen) and desalted with 0.1% TFA at 3 µL/min during 5 min. The peptides were then loaded onto an analytical column (LC Column, 3 µm C18-CL, 75 µm x 12cm, Nikkyo) equilibrated in 5% ACN 0.1% formic acid. Elution was carried out with a linear gradient of 5 to 40% B in A for 60 min (A: 0.1% formic acid; B: ACN, 0.1% formic acid) at a flow rate of 300 nL/min. Peptides were analysed in a MS nanoESIqQTOF (5600 TripleTOF, AB Sciex). For ionization conditions, see Supporting Information.

In order to identify proteins, the SCIEX.wiff data-files were processed using ProteinPilot v5.0 search engine (AB Sciex). ProteinPilot default parameters were used to generate peak list directly from 5600 TripleTofwiff files. The Paragon Algorithm [19] of ProteinPilot v5.0 was used to search the expasy database (version 01-2017) (see Supporting Information for more details). Only peptide and protein identifications with ≥ 95% confidence (unused Score ≥ 1.3) were validated. Protein identifications were accepted either if they contained at least two identified peptides or if they contained only one peptide but they have been previously reported in any of the following references [2,7,20–27].

The proteomics data and result-files from the analysis have been deposited to the ProteomeXchange Consortium via the PRIDE [28] partner repository, with the dataset identifier PXD010315 and 10.6019/PXD010315.

9. 2. 8. Label-free protein quantification using chromatographic areas

For quantification, the group file generated by ProteinPilot was used. The ions areas were extracted from the wiff files obtained from LC–MS/MS experiment by Peak View® v1.1. Only peptides assigned with confidence ≥ 95%, among those without modifications or shared by different proteins were extracted. The quantitative data obtained by PeakView® were analyzed by Marker View® v1.3 (AB Sciex). Areas were normalized by total areas summa.

9. 2. 9. CE working conditions

Conditioning of the capillary was conducted at 60 ºC by following the next steps: 10 min with 1 M NaOH, 10 min with 0.1 M NaOH, and 10 min with water. Background electrolyte (BGE) was adopted from a previous work [29] and consisted in 50 mM IDA (pH = pI = 2.30 at 25 ºC), 0.5% HEC and 6 M urea (apparent pH 3.1). Separation was carried out at 15 kV and samples were injected using hydrostatic pressure (50 mbar) for 5 s. The signal was monitored at 214 ± 4 nm (360 ± 100 nm as reference). Prior to each working session the capillary was rinsed for 30 min with the running BGE at 25 ºC. Between injections, a rinsing for 2 min with the BGE was done. At the end, the capillary was cleaned with water for 20 min.

9. 2. 10. CE fraction collection

A procedure for collecting fractions during CE separation was conducted. Collection was carried out by pressure elution, that is, peaks were moved into the collection vial by applying 50 mbar pressure. To this end, migration time when a pressure of 50 mbar was applied was first determined. This time corresponds to that needed for an injected sample plug to move from

the capillary inlet to the detector if moved by pressure only. Then, along ten consecutive injections of a human milk sample, all peaks eluted within a designated timeframe were collected in microvials with 25 μL 50 mM IDA. Based on the peak migration time, capillary length and elution mode (pressure), all detected peaks above a certain threshold (slope > 1) were collected and subjected to LC-MS/MS analysis.

9. 3. Results and discussion

9. 3. 1. Precipitation of casein micelles

As previously discussed in Introduction, human milk proteins and, in particular, human CN micelles differ in terms of both composition and structure from their ruminant counterpart. On the other hand, the interactions of the CN micelles should be understood in terms of the structure of the surface layer that changes with conditions [4]. In this sense, certain studies have proposed that κ-CN (a glycoprotein) is located on the surface of the micelles and is responsible of their stability against precipitation by calcium ions [30]. Thus, the enhanced hydrophilic nature of human κ-CN, due to its large degree of glycosylation, may be one of the factors leading to the formation of smaller-sized micelles in this sample as compared to bovine milk [31]. Since the structure of the surface layer of CN micelles changes with media conditions, the interaction with precipitating agents could play an important role in the fractionation of these proteins. **Figure 9.1** shows the SDS-PAGE analysis of supernatant and pellet fractions after using conventional isoelectric precipitation (pH 4.6). Protein bands were ascribed according to a previous work [32]. As can be seen, the isolation of CNs was incomplete (lane 2) leading to a whey fraction highly contaminated (lane 3). This fact can be explained as follows. Within the CN micelles, CN molecules are held together primarily by hydrophobic interactions and (insoluble or

CN-bound) colloidal calcium phosphate (CCP) crosslinks [3]. Besides, experimental evidence strongly favors the idea of chemical association between this CCP (inorganic phosphate) and organic phosphate (esterified to the protein via the hydroxyl group of serine of CN) [33]. The acidification of milk causes the progressive release of CCP and other ions from the interior of the micelles, leading to an eventual coagulation and precipitation of CNs. However, human CNs with higher pIs (5.3, 5.2, 8.7 for β-CN, α-S1-CN and κ-CN, respectively) [34] under the usual isoelectric pH (4.6) remain soluble, which results in a non-effective fractionation protocol.

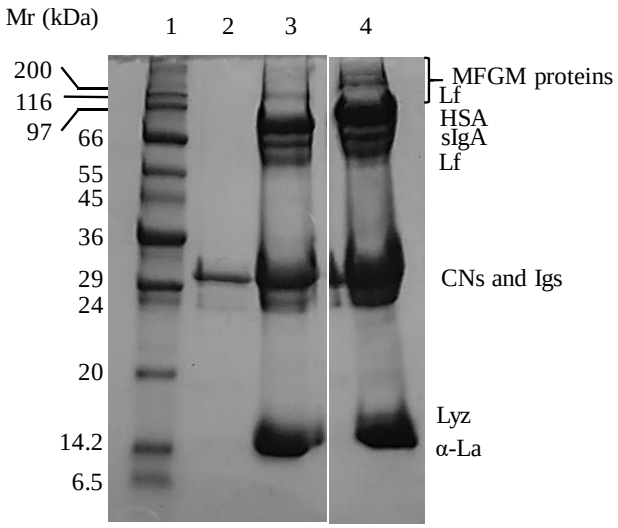

Figure 9.1. SDS-PAGE analysis of human milk. Identification: lane 1, molecular weight marker; lane 2 and 3, pellet and supernatant of isoelectric precipitation (pH 4.6), respectively; and lane 4, human milk.

On the other hand, prior studies [6] have reported that addition of calcium may facilitate the release of whey proteins from CNs due to hydrophobic interaction, repulsive forces, or entrapment. Taking into account this fact, jointly with the phosphorylated structure of CN molecules, the addition of calcium phosphate (CaP) was explored as alternative to improve the performance of the fractionation protocol. **Figure 9.2** shows the

SDS-PAGE analysis of supernatant and pellet fractions of CaP precipitation. As can be seen, the addition of calcium and phosphate ions to human milk induces the selective precipitation of CNs (lane 2), while whey proteins remain in solution (lane 5).

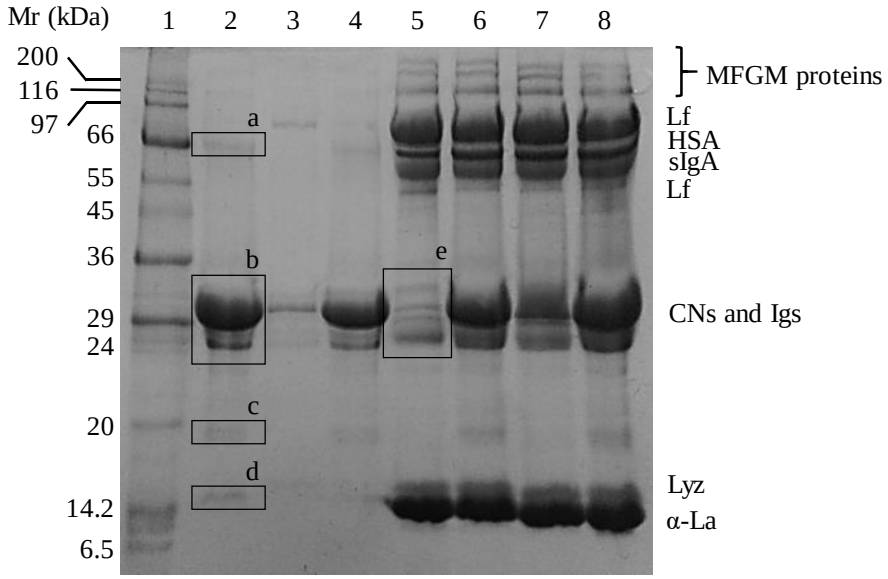

Figure 9.2. SDS-PAGE analysis of human milk. Identification: lane 1, molecular weight marker; lane 2-4, pellet of CaP, phosphate and Ca precipitation, respectively; lane 5-7, supernatant of CaP, phosphate, Ca precipitation, respectively; and lane 8, human milk.

In order to understand the role of both ions, separate experiments based on calcium or phosphate precipitation were also carried out (see Section 9.2.3). The addition of calcium gave a noticeable isolation of CNs (lane 4), although a small fraction of these proteins was still evidenced in the whey fraction (lane 7). On the other hand, the addition of phosphate just showed a slight effect in the fractionation process (lanes 3 and 6). Thus, calcium added to milk reacts with soluble phosphate and results in precipitation of CCP and, consequently, in coprecipitation of CN micelles. However, as can be seen, the addition of secondary phosphate (KH_2PO_4) has an extra benefit in the

coagulation of CN micelles due to the formation and precipitation of extra CCP. Other authors have observed a similar phenomenon in the coprecipitation of phosphopeptides with lanthanide phosphates [35]. The authors of this study attributed the coprecipitation process to the formation of stable complexes between lanthanide ions and the phosphate groups of phosphopeptides. Consequently, this possibility cannot be excluded for calcium ions in this work.

Considering these comments, an additional experiment using double amount of precipitating agent (CaP (2x) precipitation) was carried out. However, the intensity of several bands in the CN fraction increased, while other bands from the whey fraction diminished (**Figure S9.1**).

To further identify the protein bands observed in the SDS-PAGE analysis of both CaP precipitations, bands labeled as “a” to “e” (see **Figure 9.2**) and “d’” and “e’” (see **Figure S9.1**) were digested and analyzed by either MALDI-TOF/TOF or LC-MS/MS (see Sections 9.2.5 - 9.2.7). The results of MS analysis are presented in **Table S9.1**.

To evaluate the level of isolation capability reached by each fractionation approach tested, proteins from untreated human milk, whey and CN extracts were subjected to digestion and analysis by LC-MS/MS (see Sections 9.2.5, 9.2.7 and 9.2.8). A total of 123 proteins (see Supporting Information, file “Proteins in fractions”) were identified in the human milk sample, all of them previously reported [2,7,20–25]. Venn diagrams [36] jointly with normalized areas of the relevant proteins present in whey and CN fractions were used as an indicator of cross contamination degree.

From Venn diagrams (**Figure 9.3**), it can be derived that only 35 proteins are recognized in all three extracts of CaP precipitation, whereas 40 and 44 proteins are found for CaP (2x) and isoelectric precipitation protocols, respectively. Besides, the number of proteins identified both in the whey and CN fractions increases along these procedures as well.

Figure 9.4 shows the changes in normalized areas of CNs and selected whey proteins in untreated human milk, pellets and supernatants in the different fractionation protocols. As can be seen, the CN fraction (part A) after CaP precipitation is greater than that found in isoelectric and in CaP (2x) precipitations. In addition, the most "CN-free" whey protein fraction is obtained with the CaP treatment. Besides, in this protocol, the profile of CNs and whey proteins in the human milk sample is maintained with respect to the pellet and supernatant fractions. Regarding whey proteins, similar results were observed for the supernatant fractions obtained with CaP and CaP (2x) precipitations. However, the later procedure led to a higher coprecipitation of whey proteins in CN pellet. All these findings are in agreement with the results previously observed in the SDS-PAGE analysis (see **Figures 9.1**, **9.2** and **S9.1**).

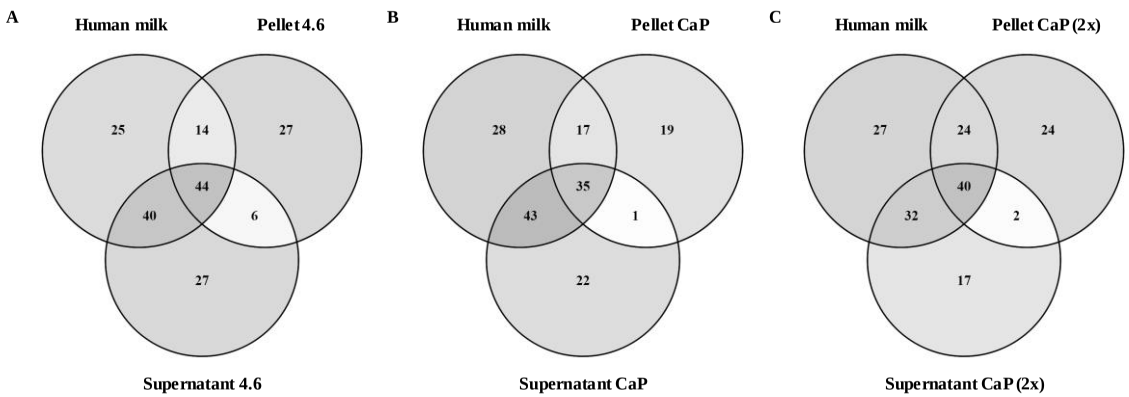

Figure 9.3. Venn diagrams of the number of unique proteins observed with the three different fractionation protocols: isoelectric precipitation (pH 4.6) (A), CaP precipitation (B), and CaP (2x) precipitation (C).

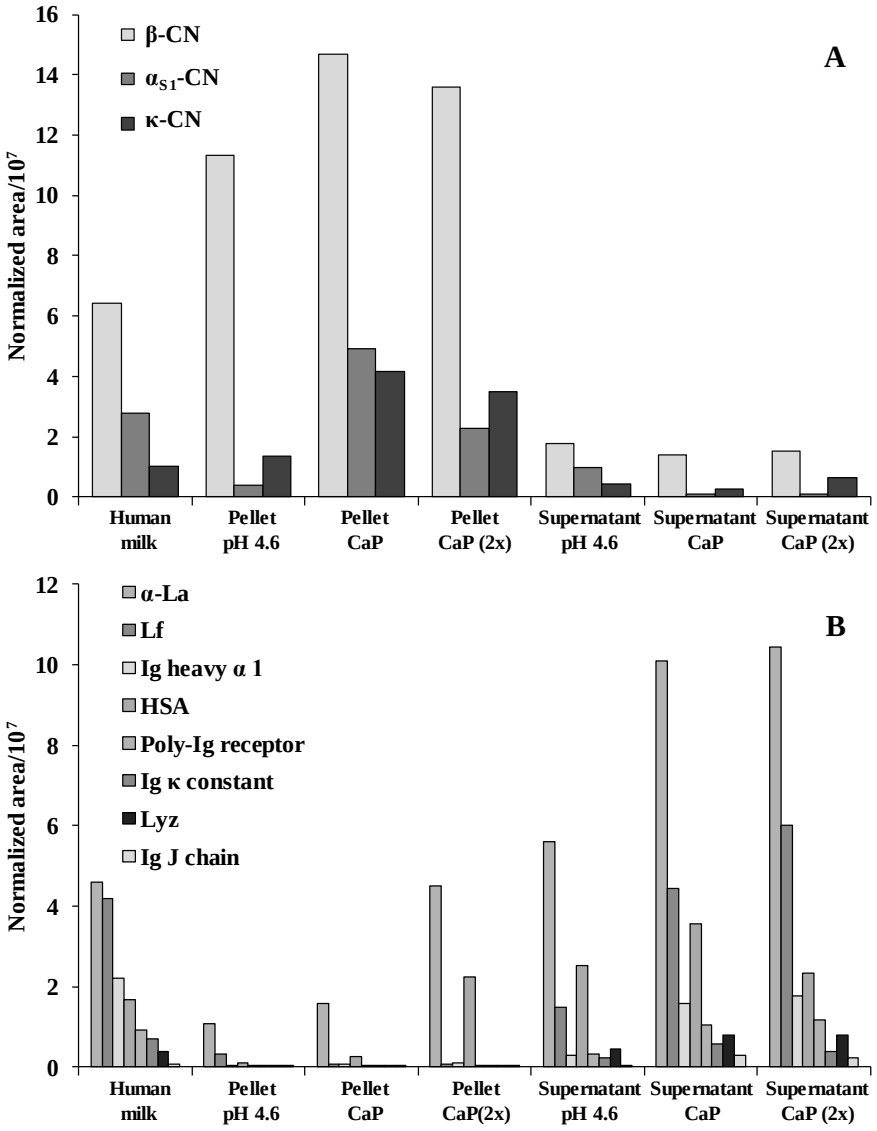

Figure 9.4. Normalized areas of selected CNs (A) and main whey proteins (B) in human milk, pellets, and supernatants of the different fractionation approaches. Abbreviations: β-CN, beta-CN; α_{S1}-CN, alpha-S1-CN; κ-CN, kappa-CN; α-La, alpha-lactalbumin; Lf, lactoferrin; Ig heavy α 1, Ig alpha-1 chain C region; HSA, human serum albumin; Poly- Ig receptor, polymeric immunoglobulin receptor; Ig κ constant, Ig kappa chain C region; Lyz, lysozyme C; Ig J chain, immunoglobulin J chain.

9. 3. 2. CE analysis

As previously stated, CE allows the development of simple, rapid, and automated methods with excellent separation of individual milk proteins based on their charge to mass ratio. However, only one study focused on the electrophoretic characterization of human milk proteins has been carried out [13]. To get more information about this challenging matrix, a fast CE procedure using isoelectric buffers was further accomplished. These BGEs show reduced conductivity [37], which is compatible with high voltage gradients, thus favoring high resolution with short migration times. The CE experiments were carried out with human skim milk. Thus, fat was removed by centrifugation at 13300 rpm for 30 min at 4 ºC. **Figure 9.5** shows the electrophoretic pattern of a human milk sample, where main proteins are successfully separated. Proteins were identified by comparison with human whey protein standards and based on the observation of migration time of bovine CNs standard. In addition, the CE pattern obtained by Manso *et al.* [13] was considered. As can be seen, whey proteins elute first (4-8 min), followed by CNs (12-16 min), whose distribution of β-CN phosphorylated forms is clearly observed. Some peaks (labelled with an asterisk in **Figure 9.5**) were ascribed to proteolysis products of CNs by endogenous plasmin [13]. On the other hand, the region ranged from 8 to 11 min was not clearly ascribed to any protein or group of proteins. To elucidate the identification of this band, CE fraction collection in this time interval was done, and the extract of digested proteins was analyzed by LC-MS/MS. This approach represents an alternative when hyphenated CE-MS techniques are not available, or when constraints related to MS compatibility such as nonvolatile BGEs or high concentrations of inorganic salts are present.

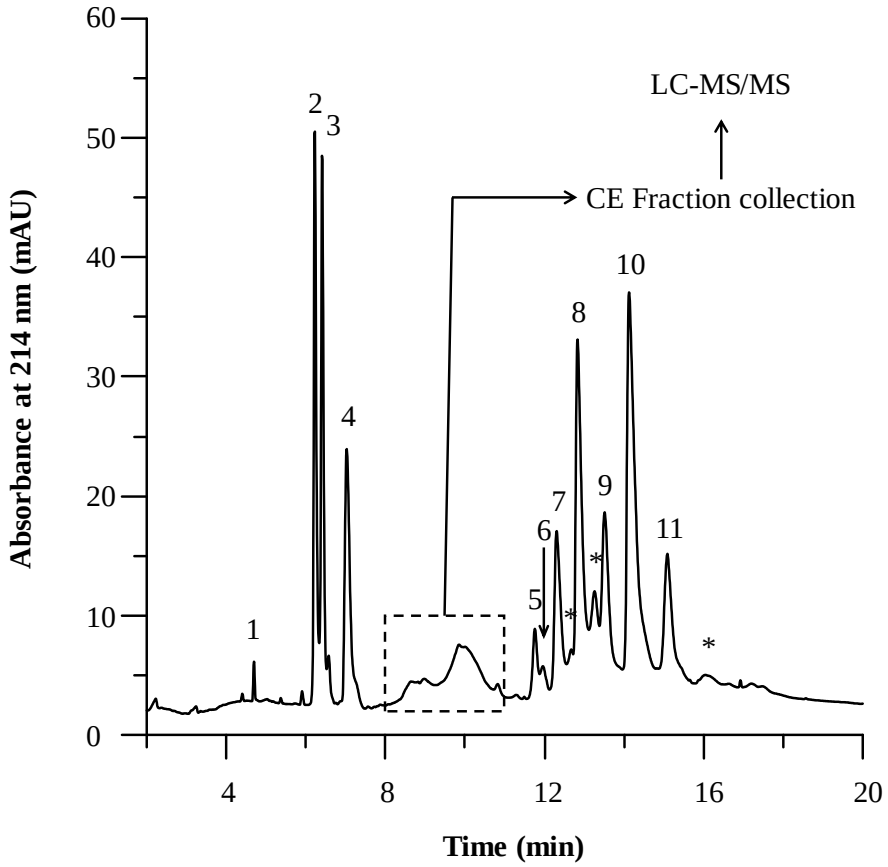

Figure 9.5. Electropherogram of human skim milk. Peak identification: (1) Lyz, (2) HSA, (3) α-La, (4) Lf, (5) β-CN 0P, (6) κ-CN, (7) β-CN 1P, (8) β-CN 2P, (9) β-CN 3P, (10) β-CN 4P, (11) β-CN 5P, and (*) proteolysis products of endogenous plasmin (γ-CN). See **Figure 9.4** for abbreviations.

Under the working conditions described in Section 9.2.10, the fractions corresponding to the broad peak comprised between 8 and 11 min (time window with discontinuous line in **Figure 9.5**) were collected into two microvials. The different fractions were then subjected to the aforementioned LC-MS/MS method. **Table S9.2** shows the list of proteins identified in the CE fraction collection study. As can be seen, 62 proteins are identified, many of which are common (45) for both fractions. This might be attributed to the

transient interruption of the electrophoretic separation during the fraction collection. The resulting laminar flow induced from hydrodynamic fractionation can cause band-broadening and detriment in resolution [38]. **Table S9.2** shows proteins such as immunoglobulins (Igs) and keratins. These later proteins were not considered contamination and therefore were not removed from the data set, since mammary epithelial cells express keratins [20]. With respect Igs, secretory IgA (a dimer of IgA) represents ~90% of total Igs in human milk [39]. However, this protein has not been previously detected by CE [13]. In **Table S9.2**, heavy and light chains of IgA appear as identified proteins in this complex matrix. On the other hand, from the proteins identified, 41 proteins are not enclosed in the proteins identified in the direct analysis of human milk, pellet, and supernatant of CaP precipitation. In addition, the presence of certain proteins such as two keratins (keratin, type I cytoskeletal 13 and keratin, type II cytoskeletal 3) and a transglutaminase (protein-glutamine gamma-glutamyltransferase K) were found in human milk for the first time. From these results, it follows that CE fraction collection is a potential tool to increase the number of proteins present in human milk.

From the molecular function classification of these 62 proteins (**Figure 9.6A**), it is derived that, a total of 45 (73%) are involved in the selective, non-covalent interaction (binding) with other molecules (such as proteins, lipids, or ions, among others). Some others appear showing structural molecule (25, 40%), catalytic activities (16, 26%) and enzyme regulatory (9, 15%) activities. With respect the biological process in which they are involved (**Figure 9.6B**), most of them (52, 84%) participate in cellular processes (e.g., cell activation, cell death, cellular metabolic processes, or secretion by cells, among others). Likewise, biological regulation (42, 68%), localization (34, 55%), immune system process (32, 52%), and multicellular organismal process (33, 53%) are also representative biological processes of these proteins. Regarding their presence in cellular components (**Figure 9.6C**),

most of them belong to the cell part group (58, 94%) as well as to organelle (57, 92%) and extracellular region part (56, 90%).

Once accomplished the identification of the human milk proteins by CE, the analysis of CN and whey fractions obtained with the proposed CaP precipitation method was performed (**Figure S9.2**). As shown in this figure, the CN fraction obtained with the traditional isoelectric precipitation protocol (trace A) shows the presence of small amounts of whey proteins, or alternatively, the CNs identified in whey fraction are also clearly distinguished (trace B). However, after fractionation with CaP, the presence of whey or CN proteins in the fractions considered is significantly lower, particularly for CN fraction (trace C), where whey proteins are not distinctly evidenced. All these data presented are in rough agreement with the results previously found by SDS-PAGE and LC-MS/MS experiments (see Section 9.3.1). Thus, the enhanced efficiency of the proposed extraction method is of great significance to go deep inside the human milk proteome.

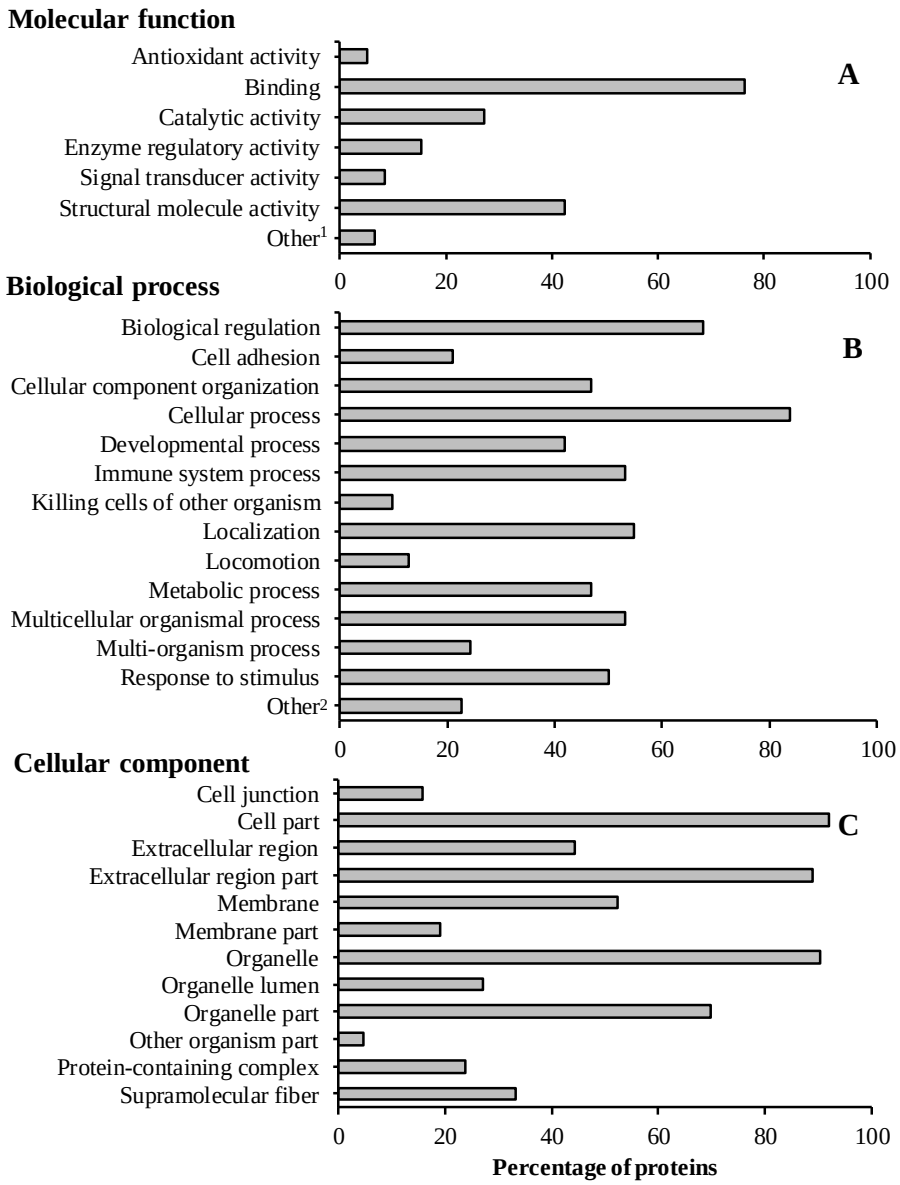

Figure 9.6. Bar charts representing the distribution of the proteins identified in the CE fraction collection according to molecular function (A), biological process (B) and cellular component (C) using UniProt KB database [40]. [1]Other: oxygen carrier activity, transcription coactivator activity, transporter activity and virus receptor activity. [2]Other: cell proliferation, cellular oxidant detoxification, estrous cycle, reproductive process, and signaling.

9. 4. Conclusions

Isoelectric precipitation of milk is a well-known technique to separate the two main classes of proteins (CNs and whey proteins). However, this conventional protocol is not fully effective since some whey proteins co-precipitate with CNs and some CNs remain in solution as well. Besides, for human milk, the distribution of CNs jointly with their distant pI value from the isoelectric pH (4.6) might hinder an efficient fractionation when isoelectric precipitation is carried out.

We have proposed here an easy fractionation method in which the addition of calcium and phosphate ions favours the formation of CCP and, hence, enhances the coprecipitation of CN micelles. This fact can be attributed to the chemical association between CCP and organic phosphate (esterified to CN subunits). On the other hand, the role of formation of complexes between phosphate groups of CN micelles and calcium ions cannot be excluded. In any case, the improvement in fractionation with CaP with respect isoelectric precipitation was evidenced through several techniques (SDS-PAGE, LC-MS/MS, and CE). In addition, CE fraction collection off-line coupled to LC-MS/MS has proved to be useful in the identification of minor proteins present in human milk. This fraction collection approach represents an affordable choice to the off-line use of expensive MS instruments, which can be shared among different research groups.

On the other hand, considering reagents, instrumentation, and labour, CaP precipitation results in a cost-effective and straightforward fractionation method for whatever purposes one may have (e.g., differences in CE pattern of human milk according to state of lactation, selection of candidate biomarkers for the diagnosis of diseases, or even the production of milk proteins at a commercial scale). Based on the outcomes of this protocol, we encourage researchers to extend it to the fractionation of proteins in milk from other mammalian species.

Author contributions

J.M.H-M and E.F.S-A conceived the study, contributed to experimental design, and revised the manuscript critically; I.T-D carried out the experimental procedure, made the comprehensive analysis of the data derived from the proteomic analysis and also wrote the manuscript. All authors read and approved the final version of the manuscript.

Conflict of Interest

The authors declare no conflict of interest.

Acknowledgements

This work was supported by project PROMETEO/2016/145 (Generalitat Valenciana). I. T-D thanks the MECD for an FPU grant for PhD studies. The authors also thank Dr. María Luz Valero Rustarazo from the Proteomic section of the SCSIE (University of Valencia), for her help in protein analysis. This proteomics laboratory is a member of Proteored, PRB3 and is supported by grant PT17/0019, of the PE I+D+i 2013-2016, funded by ISCIII and ERDF.

9. 5. References

[1] F. Anatolitou, Human milk benefits and breastfeeding, J. Pediatr. Neonatal Individ. Med. 1 (2012) 11–18. doi:10.7363/010113.

[2] Y. Liao, R. Alvarado, B. Phinney, B. Lönnerdal, Proteomic characterization of human milk fat globule membrane proteins during a 12 month lactation period, J. Proteome Res. 10 (2011) 3530–3541. doi:10.1021/pr200149t.

[3] P.F. Fox, A. Brodkorb, The casein micelle: Historical aspects, current concepts and significance, Int. Dairy J. 18 (2008) 677–684. doi:10.1016/j.idairyj.2008.03.002.

[4] D.G. Dalgleish, M. Corredig, The Structure of the casein micelle of milk and its changes during processing, Annu. Rev. Food Sci. Technol. 3 (2012) 449–467. doi:10.1146/annurev-food-022811-101214.

[5] T. Nagasawa, I. Kiyosawa, M. Takase, Lactoferrin and serum albumin of human casein in colostrum and milk, J. Dairy Sci. 57 (1974) 1159–1163. doi:10.3168/jds.S0022-0302(74)85030-7.

[6] C. Kunz, B. Lönnerdal, Human milk proteins: separation of whey proteins and their analysis by polyacrylamide gel electrophoresis, fast protein liquid chromatography (FPLC) gel filtration, and anion-exchange chromatography, Am. J. Clin. Nutr. 49 (1989) 464–470. doi:10.1016/B978-0-12-374039-7.00014-3.

[7] Y. Liao, R. Alvarado, B. Phinney, B. Lönnerdal, Proteomic characterization of human milk whey proteins during a twelve-month lactation period, J. Proteome Res. 10 (2011) 1746–1754. doi:10.1021/pr101028k.

[8] T. Morçöl, Q. He, S.J.D. Bell, Model process for removal of caseins from milk of transgenic animals, Biotechnol. Prog. 17 (2001) 577–582.

doi:10.1021/bp010023x.

[9] C.H. Yen, Y.S. Lin, C.F. Tu, A novel method for separation of caseins from milk by phosphates precipitation, Prep. Biochem. Biotechnol. 45 (2015) 18–32. doi:10.1080/10826068.2013.877030.

[10] E.S. Sørensen, L. Møller, M. Vinther, T.E. Petersen, L.K. Rasmussen, The phosphorylation pattern of human α_{s1}-casein is markedly different from the ruminant species, Eur. J. Biochem. 270 (2003) 3651–3655. doi:10.1046/j.1432-1033.2003.03755.x.

[11] E. D'Auria, C. Agostoni, M. Giovannini, E. Riva, R. Zetterström, R. Fortin, G.F. Greppi, L. Bonizzi, P. Roncada, Proteomic evaluation of milk from different mammalian species as a substitute for breast milk, Acta Paediatr. 94 (2005) 1708–1713. doi:10.1080/08035250500434793.

[12] A. Omar, N. Harbourne, M.J. Oruna-Concha, Quantification of major camel milk proteins by capillary electrophoresis, Int. Dairy J. 58 (2016) 31–35. doi:10.1016/j.idairyj.2016.01.015.

[13] M.A. Manso, M. Miguel, R. López-Fandiño, Application of capillary zone electrophoresis to the characterisation of the human milk protein profile and its evolution throughout lactation, J. Chromatogr. A 1146 (2007) 110–117. doi:10.1016/j.chroma.2007.01.100.

[14] N. Boumahrou, S. Andrei, G. Miranda, C. Henry, J.J. Panthier, P. Martin, S. Bellier, The major protein fraction of mouse milk revisited using proven proteomic tools, J. Physiol. Pharmacol. 60 (2009) 113–118.

[15] G. Álvarez, L. Montero, L. Llorens, M. Castro-Puyana, A. Cifuentes, Recent advances in the application of capillary electromigration methods for food analysis and Foodomics, Electrophoresis 39 (2017) 136–159. doi:10.1002/elps.201700321.

[16] R. O'Donnell, J.W. Holland, H.C. Deeth, P. Alewood, Milk proteomics, Int. Dairy J. 14 (2004) 1013–1023. doi:10.1016/j.idairyj.2004.04.004.

[17] U.K. Laemmli, Cleavage of structural proteins during the assembly of the head of bacteriophage T4, Nature 227 (1970) 680–685. doi:10.1038/227680a0.

[18] A. Shevchenko, O.N. Jensen, A. V. Podtelejnikov, F. Sagliocco, M. Wilm, O. Vorm, P. Mortensen, A. Shevchenko, H. Boucherie, M. Mann, Linking genome and proteome by mass spectrometry: Large-scale identification of yeast proteins from two dimensional gels, Proc. Natl. Acad. Sci. 93 (1996) 14440–14445. doi:10.1073/pnas.93.25.14440.

[19] I. V. Shilov, S.L. Seymour, A.A. Patel, A. Loboda, W.H. Tang, S.P. Keating, C.L. Hunter, L.M. Nuwaysir, D.A. Schaeffer, The Paragon Algorithm, a next generation search engine that uses sequence temperature values and feature probabilities to identify peptides from tandem mass spectra, Mol. Cell. Proteomics 6 (2007) 1638–1655. doi:10.1074/mcp.T600050-MCP200.

[20] M.J.C. van Herwijnen, M.I. Zonneveld, S. Goerdayal, E.N.M. Nolte – 't Hoen, J. Garssen, B. Stahl, A.F. Maarten Altelaar, F.A. Redegeld, M.H.M. Wauben, Comprehensive proteomic analysis of human milk-derived extracellular vesicles unveils a novel functional proteome distinct from other milk components, Mol. Cell. Proteomics 15 (2016) 3412–3423. doi:10.1074/mcp.M116.060426.

[21] M. Yang, M. Cong, X. Peng, J. Wu, R. Wu, B. Liu, W. Ye, X. Yue, Quantitative proteomic analysis of milk fat globule membrane (MFGM) proteins in human and bovine colostrum and mature milk samples through iTRAQ labeling, Food Funct. 7 (2016) 2438–2450. doi:10.1039/C6FO00083E.

[22] A. D'Alessandro, A. Scaloni, L. Zolla, Human milk proteins: strides in proteomics and benefits in nutrition research, en: S. Zibadi, R.R. Watson, V.R. Preedy (Eds.), Handb. Diet. Nutr. Asp. Hum. Breast Milk, 1ª ed., Wageningen Academic Publishers, The Netherlands, 2013: págs. 249–292.

[23] C.E. Molinari, Y.S. Casadio, B.T. Hartmann, A. Livk, S. Bringans, P.G. Arthur, P.E. Hartmann, Proteome mapping of human skim milk proteins in term and preterm milk, J. Proteome Res. 11 (2012) 1696–1714. doi:10.1021/pr2008797.

[24] A. D'Alessandro, A. Scaloni, L. Zolla, Human milk proteins: an interactomics and updated functional overview, J. Proteome Res. 9 (2010) 3339–3373. doi:10.1021/pr100123f.

[25] D.J. Palmer, V.C. Kelly, A.M. Smit, S. Kuy, C.G. Knight, G.J. Cooper, Human colostrum: Identification of minor proteins in the aqueous phase by proteomics, Proteomics 6 (2006) 2208–2216. doi:10.1002/pmic.200500558.

[26] J. Bronsky, M. Karpísek, E. Bronská, M. Pechová, B. Jancíková, H. Kotolová, D. Stejskal, R. Prusa, J. Nevoral, Adiponectin, adipocyte fatty acid binding protein, and epidermal fatty acid binding protein: proteins newly identified in human breast milk, Clin Chem. 52 (2006) 1763–1770. doi:10.1373/clinchem.2005.063032.

[27] I. Nischang, Porous polymer monoliths: Morphology, porous properties, polymer nanoscale gel structure and their impact on chromatographic performance, J. Chromatogr. A 1287 (2013) 39–58. doi:10.1016/j.chroma.2012.11.016.

[28] J.A. Vizcaíno, E.W. Deutsch, R. Wang, A. Csordas, F. Reisinger, D. Ríos, J.A. Dianes, Z. Sun, T. Farrah, N. Bandeira, P.A. Binz, I. Xenarios, M. Eisenacher, G. Mayer, L. Gatto, A. Campos, R.J.

Chalkley, H.J. Kraus, J.P. Albar, S. Martinez-Bartolomé, R. Apweiler, G.S. Omenn, L. Martens, A.R. Jones, H. Hermjakob, ProteomeXchange provides globally coordinated proteomics data submission and dissemination, Nat. Biotechnol. 32 (2014) 223–226. doi:10.1038/nbt.2839.

[29] J.M. Herrero-Martínez, E.F. Simó-Alfonso, G. Ramis-Ramos, C. Gelfi, P.G. Righetti, Determination of cow's milk in non-bovine and mixed cheeses by capillary electrophoresis of whey proteins in acidic isoelectric buffers, J. Chromatogr. A 878 (2000) 261–271. doi:10.1016/S0021-9673(00)00299-5.

[30] S.M. Sood, P.J. Herbert, C.W. Slattery, Structural studies on casein micelles of human milk: Dissociation of beta-casein of different phosphorylation levels induced by cooling and ethylenediaminetetraacetate, J. Dairy Sci. 80 (1997) 628–633. doi:10.3168/jds.S0022-0302(97)75980-0.

[31] B.C. Dev, S.M. Sood, S. DeWind, C.W. Stattery, k-casein and ß-casein in human milk micelles: Structural studies, Arch. Biochem. Biophys. 314 (1994) 329–336. doi:10.1006/abbi.1994.1450.

[32] I. Ten-Doménech, E.F. Simó-Alfonso, J.M. Herrero-Martínez, Isolation of human milk whey proteins by solid phase extraction with a polymeric material modified with gold nanoparticles, Microchem. J. 133 (2017) 320–326. doi:10.1016/j.microc.2017.03.058.

[33] P.F. Fox, T. Uniacke-Lowe, P.L.H. McSweeney, J.A. O'Mahony, Chapter 4. Milk Proteins, en: Encycl. Dairy Sci., 2ª ed., Springer, Switzerland, 2015: págs. 145–239. doi:10.1007/978-3-319-14892-2.

[34] L.P. Kozlowski, IPC - Isoelectric Point Calculator, Biol. Direct. 11 (2016) 55. doi:10.1186/s13062-016-0159-9.

[35] M.R. Mirza, M. Rainer, Y. Güzel, I.M. Choudhary, G.K. Bonn, A

novel strategy for phosphopeptide enrichment using lanthanide phosphate co-precipitation, Anal. Bioanal. Chem. 404 (2012) 853–862. doi:10.1007/s00216-012-6215-0.

[36] J.C. Oliveros, Venny. An interactive tool for comparing lists with Venn's diagrams, (2007). Disponible en: http://bioinfogp.cnb.csic.es/tools/venny/index.html (Fecha de acceso 15/05/2018).

[37] P.G. Righetti, C. Gelfi, A. Bossi, E. Olivieri, L. Castelletti, B. Verzola, A. V. Stoyanov, Capillary electrophoresis of peptides and proteins in isoelectric buffers: An update, Electrophoresis 21 (2000) 4046–4053. doi:10.1002/1522-2683(200012)21:18<4046::AID-ELPS4046>3.0.CO;2-5.

[38] H. Stutz, Advances in the analysis of proteins and peptides by capillary electrophoresis with matrix-assisted laser desorption/ionization and electrospray-mass spectrometry detection, Electrophoresis 26 (2005) 1254–1290. doi:10.1002/elps.200410130.

[39] B. Lönnerdal, Bioactive proteins in breast milk, J. Paediatr. Child Health. 49 (2013) 1–7. doi:10.1111/jpc.12104.

[40] A. Bateman, C. Wu, I. Xenarios, The Universal Protein Resource (UniProt). UniProt Knowledgebase, (2002). Disponible en: https://www.uniprot.org/ (Fecha de acceso: 05/06/2018).

[41]† Y. Liao, R. Alvarado, B. Phinney, B. Lönnerdal, Proteomic characterization of specific minor proteins in the human milk casein fraction, J. Proteome Res. 10 (2011) 5409–5415. doi:10.1021/pr200660t.

† Only included in Supplementary Information.

9. 6. Supporting Information

9. 6. 1. LC-MS/MS analysis

Ionization conditions of MS/MS

Sample was ionized applying 2.8 kV to the spray emitter. Analysis was carried out in a data-dependent mode. Survey MS1 scans were acquired from 350–1250 m/z for 250 ms. The quadrupole resolution was set to 'UNIT' for MS2 experiments, which were acquired 100–1500 m/z for 50 ms in 'high sensitivity' mode. Following switch criteria were used: charge: 2+ to 5+; minimum intensity; 70 counts per second (cps). Up to 50 ions were selected for fragmentation after each survey scan. Dynamic exclusion was set to 15 s. The system sensitivity was controlled with 2 fmol of 6 proteins (LC Packings).

Protein identification

Searching in the expasy database (version 01-2017) was done with the following parameters: trypsin specificity, cys-alkylation, taxonomy restricted to human, and the search effort set to through. To avoid using the same spectral evidence in more than one protein, the identified proteins were grouped based on MS/MS spectra by the ProteinPilot Pro Group algorithm. A protein group in a Pro Group Report is a set of proteins that share some physical evidence. Unlike sequence alignment analyses where full length theoretical sequences are compared, the formation of protein groups in Pro Group is guided entirely by observed peptides only. Since the observed peptides are actually determined from experimentally acquired spectra, the grouping can be considered to be guided by usage of spectra. Then, unobserved regions of protein sequence play no role in explaining the data.

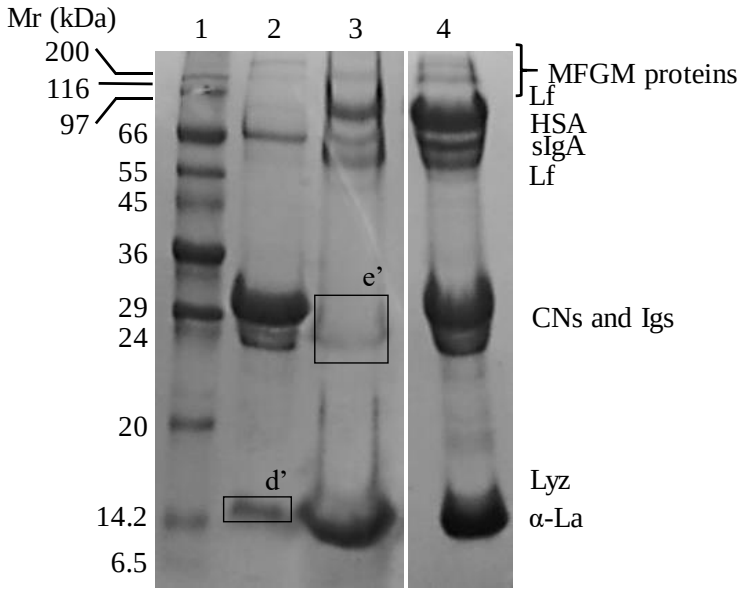

Figure S9.1. SDS-PAGE analysis of human milk. Identification: lane 1, molecular weight marker; lane 2 and 3, pellet and supernatant of CaP precipitation (2x), respectively; and lane 4, human milk.

Table S9.1. Identified human milk proteins in the SDS-PAGE bands digested (see **Figure 9.2** and **S9.1**). Unless indicated, all listed proteins have been reported at least in two of the following references: [2,7,20–25,41].

Band	Protein Name	Accession No.	Mascot Score[1]/ Unused[2]	%Cov (95)	Peptides (95%)
a[1]	Beta-casein	P05814	70	11	3
	Kappa-casein	P07498	173	45	8
b[1]	Beta-casein	P05814	100	19	6
c[2]	Alpha-S1-casein	P47710	3.8	9.7	2
	Beta-casein	P05814	11.6	13.3	6
	Butyrophilin subfamily 1 member A1	Q13410	2.0	2.3	1
	Golgi-associated plant pathogenesis-related protein 1	Q9H4G4	6.0	23.4	3
	Hornerin[3]	Q86YZ3	2.0	2.8	1
	Keratin, type I cytoskeletal 10	P13645	8.0	9.1	5
	Keratin, type I cytoskeletal 14	P02533	2.0	15.0	6
	Keratin, type I cytoskeletal 16	P08779	11.1	14.8	6
	Keratin, type I cytoskeletal 17[3]	Q04695	2.0	6.7	3
	Keratin, type I cytoskeletal 9	P35527	15.5	15.6	9
	Keratin, type II cytoskeletal 1	P04264	27.8	19.4	14
	Keratin, type II cytoskeletal 2 epidermal	P35908	10.8	12.7	7
	Keratin, type II cytoskeletal 5	P13647	6.0	8.5	4
	Keratin, type II cytoskeletal 6A	P02538	2.0	9.9	5
	Keratin, type II cytoskeletal 6C	P48668	9.1	9.9	5
d[2]	Alpha-lactalbumin	P00709	8.1	21.8	5
	Beta-casein	P05814	4.1	8.9	2
	Fatty acid-binding protein, heart	P05413	10.1	44.4	7
	Kappa-casein	P07498	4.0	14.3	2
	Keratin, type I cytoskeletal 10	P13645	8.0	9.2	5
	Keratin, type I cytoskeletal 14	P02533	10.4	11.4	5
	Keratin, type I cytoskeletal 9	P35527	9.1	7.9	4
	Keratin, type II cytoskeletal 1	P04264	18.6	13.3	9
	Keratin, type II cytoskeletal 2 epidermal	P35908	10.4	9.7	6
	Keratin, type II cytoskeletal 5	P13647	4.0	4.2	2
	Vitronectin	P04004	2.0	2.3	1

Band	Protein Name	Accession No.	Mascot Score[1]/ Unused[2]	%Cov (95)	Peptides (95%)
e[1]	Beta-casein	P05814	96	15	4
	Ig kappa chain C region	P01834	78	37	4
	Lactoferrin	P02788	113	27	20
d'[2]	Alpha-lactalbumin	P00709	43.1	64.1	63
	Beta-casein	P05814	4.0	11.9	5
	Fatty acid-binding protein, heart	P05413	18.6	61.7	11
	Kappa-casein	P07498	14.0	47.2	15
	Keratin, type I cytoskeletal 10	P13645	14.7	20.6	13
	Keratin, type I cytoskeletal 14	P02533	6.6	22.9	9
	Keratin, type I cytoskeletal 16	P08779	22.7	32.8	12
	Keratin, type I cytoskeletal 9	P35527	32.0	37.6	19
	Keratin, type II cytoskeletal 1	P04264	50.3	39.8	28
	Keratin, type II cytoskeletal 2 epidermal	P35908	13.2	21.4	13
	Keratin, type II cytoskeletal 5	P13647	2.0	8.6	6
	Keratin, type II cytoskeletal 6A	P02538	17.6	23.4	12
	Lysozyme C	P61626	6.1	22.3	3
	Macrophage migration inhibitory factor[3]	P14174	4.0	17.4	2
	Serum albumin	P02768	35.3	34.8	18
e'[2]	Alpha-1-antichymotrypsin	P01011	6.4	9.5	3
	Alpha-lactalbumin	P00709	15.9	43.0	8
	Alpha-S1-casein	P47710	5.8	14.6	6
	Apolipoprotein A-I	P02647	2.0	5.2	1
	Beta-1,4-galactosyltransferase 1	P15291	2.0	2.0	1
	Beta-casein	P05814	27.9	44.7	31
	Bile salt-activated lipase	P19835	39.6	27.9	26
	Butyrophilin subfamily 1 member A1	Q13410	13.3	19.6	9
	Cell death activator CIDE-A[3]	O60543	7.9	21.0	4
	Chordin-like protein 2	Q6WN34	2.0	3.7	1
	Clusterin	P10909	6.1	11.4	3
	Complement C4-B	P0C0L5	4.0	1.8	2
	GTP-binding protein SAR1b	Q9Y6B6	1.4	5.6	1
	Heat shock protein beta-1	P04792	2.0	4.9	1
	Ig alpha-1 chain C region	P01876	11.3	19.8	8

Band	Protein Name	Accession No.	Mascot Score[1]/ Unused[2]	%Cov (95)	Peptides (95%)
	Ig gamma-1 chain C region	P01857	5.8	13.3	3
	Ig kappa chain C region	P01834	45.1	97.2	60
	Ig lambda-2 chain C regions	P0DOY2	26.5	74.5	29
	Immunoglobulin J chain	P01591	24.3	56.0	18
	Immunoglobulin kappa variable 1-17[4]	P01599	2.0	34.2	6
	Immunoglobulin kappa variable 1-33[3]	P04432	2.0	29.1	4
	Immunoglobulin kappa variable 1-5[3]	P01602	8.1	34.2	5
	Immunoglobulin kappa variable 1D-39[5]	P04432	6.3	34.2	8
	Immunoglobulin kappa variable 2-30	P06310	2.0	16.7	3
	Immunoglobulin kappa variable 2D-28[3]	P01615	4.7	37.5	7
	Immunoglobulin kappa variable 3-11	P04433	2.0	35.6	8
	Immunoglobulin kappa variable 3-15[3]	P01624	6.0	41.7	4
	Immunoglobulin kappa variable 3-20	P01619	10.4	61.2	11
	Immunoglobulin kappa variable 3-20[5]	A0A0C4	4.0	37.1	9
	Immunoglobulin kappa variable 4-1	P06312	4.0	22.3	2
	Immunoglobulin lambda variable 1-47	P01700	8.9	43.6	7
	Immunoglobulin lambda variable 1-51[5]	P01701	3.2	32.5	4
	Immunoglobulin lambda variable 3-19	P01714	4.1	24.1	3
	Immunoglobulin lambda variable 3-21	P80748	4.0	29.1	2
	Immunoglobulin lambda variable 3-25	P01717	6.1	35.7	4
	Immunoglobulin lambda variable 7-43[3]	P04211	1.9	7.7	1
	Immunoglobulin lambda-like polypeptide 5	B9A064	8.0	40.7	26
	Interleukin-19[6]	Q9UHD0	3.7	14.7	2
	Kallikrein-6	Q92876	2.0	4.9	1
	Kappa-casein	P07498	4.0	14.3	3
	Keratin, type I cytoskeletal 10	P13645	28.9	28.6	15
	Keratin, type I cytoskeletal 16	P08779	2.8	9.7	4
	Keratin, type I cytoskeletal 9	P35527	16.6	26.5	11
	Keratin, type II cytoskeletal 1	P04264	43.7	40.8	27
	Keratin, type II cytoskeletal 2 epidermal	P35908	17.9	25.2	12
	Keratin, type II cytoskeletal 5	P13647	1.9	3.4	2
	Keratin, type II cytoskeletal 6B[3]	P04259	2.0	7.1	4
	Lactadherin	Q08431	5.9	11.1	3
	Lactotransferrin	P02788	149.3	70.0	134
	Lysozyme C	P61626	6.5	22.3	3
	Metalloproteinase inhibitor 1	P01033	3.5	9.2	2

Band	Protein Name	Accession No.	Mascot Score[1]/ Unused[2]	%Cov (95)	Peptides (95%)
	Methyltransferase-like protein 7A[3]	Q9H8H3	2.0	6.1	1
	Mucin-1	P15941	2.0	1.1	1
	Peptidyl-prolyl cis-trans isomerase B	P23284	2.0	7.4	1
	Perilipin-2	Q99541	10.4	21.7	6
	Polymeric immunoglobulin receptor	P01833	10.0	9.8	5
	Sclerostin domain-containing protein 1	Q6X4U4	6.1	15.0	3
	Serum albumin	P02768	60.2	52.4	39
	Triosephosphate isomerase	P60174	4.0	12.2	2
	Xanthine dehydrogenase/oxidase	P47989	2.2	1.0	2

[1]MALDI-TOF.
[2]LC-MS/MS.
[3]Only reported in reference [20].
[4]Only reported in reference [22].
[5]Not previously reported in human milk.
[6]Only reported in reference [21].

Table S9.2. Identified proteins in CE fraction collection. Unless indicated, all proteins have been reported at least in two of the following references: [2,7,20–25,41].

		Fraction 1			Fraction 2		
Protein Name	**Accession No.**	**Unused**	**%Cov (95)**	**Peptides (95%)**	**Unused**	**%Cov (95)**	**Peptides (95%)**
Actin, cytoplasmic 2	P63261	4.5	9.1	2	3.0	9.1	2
Alpha-amylase 1	P04745	4.0	6.1	2	-	-	-
Annexin A1	P04083	21.4	32.9	11	2.2	3.2	1
Annexin A2	P07355	9.3	21.5	6	8.2	12.7	4
Arginase-1[1]	P05089	6.7	16.2	4	2.5	5.6	1
Beta-casein	P05814	6.0	28.3	5	4.0	11.9	5
Bilesalt-activatedlipase	P19835	-	-	-	2.0	1.6	1
C4b-binding protein alpha chain	P04003	2.0	2.0	1	-	-	-
Calmodulin-likeprotein 5	Q9NZT1	2.0	15.7	2	2.3	7.5	1
Cathepsin D	P07339	2.1	3.2	1	-	-	-
Clusterin	P10909	3.5	8.9	2	-	-	-
Cystatin-A[1]	P01040	-	-	-	3.4	26.5	2
Dermcidin	P81605	6.0	25.5	3	7.9	36.4	4
Desmocollin-1[1]	Q08554	1.4	3.2	2	4.3	4.4	3
Desmoglein-1[1]	Q02413	12.4	10.1	10	9.2	9.4	6
Desmoplakin[1]	P15924	41.8	10.7	24	32.5	7.6	16
Fatty acid-binding protein, epidermal[2]	Q01469	-	-	-	2.1	15.6	1
F-box onlyprotein 50[1]	Q6ZVX7	2.0	4.4	1	-	-	-
Filaggrin-2[1]	Q5D862	5.9	3.9	4	2.9	0.8	2
Galectin-7[1]	P47929	1.5	10.3	1	2.5	18.4	2
Glyceraldehyde-3-phosphate dehydrogenase	P04406	2.6	8.7	2	2.1	4.5	1
Heat shock protein beta-1	P04792	4.6	21.0	3	2.0	4.9	1
Hemoglobinsubunit beta	P68871	-	-	-	2.0	8.8	1
Histone H4[1]	P62805	-	-	-	4.8	25.2	3
Hornerin	Q86YZ3	16.0	17.1	9	6.0	5.2	4
Ig alpha-1 chain C region	P01876	4.2	9.1	3	4.0	9.1	3
Ig kappa chain C region	P01834	8.0	64.1	4	2.0	17.0	1

		Fraction 1			Fraction 2		
Protein Name	**Accession No.**	**Unused**	**%Cov (95)**	**Peptides (95%)**	**Unused**	**%Cov (95)**	**Peptides (95%)**
Ig lambda-3 chain C regions	P0DOY3	2.0	14.1	1	-	-	-
Junction plakoglobin[1]	P14923	17.5	16.5	9	18.1	16.8	9
Kappa-casein	P07498	1.8	7.1	1	-	-	-
Keratin, type I cytoskeletal 10	P13645	84.2	57.0	68	66.1	56.0	51
Keratin, type I cytoskeletal 13[3]	P13646	24.2	39.5	24	9.9	25.3	16
Keratin, type I cytoskeletal 14	P02533	32.5	61.9	40	43.5	52.3	27
Keratin, type I cytoskeletal 16	P08779	53.4	65.1	37	20.0	53.5	25
Keratin, type I cytoskeletal 17[1]	Q04695	12.2	34.3	18	8.0	32.2	15
Keratin, type I cytoskeletal 9	P35527	73.4	76.4	56	65.7	77.2	58
Keratin, type II cytoskeletal 1	P04264	98.9	71.1	85	101.8	65.5	77
Keratin, type II cytoskeletal 1b[1]	Q7Z794	10.3	16.6	11	10.0	15.2	10
Keratin, type II cytoskeletal 2 epidermal	P35908	109.5	84.2	71	75.1	66.4	53
Keratin, type II cytoskeletal 3[3]	P12035	8.1	23.7	19	-	-	-
Keratin, type II cytoskeletal 4[1]	P19013	46.1	51.5	26	6.1	13.5	6
Keratin, type II cytoskeletal 5	P13647	59.0	52.4	48	40.8	45.4	32
Keratin, type II cytoskeletal 6A	P02538	40.3	61.5	45	27.8	42.2	30
Keratin, type II cytoskeletal 6B[1]	P04259	5.8	59.8	42	3.6	40.4	28
Keratin, type II cytoskeletal 78[1]	Q8N1N4	11.3	17.5	10	15.9	17.5	9
Keratin, type II cytoskeletal 80[1]	Q6KB66	2.0	5.1	2	3.6	7.5	3
Lactotransferrin	P02788	32.9	31.7	18	8.4	8.9	5
Lysozyme C	P61626	2.0	8.1	1	2.0	8.1	1
Plakophilin-1[1]	Q13835	2.0	2.0	1	2.0	2.0	1
Prolactin-inducible protein	P12273	6.2	26.0	3	4.1	15.1	2
Protein S100-A8	P05109	1.5	11.8	1	4.6	37.6	3

		Fraction 1			Fraction 2		
Protein Name	**Accession No.**	**Unused**	**%Cov (95)**	**Peptides (95%)**	**Unused**	**%Cov (95)**	**Peptides (95%)**
Protein S100-A9	P06702	3.7	28.1	3	5.1	28.9	3
Protein-glutamine gamma-glutamyltransferase E[1]	Q08188	4.0	5.5	2	4.0	5.2	2
Protein-glutamine gamma-glutamyltransferase K[3]	P22735	2.0	2.0	1	2.7	3.8	2
Serpin B12[1]	Q96P63	3.4	7.7	3	5.4	6.9	3
Serpin B3[1]	P29508	3.8	4.9	2	12.7	22.8	7
Serumalbumin	P02768	29.2	28.2	19	12.3	14.8	7
Suprabasin[1]	Q6UWP8	4.0	15.3	2	-	-	-
Thioredoxin	P10599	1.5	12.4	1	-	-	-
Tubulin alpha-1C chain[1]	Q9BQE3	-	-	-	2.0	3.3	1
Ubiquitin-60S ribosomal protein L40	P62987	4.2	22.7	2	2.0	12.5	1
Zinc-alpha-2-glycoprotein	P25311	2.5	11.1	2	-	-	-

[1]Only reported in reference [20].

[2]Only reported in reference [26].

[3]Not previously reported in human milk.

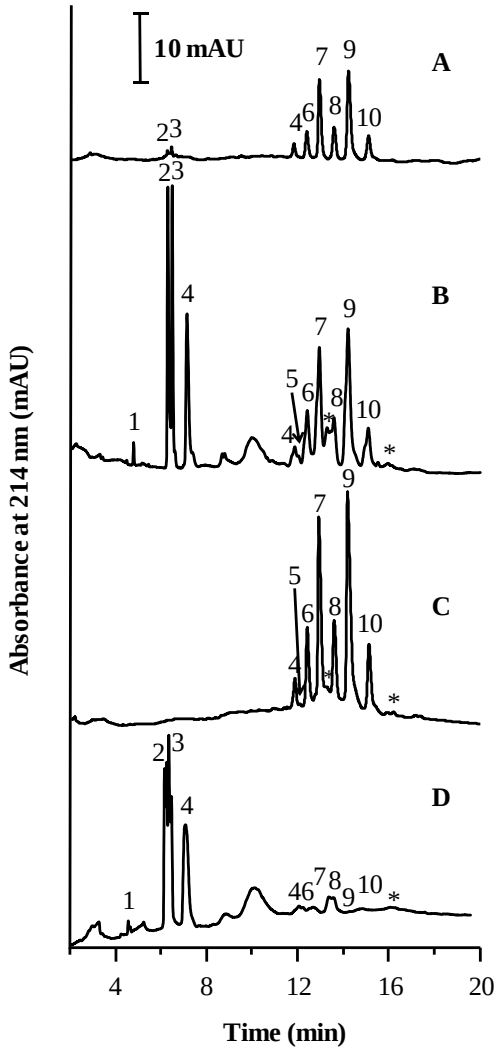

Figure S9.2. Electropherograms of pellet (A) and supernatant (B) of isoelectric precipitation, and pellet (C) and supernatant (D) of CaP precipitation. See **Figure 9.5** for peak identification.

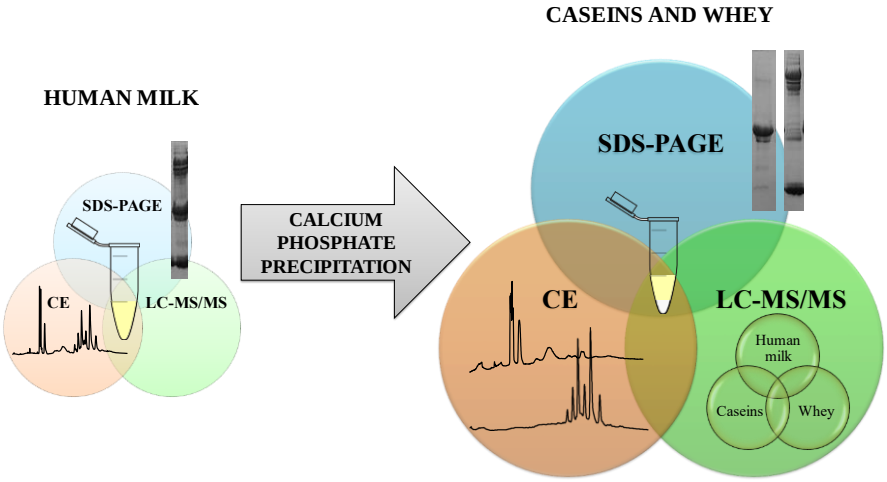
HUMAN MILK
SDS-PAGE
CE
LC-MS/MS
CALCIUM
PHOSPHATE
PRECIPITATION
CASEINS AND WHEY
SDS-PAGE
CE
LC-MS/MS
Human
milk
Caseins
Whey

BLOQUE IV. RESUMEN DE RESULTADOS Y CONCLUSIONES

A. Análisis de la fracción lipídica de la leche materna

A.1. Triacylglycerol analysis in human milk and other mammalian species: small-scale sample preparation, characterization and statistical classification using HPLC-ELSD profiles

En este trabajo se llevó a cabo la separación de TAG presentes en la leche materna y en la procedente de otros mamíferos (vaca, cabra y oveja) por RP-HPLC empleando una columna particulada de "corazón fundido" (*fused core*) con detector UV-vis y ELSD. Para la separación cromatográfica se empleó una fase móvil de ACN/*n*-pentanol, resolviéndose de manera satisfactoria más de 50 TAG, cuya identificación se llevó a cabo posteriormente por APCI-MS.

Además, se puso a punto un método de extracción a escala reducida, el cual requiere unos volúmenes de reactivos y muestra inferiores al método tradicional. El método propuesto se comparó con el método tradicional, observándose que no existían diferencias significativas entre ambos en el contenido de grasa y para un 85% de los TAG identificados. Además, cabe destacar que, el método de tratamiento de muestra propuesto no sólo supone una reducción en la cantidad de reactivos necesaria, sino que, debido a la sencillez asociada a la manipulación del material requerido, permite el procesamiento de un mayor número de muestras respecto al método tradicional.

Por último, con el fin de distinguir el origen de la leche de diversos mamíferos, se realizó un estudio estadístico donde se construyó un modelo LDA a partir del perfil de TAG obtenido mediante HPLC-ELSD. Los resultados obtenidos permitieron discernir entre las variedades de leche estudiadas (humana, bovina, ovina y caprina). Este estudio resulta de interés no solo por su aplicabilidad sobre leche materna, sino también sobre productos derivados de la leche de otros mamíferos.

A.2. Solid-phase extraction of phospholipids using mesoporous silica nanoparticles. Application to human milk samples

En este trabajo se evaluaron diversos MSM (MCM-41 y UVM-7, tanto pura como dopada con Ti) y una fase estacionaria comercial de sílice (SupelClean^{TM}) como sorbentes de SPE para el aislamiento de PL empleando PC como soluto test. La caracterización morfológica de los materiales sintetizados y del material comercial se llevó a cabo por técnicas tales como SEM, TEM, incluyéndose también medidas de área superficial y tamaño de poro.

Por otra parte, se abordó el mecanismo de interacción entre el analito de interés y los MSM, proponiéndose que éste tenía lugar en dos pasos: (i) difusión de las micelas invertidas de PC a lo largo del sistema de poros de la sílice; y (ii) ruptura de las micelas de PC inducida por la interacción favorable del PL con los grupos silanoles de la superficie de la sílice (Si-OH⋯PC).

Con respecto al protocolo SPE, se investigaron diversos parámetros experimentales que afectan al proceso como p.ej. disolvente de carga y elución, volumen de ruptura, capacidad de carga y reutilización.

De entre los materiales testados, incluyendo el de sílice comercial, el material UVM-7-Ext, en el que los restos de surfactante de la síntesis habían sido retirados por extracción química, fuel el que proporcionó los mejores resultados. Este hecho, se atribuyó al entorno más hidrofílico (mayor proporción de grupos silanoles) de dicho material con respecto al MCM-41 y SupelClean^{TM}, junto con el segundo sistema de poros bimodal característico del material UVM-7. Así pues, el material UVM-7-Ext proporcionó una elevada capacidad de adsorción (544 µg de PC por mg de sorbente), reutilización (más de 15 usos) y capacidad de preconcentración (hasta 16 veces), características de gran importancia con fines de tratamiento de muestra.

Finalmente, la utilidad del material UVM-7-Ext como sorbente SPE quedó demostrada por su satisfactoria aplicación a extractos de grasa de leche materna, observándose una limpieza efectiva (*clean up*) de la muestra (especialmente en la eliminación de TAG) y una preconcentración de los PL, preservando así la integridad estructural de la columna cromatográfica.

Este trabajo supone la primera aplicación de los MSM a la preconcentración de PL en esta matriz compleja, por lo que los materiales tipo UVM-7 merecen ser considerados como sorbentes prometedores para la extracción de estos analitos en muestras biológicas.

A.3. Polymer-based materials modified with magnetite nanoparticles for enrichment of phospholipids

En este trabajo se preparó un material polimérico de GMA, el cual fue posteriormente modificado con MNP para ser evaluado como sorbente tanto en SPE como en MSPE para el aislamiento de PL en muestras de leche materna. El material sintetizado se caracterizó por SEM, observándose claramente el anclaje de las NP de magnetita sobre la superficie del polímero. También, se determinó el contenido de Fe (1.6 - 1.7% m/m) en el material sintetizado por UV-vis e ICP-MS. Asimismo, las medidas de área superficial en los polímeros funcionalizados con MNP mostraron un incremento en la misma (15.17 m^2/g) respecto al polímero sin modificar (6.14 m^2/g), favoreciéndose así la retención de los analitos de interés.

Por otra parte, se investigaron diversas variables que intervienen en el proceso de extracción (p. ej. disolvente de carga, volumen de ruptura y capacidad de carga) y se comparó la modalidad de SPE convencional con la MSPE. En las condiciones de carga y elución establecidas, la capacidad de adsorción del sorbente en SPE fue superior (5.7 µg de PC por mg de sorbente) a la mostrada en dispersiva (MSPE) (3.3 µg de PC por mg de sorbente). Además, la reutilización de los cartuchos de SPE fue claramente superior

(10 usos) a la mostrada en MSPE (un único uso), atribuyéndose este resultado principalmente a la pérdida de material magnético tras el proceso de regeneración de éste.

La metodología propuesta se aplicó satisfactoriamente a la extracción de PL de extractos de grasa de leche materna en diferentes etapas de lactancia, analizándose los PL extraídos mediante HILIC-ELSD. Por otra parte, gracias a la extracción previa de los PL con la concomitante eliminación de lípidos no polares (TAG), la integridad estructural de la columna cromatográfica se ve preservada. Así pues, este trabajo representa también una alternativa prometedora para la extracción de PL de muestras biológicas.

A.4. Molecularly imprinted polymers for selective solid-phase extraction of phospholipids from human milk samples

En este trabajo se han sintetizado diversos MIP por polimerización térmica empleándose PC como molécula plantilla (T), MA como monómero funcional (M) y EDMA como agente entrecruzante (C). En primer lugar, se llevó a cabo un estudio de pre-polimerización por FTIR, en el que se estudiaron las interacciones moleculares T-M en diferentes disolventes (ACN, MeOH y THF), seleccionándose ACN como disolvente porogénico para la síntesis. Se estudiaron también diferentes proporciones de T:M:C y porcentaje de iniciador. De entre los MIP sintetizados, el MIP con una relación T:M:C de 1:6:30 y un 4.2% de iniciador mostró la mejor capacidad de reconocimiento de la molécula plantilla. Se investigó la selectividad del MIP frente a otros PL, observándose que éste mostraba una elevada afinidad no solo por la PC, sino por otros PL como la SM y la PE. Este fenómeno, conocido como reactividad cruzada, es de gran utilidad para el fin que se perseguía inicialmente en el trabajo: la extracción del conjunto de PL.

El MIP seleccionado se empleó en la extracción de PL de extractos de grasa de leche materna, observándose una limpieza efectiva de la matriz de la

muestra (eliminación de TAG) y una preconcentración de los analitos de interés (analizados por HILIC-ELSD). Asimismo, el MIP mostró una buena capacidad de carga (41 μg PC por mg de sorbente) y una reutilización de al menos 20 veces para disoluciones patrón de PC y de al menos 6 veces para extractos de grasa.

Este trabajo supone la primera aplicación de la tecnología de impronta molecular para el aislamiento de PL de matrices complejas.

B. Análisis de la fracción proteica de la leche materna

B.1. Isolation of human milk whey proteins by solid-phase extraction with a polymeric material modified with gold nanoparticles

En este trabajo se describe un método para el aislamiento de las proteínas del suero de la leche materna mediante SPE empleando un material polimérico de GMA modificado con AuNP. El contenido de Au resultante, medido colorimétricamente previa calcinación del material híbrido fue de un 1.3% m/m. Asimismo, las micrografías SEM mostraron la presencia de las AuNP en la superficie del sorbente, presentando éstas una elevada afinidad por los grupos tiol y amino, habitualmente presentes en biomoléculas como las proteínas.

En concreto, se seleccionaron una serie de proteínas séricas como son la HSA, la α-La, la Lf y la Lyz y se investigaron diferentes variables (pH, fuerza iónica) con el fin de conseguir el máximo rendimiento en el proceso de extracción. En las mejores condiciones establecidas (pH de carga 5.0, pH de elución 12 con 0.25 M de NaCl), el sorbente SPE proporcionó excelentes recuperaciones, ofreciendo una alta permeabilidad y reutilización (más de 20 veces).

Cabe destacar que, este trabajo supone la primera aproximación basada en la inmovilización de AuNP sobre soportes poliméricos y su

interacción con las proteínas presentes en la leche para su empleo como sorbente de extracción en SPE. Asimismo, la viabilidad de la metodología propuesta, seguida por SDS-PAGE, quedó satisfactoriamente demostrada con el aislamiento de las proteínas de interés tanto de extractos de suero de leche materna, como directamente de muestras de leche diluidas, es decir, sin haber llevado a cabo previamente la precipitación isoeléctrica de las CN.

B.2. Improving fractionation of human milk proteins through calcium phosphate coprecipitation and their rapid characterization by capillary electrophoresis

En este estudio se describe un método sencillo de tratamiento de muestra para el fraccionamiento efectivo de las proteínas de la leche materna en sus dos grupos principales: suero y CN. El protocolo de extracción consistió en la adición de iones calcio y fosfato a la leche sin ajuste previo de pH, seguido de etapas de lavado y centrifugación. La combinación de ambos iones dio lugar a la precipitación de fosfato cálcico y como resultado, a una coprecipitación efectiva de las CN. La efectividad del fraccionamiento por coprecipitación, así como por precipitación en el pI se siguió por SDS-PAGE, LC-MS/MS y CE. Los resultados obtenidos mostraron una disminución significativa en la contaminación de la fracción de CN con proteínas del suero y viceversa, en comparación con el método convencional de precipitación de CN basado en el pI.

En lo referente al análisis de la leche materna por CE, se empleó un tampón isoeléctrico constituido por urea, hidroxietilcelulosa y ácido iminodiacético (pH aparente 3.1), obteniéndose un perfil electroforético en el que las principales proteínas del suero y CN se encontraban adecuadamente resueltas en un tiempo de análisis corto. Además, se aplicó satisfactoriamente la recolección de fracciones en CE acoplada a LC-MS/MS (acoplamiento fuera de línea) para la identificación de proteínas minoritarias en esta matriz

compleja. Esta combinación permitió identificar proteínas tales como Ig, las cuales no habían sido identificadas previamente mediante esta técnica separativa.

Cabe destacar que, en lo que respecta a reactivos, instrumentación y esfuerzo, la metodología de fraccionamiento propuesta supone una aproximación de bajo coste y gran alcance para acrecentar el conocimiento del proteoma de la leche materna. Los datos obtenidos en este trabajo se encuentran disponibles en el consorcio *ProteomeXchange* con el identificador PXD010315.

VNIVERSITAT DE VALÈNCIA